Symmetries of Curves and Surfaces

Thesis submitted in accordance with the requirements of the University of Liverpool for the degree of Doctor in Philosophy

by

John Paul Warder

May 2009

UNIVERSITY OF LIVERPOOL

Contents

List of Figures

List of Abbreviations

AASS	=	Affine Area Symmetry Set
ADSS	=	Affine Distance Symmetry Set
AESS	=	Affine Envelope Symmetry Set
BPC	=	Bi-tangent Plane Curve
CGI	=	Computer-Generated Imagery
CSS	=	Centre Symmetry Set
CT	=	Computerised Tomography
FC	=	Flecnodal Curve
LHS	=	Left Hand Side
LSMP	=	Liverpool Surface Modeling Package
MPL	=	Mid-Point Locus
MPTL	=	Mid-Parallel Tangents Locus
MPTS	=	Mid-Parallel Tangents Surface
ODE	=	Ordinary Differential Equation
PC	=	Parabolic Curve
PSS	=	Pre-Symmetry Set
PTBC	=	Parallel Tangents Boundary Curve
RHS	=	Right Hand Side
SS	=	Symmetry Set

Acknowledgements

My thanks go to my supervisor Professor Peter Giblin for devoting so much of his valuable time during these past three and a half years. His enduring patience and good humour in working through many difficult concepts with me has been quite invaluable. Special thanks must also go to Professor Vladimir Zakalyukin for suggesting areas of investigation and for patiently explaining, and expanding upon, his work on determining normal forms for equidistants.

I am indebted to the Department of Mathematical Sciences for providing a friendly and effective working environment and to the Engineering and Physical Sciences Research Council (EPSRC) for their generous funding.

Last, and by no means least, I wish to thank my partner Rachel for her love, encouragement and understanding throughout what has been a long and at times arduous process ... for both of us!

Chapter 1

Introduction

This thesis is concerned with the differential geometry of plane curves and surfaces in 3-space, with a particular emphasis on the properties of symmetry revealing or encoding type constructions. Such constructions are used in a wide variety of real world applications, mostly falling under the umbrella term *Computer Vision.* These include: object recognition (e.g. iris and finger print scanning), object reconstruction (e.g. from partly occluded or poorly resolved photo and video images), medical imaging (e.g. 3D reconstructions from multiple CT scans) and CGI (skeletonisation and shading effects).

To form such symmetry constructions it is necessary to identify for a given curve, or surface, the set of pairs of points which have parallel tangents or which both touch a bi-tangent circle or sphere. We call these objects *pre-sets* and they have a rich mathematical structure of their own. Once the pre-set is known, and if it is sufficiently well behaved, we can use it to form symmetry constructions. Many different symmetry constructions have been studied in the literature and creation of new types and variations on the existing models is an active research area. They all have differing applications and/or reveal special features of the host geometry. The work described here considers two such constructions: (i) a symmetry construction to smooth plane curves called the *Mid-Point Locus* and (ii) a family of symmetry constructions to smooth surfaces known collectively as *equidistants* of the surface. A chapter summary now follows:

In chapter 2 we introduce the Mid-Point Locus to a plane curve. The pre-set here is the set of pairs of points through which we can draw a bi-tangent circle, whilst the mid-points of chords joining such pairs forms the Mid-point Locus itself. We describe conditions under which the Mid-Point Locus fails to be smooth and investigate factors influencing the angle between the tangents to the Mid-Point Locus and its host curve at points of contact. We study special branches of the Mid-Point Locus formed as midpoints of lines connecting pairs of points with parallel tangents on the host curve (a 2D analogue of the equidistants). The Mid-Point Locus can be used to skeletonise a closed curve (or indeed any 2D shape) and in chapter 3 we look at various methods of reconstructing the original curve given its Mid-Point Locus.

The remainder of the thesis is devoted to surface symmetry. We consider the pre-set Π of pairs of surface points with parallel tangent planes; either on disjoint surfaces or local to a parabolic point of a single surface piece. From this pre-set we can construct the *equidistants* which are affine invariants of the surface. If we have points $p, q \in \Pi$ then the corresponding equidistant point is given by $(1-\lambda)\,p + \lambda\,q$ where $\lambda \in [0,1]$ is some fixed proportion along the chord. Since λ and $1-\lambda$ give the same equidistant we find that the equidistant with $\lambda = \frac{1}{2}$ has a special symmetry. We call it the *Mid-Parallel Tangents Surface* (MPTS) and show that it has some unique singular behaviour quite apart from the other equidistants.

In chapter 4 we study the pre-set Π itself for the case of disjoint surface pieces, exploring the maps linking the parameters at the two points of tangency and some of their singularities. For Π in the local case we consider the same issues and also the effect of the parabolic point being an ordinary cusp of Gauss. In this setting we describe the necessary arrangement of a number of special curves on the surface through the cusp of Gauss. In chapter 5 we study the MPTS in the disjoint surfaces case, obtaining exact conditions for cusp edge and swallowtail singularities and their corresponding versal unfolding criteria. We also consider the case of bi-tangent plane pairs and the ruled surface formed by chords joining such pairs. Some interesting results are obtained concerning the relationship of this surface to the MPTS. In the

local case we consider similar phenomena but now with an emphasis on forming the equidistants as envelopes of certain *generating families*. We show how the MPTS has some interesting singular behaviour local to special parabolic points, designated A_2^*, which have never been previously studied. In the A_3 case we show how the equidistant has interesting singular behaviour for certain special (and symmetric) values of λ. In both cases we look at how these singularities transition either side of the special λ values. Chapter 6 contains detailed proofs that the generating families used to form equidistants local to A_2, A_2^* and A_3 points are valid. The chapter is separated into sections for equidistants to plane curves and surfaces.

The final chapter contains some experimental results for equidistants local to special surface points occurring in families of surfaces, e.g. equidistants local to a parabolic point undergoing a Morse transition (non-versal A_3) and also transitions about points of the surface where the height function on the surface is A_4 or D_4 singular. The D_4 cases are particularly elusive as Π is not easily parameterised and alternative approaches are required. We obtain some useful qualitative information using simpler diffeomorphic settings.

Chapter 2

The Mid-Point Locus

2.1 Introduction

The Mid-Point Locus (MPL) was introduced in the early 1980s by Asada and Brady [3] as a means of capturing the essential symmetry of a planar shape. The pre-set in this case is the set of pairs of points through which we can draw a bi-tangent circle. This is the 2D *pre-symmetry set* and its structure has been extensively studied so here we concentrate on the MPL itself (which is formed as the mid-points of chords joining pairs of points in the pre-symmetry set). The work elaborates on that of Giblin and Brassett [8] and a summary of this chapter is as follows:

1. We describe conditions under which the MPL fails to be smooth and investigate its local structure under such circumstances.

2. If γ is a plane curve to which we form the MPL then the angle between the tangents to γ and the MPL at a point of contact (which is always at a vertex on γ) varies considerably. We study a number of the factor influencing this phenomenon.

3. In plotting the MPL it is possible to generate 'false' branches, corresponding to midpoints of lines connecting pairs of points with parallel tangents on γ. We study such branches and also their interaction with the MPL.

2.2 Some Preliminaries

Here we establish a number of results concerning the local structure of the MPL and one global result regarding closed curves that we will need later in the chapter. First some definitions:

Definition 2.2.1 *Given a smooth curve γ in $\mathbb{R}^2$ the Mid-Point Locus (MPL) is the locus of mid-points of chords of the contact points of circles bi-tangent to γ together with all limit points of this set. Thus, if $\gamma_1 = \gamma(s)$ and $\gamma_2 = \gamma(t)$ are the two points of tangency then the corresponding point of the MPL is, $m(s,t) = (\gamma_1 + \gamma_2)/2$.*

Definition 2.2.2 *Given a smooth curve γ in $\mathbb{R}^2$ the Pre-Symmetry Set (PSS) of γ is the set of all pairs of points on γ to which we can construct a bi-tangent circle.*

Local Structure of the Mid-Point Locus

Locally, let $\gamma_1 = \gamma(s)$ and $\gamma_2 = \gamma(t)$ be *unit speed parameterisations*[1] of disjoint arcs of a smooth curve γ near points of contact with a bi-tangent circle[2] (oriented as shown in figure 2.1) with T_1, T_2 and N_1, N_2 their unit tangents and normals. Now consider

$$h(s,t) = (\gamma_1 - \gamma_2) \cdot (T_1 - T_2). \tag{2.1}$$

Clearly $\gamma_1 = \gamma_2$ and $T_1 = T_2$ are both impossible in our setup and we claim:

Proposition 2.2.3 *The closure of $h^{-1}(0)$ is exactly the local PSS.*

Proof: $h = 0$ if and only if $\gamma_1 - \gamma_2 \perp T_1 - T_2$ if and only if $\gamma_1 - \gamma_2 \parallel N_1 - N_2$, i.e. $\gamma_1 - \gamma_2 + r(N_1 - N_2) = 0$ for some $r \in \mathbb{R}$. Thus, $\gamma_1 + rN_1 = \gamma_2 + rN_2$ and the common vector $u = \gamma_i + rN_i$ is the centre of a bi-tangent circle to γ of radius $r > 0$ (see figure 2.1). □

[1] i.e. $\|\gamma'(s)\| = \|\gamma'(t)\| = 1 \, \forall \, s, t$

[2] Note: In figure 2.1 the orientation of the circle agrees with that of γ_1 and γ_2 at the points of tangency. We call this a *coherent* bi-tangent circle and locally we can always set things up this way. However, given a global parameterisation for γ this may not hold, e.g. the larger circle in figure 2.2.

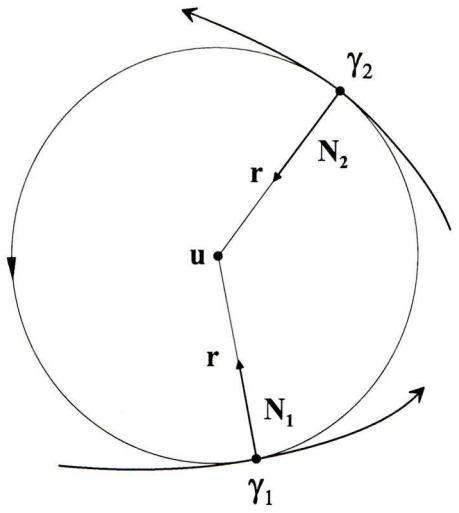

Figure 2.1: Local geometry of a bi-tangent circle to $\gamma(t)$.

We can now use proposition 2.2.3 to find the local structure of the MPL (except in the case of a bi-tangent line which will be considered separately). Firstly, let us take a point (s,t) in the PSS of γ and determine the slope of the tangent here. Let $\gamma_1 = \gamma(s)$ and $\gamma_2 = \gamma(t)$ be the points of tangency and furthermore assume $1 - r\kappa_2(0) \neq 0$, where κ_2 is the curvature at γ_2 and r is the radius of the bi-tangent circle. This being the case then the Jacobian of the map h has maximal rank and by the inverse function theorem we can write $t = t(s)$. Substituting $t = t(s)$ into $h(s,t) = 0$ and differentiating with respect to s we obtain

$$(T_1 - T_2 t') \cdot (T_1 - T_2) + (\gamma_1 - \gamma_2) \cdot (\kappa_1 N_1 - \kappa_2 N_2 t') = 0.$$

If we now expand, substitute $\gamma_1 - \gamma_2 = r(N_2 - N_1)$, and simplify we obtain, $1 - r\kappa_1 - t'(1 - r\kappa_2) = 0$, from which we state:

Proposition 2.2.4 *Given a point (s,t) in the PSS of a smooth curve γ then the slope of the PSS here is*

$$\frac{dt}{ds} = -\left(\frac{1 - r\kappa_1}{1 - r\kappa_2}\right)$$

provided $1 - r\kappa_2 \neq 0$, where κ_2 is the curvature at γ_2 and r is the radius of the bi-tangent circle.

We now ask, when is the MPL $(= m(h^{-1}(0))$ a smooth curve? If m is a local diffeomorphism then $h^{-1}(0)$ and the MPL have the same local structure up to a smooth

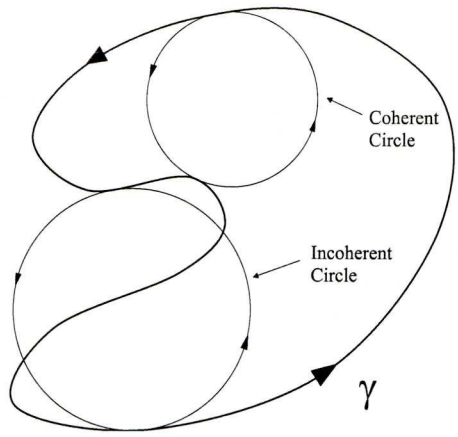

Figure 2.2: Coherent and incoherent bi-tangent circles.

change of coordinates in the plane. Taking (s,t) as a point in the PSS then m is a local diffeomorphism here provided Dm, the 2×2 Jacobian matrix of the map m, has maximal rank here, i.e. $\det(Dm) = \det\left(T_1/2 \;\; T_2/2\right) \neq 0$. This only fails to hold if $T_1 = \lambda T_2$ for some $\lambda \in \mathbb{R}$, but since our parameterisation is unit speed then $\lambda = \pm 1$. Now $T_1 = T_2$ is impossible thus $T_1 = -T_2$ and so the points lie at either end of a diameter on the bi-tangent circle.

When is $h^{-1}(0)$ a smooth curve? Again this will be the case provided

$$Dh = \left((1 - T_1 \cdot T_2)(1 - r\kappa_1) \quad (1 - T_1 \cdot T_2)(1 - r\kappa_2) \right)$$

has maximal rank, and this only fails to hold if both entries are zero. Now $T_1 \cdot T_2 = 1$ if and only if $T_1 = T_2$ which we have already discounted, so Dh has maximal rank, and $h^{-1}(0)$ is smooth, provided $1 - r\kappa_1 \neq 0$ or $1 - r\kappa_2 \neq 0$, i.e. provided the circle is not bi-osculating. So, given that $h^{-1}(0)$ is smooth, the MPL is smooth provided the only vector mapped to zero by both Dh and Dm is the zero vector. Suppose $\mu = (u, v)$ is a non-zero vector mapped to zero by both Dh and Dm. If we form the 3×2 matrix $\tilde{M}$, which is Dh on top of Dm (ignoring non-zero row multipliers) then

$$\tilde{M}\,\mu = \begin{pmatrix} 1 - r\kappa_1 & 1 - r\kappa_2 \\ T_1 & T_2 \end{pmatrix} \begin{pmatrix} u \\ v \end{pmatrix} = \mathbf{0}.$$

Thus, $u\,(1 - r\kappa_1) + v\,(1 - r\kappa_2) = 0$ and $u\,T_1 + v\,T_2 = 0$. The second equation tells us that both u and v must be non-zero and furthermore that $u = \pm v$, since T_1 and T_2 are

both unit vectors. Now, since we have discounted $T_1 = T_2$ we must have $u = v \neq 0$. Cancelling the u's and v's from both equations gives us the following:

Proposition 2.2.5 *Given a smooth plane curve γ with γ_1 and γ_2 being points of contact of a bi-tangent circle, then the MPL of γ is smooth here provided $T_1 \neq -T_2$ or $\kappa_1 + \kappa_2 \neq 2/r$. Remark: For the MPL to be singular would mean imposing four conditions on the variables s, t and r, so singular points of the MPL are clearly non-generic phenomena.*

We now determine the tangent direction to the MPL at a given point. Provided the MPL is smooth then we know from the discussion above that the tangent direction to $h^{-1}(0)$ in the st–plane is taken by the map Dm to the tangent direction to the MPL. The tangent vectors to $h^{-1}(0)$ lie in the kernel of the map Dh and if (u, v) is such a vector then, $(1 - T_1 \cdot T_2)(u\,(1 - r\kappa_1) + v\,(1 - r\kappa_2)) = 0$, so that (u, v) is parallel to $((1 - r\kappa_2), -(1 - r\kappa_1))$. We know that $2Dm = (T_1\ T_2)$ and hence we state:

Proposition 2.2.6 *Given a smooth plane curve γ with bi-tangent circle contacts at γ_1 and γ_2 then the tangent direction to the MPL at the point corresponding to this pair is given by*

$$(T_1\ T_2)\begin{pmatrix} 1 - r\kappa_2 \\ -1 + r\kappa_1 \end{pmatrix} = T_1(1 - r\,\kappa_2) - T_2(1 - r\,\kappa_1)$$

where T_1, T_2 and κ_1, κ_2 are unit tangents and curvatures at the two points respectively, and r is the radius of the bi-tangent circle.

Global Considerations

As stated above, if we have a global parameterisation for γ then $h = 0$ may not find all possible bi-tangent circles to γ. In fact we demonstrated that $h = 0$ will only pick out coherently oriented circles. To find all possible bi-tangent circles we would need to also consider

$$g(s, t) = (\gamma_1 - \gamma_2) \cdot (T_1 + T_2). \tag{2.2}$$

Now $g = 0$ has the trivial solutions $s = t$ and any pair of points for which $T_1 = -T_2$ but a similar argument to that given above shows that the non-trivial solutions pick

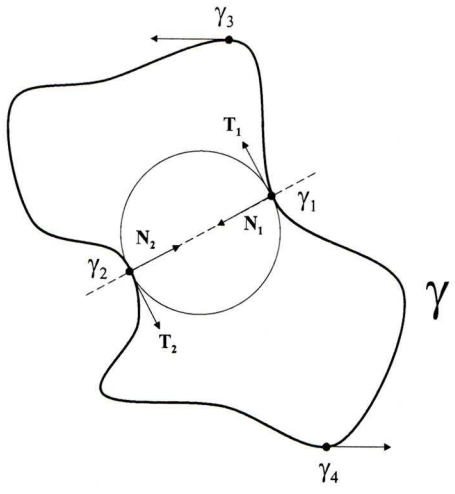

Figure 2.3: Parallel tangents and common normals on a smooth closed curve γ.

out all incoherent bi-tangent circles to γ. Thus, if G is the closure of $g^{-1}(0)$ and H is the closure of $h^{-1}(0)$ (excluding all trivial solutions) then we state:

Proposition 2.2.7 *Given a smooth curve γ in $\mathbb{R}^2$ then $PSS_\gamma = G \cup H$.*

Now we prove a useful global result concerning smooth closed curves. Let γ be a smooth closed curve and γ_i and γ_j be any two distinct points on γ. If we fix γ_i then it is easy to show that we can find a point γ_j such that the tangents at γ_i and γ_j are parallel, e.g. γ_3 and γ_4 in figure 2.3. What isn't immediately obvious is that we can find any pair γ_i, γ_j on γ with parallel tangents **and** a *common normal*[3], e.g. γ_1 and γ_2 in figure 2.3. However, we claim that this is indeed the case by:

Proposition 2.2.8 *For any smooth closed curve γ there exists at least one pair of distinct points on γ with a common normal.*

Proof: Consider the lengths of all possible chords to γ. This is clearly a closed interval of real numbers and so the absolute maximum must be achieved. We claim that the chord, pq say, of maximal length is normal to γ at both ends since if we fix one end, p, and consider the *distance-squared function*[4] from p to γ, which by choice of pq has a maximum at q, then the chord is normal at q. If we now repeat the argument with p and q reversed the result follows. □

[3]By which we mean that the normal line through γ_1 is the same as that through γ_2 (equivalent to γ_1 and γ_2 lying at either end of a diameter of a bi-tangent circle to γ).

[4]i.e. $F = \|p - \gamma\|^2 = (p - \gamma) \cdot (p - \gamma)$.

2.3 Singular Structure of the Mid-Point Locus

The MPL is generically smooth but, by proposition 2.2.5, if the contact points lie at either end of a diameter on a bi-tangent circle and, in addition, the curvatures κ_1 and κ_2 at the two points satisfy $\kappa_1 + \kappa_2 = 2/r$, then the MPL fails to be smooth. Our aim in this section is to describe, by means of an example, the singular structure of the MPL under such circumstances and also to determine conditions for the singularity to be an ordinary cusp.

A Closed Curve Example

We start with a smooth simple closed curve $\gamma(t)$ for which the tangents at $t = 0$ and $t = \pi$, corresponding to the origin and another point on the y–axis, are both parallel to the x–axis. This is the same as saying that the two points share a common normal and there must always be such a pair of points by proposition 2.2.8. If we write $\gamma(t) = (X(t), Y(t))$ then we can express the above requirements as, $X(0) = Y(0) = 0$, $Y'(0) = Y'(\pi) = 0$ and $X(\pi) = 0$. To satisfy these conditions with a closed curve we can choose for example X and Y to have the form

$$X(t) = a\sin t + b(1 - \cos 2t)\ ,\ Y(t) = c(1 - \cos t) + d(1 - \cos 2t).$$

For the MPL to be singular we also need to satisfy the condition $\kappa(0) + \kappa(\pi) = 2/r$. Using the standard Cartesian formula for curvature

$$\kappa = \frac{Y''X' - X''Y'}{((X')^2 + (Y')^2)^{\frac{3}{2}}}$$

and taking positive square roots we obtain the following for $\kappa(0)$ and $\kappa(\pi)$

$$\kappa(0) = \frac{c + 4d}{a^2} \text{ and } \kappa(\pi) = \frac{c - 4d}{a^2}.$$

Now, $r = Y(\pi)/2 = c$, so the condition on curvatures is satisfied by

$$\frac{2c}{a^2} = \frac{2}{c} \Rightarrow c = \pm a.$$

Writing X and Y as Taylor series about $t = 0$ we obtain

$$x = X(t) = at + 2bt^2 - \frac{a}{6}t^3 - \frac{2b}{3}t^4 + \frac{a}{120}t^5 + \frac{4b}{45}t^6 + \ldots,$$

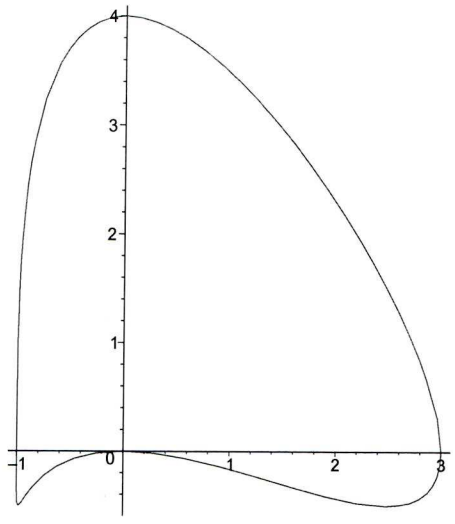

Figure 2.4: $\gamma(t) = (2\sin t + \frac{1}{2} - \frac{1}{2}\cos 2t,\ 1 - 2\cos t + \cos 2t)$.

$$y = Y(t) = \frac{c+4d}{2}t^2 - \frac{1+16d}{24}t^4 + \frac{1+64d}{720}t^6 + \ldots$$

If we now solve for t as a function of x from the equation $x = X(t)$ we obtain

$$t = \frac{1}{a}x - \frac{2b}{a^3}x^2 + \frac{48\,b^2+a^2}{6a^5}x^3 - \frac{b\,(40\,b^2+a^2)}{a^7}x^4 + \ldots$$

and substituting this t into the expression for $Y(t)$ gives

$$Y(t(x)) = \frac{c+4d}{2a^2}x^2 - \frac{(2c+8d)\,b}{a^4}x^3 + \frac{80\,cb^2+ca^2+320db^2}{8a^6}x^4 + \ldots = f(x)$$

where $f(x)$ is the graph of $\gamma(t)$ close to $t = 0$ (the origin in our setup). We can now set $t = s + \pi$ in our original functions for $X(t)$ and $Y(t)$ so that $s = 0$ corresponds to $t = \pi$, repeat the above procedure and obtain a function $g(x)$ which is the graph of $\gamma(t)$ close to $t = \pi$. The expression for $g(x)$ turns out to be

$$g(x) = 2c - \frac{c-4d}{2a^2}x^2 + \frac{(2c-8d)\,b}{a^4}x^3 - \frac{80cb^2+ca^2-320db^2}{8a^6}x^4 + \ldots$$

If we now write $f = f(t)$ and $g = g(s)$ and solve equation (2.1) for t as a function of s, i.e.

$$h(s,t) = ((t, f(t)) - (s, g(s))) \cdot (T_f(t) - T_g(s)) = 0$$

(where $T_f(t)$ and $T_g(s)$ are the unit tangents to f and g respectively) then we can obtain the MPL as

$$m : (s, t(s)) \mapsto \left(\frac{1}{2}(s + t(s)),\ \frac{1}{2}(f(t(s)) + g(s))\right).$$

We are now in a position to derive the general condition for our singularity to be an ordinary cusp since if $C_x(i)$ and $C_y(i)$ denote the coefficients of the i^{th} term in the series expansions of the x and y coordinates of the MPL then, according to Porteous [20] (p.12), our condition is

$$\det \begin{pmatrix} C_x(2) & C_y(2) \\ C_x(3) & C_y(3) \end{pmatrix} \neq 0.$$

Substituting $c = \pm a$ from our earlier requirement on curvatures we obtain the condition $\pm 8(d^2 - b^2)/a^5 \neq 0$. So summarising the above we have:

Proposition 2.3.1 *The smooth closed curve*

$$\gamma(t) = (a \sin t + b\,(1 - \cos 2t), c\,(1 - \cos t) + d\,(1 - \cos 2t))$$

has singular MPL if $a = \pm c$ and the singular points will be ordinary cusps provided $b \neq \pm d$.

We will now choose particular values for a, b, c and d in order to see more clearly what is going on, say $a = 2$, $b = \frac{1}{2}$, $c = 2$ $(= a)$ and $d = -1$. Thus

$$X(t) = 2 \sin t + \frac{1}{2} - \frac{1}{2} \cos 2t, \quad Y(t) = 1 - 2 \cos t + \cos 2t.$$

This is the lung shaped curve in figure 2.4. Our expressions f and g become

$$f(t) = -\frac{1}{4} t^2 + \frac{1}{8} t^3 - \frac{1}{16} t^4 + \ldots, \quad g(s) = 4 - \frac{3}{4} s^2 - \frac{3}{8} s^3 - \frac{1}{4} s^4 + \ldots$$

We can now calculate the PSS as the zeros of equation (2.1). This is a function in s and t and if we solve $h(s,t) = 0$ in t as a function of s we obtain

$$t = s + \frac{3}{2} s^2 + \frac{3}{4} s^3 - 2\, s^4 - \frac{85}{16} s^5 + \ldots$$

All that remains is to map these points to the MPL using the map m to obtain

$$m(s) = \left(\frac{3}{4} s^2 + \frac{3}{8} s^3 - s^4 - \frac{85}{32} s^5 + \ldots,\ 2 - \frac{1}{2} s^2 - \frac{1}{2} s^3 - \frac{11}{32} s^4 + \frac{19}{32} s^5 + \ldots \right)$$

which clearly has an ordinary cusp when $s = 0$, corresponding to the point $(0, 2)$, since $m'(0) = (0,0)$, $m''(0) = (3/2, -1)$ and $m'''(0) = (9/4, -3)$. So $m''(0)$ and $m'''(0)$ are linearly independent. Figure 2.5 shows the entire MPL for γ with a cusp

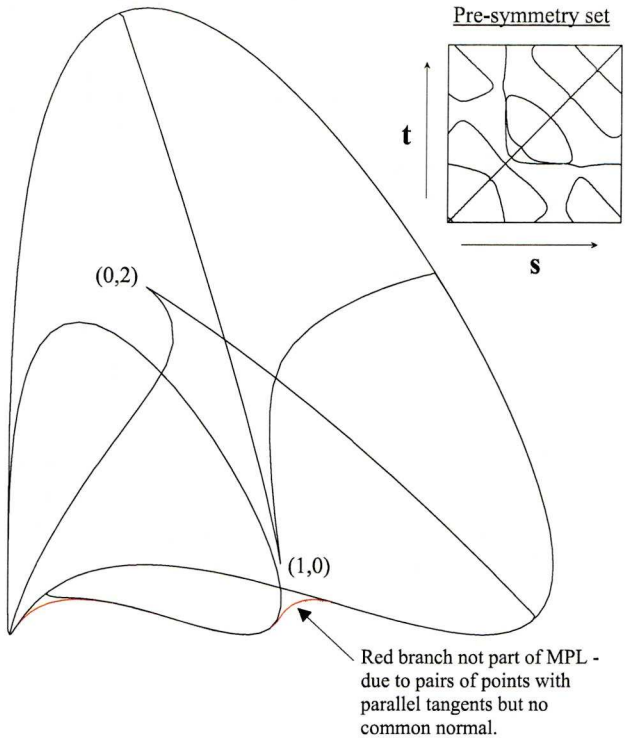

Figure 2.5: The curve γ with MPL overlaid. The arrowed red coloured branch (which terminates at inflexions on γ) is *not* part of the MPL.

clearly visible at the point $(0, 2)$. We also see a cusp at the point $(1, 0)$ which we might expect since $X'(\pi/2) = X'(3\pi/2) = 0$ and $\kappa(\pi/2) = 1$, $\kappa(3\pi/2) = 0$ so that $\kappa(\pi/2) + \kappa(3\pi/2) = 1 = 2/r$ since $r = 2$ here, and so the parallel tangent and curvature condition is satisfied here also. Figure 2.5 also shows a false branch which is the locus of midpoints of lines joining points on γ with parallel tangents but not necessarily a common normal. Clearly these pairs of points satisfy equation (2.2) but say something entirely different about the symmetry of γ. We will study these branches in more detail later in the chapter. Figures 2.6 and 2.7 show the result of perturbing γ by altering the value of c. We know by proposition 2.3.1 that for a non-smooth MPL we must have $c = \pm a$. Figure 2.6 shows that making c slightly smaller than a ($c = 1.8$) results in blunting of the points of the cusps, whilst figure 2.7 shows that making c slightly larger than a ($c = 2.2$) turns the cusps into tight loops. Note: Figures 2.4 to 2.7 where produced using the Linux based Liverpool Surface Modeling Package (LSMP) written by Richard J. Morris [16].

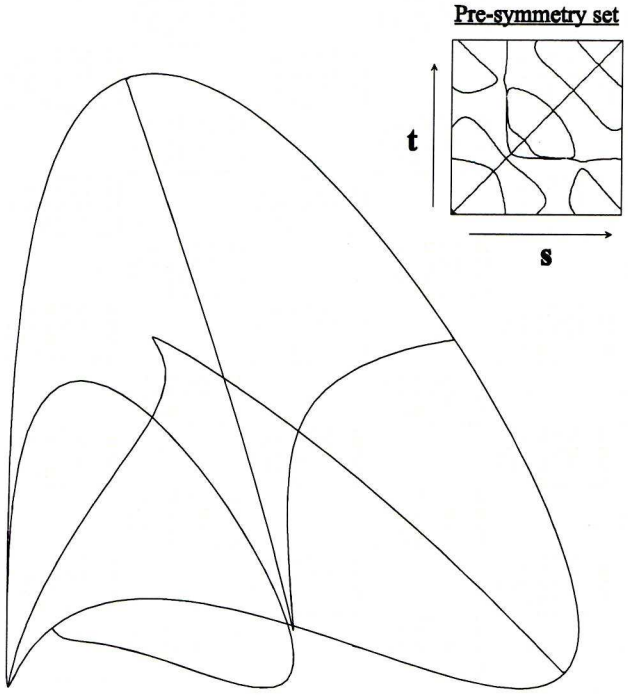

Figure 2.6: Effect of reducing c to 1.8. Notice the blunting of the cusps on the MPL.

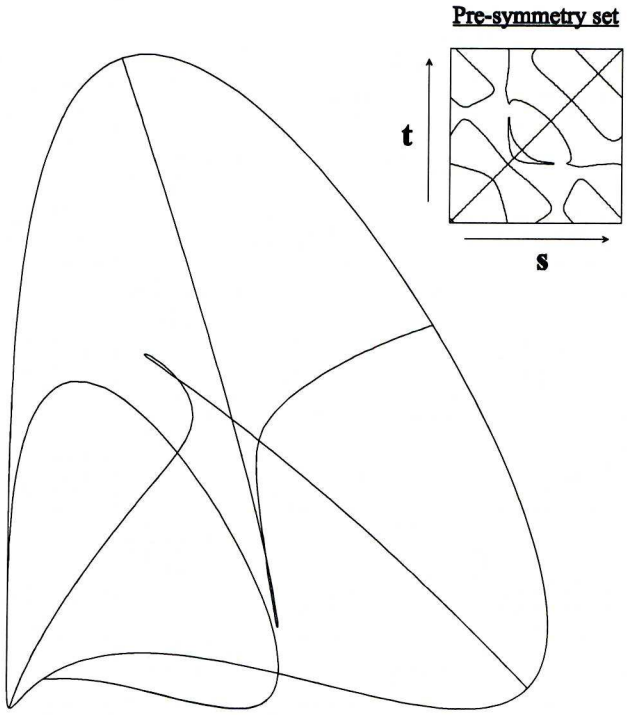

Figure 2.7: Effect of increasing c to 2.2. The cusps on the MPL are now tight loops.

General Common Normal Case

We now consider a general common normal situation where the two points of tangency need not even belong to the same curve. We choose axes so that one point is at the origin and the other lies at the point $(0, 2r)$ on the positive y–axis with tangents at both points being parallel to the x–axis. The curve piece passing through the origin we will call $\gamma_1(s) = (s, f_2s^2 + f_3s^3 + ...)$ and that passing through $(0, 2r)$ we will call $\gamma_2(t) = (-t, 2r + g_2t^2 - g_3t^3 + ...)$. Note: we parameterise γ_2 using $(-t)$ in order to render our bi-tangent circle coherent. The setup is thus

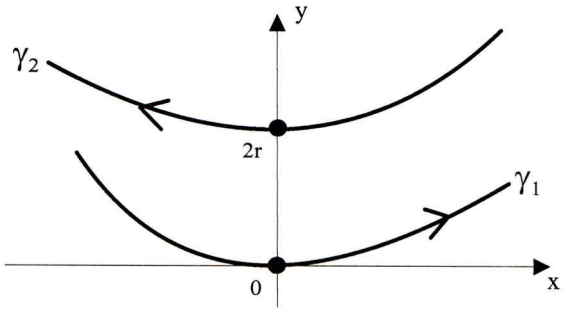

Let, $f(s) = f_2s^2+f_3s^3+f_4s^4+f_5s^5+...$ and $g(t) = 2r+g_2t^2-g_3t^3+g_4t^4-g_5t^5+...$ then the curvatures $\kappa_f(0)$ and $\kappa_g(0)$ at the points of tangency are $2f_2$ and $-2g_2$ respectively, so the condition for a non-smooth MPL is, $\kappa_f(0) + \kappa_g(0) = 2/r \Rightarrow g_2 = f_2 - 1/r$. We now solve $h(s, t) = 0$ for t as a function of s to obtain

$$t = s + \frac{3r(f_3 + g_3)}{2f_2r - 1}s^2 + ...$$

provided $f_2 \neq 1/(2r)$. We observe that the slope of the tangent to the PSS at $s = t = 0$ is $+1$. This is what we expect since by proposition 2.2.4 the unique condition for this to occur is indeed $\kappa_f + \kappa_g = 2/r$. We also note that the denominator in the coefficient of the s^2 term is non-zero provided the circle is not osculating at γ_1. We now apply the MPL map[5]

$$m : (s, t(s)) \mapsto \left(\frac{1}{2}(s - t(s)), \frac{1}{2}(f(s) + g(t(s)))\right)$$

to obtain

$$m(s) = \left(\frac{3r(f_3 + g_3)}{2(2f_2r - 1)}s^2 + ..., r + \frac{2f_2r - 1}{2r}s^2 + ...\right).$$

[5]Here we use $s - t(s)$ in the x-component as $(-t)$ is our parameter on γ_2.

Clearly $m'(0) = 0$ and the condition for the singular point to be an ordinary cusp is

$$(20f_2)\,r - (52f_2^2)\,r^2 + (64{f_2}^3 - 4g_4 + 4f_4)\,r^3 +$$

$$(-32{f_2}^4 + 27f_3g_3 + 21{f_3}^2 + 16f_2g_4 - 3{g_3}^2 - 16f_2f_4)\,r^4 +$$

$$(24f_2{g_3}^2 - 16g_4{f_2}^2 - 24{f_3}^2f_2 + 16f_4{f_2}^2)\,r^5 \neq 3.$$

2.4 Slope of the Mid-Point Locus at a Vertex

Looking at figure 2.5 we observe that the MPL terminates on γ at a number of points. If we imagine a bi-tangent circle in the lower right interior of γ we can see how, as the circles get smaller and approach the lower right extremity of γ, the points of tangency (2-point contact) get closer together until in the limit they coincide in a place of 4-point contact with γ, i.e. a vertex. So the MPL terminates on γ at points of maximum or minimum curvature. However, as figure 2.5 shows, the angle at which the MPL meets the curve varies considerably and here we consider this phenomenon.

We simplify the calculations by choosing axes so that γ passes through the origin at the vertex and also such that the x–axis is tangent to γ at this point. Since we are only interested in local effects we will express γ as a power series about the origin, say $\gamma(s) = (s, f(s))$ where $f(s) = a_2s^2 + a_3s^3 + a_4s^4 + a_5s^5 + \ldots$ Note: we have no constant or linear terms as a result of our choice of axes. Also, since we know that the origin is a vertex on γ we can also eliminate the cubic term since

$$\kappa = \frac{f''}{(1+(f')^2)^{\frac{3}{2}}} \Rightarrow \kappa' = \frac{-3f''(2f'f'')}{2(1+(f')^2)^{\frac{5}{2}}} + \frac{f'''}{(1+(f')^2)^{\frac{3}{2}}}.$$

Now $f'(0) = 0$ so $\kappa'(0) = 0 \Leftrightarrow f'''(0) = 6a_3 = 0 \Leftrightarrow a_3 = 0$. Thus we can write $f(s) = a_2s^2 + a_4s^4 + a_5s^5 + \ldots$ and use $g(t) = a_2t^2 + a_4t^4 + a_5t^5 + \ldots$ to describe the other point of tangency. Now we can calculate the PSS as the zeros of equation (2.1). This is a function in s and t and writing it as a power series we obtain

$$h(s,t) = 2a_2\,({a_2}^3 - a_4)s^5 - 6a_2\,({a_2}^3 - a_4)ts^4 + 4a_2\,({a_2}^3 - a_4)t^2s^3$$

$$+4a_2\,({a_2}^3 - a_4)t^3s^2 - 6t^4s + 2a_2\,({a_2}^3 - a_4)t^5 + \ldots$$

We now solve $h(s,t) = 0$ in t, eliminating the trivial solution $t = s$ by writing $t = -s + t_2 s^2 + t_3 s^3 + ...$, equating coefficients of $h(s, t(s))$ to zero and solving for the t_i to obtain

$$t = -s + \frac{a_5}{{a_2}^3 - a_4} s^2 - \frac{{a_5}^2}{{a_2}^3 - a_4} s^3 - \frac{1}{2({a_2}^3 - a_4)}(2a_5 a_2^8 - 3a_7 a_2^6 + 8a_4 a_5 a_2^5 - 6a_2^3 a_5 a_6$$

$$+6a_2^3 a_4 a_7 - 10a_4^2 a_5 a_2^2 + 6a_5 a_6 a_4 - 5a_5^3 - 3a_7 a_4^2) s^4 + ...$$

We can now determine the MPL using

$$m : (s, t(s)) \mapsto \left(\frac{1}{2}(s + t(s)),\ \frac{1}{2}(f(t(s)) + g(s)) \right)$$

which gives us the following

$$m(s) = \left(\frac{a_5}{2({a_2}^3 - a_4)} s^2 - \frac{{a_5}^2}{2({a_2}^3 - a_4)^2} s^3 + ...\ ,\ a_2 s^2 - \frac{a_2 a_5}{({a_2}^3 - a_4)} s^3 + ... \right).$$

Hence

$$\frac{dm}{ds} = \left(\frac{a_5}{({a_2}^3 - a_4)} s - \frac{3{a_5}^2}{2({a_2}^3 - a_4)^2} s^2 + ...\ ,\ 2a_2 s - \frac{3a_2 a_5}{({a_2}^3 - a_4)} s^2 + ... \right)$$

and thus we state:

Proposition 2.4.1 *Given a smooth curve* $\gamma(s) = (s\ ,\ a_2 s^2 + a_4 s^4 + a_5 s^5 + ...)$ *with an ordinary vertex at the origin and the* x*–axis tangent to the curve here, then the limiting tangent direction of the MPL as it meets* γ *at the vertex is*

$$\lim_{s \to 0} \{T_{MPL}\} = \left(a_5,\ 2a_2({a_2}^3 - a_4) \right).$$

Immediately we can make various observations, which are borne out by figure 2.5:

(i) If $a_5 = 0$ so that γ is highly symmetric about the y–axis, then the MPL approaches γ along the normal to γ at the point of contact. We see examples like this in the uppermost and rightmost vertices of figure 2.5.

(ii) If a_2 is small compared with a_5, so that γ has small curvature, then the MPL approaches γ almost along the tangent to γ at the point of contact. We see an example like this in the vertex on the left side of figure 2.5.

(iii) If a_2 is large compared with a_5, so that γ has large curvature and is highly symmetric about the y–axis, then the MPL approaches γ almost along the normal to γ at the point of contact. We see an example like this in the vertex in the bottom left of figure 2.5.

(iv) Finally, if we look at the expressions for h, t and m above we see the term ${a_2}^3 - a_4$ appearing over and over again. If we look at the distance squared function from a point on γ to the point $u = (0, 1/(2a_2))$, the centre of curvature to γ at the origin, we have

$$F(t) = \|\gamma(t) - u\|^2 = t^2 + \left(-\frac{1}{2a_2} + a_2 t^2 + a_4 t^4 + ...\right)^2 = \frac{1}{4{a_2}^2} + \frac{{a_2}^3 - a_4}{a_2} t^4 + ...$$

from which we see the significance of the ${a_2}^3 - a_4$ term. If this is zero we have a higher vertex at the origin and, if $a_5 \neq 0$, then the MPL approaches γ directly along the tangent to γ at the point of contact.

2.5 Parallel Tangents and the Mid-Point Locus

If we look at the bottom left part of figure 2.5 we observe what appears to be two branches of the MPL outside of γ in very close contact with one another. In fact of these branches the one which crosses γ then terminates at a vertex on γ is a true part of the MPL. The other branch, which meets γ at inflexions (the red branch), is not actually part of the MPL but is generated as the locus of midpoints of lines connecting points with parallel tangents but not necessarily a common normal on γ. This branch is actually part of a construction called the Mid-Parallel Tangents Locus (MPTL) and it says something quite different about the symmetry of γ. We will investigate its properties in more detail later in the chapter.

The interesting part as far as the MPL is concerned is that the two branches seem to display a very high degree of contact with one another, looking almost coincident over a large part of their respective lengths. We will investigate if there is a generic effect or of in fact it is just a quirk of our chosen example. Again we will simplify the geometry by choosing the x–axis to be bi-tangent to γ with one of the points of

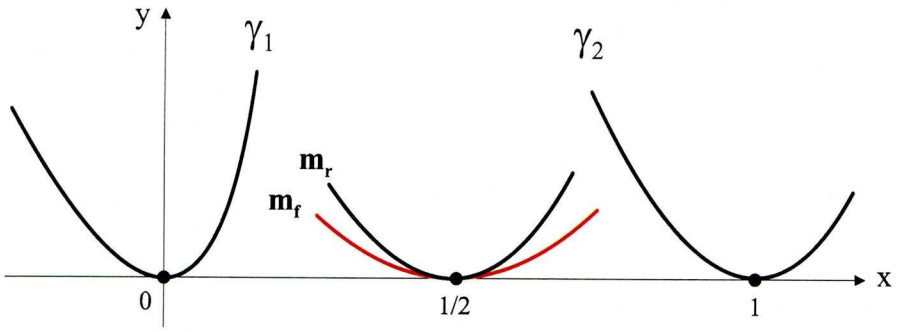

Figure 2.8: Geometrical setup for bi-tangent line case.

tangency at the origin and the other at the point $(1, 0)$. Hence we are interested in the degree of contact of the two branches at $(\frac{1}{2}, 0)$. We now let

$$\gamma_1(s) = (s,\ as^2 + bs^3 + cs^4 + ds^5 + ...)\ ,\ \gamma_2(t) = (t+1,\ a_1t^2 + b_1t^3 + c_1t^4 + d_1t^5 + ...)$$

represent pieces of γ in neighbourhoods of the two points of tangency with the line. Hence the geometrical setup is as shown in figure 2.8. We now calculate the PSS as the zeros of equation (2.1), i.e.

$$h(s,t) = ((s, f(s)) - (t+1, g(t))) \cdot (T_f(s) - T_g(t))$$

where $f(s) = as^2 + bs^3 + cs^4 + ds^5 + \ldots$, $g(t) = a_1t^2 + b_1t^3 + c_1t^4 + d_1t^5 + \ldots$ and $T_f(s)$ and $T_g(t)$ represent the respective unit tangents. This is a function in s and t and writing it as a power series we obtain

$$h(s,t) = (2a^2)\,s^2 - (2{a_1}^2)\,t^2 + (6ab)\,s^3 + (2a^2 - 2aa_1)\,ts^2 + (2{a_1}^2 - 2aa_1)\,t^2s - (6a_1b_1)\,t^3$$

$$+(8ac + 9b^2/2 - 6a^4 - ab)\,s^4 + (6ab - 2ba_1)\,ts^3 + (-3ba_1 - 3ab_1)\,t^2s^2$$

$$+(6a_1b_1 - 2ab_1)\,t^3s + (-8a_1c_1 - 9b_1^2/2 + 6{a_1}^4 - a_1b_1)\,t^4 + \ldots$$

Immediately we see that $h(s,t) = 0$ has two solution sets, one for each branch. Solving for t as a function of s we obtain

$$t_f = \frac{a}{a_1}s - \frac{3(b_1a^2 - b{a_1}^2)}{2{a_1}^3}s^2 - \frac{9b_1a{a_1}^2b - 4c{a_1}^4 - 9a^3{b_1}^2 + 4a^3c_1a_1}{2{a_1}^5}s^3 + \ldots,$$

$$t_r = -\frac{a}{a_1}s + \frac{2a^2a_1 - 3b_1a^2 - 3ba_1{}^2 - 2aa_1{}^2}{2a_1{}^3}s^2 - \frac{1}{2a_1{}^5}(6a^2b1a_1{}^2 - 4a^2a_1{}^3 + 2aa_1{}^4$$
$$-6aba_1{}^3 - 10a^3b_1a_1 + 9b_1aa_1{}^2b + 2ba_1{}^4 + 4ca_1{}^4 + 2a^3a_1{}^2 + 9a^3b_1{}^2 - 4a^3c_1a_1)s^3 + ...$$

as the domains of the false (f = false) and real (r = real) branches. We can now map these to the distinct branches using

$$m : (s, t(s)) \mapsto \left(\frac{1}{2}(s + t(s) + 1),\ \frac{1}{2}(f(t(s)) + g(s))\right).$$

If we express the results as graphs of functions, m_f and m_r say, about the point $(\frac{1}{2}, 0)$ we have

$$m_f(x) = \frac{2aa_1}{a + a_1}x^2 + \frac{4(a^3b_1 + ba_1{}^3)}{(a + a_1)^3}x^3 + \dots,$$

$$m_r(x) = \frac{2a\,(a_1 + a)\,a_1}{(a - a_1)^2}x^2 + \frac{4(4a^2a_1{}^3 + 5a^3b_1a_1 + 5aba_1{}^3 + a^4b_1 + ba_1{}^4 - 4a^3a_1{}^2)}{(a - a_1)^4}x^3 + \dots$$

So the two branches are clearly tangential (both have no constant or linear term) but is there higher degree contact? Equating the coefficients of the x^2 terms leads to either $a = 0$ or $a_1 = 0$ and setting a (or a_1) to zero in m_f and m_r leads to the same coefficient for x^3 in both cases, namely $4b$ (or $4b_1$), so the two branches have fourth (or higher) order contact. Of course, in general neither a nor a_1 are zero and the branches will merely be tangential.

Remark: Returning to the example of figure 2.5, if we move γ by 0.5 in the positive y direction then the x–axis will be tangential to γ when $t = \pm\pi/3$ and also at the point of contact of the two branches. If we now express the two pieces of γ in neighbourhoods of the points of tangency as power series then we can calculate the coefficients a and a_1 analogous to our setup above. These turn out to be $a = 6/(\sqrt{3} + 2)^2$ and $a_1 = 6/(\sqrt{3} - 2)^2$. If we now calculate the coefficients of x^2 in the expansions of m_f and m_r above we obtain

$$\frac{2aa_1}{a + a_1} = \frac{6}{7}\ ,\quad \frac{2a(a + a_1)a_1}{(a - a_1)^2} = \frac{7}{8}$$

or 0.857 compared to 0.875. So although the two branches are in fact only tangential they are extremely close, much as $y = x^2$ and $y = (1 + 10^{-10})x^2$ are only tangential at the origin but appear indistinguishable to the eye.

Singular Mid-Point Locus in Bi-Tangent Line Case

A bi-tangent line to γ can be regarded as a limiting case of a bi-tangent circle of infinite radius. However the condition for the MPL to be singular in this case is different and we now determine it. Following the argument set out after proposition 2.2.4 we know that the MPL fails to be smooth if we can find a non-zero vector $\mu = (u, v)$ such that $\tilde{M}\mu = \mathbf{0}$ where $\tilde{M}$ is the 3×2 matrix which is Dh on top of Dm (ignoring any non-zero row multipliers). For this case we will need an alternative form for the function $h(s,t)$ of equation (2.1) which is equivalent to the previous form but avoids the term $1 - T_1 \cdot T_2$ appearing in Dh (since this term is zero at the point of interest). Hence we use

$$h(s,t) = (\gamma_1 - \gamma_2) \cdot (N_1 + N_2)$$

whence

$$Dh = (\, T_1 \cdot N_2 - \kappa_1\lambda(1 + T_1 \cdot T_2) \,,\; -T_2 \cdot N_1 - \kappa_2\lambda(1 + T_1 \cdot T_2)\,)$$

where λ is the analogue of r in the bi-tangent circle case. At the point of bi-tangency with the line we have $T_1 \cdot N_2 = T_2 \cdot N_1 = 0$ and so $Dh = -2\lambda\,(\,\kappa_1, \kappa_2\,)$. As before $Dm = (\,T_1, T_2\,)/2$ and so we require

$$\tilde{M}\,\mu = \begin{pmatrix} \kappa_1 & \kappa_2 \\ T_1 & T_2 \end{pmatrix} \begin{pmatrix} u \\ v \end{pmatrix} = \mathbf{0}.$$

but $T_1 = T_2$ which implies $u = -v$ and we state:

Proposition 2.5.1 *Given a smooth curve γ with a line bi-tangent at γ_1 and γ_2 then the MPL is singular at the mid-point of the line γ_1 and γ_2 when $\kappa_1 = \kappa_2$.*

Referring to the geometry of figure 2.8 again with now $\kappa_f = \kappa_g$ at the points of tangency (i.e. $f_2 = g_2$ in the respective Taylor expansions) then the parameterisation of the MPL is

$$m(s) = \left(\frac{1}{2} - \frac{3(f_3 + g_3)}{4f_2}\, s^2 + \ldots \,,\; f_2 s^2 + \ldots \right)$$

which is clearly singular at $(\frac{1}{2}, 0)$. The condition for the singularity to be an ordinary cusp is given by

$$f_2 \neq \frac{3({f_3}^2 - {g_3}^2)}{2(f_3 + g_4 + g_3 - f_4)}.$$

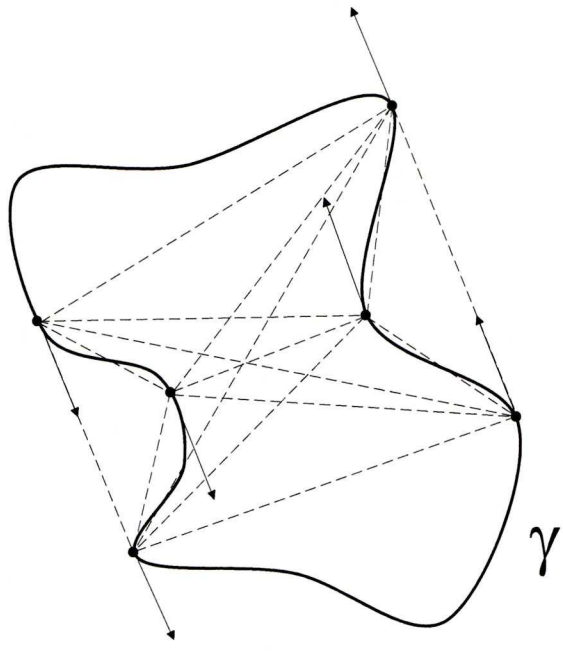

Figure 2.9: Construction of the MPTL.

2.6 The Mid-Parallel Tangents Locus

Although our principal area of interest in this chapter is the MPL it is appropriate to conclude this chapter by looking at the MPTL in a bit more detail and to construct the full locus for our example of figure 2.5. First a definition:

Definition 2.6.1 *Given a smooth closed curve γ, the MPTL is formed as the mid-points of lines joining* **any** *two points of γ with parallel tangents.*

It is clear that every point of γ will contribute to the MPTL and that some points will contribute more than once. If we pick a point on γ, draw the tangent line, and then drag an imaginary ruler parallel to this line across γ then we are guaranteed at least one other point on γ where the ruler touches. Figure 2.9 shows an example where six points each contribute five points to the MPTL, i.e. the midpoints of the dashed lines connecting each point with the other five. To determine the domain of the MPTL we need an expression whose zeros will pick out points with parallel tangents on γ. If $\gamma_1 = \gamma(s)$ and $\gamma_2 = \gamma(t)$ are any two points on γ with T_1, T_2 and N_1, N_2 their respective unit tangents and normals then consider

$$f(s,t) = T_1 \cdot N_2.$$

We have some trivial solutions (since $f = 0$ when $\gamma_1 = \gamma_2$) but all other solution pairs (s, t) designate distinct points on γ with parallel tangents. To find conditions for the MPTL to be singular we again use the argument set out after proposition 2.2.4, i.e. given $f^{-1}(0)$ is smooth, then the MPTL is smooth provided there is no non-zero vector $\mu = (u, v)$ such that $\tilde{M}\mu = \mathbf{0}$ where $\tilde{M}$ is the 3×2 matrix which is Df on top of Dm (ignoring non-zero row multipliers). Now

$$Df = (\, \kappa_1 N_1 \cdot N_2 \;,\; -\kappa_2 T_1 \cdot T_2 \,)$$

so $Df = (\, \pm\kappa_1, \mp\kappa_2 \,)$ when $f = 0$ (as $T_1 = \pm T_2$) and $Dm = (\, T_1 \;\; T_2 \,)/2$ so

$$\tilde{M}\,\mu = \begin{pmatrix} \pm\kappa_1 & \mp\kappa_2 \\ T_1 & T_2 \end{pmatrix} \begin{pmatrix} u \\ v \end{pmatrix} = \mathbf{0}.$$

Since $T_1 = \pm T_2$ when $f = 0$ then $u = \pm v$ and we state:

Proposition 2.6.2 *Given a smooth curve γ with parallel tangents at γ_1 and γ_2 then the MPTL is singular at the mid-point of the line joining these points if: (i) $\kappa_1 = -\kappa_2$ when $T_1 = T_2$, or (ii) $\kappa_1 = \kappa_2$ when $T_1 = -T_2$.*

We can use the above information to determine the slope of the tangent to the MPTL at a given point since the tangent to $m(f^{-1}(0))$ is the image under Dm of a non-zero kernel vector of Df. If (u, v) is such a vector then we know from the above that $v = \pm(\kappa_1/\kappa_2)\, u$. So (u, v) is parallel to $(\kappa_1, \pm\kappa_2)$ and since we have parallel tangents $Dm = (T_1 \,,\, \pm T_1)/2$. Hence

$$Dm \begin{pmatrix} u \\ v \end{pmatrix} = \lambda\,(T_1 \,,\, \pm T_1) \begin{pmatrix} \kappa_2 \\ \pm\kappa_1 \end{pmatrix} = \lambda\,(\kappa_2 \pm \kappa_1)\, T_1 \quad \text{for some } \lambda \in \mathbb{R}.$$

So the tangent to the MPTL is always parallel to T_1 (or T_2) and since any smooth curve is the envelope of its tangent lines we have the following:

Proposition 2.6.3 *On the MPTL of a smooth curve γ the tangent at any point is parallel to the pair of parallel tangents on γ which generated that point. Moreover the MPTL is the envelope of mid-lines parallel to pairs of parallel tangents on γ.*

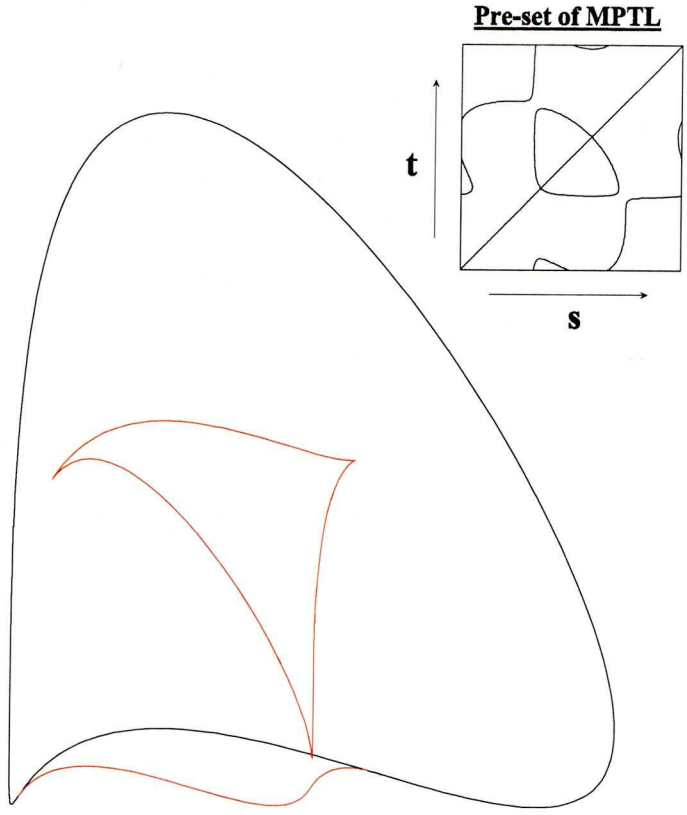

Figure 2.10: The full MPTL of the example of figure 2.5. The smaller figure is the graph of $f^{-1}(0)$, the preset of the MPTL.

Figure 2.10 shows the full MPTL for the example of figure 2.5. We see that it consists of two branches: the one outside of γ that we have already discussed, and a second closed branch, like a distorted triangle, which displays three singular points that look like ordinary cusps. Since parallelism is an affine invariant property we can use a simplified model to determine an ordinary cusp condition for the MPTL.

We will place one parallel tangent at the origin pointing along the positive x–axis and perform a shear transformation to place the other parallel tangent on the y–axis at $(0, 2k)$ and pointing in the direction of the positive or negative x–axis (depending as $T_1 = \pm T_2$). Hence we are left with a model very similar to that used in section 2.3 but with a different domain for our mid-point map, namely $f^{-1}(0)$, and a different singularity condition, namely that given by proposition 2.6.2.

The curve piece passing through the origin we will call $\gamma_1(s) = (s, f_2s^2 + f_3s^3 + ...)$ and that passing through $(0, 2k)$ we will call $\gamma_2(t) = (\varepsilon t, 2k + g_2t^2 + \varepsilon g_3t^3 + ...)$. So if $T_1 = T_2$ then $\varepsilon = 1$ whilst if $T_1 = -T_2$ then $\varepsilon = -1$.

Let, $f(s) = f_2s^2 + f_3s^3 + f_4s^4 + f_5s^5 + ...$ and $g(t) = 2k + g_2t^2 + \varepsilon g_3t^3 + g_4t^4 + \varepsilon g_5t^5 + ...$ then the curvatures κ_f and κ_g at the points of tangency are $2f_2$ and $2\varepsilon g_2$ respectively, so the condition for a non-smooth MPTL is, $g_2 = -f_2$ in either case. We now solve $f(s,t) = 0$ for t as a function of s to obtain

$$t = -\varepsilon\, s - \frac{3\varepsilon\,(-\varepsilon^2 g_3 + f_3)}{2f_2} s^2 + ...$$

We observe that the slope of the tangent to $f^{-1}(0)$ at $s = t = 0$ is ∓ 1 depending as $T_1 = \pm T_2$. We now apply the mid-point map to obtain the following parameterisation for the MPTL

$$MPTL(s) = \left(\frac{3(g_3 - f_3)}{4f_2}\, s^2 + ...\,,\; k + (g_3 - f_3)\, s^3 + ... \right).$$

Clearly $MPTL'(0) = 0$ and the condition for the singular point at $(0, k)$ to be an ordinary cusp is given by, $9(f_3 - g_3)^2 \neq 0$. So provided $f_3 \neq g_3$ then the singular point will be an ordinary cusp.

2.7 Chapter Summary

In this chapter we have investigated the local structure of a symmetry construction to plane curves called the Mid-Point Locus (MPL). It is formed as the midpoints of chords joining points on a smooth curve γ to which we can fit a bi-tangent circle. It has some appealing features that are not shared by more well documented symmetry constructions, e.g. it is generically a smooth curve and has end points actually at vertices on γ (rather than some distance away as with the symmetry set and medial axis). In proposition 2.2.5 we determined the (non-generic) condition for the MPL to be singular whilst in proposition 2.4.1 we found an expression for the limiting tangent direction to the MPL as it meets a vertex on γ.

We also considered the limiting case of bi-tangent lines to γ (which can be regarded as bi-tangent circles of infinite radius) and in proposition 2.5.1 determined the condition for the MPL to be singular in this case. Bi-tangent lines to γ also contribute points to another symmetry construction called the Mid-Parallel Tangents Locus (MPTL) which is formed as the mid-points of chords joining points on γ with parallel tangent lines. We investigated the relationship between the MPL and MPTL at shared points and showed that, in general, they are merely tangential. We also considered the MPTL in its own right, showing in proposition 2.6.3 that the tangent to the MPTL at any point is parallel to the pair of tangent lines on γ which generated that point. Also in proposition 2.6.2 we gave the condition for the MPTL to be singular.

Chapter 3

Reconstruction from the Mid-Point Locus

3.1 Introduction

In this chapter we consider the following important question: If we are given a parameterisation for the MPL, say $m(t) = (u(t), v(t))$, of a smooth curve $\gamma(t)$ what additional information do we need in order to reconstruct γ? We will look at two possible options: (i) The radius function r (i.e. for each point on m we know the radius of the bi-tangent circle which gave rise to that point) and (ii) The chord angle function ϕ (i.e. for each point on m we know the angle between the tangent to m and the chord of which m is the mid-point). First a definition:

Definition 3.1.1 *Given a smooth curve γ in $\mathbb{R}^2$ the Symmetry Set (SS) is the locus of centres of circles bi-tangent to γ. Thus, if $\gamma_1 = \gamma(s)$ and $\gamma_2 = \gamma(t)$ are two points of tangency with a circle then the corresponding point of the SS is*

$$c(s,t) = \gamma_1 + r\,N_1 \ (= \gamma_2 + r\,N_2)$$

where r is the radius of the bi-tangent circle.

If we are given the SS as a parameterised curve, say $c(s) = (x(s), y(s))$ and the radius function $r(s)$ (where s is arclength on c so that c is unit speed) then we can

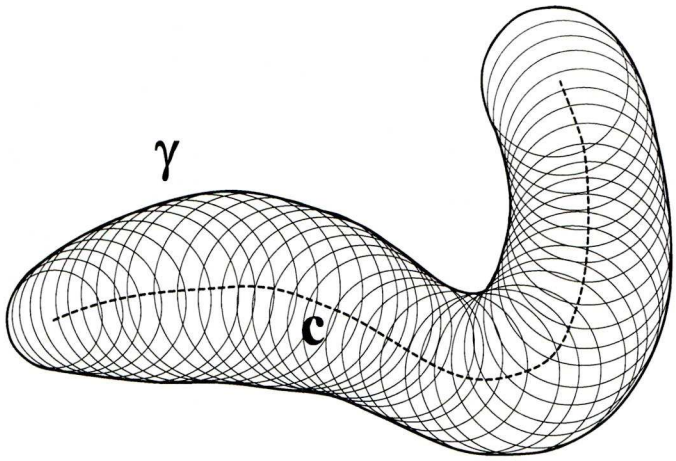

Figure 3.1: A smooth curve $\gamma(t)$ as the envelope of bi-tangent circles centred on a smooth curve $c(t)$ (shown dashed).

reconstruct γ as the envelope of the circles[1] (e.g. figure 3.1). If ω is a point on the circumference of a circle of radius r centred on c, then the family of such circles can be written as

$$F(s,\omega) = (c-\omega)\cdot(c-\omega) - r^2.$$

Hence we have

$$\frac{\partial F}{\partial s} = 2(c-\omega)\cdot T - 2r\frac{dr}{ds}$$

and

$$\mathcal{D}_F = \{\,\omega \in \mathbb{R}^2 : \exists s \in \mathbb{R} \text{ with } F = \partial F/\partial s = 0\,\}$$

is the envelope of the circles. If T and N are the unit tangent and normal to c then they are linearly independent and so can be used as a basis for $\mathbb{R}^2$. So writing $c-\omega = \lambda T + \mu N$ (where $\lambda,\mu \in \mathbb{R}$) and substituting into $\partial F/\partial s = 0$ we obtain, $2\lambda - 2r\,(dr/ds) = 0$ so that $\lambda = r\,(dr/ds)$. Substituting into $F = 0$ we obtain, $\lambda^2 + \mu^2 = r^2$ so that $\mu = r\sqrt{1-(dr/ds)^2}$ and so for each circle the two points of tangency are at

$$\gamma_i = c - \left(r\frac{dr}{ds}\right)T \pm \left(r\sqrt{1-\left(\frac{dr}{ds}\right)^2}\right)N \quad (i=1,2). \tag{3.1}$$

[1]Provided $|dr/ds| \leq 1$. In a physical sense, if the circles are growing (or shrinking) in size at a faster rate than we are moving along $c(t)$ then a real envelope cannot form. We can express the requirement as, $r'(t)^2 \leq x'(t)^2 + y'(t)^2$. See 'Curves and Singularities' [6] Ch.5 for more detail on reconstruction from the SS.

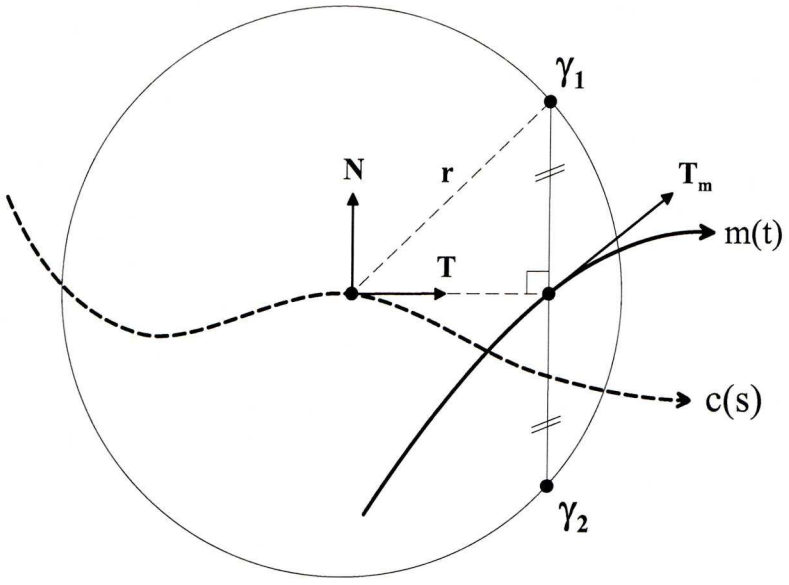

Figure 3.2: Geometrical relation between the symmetry set and the MPL.

3.2 Reconstructing γ from m and r

Unfortunately we cannot directly reconstruct γ from m and r using the above method since although we know the radius of the circle generating each point of m we do not have sufficient information to place its centre. We can however use equation (3.1) to derive a relationship between c and m. If we can reconstruct c from m and r then we will be able to reconstruct γ from c and r using the envelope method. As figure 3.2 shows, m is the mid-point of the line joining the two points of tangency, γ_1 and γ_2, and the line perpendicular to this through m is tangent to c. Using equation (3.1) we have

$$m = c - \left(r \frac{dr}{ds} \right) T \tag{3.2}$$

where s is arclength on c. If we now write everything in terms of some general parameter t (i.e. not necessarily arclength) then

$$m(t) = c(t) - r(t) \left(\frac{dr}{dt}\frac{dt}{ds} \right) \left(\frac{dc}{dt}\frac{dt}{ds} \right) = c(t) - r(t)r'(t)\frac{c'(t)}{s'(t)^2}$$

where $' \equiv d/dt$. Also since $c(s)$ is unit speed we have

$$\left(\frac{dc}{dt}\frac{dt}{ds} \right) \cdot \left(\frac{dc}{dt}\frac{dt}{ds} \right) = 1 \quad \Rightarrow \quad c'(t) \cdot c'(t) = s'(t)^2.$$

If we now let $R(t) = r(t) \cdot r'(t)$ then

$$m(t) = c(t) - \left(\frac{R(t)}{c'(t) \cdot c'(t)} \right) c'(t).$$

This represents a pair of simultaneous ODE's for which m and R are known and we seek to find c. If we write this as $(c - m)\, c' \cdot c' = R\, c'$ then we can eliminate the non-linear terms by dotting both sides in turn with the linearly independent vectors, $\| c' \| T = (x', y')$ and $\| c' \| N = (-y', x')$, to give the following pair of simultaneous ODE's

$$(x - u, y - v) \cdot (x', y') = R \text{ and } (x - u, y - v) \cdot (-y', x') = 0$$

where $m(t) = (u(t), v(t))$. If we write these in matrix form we obtain

$$\begin{pmatrix} y - v & -x + u \\ x - u & y - v \end{pmatrix} \begin{pmatrix} x' \\ y' \end{pmatrix} = \begin{pmatrix} 0 \\ R \end{pmatrix}$$

and inverting the 2×2 matrix we obtain

$$\begin{pmatrix} x' \\ y' \end{pmatrix} = \frac{1}{(x - u)^2 + (y - v)^2} \begin{pmatrix} y - v & x - u \\ -x + u & y - v \end{pmatrix} \begin{pmatrix} 0 \\ R \end{pmatrix}$$

which holds provided $(x - u)^2 + (y - v)^2 \neq 0$, i.e. provided $c \neq m$. If we now let $X = x - u$ and $Y = y - v$ then

$$\begin{pmatrix} X' + u' \\ Y' + v' \end{pmatrix} = \frac{1}{X^2 + Y^2} \begin{pmatrix} Y & X \\ -X & Y \end{pmatrix} \begin{pmatrix} 0 \\ R \end{pmatrix}$$

whence

$$X' = \frac{RX}{X^2 + Y^2} - u' \quad \text{and} \quad Y' = \frac{RY}{X^2 + Y^2} - v'.$$

With the equations in this form a method of numerical solution becomes apparent since if we are given a boundary condition, say $X(0) = a, Y(0) = b$, then we can calculate the slope to the solution curve at $(0, 0)$ as

$$(X'(0), Y'(0)) = \left(\frac{a\, R(0)}{a^2 + b^2} - u'(0) \, , \, \frac{b\, R(0)}{a^2 + b^2} - v'(0) \right).$$

If we now increment t by an infinitesimal amount δt, move to a new position

$$(X(0) + \delta t X'(0), Y(0) + \delta t Y'(0))$$

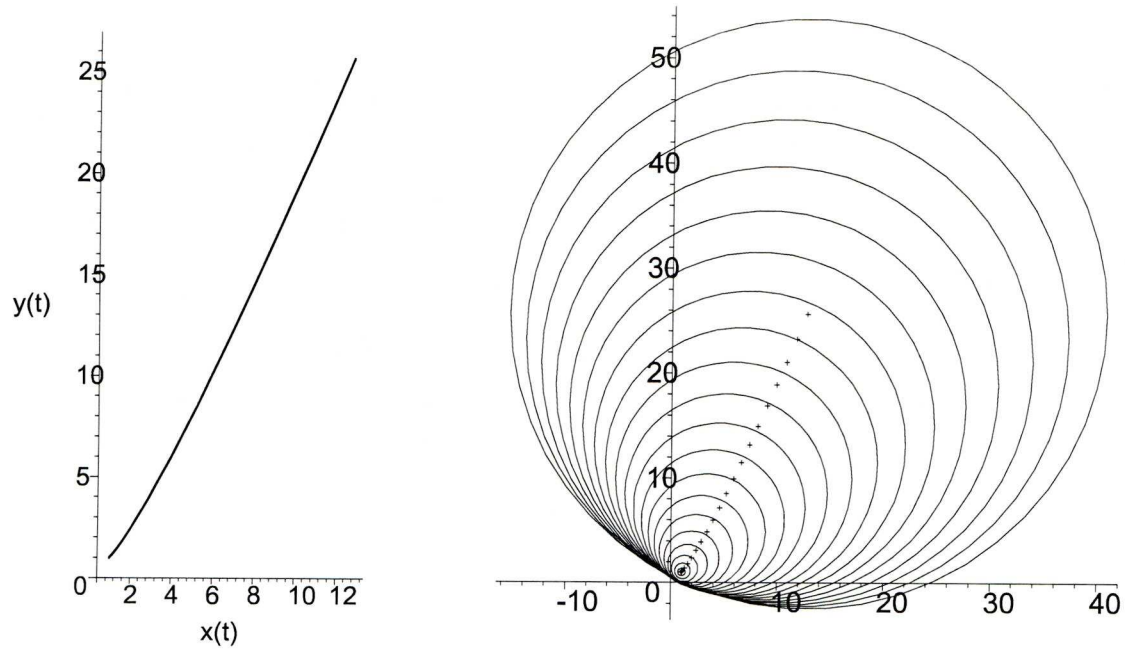

Figure 3.3: A solution curve and bi-tangent circle envelope in the m and r case with $m(t) = (t, 0)$ and $r(t) = 0.1 + 2t + 6t^2$.

and repeat the process we can form a unique solution curve. Note: existence and uniqueness are assured, provided we keep away from points where $X = Y = 0$ (i.e. crossing points of m and c), as the Lipschitz condition for a system of linear first order equations is satisfied (see Ince [12] section 3.3). Importantly, there is nothing to restrict us on our choice of boundary condition so given m and r we obtain a two parameter family of corresponding symmetry sets, although not all of these will enable us to form an envelope and thus reconstruct γ. We now summarise the above findings in:

Proposition 3.2.1 *Given the MPL, m, of a smooth curve γ and a smooth function r describing the radius of the circle generating each point of m, then we can reconstruct the unique symmetry set c of γ provided we know at least one point on c. Moreover, whenever $\mid dr/ds \mid \leq 1$ on c, where s is arclength on c, then γ can be locally reconstructed as the envelope of bi-tangent circles centred on c. Without a given point on c we are left with a 2-parameter family of symmetry sets corresponding to m not all of which will yield a real envelope.*

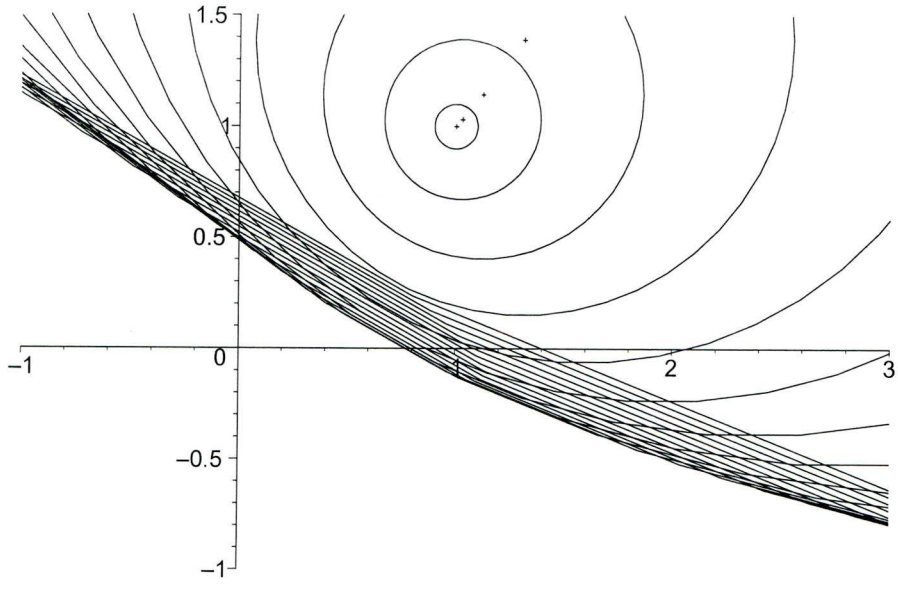

Figure 3.4: Detail of envelope formation for m and r case with $m(t) = (t, 0)$ and $r(t) = 0.1 + 2t + 6t^2$.

Example 3.2.2 We will choose the MPL to be a line segment, say $m(t) = (t, 0)$ where $t \in [0, 2]$ and $r(t) = 0.1 + 2t + 6t^2$. Thus $u(t) = t$, $v(t) = 0$ and $R(t) = (0.1 + 2t + 6t^2)(2 + 12t)$. Hence we must solve

$$x'(t) = \frac{(1+6t)(1+20t+60t^2)(x(t)-t)}{5(x(t)^2 - 2tx(t) + t^2 + y(t)^2)}, \quad y'(t) = \frac{(1+6t)(1+20t+60t^2)y(t)}{5(x(t)^2 - 2tx(t) + t^2 + y(t)^2)}.$$

If we take as a boundary condition $x(0) = y(0) = 1$ then the solution curve, $c(t)$, is shown in the left half of figure 3.3. On the right half of this figure we draw a number of the bi-tangent circles centred on $c(t)$ and see an envelope forming in the lower left portion of the figure. A detail of this region is shown in figure 3.4.

3.3 Reconstructing γ from m and ϕ

Here we exploit the fact that the line perpendicular to the chord generating each point of m, is always tangent to c. If we form the envelope of these lines we should be able to reconstruct c and moreover we will be able to retrieve the radius function as part of the process. Let $m(t) = (u(t), v(t))$, $\phi(t)$ be the angle between the normal to $m(t)$ and the chord at each point (measured anti-clockwise) and $p = (x, y)$ be a general point on the line through $m(t)$ perpendicular to the chord, i.e.

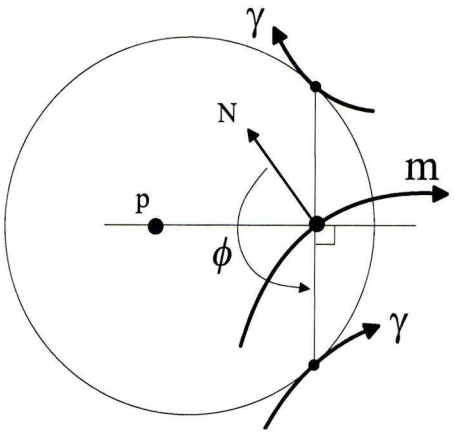

Now $\|m'\|N = (-v', u')$ and rotating this vector ϕ radians anti-clockwise gives

$$(x-u,\, y-v)\cdot((\cos\phi)u' - (\sin\phi)v',\, (\sin\phi)u' + (\cos\phi)v') = 0$$

leading to a family of lines

$$F(t,p) = (x-u)((\cos\phi)u' - (\sin\phi)v') + (y-v)((\sin\phi)u' + (\cos\phi)v') = 0. \quad (3.3)$$

If we now solve $F = \partial F/\partial t = 0$ for x and y we obtain $c(t) = (x(t), y(t))$ as an envelope of this family of lines. We know from equation (3.2) that for each point on m we have

$$r\frac{dr}{ds} = -\sqrt{(x(t)-u(t))^2 + (y(t)-v(t))^2} \quad \left(= r\frac{dr}{dt} \Big/ \frac{ds}{dt}\right).$$

Now

$$\frac{ds}{dt} = \sqrt{\frac{dx}{dt}^2 + \frac{dy}{dt}^2} \quad \text{and} \quad r\frac{dr}{dt} = \frac{d}{dt}\left(\frac{r^2}{2}\right)$$

So

$$r(t)^2 = -2\int_0^t \sqrt{\{x'(t)^2 + y'(t)^2\}\,\{(x(t)-u(t))^2 + (y(t)-v(t))^2\}}\,dt \;+\; C. \quad (3.4)$$

We can choose C so that the RHS here is non-negative throughout the range of values for t but we are still faced with a choice over the sign of the square root in the integrand. Clearly though, only one of the options will allow us to get back to m given x, y and r. From equation (3.2) we have

$$m = c - \left(r\frac{dr}{dt}\right)\left(\frac{ds}{dt}\right)^{-1} T$$

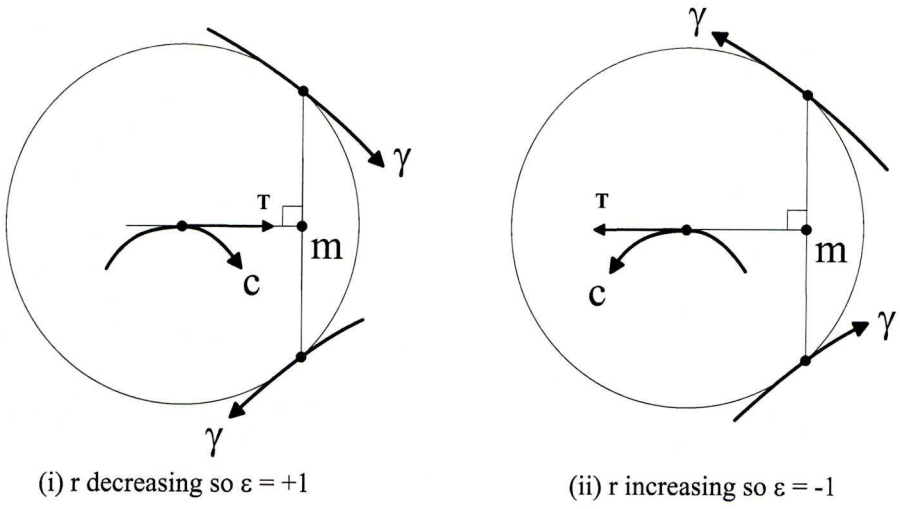

Figure 3.5: Determining the sign of ε.

and from equation (3.4)

$$r\frac{dr}{dt} = \frac{1}{2}\frac{d}{dt}(r^2) = -\varepsilon\left(\frac{ds}{dt}\right) \parallel m - c \parallel$$

where

$$\varepsilon = \begin{cases} +1 \text{ for } +\text{ve square root,} \\ -1 \text{ for -ve square root.} \end{cases}$$

Thus

$$m = c + \varepsilon\, ||m - c||\, T.$$

Now when r is decreasing, T points towards the corresponding point on m so that $\varepsilon = 1$ (and vice-versa) as shown in figure 3.5. The radius function need not be monotone over the range of t so ε can change sign, but with this in mind we now have (at least in principle) the SS and radius function, and so can reconstruct γ as the envelope of bi-tangent circles. Of course in the real world equation (3.4) will most often only be solvable numerically and we will be left with a table of values for r versus t. Note: we choose C so that the RHS of equation (3.4) is always non-negative but we still have infinitely many choices so given m and ϕ we obtain a one parameter family of corresponding symmetry sets. This is in some sense an improvement on the m and r case as we only have one degree of freedom. Summarising we have:

Proposition 3.3.1 *Given the MPL, m, of a smooth curve γ and a smooth function ϕ describing the angle between the chord generating each point of m and the normal to m (measured anti-clockwise), then we can reconstruct the unique symmetry set c of γ provided we know the radius of at least one bi-tangent circle generating a point on m. Moreover, wherever the envelope existence criterion is met then γ can be locally reconstructed as the envelope of bi-tangent circles centred on c. Without a given radius for a point on m we are left with a 1-parameter family of symmetry sets corresponding to m not all of which will yield a real envelope.*

Example 3.3.2 Again we will choose the MPL to be a line segment, say $m(t) = (t, 0)$ where $t \in [0, 1]$ and $\phi(t) = \pi t$. Thus $u(t) = t$, $v(t) = 0$ and $\phi'(t) = \pi$. Solving the envelope equations $F = \partial F/\partial t = 0$ gives us the following for the SS

$$c(t) = \left(\frac{\pi\, t\, (\tan(\pi\, t))^2 + \pi\, t - \tan(\pi\, t)}{\pi\, \left((\tan(\pi\, t))^2 + 1\right)}, \frac{1}{\pi\, \left((\tan(\pi\, t))^2 + 1\right)} \right)$$

In this case we can actually solve the integral equation explicitly and if we take $C = 1.5$ we obtain

$$r(t) = \sqrt{1.5 + \frac{\cos(2\,\pi\, t)}{\pi^2}}.$$

Although r is decreasing for $t \in [0, 0.5)$ and increasing for $t \in (0.5, 1]$ the integrand of equation (3.4) conveniently changes sign at the crossover point to give us the correct ε throughout. Figure 3.6 shows m (the straight line segment from 0 to 1), c (the U-shaped curve touching m at $(0.5, 0)$) and twenty bi-tangent circles of appropriate radius centred on c. The envelope of these circles (i.e. γ) is shown in pieces (one each in the upper and lower half planes). The figure also shows the chords appropriate to each circle crossing m at the mid-point of each.

Example 3.3.3 This time we will have a non-straight MPL and keep ϕ constant. So we choose the MPL to be an ellipse, say $m(t) = (2\cos(t), \sin(t))$ where $t \in [0, 2\pi]$ and $\phi(t) = \Phi$, a constant angle between 0 and 2π. Thus $u(t) = 2\cos(t)$, $v(t) = \sin(t)$ and $\phi'(t) = 0$. Solving the envelope equations $F = \partial F/\partial t = 0$ gives us the following for the components of $c = (x, y)$

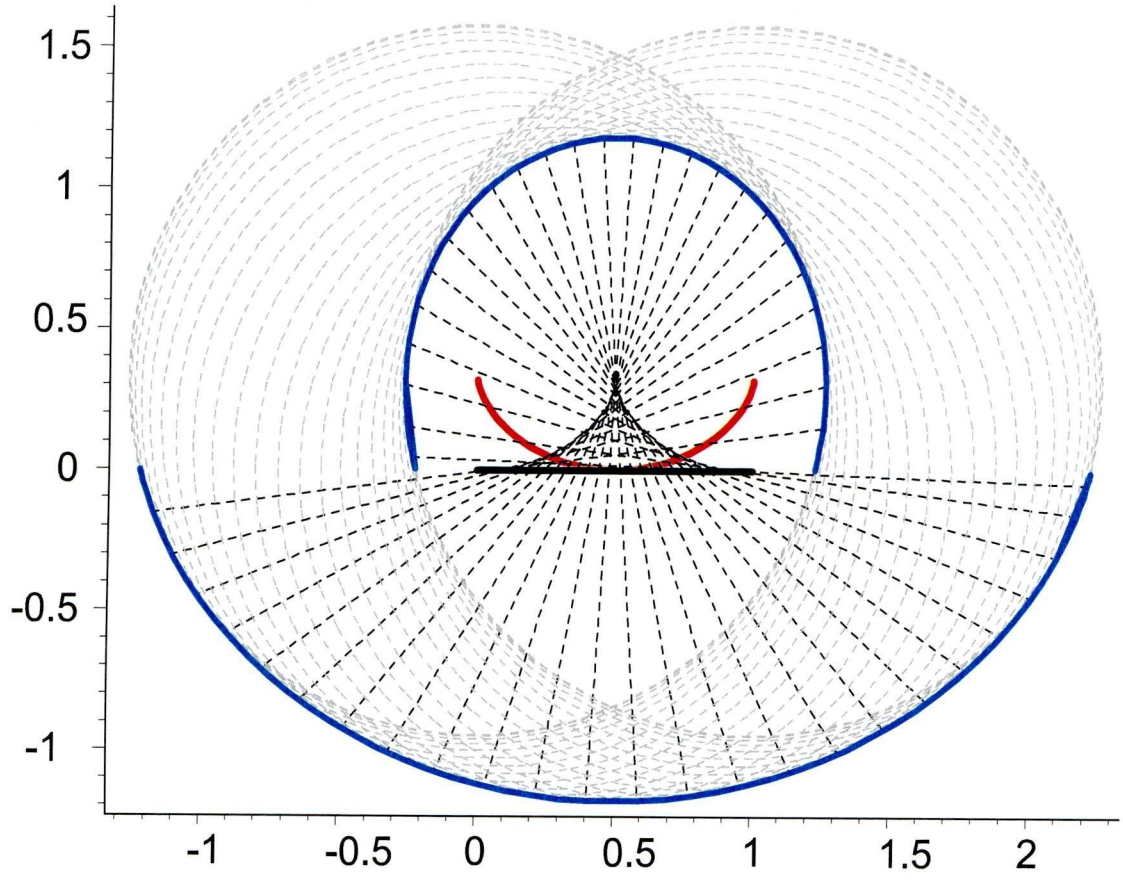

Figure 3.6: Formation of γ given $m(t) = (t, 0)$ (line segment from $(0, 0)$ to $(1, 0)$) and $\phi(t) = \pi t$. The symmetry set, c, is marked in red whilst the blue curve pieces (the envelope of circles) represent γ.

$$x(t) = \frac{3}{2}\left(\cos\left(\Phi\right)\right)^2\left(\cos\left(t\right)\right)^3 - 3\,\cos\left(\Phi\right)\left(\cos\left(t\right)\right)^2\sin\left(\Phi\right)\sin\left(t\right)$$
$$-\,2\,\cos\left(t\right)\left(\cos\left(\Phi\right)\right)^2 + \,2\,\cos\left(t\right) + 4\,\cos\left(\Phi\right)\sin\left(\Phi\right)\sin\left(t\right)\,,$$

and

$$y(t) = -4\,\sin\left(t\right)\left(\cos\left(\Phi\right)\right)^2 + 3\,\sin\left(t\right)\left(\cos\left(\Phi\right)\right)^2\left(\cos\left(t\right)\right)^2$$
$$-\,2\,\sin\left(\Phi\right)\cos\left(t\right)\cos\left(\Phi\right) + \frac{3}{2}\,\sin\left(\Phi\right)\left(\cos\left(t\right)\right)^3\cos\left(\Phi\right) + \sin\left(t\right).$$

If we take $\Phi = 0$ then c is the envelope of normals to m (i.e. the evolute of m)

$$c(t) = \left(\frac{3}{2}(\cos(t))^3,\ -3\,\sin\left(t\right) + 3\,\sin\left(t\right)\left(\cos\left(t\right)\right)^2\right).$$

Again the integral equation is explicitly solvable and taking $C = 15$ we obtain

$$r(t) = \frac{1}{2}\sqrt{60 + 9\,\left(3\,\left(\cos\left(t\right)\right)^4 - 9\,\left(\cos\left(t\right)\right)^2 + 7\right)\left(\sin\left(t\right)\right)^2}.$$

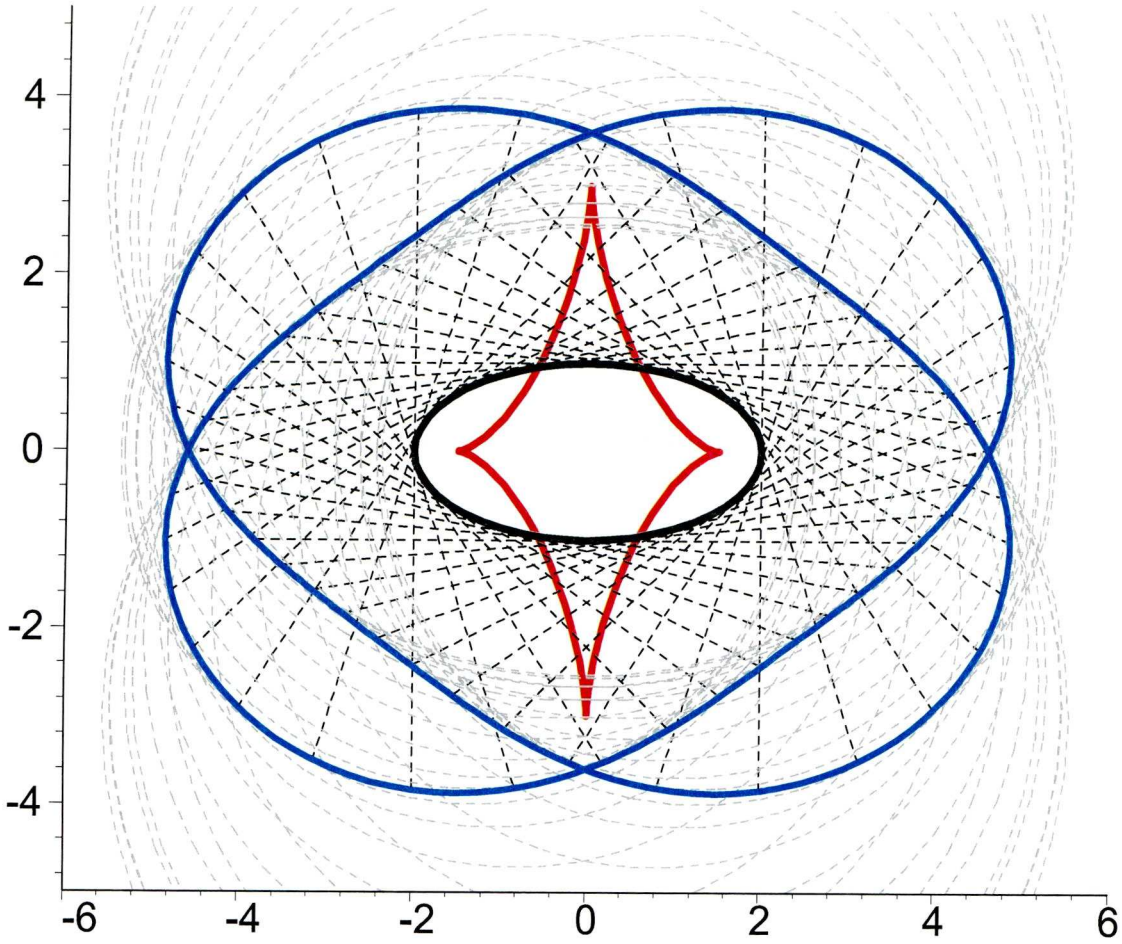

Figure 3.7: Formation of γ given $m(t) = (2\cos t, \sin t)$ (the central ellipse) and $\phi(t) = 0$. The symmetry set, c, is marked in red whilst the blue curves (the envelope of circles) represent γ.

In this example r is increasing for $t \in (0, \pi/2) \cup (\pi, 3\pi/2)$ and decreasing for $t \in (\pi/2, \pi) \cup (3\pi/2, 2\pi)$. However the integrand of equation (3.4) changes sign at the transition points to give us the correct ε throughout. Figure 3.7 shows m (the ellipse), c (the curved four point star) and twenty bi-tangent circles of appropriate radius centred on c. The envelope of these circles (i.e. γ) is shown as two intersecting flattened ovals. The figure also shows the chords appropriate to each circle, the mid-point of each touching m so that m is actually the envelope of the chords.

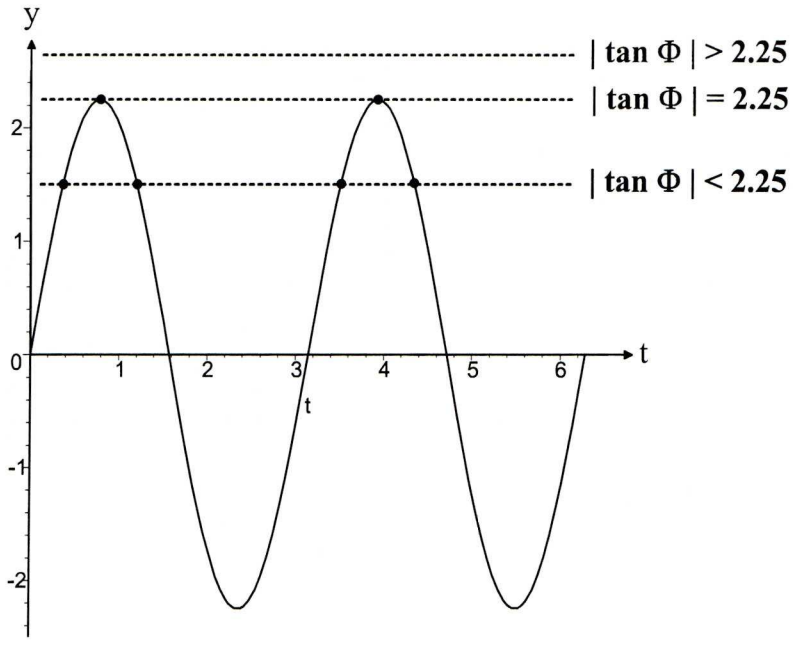

Figure 3.8: The graph of $y = \frac{9}{2}\cos(t)\sin(t)$ showing the relationship between number of singular points on c and the angle Φ in Example 3.3.3.

We can extend this example by asking: what is the relationship between Φ and the existence of singular points on c? With $\Phi = 0$ then c is the evolute of m and we have four singular points on m where $t = 0$, π and $\pm\pi/2$. Solving $x'(t) = y'(t) = 0$ for Φ in the general expressions for x and y above gives

$$\tan(\Phi) = \frac{9}{2}\cos(t)\sin(t)$$

but the maximum magnitude of the RHS here is 2.25 (when $t = n\pi/4$ where n is an odd integer) so as figure 3.8 shows, when $|\tan(\Phi)| > 2.25$ there are no real solutions and c is smooth. When $|\tan(\Phi)| < 2.25$ there are four real solutions and c has four singular points, and when $|\tan(\Phi)| = 2.25$ the solutions coincide in pairs to give two degenerate singular points on c. Figure 3.7 shows that with $\Phi = 0$ the solutions are equispaced along the t–axis at $t = 0$, $\pi/2$, π and $3\pi/2$.

3.4 Fixed Angle Envelopes

We conclude this chapter with a general discussion of the fixed angle envelopes introduced in example 3.3.3 above. We seek to find a relationship between the constant Φ and the existence of singular points on the resulting envelope for a general smooth curve $\gamma(t) = (u(t), v(t))$ and also determine the condition for any singular points that do arise to be ordinary cusps.

We start by simplifying our geometry by translating the point of interest on γ to the origin and rotating in the plane so that, locally, γ lies in the upper half plane and is tangent to the t–axis at the origin. Hence, close to the origin we can write

$$\gamma(t) = (t, a_2t^2 + a_3t^3 + a_4t^4 + \dots).$$

Solving $F = \partial F/\partial t = 0$, where F is the family of lines given by equation (3.3) and $\phi = \Phi$ (a constant) we obtain the fixed angle envelope, $\Psi(t) = (x(t), y(t))$, of γ. Extracting the coefficients of the linear terms of x and y we have

$$C_x(1) = \frac{\tan\Phi\,(3a_3 + 2a_2^2\tan\Phi)}{2a_2^2\left((\tan\Phi)^2 + 1\right)}\ ,\ C_y(1) = \frac{-3a_3 - 2a_2^2\tan\Phi}{2a_2^2\left((\tan\Phi)^2 + 1\right)} \tag{3.5}$$

with $C_{x,y}(i)$ denoting the coefficient of t^i in the Taylor expansion of x (or y) about $t = 0$. Thus $x'(0) = y'(0) = 0$ when $3a_3 + 2a_2^2\tan\Phi = 0$. When $\tan\Phi = 0$ (i.e. $\Phi = n\pi$ where $n \in \mathbb{Z}$) then $x'(0) = 0$ and $y'(0) = 0$ also when $a_3 = 0$. When $\Psi'(0) = 0$ the condition for the singular point to be an ordinary cusp is that $\Psi''(0)$ and $\Psi'''(0)$ are linearly independent, which is equivalent to

$$C_x(2)\,C_y(3) - C_x(3)\,C_y(2) = \frac{12\,(2\,{a_2}^4 - 2\,a_2\,a_4 + 3\,{a_3}^2)^2}{a_2\,(4\,{a_2}^4 + 9\,{a_3}^2)} \neq 0. \tag{3.6}$$

Finally, if the singularity is degenerate then it will be exactly A_3 (i.e. $F = F' = F'' = F''' = 0$ but $F^{(4)} \neq 0$) when

$$a_5 \neq \frac{a_3\,(38\,{a_2}^4 + 27\,{a_3}^2)}{10\,{a_2}^2}. \tag{3.7}$$

If we now calculate the curvature κ of γ and its first three derivatives at $t = 0$ we obtain $\kappa(0) = 2a_2$, $\kappa'(0) = 6a_3$, $\kappa''(0) = 24(a_4 - a_2^3)$ and $\kappa'''(0) = 120\,a_5 - 456\,a_3\,a_2^3$. We can now express the above results in terms of κ and its derivatives and state:

Proposition 3.4.1 *Let γ be a smooth curve in the plane and F be the family of lines that at each point p of γ makes a constant angle Φ to the normal to γ at p, then the curve Ψ formed as the envelope of this family is smooth at the point corresponding to p on γ provided*

$$\kappa_p{}^2 \tan\Phi + \kappa_p' \neq 0 \tag{3.8}$$

where κ_p is the curvature of γ at p and derivatives are with respect to arclength on γ. For points p where equation (3.8) fails to hold then the singular point on Ψ will be an ordinary cusp provided

$$2\,\kappa_p'{}^2 - \kappa_p\,\kappa_p'' \neq 0. \tag{3.9}$$

If equations (3.8) and (3.9) both fail to hold then the singular point will be exactly A_3 provided

$$\kappa_p{}^2\kappa_p''' - 6\kappa_p'{}^3 \neq 0. \tag{3.10}$$

** In the special case $\Phi = 0$ then Ψ is smooth at the point corresponding to p on γ provided $\kappa_p' \neq 0$, i.e. p is not a vertex on γ.*

Remark: Looking back to example 3.3.3 we see that the last part of proposition 3.4.1 is verified since c displays singular points precisely at values of t giving vertices on m. Note: In many of the expressions above we see a_2 appearing as a factor in the denominator, hence we must have $a_2 \neq 0$. If $a_2 = 0$ then γ has an inflexion at the origin and the corresponding point on ε goes to infinity for all Φ.

A General Expression for Ψ

We can underline this point regarding inflexions on γ by finding a general expression for the fixed angle envelope Ψ. Let p be a point on γ (parameterised by arclength s) and x be a general point on the line through p at an angle Φ to N (the normal to γ at p) as shown in figure 3.9. Note: here $\Phi = \phi - \pi/2$ where ϕ is the angle used in example 3.3.3. Hence we have

$$(x - \gamma) \cdot N = ||x - \gamma|| \cos\Phi.$$

Since N and T (the tangent to γ at p) are linearly dependent they can be used as a

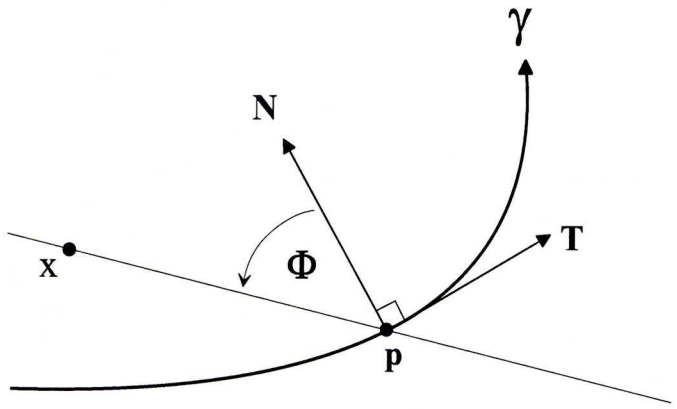

Figure 3.9: Construction of the fixed angle envelope Ψ.

basis for $\mathbb{R}^2$ and we can write, $x - \gamma = \lambda T + \mu N$, where λ, $\mu \in \mathbb{R}$. Hence

$$\lambda = (x-\gamma)\cdot T = -\sin\Phi\,||x-\gamma|| \quad \text{and} \quad \mu = (x-\gamma)\cdot N = \cos\Phi\,||x-\gamma||.$$

Multiplying the first expression by $\cos\Phi$ and the second by $\sin\Phi$ and adding we obtain

$$\lambda\cos\Phi + \mu\sin\Phi = 0, \tag{3.11}$$

and

$$F = (x-\gamma)\cdot(T\cos\Phi + N\sin\Phi) = 0.$$

Now, F can be regarded as the family of lines through γ at an angle Φ to the normal to γ at each point and differentiating with respect to s we obtain

$$\frac{\partial F}{\partial s} = (\mu\kappa - 1)\cos\Phi - \lambda\kappa\sin\Phi = 0. \tag{3.12}$$

Now solving $F = \partial F/\partial s = 0$, which is equivalent to solving equations (3.11) and (3.12) for λ and μ, we obtain $\lambda = (\sin\Phi\cos\Phi)/\kappa$ and $\mu = (\cos^2\Phi)/\kappa$. Hence we state:

Proposition 3.4.2 *Let γ be a smooth curve and Ψ be the envelope of lines at a fixed angle Φ to the normal to γ at each point, then*

$$\Psi = \gamma + \left(\frac{\sin\Phi\,\cos\Phi}{\kappa}\right)T + \left(\frac{\cos^2\Phi}{\kappa}\right)N$$

whence it is clear that as $\kappa \to 0$ then $\Psi \to \infty$.

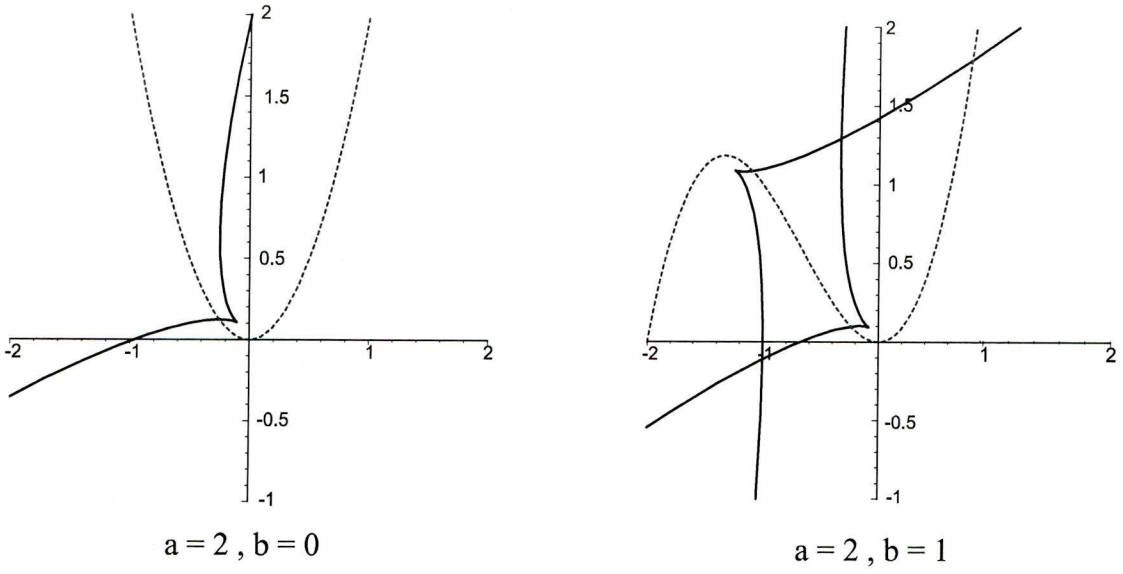

Figure 3.10: $\gamma(t) = (t,\ at^2 + bt^3)$ shown dotted with fixed angle envelope Ψ in bold. Here $\Phi = \pi/4$.

Example 3.4.3 As a simple example we will take $\gamma(t) = (t,\ at^2 + bt^3)$ and $\Phi = \pi/4$ so that $\tan\Phi = 1$. If we let $a = 2$, $b = 0$ and solve equation (3.8) we obtain the unique solution $t = 1/12$, so that the envelope, Ψ, has one singular point. Also equation (3.9) has no real solutions so the singular point is in fact an ordinary cusp. The left half of figure 3.10 shows γ as the dotted parabola with Ψ, shown in bold, displaying a single ordinary cusp where $t = 1/12$.

If we now let $a = 2$ and $b = 1$ then equation (3.8) has four solutions, two real and two complex. The real solutions are $t = -2/3 \pm (\sqrt{55 + 5\sqrt{246}})/15$. Again equation (3.9) has no real solutions so the two singular points on the envelope are ordinary cusps. The right half of figure 3.10 shows γ as the dotted cubic with the fixed angle envelope Ψ, shown in bold, displaying two ordinary cusps.

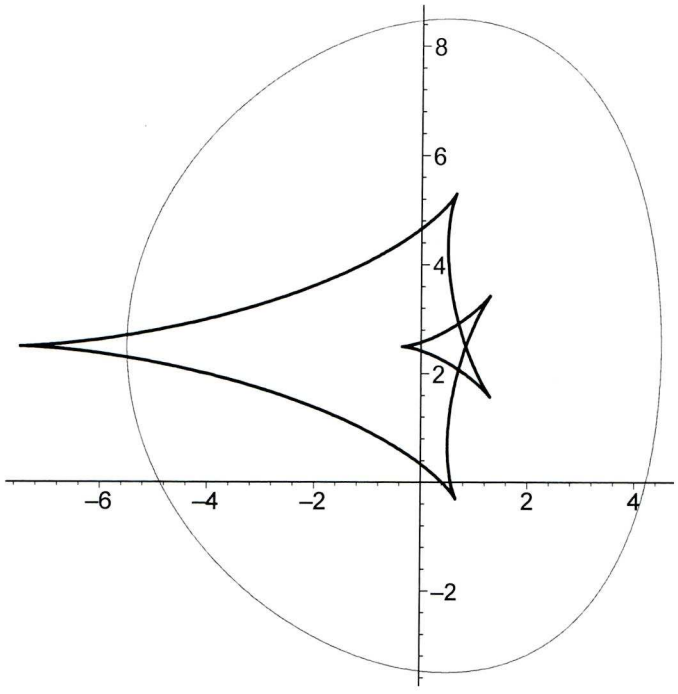

Figure 3.11: Example 3.4.4 with $\Phi = 0$. γ (in light) with fixed angle envelope Ψ (in bold) showing six ordinary cusps.

Example 3.4.4 We will now look at a more involved example, choosing γ to be a smooth closed convex curve with six vertices, $\gamma(t) = (5\sin t + \frac{1}{2}\cos 2t\,,\, \frac{5}{2} + \cos t\,)$. We will look at three values of Φ, determining the number of singular points on Ψ in each case:

(i) First we take $\Phi = 0$ whence Ψ is the evolute of γ and, by proposition 3.4.1, we anticipate six singular points on Ψ corresponding to the six vertices on γ. We find that equation (3.8) has six real solutions whilst equation (3.9) is non-zero at each. Thus Ψ has six ordinary cusps as shown in figure 3.11.

(ii) Now taking $\Phi = \pi/5$ we find that equation (3.8) has four real solutions and that equation (3.9) is non-zero at each. Thus Ψ has four ordinary cusps as shown in figure 3.12.

(iii) Finally we take $\Phi = 0.45\pi$ and find that equation (3.8) has no real solutions thus Ψ is smooth as shown in figure 3.12. Of course this is as we might expect since we are very close to $\Phi = \pi/2$, whence Ψ is the envelope of tangents to γ, which just reproduces γ itself.

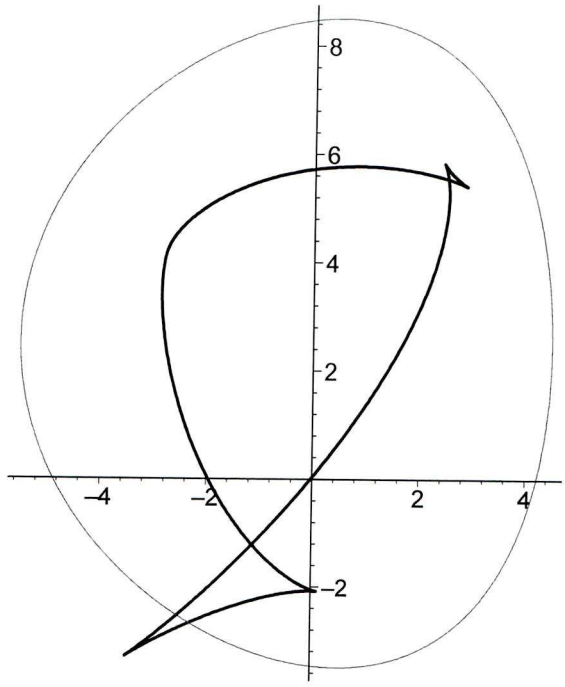

Figure 3.12: Example 3.4.4 with $\Phi = \pi/5$. γ (in light) with fixed angle envelope Ψ (in bold) showing four ordinary cusps.

So much for our three particular values of Φ but the overall picture as Φ ranges smoothly from 0 to $\pi/2$ is that we start with six cusps on Ψ and finish with $\Psi = \gamma$. Between these two extremes pairs of cusps come together in degenerate singular points and then disappear[2]. It is natural to ask: what is the nature of these degenerate singularities?

To answer this we return to our general setup and choose axes so that a point on γ giving rise to such a degenerate singularity is at the origin. We know from equation (3.5) that Ψ is singular when $\tan\Phi = (-3a_3)/(2a_2)$ and from equation (3.6) that this singular point is degenerate (i.e. $A_{\geq 3}$) if $a_4 = (2{a_2}^4 + 3{a_3}^2)/(2a_2)$. If Φ_0 is the value of Φ giving a singular point on Ψ when $t = 0$ then the components of Ψ here are, $x_0 = \tan\Phi_0/(2a_2(1 + \tan{\Phi_0}^2))$ and $y_0 = 1/(2a_2(1 + \tan{\Phi_0}^2))$.

[2]This is close to occurring for the cusp pair in the upper right quadrant of figure 3.12.

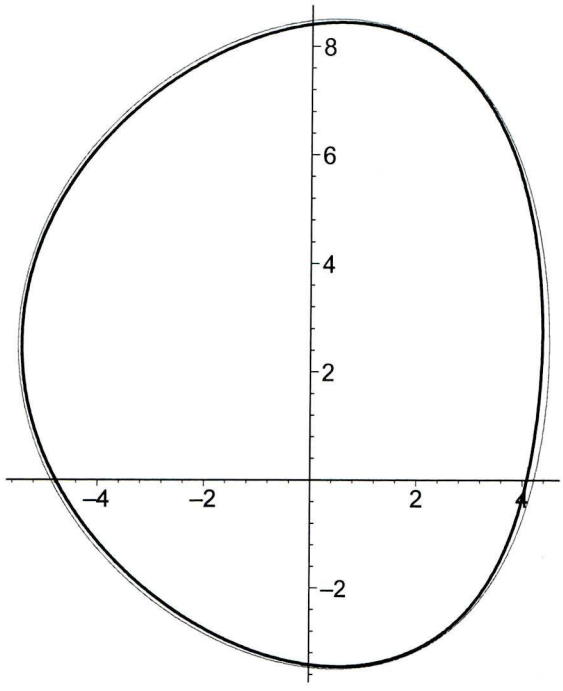

Figure 3.13: Example 3.4.4 with $\Phi = 0.45\pi$. γ (in light) with smooth fixed angle envelope Ψ.

We will now use the theory of unfoldings[3] to determine whether the family of lines $F(t, x, y, \Phi)$ is a versal unfolding of an A_3 singularity on Ψ when $t = 0$. To do this we create a new variable, say $m = \tan\Phi$ (so our unfolding parameters are now x, y and m), and calculate the 2-jets with constant of $\partial F/\partial x$, $\partial F/\partial y$ and $\partial F/\partial m$ evaluated at $t = 0$, $x = x_0$, $y = y_0$ and $m = m_0 = \tan\Phi_0$. These turn out to be

$$\begin{aligned}
j^2\,\tfrac{\partial F}{\partial x}(\text{t=0}) &= 1 + \tfrac{3a_3}{a_2}\,t + \tfrac{9{a_3}^2}{2{a_2}^2}\,t^2,\\
j^2\,\tfrac{\partial F}{\partial y}(\text{t=0}) &= -\tfrac{3a_3}{2{a_2}^2} + 2a_2\,t + 3a_3\,t^2,\\
j^2\,\tfrac{\partial F}{\partial m}(\text{t=0}) &= \tfrac{2{a_2}^3}{4{a_2}^4+9{a_3}^2} - \tfrac{6{a_2}^2a_3}{4{a_2}^4+9{a_3}^2}\,t + \tfrac{4{a_2}^5}{4{a_2}^4+9{a_3}^2}\,t^2.
\end{aligned}$$

Now, $F(t, x, y, \Phi)$ is a versal unfolding of an A_3 singularity on Ψ when $t = 0$ provided these 2-jets form a basis for the space of all polynomials of degree ≤ 2 over $\mathbb{R}$.

[3]See 'Curves and Singularities' [6] Ch.6 for details.

This is equivalent to saying that the 3×3 matrix

$$Q = \begin{pmatrix} C_{F_x}(0) & C_{F_x}(1) & C_{F_x}(2) \\ C_{F_y}(0) & C_{F_y}(1) & C_{F_y}(2) \\ C_{F_m}(0) & C_{F_m}(1) & C_{F_m}(2) \end{pmatrix}$$

formed with the coefficients of the 2-jets, is non-singular. However, $\det Q = (4{a_2}^4 + 9{a_3}^2)/(2{a_2}^2)$ which is always positive[4] and so the unfolding $F(t, x, y, \Phi)$ is always versal here. Hence we can state:

Proposition 3.4.5 *Let γ be a smooth plane curve and $\gamma(t_0)$ be a point of γ with Φ_0 a value of Φ such that the fixed angle envelope, $\Psi(t) = (x(t), y(t))$, of γ has exactly an A_3 singularity when $t = t_0$, then the 'big discriminant' surface of γ namely, $M(t, \Phi) = (x(t), y(t), \Phi)$, has a swallowtail at (x_0, y_0, Φ_0).*

Remark: Returning to example 3.4.4 we see that figures 3.11 to 3.13 represent horizontal slices through the 'big discriminant' surface M at $\Phi = 0$, $\pi/5$ and 0.45π. The surface M is shown from various angles in figures 3.14 to 3.17 from which it is evident that there are three degenerate singular points for $t \in [0, 2\pi]$ and $\Phi \in [0, \pi/2]$ (other ranges for Φ just repeat part of this surface).

We can find these points by simultaneously solving equations (3.8) and (3.9) using numerical methods, whence we obtain (to two decimal places): $(t_1, \Phi_1) = (2.02, 0.36\pi)$, $(t_2, \Phi_2) = (4.22, 0.16\pi)$ and $(t_3, \Phi_3) = (6.13, 0.28\pi)$. Also equation (3.10) is non-zero at each point. The three swallowtail points are highlighted in figures 3.14 to 3.17.

[4]Note: $\det Q$ is undefined when $a_2 = a_3 = 0$.

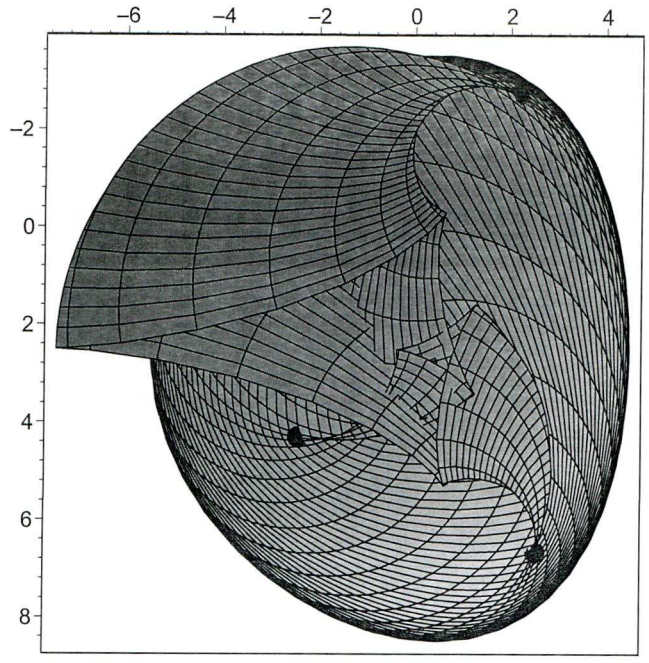

Figure 3.14: Big discriminant surface M of example 3.4.4. Bottom view.

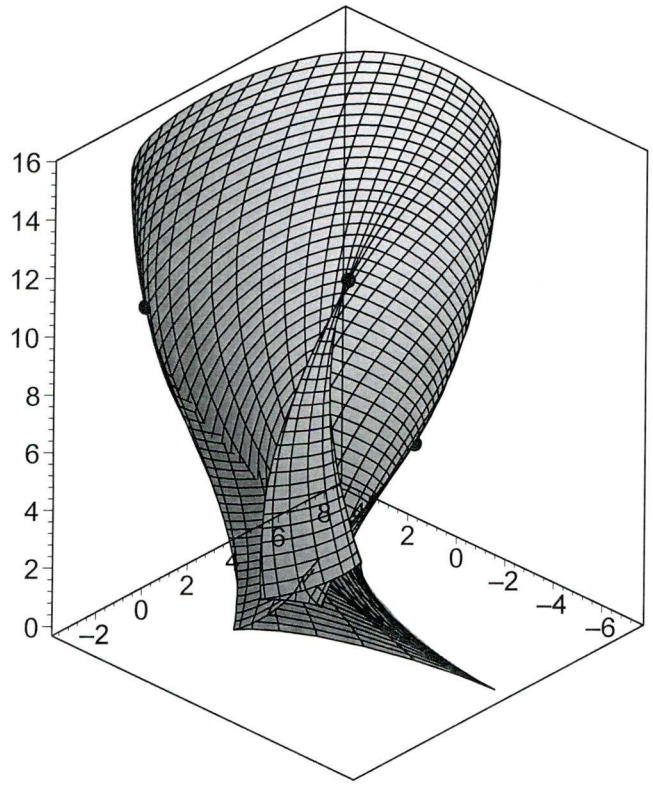

Figure 3.15: Big discriminant surface M of example 3.4.4. Oblique view.

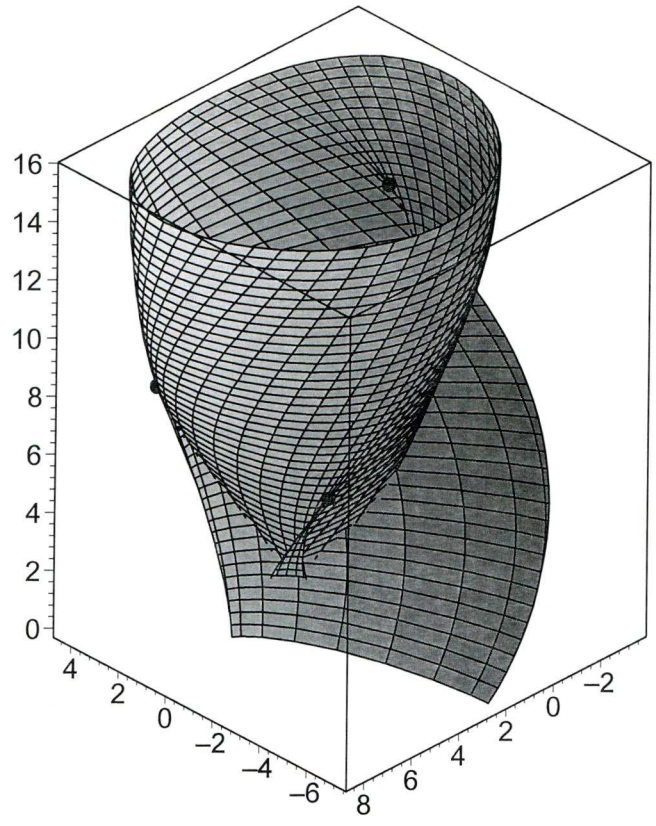

Figure 3.16: Big discriminant surface M of example 3.4.4. Oblique view.

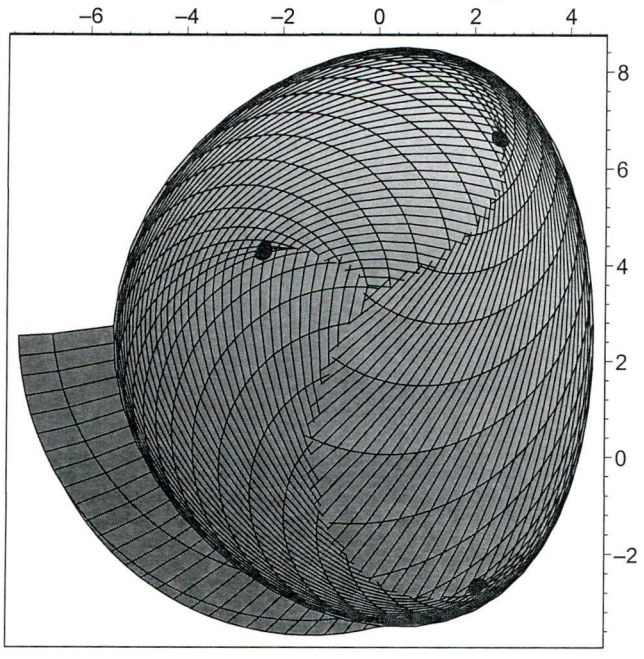

Figure 3.17: Big discriminant surface M of example 3.4.4. Top view.

3.5 Chapter Summary

In this chapter we demonstrated two methods of reconstructing a smooth curve γ given its MPL and some additional information: (i) In proposition 3.2.1 we showed that, given the MPL and a smooth function r describing the radius of the circle generating each point of the MPL, we can reconstruct the unique symmetry set c to γ (given at least one point of c) and that using c and r we can reconstruct γ as the envelope of circles centred on c. (ii) In proposition 3.3.1 we showed that, given the MPL and a smooth function ϕ describing the angle between the chord generating each point of the MPL and its normal here, we can reconstruct the unique symmetry set c of γ (provided we know the radius of at least one bi-tangent circle generating a point on the MPL). Here too we can reconstruct γ as the envelope of bi-tangent circles centred on c since the radius function r is retrieved as part of the method.

The second reconstruction method motivated the general study of fixed angle envelopes. If F is the family of lines that at each point of γ makes a constant angle Φ to the normal to γ then the fixed angle envelope Ψ is formed as the envelope of these lines. In proposition 3.4.1 we obtained conditions for Ψ to be singular and also additional conditions to determine when a singular point is A_2 (ordinary cusp) or more degenerate. In proposition 3.4.2 we obtained a parameterisation for Ψ (using Φ and the curvature function on γ) and showed that $\Psi \to \infty$ local to inflexions of γ. Finally we looked at examples of families of envelopes for varying Φ, noting changes in the numbers of cusps which occur at swallowtail points of the big bifurcation set.

Chapter 4

Parallel Tangency in $\mathbb{R}^3$

4.1 Introduction

There are many constructions available to measure the local symmetry of 3D shapes. Two of the most well documented are the Symmetry Set and Medial Axis which are formed as the centres of spheres bi-tangent to the shape. Both of these constructions have important applications in computer vision but they are restricted by their dependence on spheres whose essential properties are lost under all but Euclidean transformations of $\mathbb{R}^3$. As a result we are motivated to study symmetry constructions which are invariant under the much wider range of affine transformations of $\mathbb{R}^3$. One such construction is the Centre Symmetry Set (CSS) which is formed as the envelope of chords joining parallel tangent pairs on the shape. It measures the departure of the shape from central symmetry and since its construction only depends on parallelism it is affinely invariant. See Giblin and Holtom [9] for more detail on the CSS and its properties.

The singularities of the CSS have been extensively studied by Giblin and Zakalyukin [11] so here we consider a closely related affinely invariant family of constructions called *equidistants*. These are formed by points at a fixed proportion along chords joining parallel tangent pairs and we find that the CSS is swept out by the singularities of this family, much as the evolute or focal set is swept out by the singularities of offsets to curves or surfaces. This introductory chapter will concentrate

purely on the set of pairs of points on a surface (or surfaces) which have parallel tangent planes and the properties of maps linking the parameters describing such points. We start by recalling some basic differential geometry of surfaces and introducing some important notation.

Some Basic Notions

Let p be a smooth point on a surface piece M in $\mathbb{R}^3$. If we perform Euclidean transformations which take p to the origin and rotate so that the xy–plane is tangent to M here, then M is said to be locally in *special Monge form*. In this form our calculations are simplified as M can be locally described as the graph of a function $z = f(x, y)$ where $f = f_x = f_y = 0$ and the unit normal $\mathbf{n} = (0, 0, 1)$ at $p = \mathbf{0}$. When f is a smooth function in x and y we can write

$$f(x, y) = (a_0x^2 + a_1xy + a_2y^2) + (b_0x^3 + b_1x^2y + b_2xy^2 + b_3y^3) + \text{h.o.t.} \qquad (4.1)$$

where 'h.o.t.' is used to designate all terms in a series expansion of higher degree than those displayed before it. The behaviour of M in a neighbourhood of p is generically of three distinct types depending on the intersection of M with its tangent plane here: (i) p is called an *elliptic point* if M meets its tangent plane in an isolated point, e.g. $f(x, y) = x^2 + y^2$ at $p = \mathbf{0}$. (ii) p is called a *hyperbolic point* if M meets its tangent plane in two curves crossing transversely, e.g. $f(x, y) = x^2 - y^2$ at $p = \mathbf{0}$, and (iii) p is called a *parabolic point* if M meets its tangent plane in a cuspidal curve, e.g. $f(x, y) = x^2 + y^3$ at $p = \mathbf{0}$. The upper half of figure 4.1 shows these three contact types.

If we consider the family of planes through the origin which contain the z–axis then each will intersect M forming a curve in that plane. The signed curvature of such curves at $\mathbf{0}$ are called *sectional curvatures* of M at $\mathbf{0}$. Their extrema, say κ_1 and κ_2, are called *principal curvatures* and the directions in which they occur are called *principal directions*. Also, the product $K := \kappa_1 \kappa_2$ is called the *Gauss curvature* of M at $\mathbf{0}$. All of this gives us another way of characterising the three types of point described above since at elliptic points $K > 0$ (i.e. κ_1 and κ_2 have the same sign), at hyperbolic points $K < 0$ (i.e. κ_1 and κ_2 have opposite signs) and at parabolic points $K = 0$ (i.e. $\kappa_1 = 0$ and/or $\kappa_2 = 0$). Directions in which the sectional

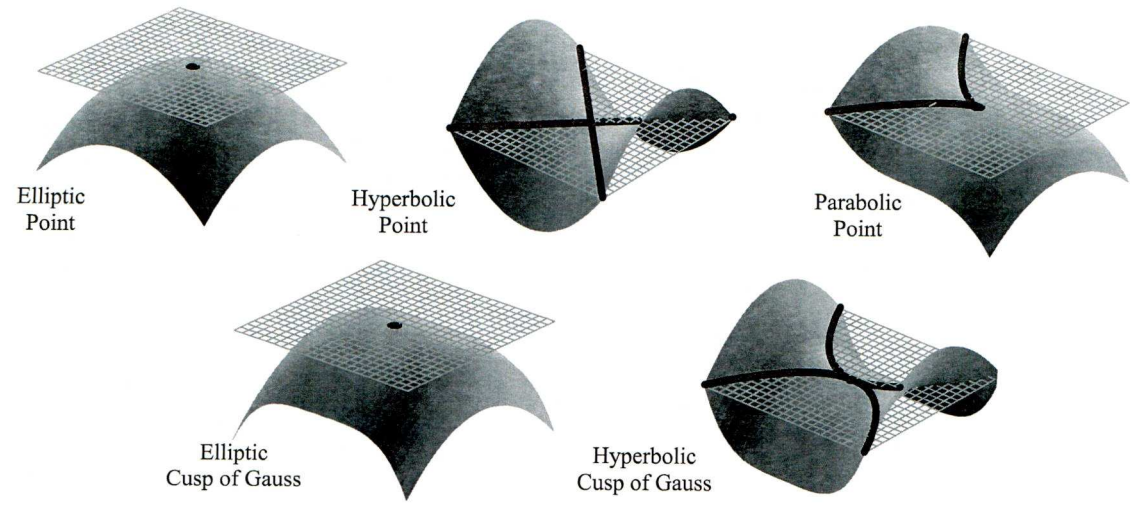

Figure 4.1: Contact with tangent plane at elliptic, hyperbolic, parabolic and cusp of Gauss points. The bold black lines show the curve of intersection between the surface and its tangent plane.

curvature is zero are called *asymptotic directions* and if $\kappa_1 = \kappa_2 = 0$ then $\mathbf{0}$ is a degenerate parabolic (or planar) point. Generically the locus of points on M which are parabolic consists of smooth disjoint curves called *parabolic curves*. These curves separate regions of elliptic and hyperbolic points on M and have major significance in computer vision applications, e.g. parabolic points appear as inflexions on the apparent contour of a surface. Parabolic points are clearly points where the tangent plane has especially high *contact* with M. With the surface in Monge form the function f can be regarded as the *height function* on M in the direction $(0, 0, 1)$. We can parameterise all directions close to $(0, 0, 1)$ by $(a, b, 1)$, with a and b both close to zero, so that the family of height functions takes the local form

$$H(x, y; a, b) = (x, y, f(x, y)) \cdot (a, b, 1) = f(x, y) + ax + by.$$

The degree of contact of M with its tangent plane is now measured by singularities of this height function and using Arnold's standard notation for singularities of functions [1] we say f is of type ${A_k}^+$ (resp. ${A_k}^-$) if, by a smooth change of coordinates in x and y, we can reduce to the *normal form* $\pm x^2 + y^{k-1}$ (resp. $\pm x^2 - y^{k-1}$). More specifically, and with reference to f as given in equation (4.1):

(i) f is of type A_1 at $\mathbf{0}$ if and only if its quadratic terms do not form a perfect square. This is equivalent to saying that $\mathbf{0}$ is not a parabolic point for which the algebraic condition is ${a_1}^2 \neq 4a_0a_2$. When this holds f is described as a *Morse function* and can be reduced to one of $\pm(x^2+y^2)$, $\pm(x^2-y^2)$. So the zero set of f is locally an isolated point or two transversely intersecting curves, i.e. elliptic and hyperbolic points as described above.

(ii) f is of type $A_{\geq 2}$ at $\mathbf{0}$ if and only if its quadratic terms form a perfect square. Thus $\mathbf{0}$ is a parabolic point, ${a_1}^2 = 4a_0a_2$, and f can be reduced to $a_0x^2 + b_0x^3 + b_1x^2y + b_2xy^2 + b_3y^3 + \text{h.o.t.}$ If in addition $a_0 \neq 0$ and $b_3 \neq 0$ then f is exactly A_2 and can be reduced to $\pm x^2 + y^3$. Thus the zero set of f is locally an ordinary cusp as described above.

(iii) f is of type $A_{\geq 3}$ at $\mathbf{0}$ if and only if its quadratic terms form a perfect square, so that ${a_1}^2 = 4a_0a_2$, but with $a_0 \neq 0$ and $b_3 = 0$. In this case x divides the cubic part of f and it can be reduced to $a_0x^2 + (c_4 - {b_2}^2/4a_0)y^4$. If the coefficient of y^4 here is non-zero then f is exactly A_3. When $b_2 \neq 0$ then $\mathbf{0}$ is called an *ordinary cusp of Gauss* of elliptic or hyperbolic type. For the elliptic type (${A_3}^+$ with ${b_2}^2 < 4a_0c_4$) the intersection of the surface with its tangent plane is an isolated point whilst for the hyperbolic type (${A_3}^-$ with ${b_2}^2 > 4a_0c_4$) it is a *tacnode*. The lower half of figure 4.1 shows these two contact types.

This covers all the generic cases which can occur for a given surface but in 1-parameter families of surfaces more complicated situations are possible. At an A_4 we have $c_4 - {b_2}^2/4a_0 = 0$ with the intersection of M and its tangent plane at $\mathbf{0}$ forming a *rhamphoid cusp*. Such points generically represent a degenerate cusp of Gauss where two ordinary cusps of Gauss have momentarily come together. Another degenerate case is that of D_4 points at which the quadratic terms of f vanish completely forming what is termed a *flat umbilic*. We will say something about such non-generic points in the final chapter but now we go on to describe the geometrical setting for the disjoint surface pieces case.

4.2 Disjoint Surfaces

Let M and N be disjoint surface pieces in $\mathbb{R}^3$. As usual we seek to simplify our geometry and so we translate such that the centre of our neighbourhood of interest on N lies at the origin and rotate so that the xy–plane is tangent here. Since parallelism is an affine invariant property we can also perform a shear transformation so that the centre of our neighbourhood of interest on M lies on the z–axis (at $z = k$ say). Clearly the tangent plane to M at $(0, 0, k)$ is also parallel to the xy–plane. Now, writing M as the graph of a function f of local variables s and t, and N as the graph of a function g of local variables u and v we have

$$M : (s,\, t) \mapsto (s,\, t,\, k + f(s,t)) \;\text{ and }\; N : (u,\, v) \mapsto (u,\, v,\, g(u,v))$$

with $f_x = f_y = g_x = g_y = 0$ at $(0,0)$. Note: here we are using x and y as place holders to denote differentiation with respect to the first and second local variables respectively. Now, the condition for parallel tangent planes on M and N is simply, $f_x(s,t) = g_x(u,v)$ and $f_y(s,t) = g_y(u,v)$. We can now define a map

$$\pi : (s,t,u,v) \mapsto (f_x - g_x\,,\; f_y - g_y) \tag{4.2}$$

the zeros of which will give us precisely those pairs of points (s,t) on M and (u,v) on N with parallel tangent planes. The geometry of the setup is shown schematically in figure 4.2.

Structure of the Set of Parallel Tangent Pairs

We now consider the set $\Pi = \{(s,t,u,v) \in \mathbb{R}^4 : \pi(s,t,u,v) = 0\}$, determine conditions for it to be smooth, investigate ways in which it can be parameterised and study some features of the maps associated with such parameterisations. Our motivation is clear since any calculations here will be greatly simplified if we are able to write any two of s, t, u and v as functions of the remaining two. To this end we examine some of the classical theory of maps from the plane to the plane and see how it can be used in this context. First a definition:

Definition 4.2.1 *Let D be an open set in $\mathbb{R}^n$ and $f : D \to \mathbb{R}^m$. The Critical Set, Σ_f, of f is that subset of D for which the rank of the Jacobian of f falls below maximal*

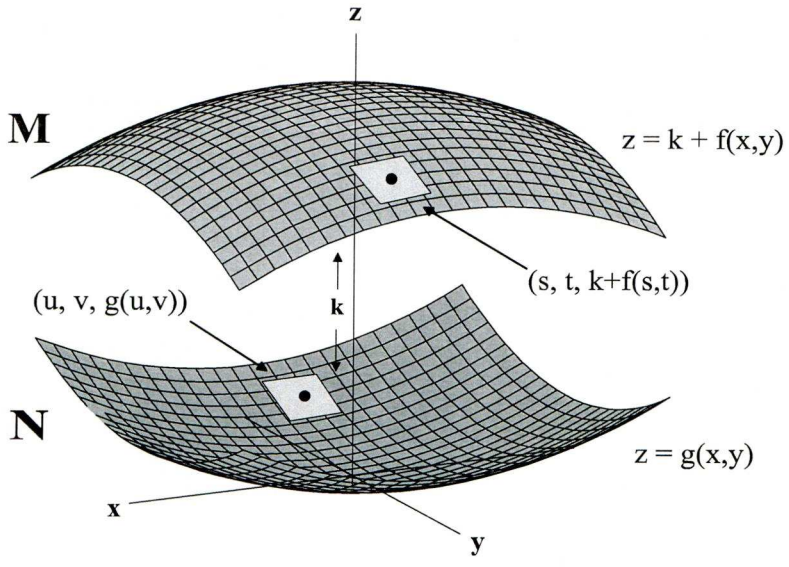

Figure 4.2: Geometry of setup for disjoint surface pieces.

rank i.e. $\min(n, m)$. *Points in* Σ_f *are known as critical points and their images in* $\mathbb{R}^m$ *are known as critical values. The set* $f(\Sigma_f)$ *is called the discriminant or critical locus of* f.

We will take our points of parallelism at $(s, t) = (u, v) = \mathbf{0}$ so that all expressions below are evaluated at these points. Now

$$J_\pi = \begin{pmatrix} f_{xx} & f_{xy} & -g_{xx} & -g_{xy} \\ f_{xy} & f_{yy} & -g_{xy} & -g_{yy} \end{pmatrix}. \tag{4.3}$$

This has maximal rank, and thus Π is smooth at $\mathbf{0}$, provided some 2×2 minor has non-zero determinant. The first two columns represent H_f, the Hessian matrix of f, whilst the last two represent (-1 times) H_g, the Hessian matrix of g. Hence Π is certainly smooth provided either M or N is non-parabolic at $\mathbf{0}$ (since this is equivalent to either $\det(H_f) \neq 0$ or $\det(H_g) \neq 0$).

The remaining possibility is that M and N are both parabolic at $\mathbf{0}$ but there exists a 2×2 minor using one the first two columns with one of the last two columns which has a non-zero determinant. If we rotate the setup in the z–axis so that the principal directions on M at $\mathbf{0}$ are aligned with the x and y axes then we can write $f(x, y) = x^2 + \text{h.o.t.}$ and thus $f_{xx}(\mathbf{0}) = 2$ and $f_{xy}(\mathbf{0}) = 0$. If we consider the first and

third columns of J_π then the 2×2 matrix formed by them has non-zero determinant at $\mathbf{0}$ if and only if $g_{xy}(\mathbf{0}) \neq 0$. Similarly the matrix formed by the first and last columns of J_π has non-zero determinant if and only if $g_{yy}(\mathbf{0}) \neq 0$. Note: we need not consider options using the second column since we know, by assumption, that this is linearly dependent on the first. Hence we can still find a 2×2 minor with non-zero determinant provided either $g_{xy}(\mathbf{0}) \neq 0$ or $g_{yy}(\mathbf{0}) \neq 0$. When both are zero (a non-generic situation since we are imposing three conditions on N) then the unique asymptotic directions at the two parabolic points coincide and we state:

Proposition 4.2.2 *With the geometry stated above then* Π *is smooth at* $\mathbf{0}$ *unless both points are parabolic and their unique asymptotic directions are parallel.*

We will return to the both points parabolic case at the end of this section but for now we can assume, without loss of generality, that M is non-parabolic at $(0, 0, k)$. Hence by the implicit function theorem, there exists a map

$$h : (u,\, v) \mapsto (s(u, v),\, t(u, v)) \tag{4.4}$$

such that $\pi(s(u, v), t(u, v), u, v) \equiv \mathbf{0}$. We can determine when h is a local diffeomorphism but studying its Jacobian

$$J_h = \begin{pmatrix} s_u & s_v \\ t_u & t_v \end{pmatrix}.$$

We know that for $(s, t, u, v) \in \Pi$ we have $f_x(s(u, v), t(u, v)) = g_x(u, v)$ and $f_y(s(u, v), t(u, v))$ $= g_y(u, v)$. If we differentiate both of these expressions in turn with respect to u and v we obtain

$$\{f_{xx}(s(u, v), t(u, v))\}\, s_u + \{f_{xy}(s(u, v), t(u, v))\}\, t_u = g_{xx}(u, v),$$

$$\{f_{xx}(s(u, v), t(u, v))\}\, s_v + \{f_{xy}(s(u, v), t(u, v))\}\, t_v = g_{xy}(u, v)$$

and

$$\{f_{xy}(s(u, v), t(u, v))\}\, s_u + \{f_{yy}(s(u, v), t(u, v))\}\, t_u = g_{xy}(u, v),$$

$$\{f_{xy}(s(u, v), t(u, v))\}\, s_v + \{f_{yy}(s(u, v), t(u, v))\}\, t_v = g_{yy}(u, v).$$

These can be written in matrix form as, $H_f\, J_h = H_g$, and we know that H_f is non-singular at $\mathbf{0}$ hence $J_h = {H_f}^{-1}\, H_g$. From this expression we see that $J_h(\mathbf{0})$ is singular (or non-singular) as $H_g(\mathbf{0})$ is and so we state:

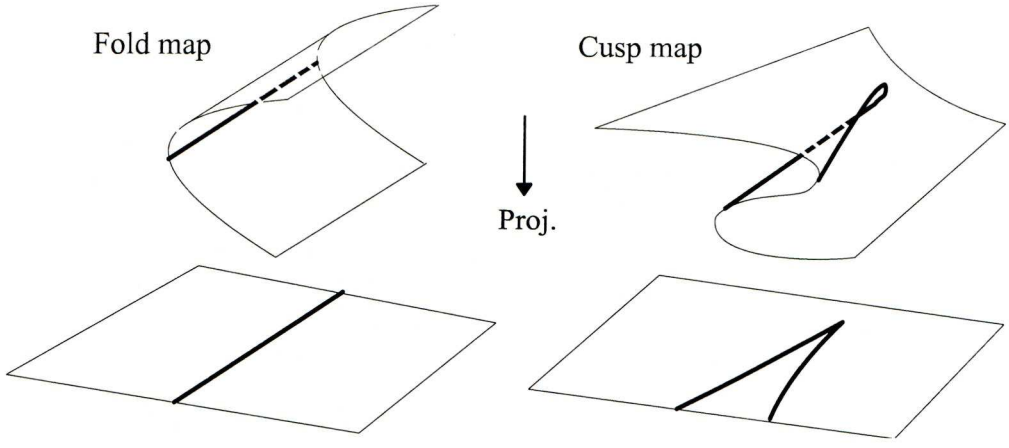

Figure 4.3: Fold and Cusp maps. The dark line in the upper figures represents the *contour generator* (or *critical set*) of the vertical projection and, in the lower figures, the *apparent contour* or *critical locus* of the projection.

Proposition 4.2.3 *With the geometry stated above then the map* $h : (u, v) \mapsto (s, t)$ *is a local diffeomorphism if and only if both* M *and* N *are non-parabolic at* $(0, 0)$.

Fold and Cusp Maps

We have dealt with the case where h is a local diffeomorphism but Whitney showed in [24] that there are two further stable maps from the plane to the plane, namely the *fold* map and the *cusp* map. We now recall some of their basic properties. Firstly, provided J_h does not have zero rank at $\mathbf{0}$ then we can make diffeomorphic changes of coordinate in the source and target spaces[1] to write $h(u, v) = (u,\ t(u, v))$, the so-called *canonical form* (Note: u, v and t here are not the same as those above, but we will retain these names for simplicity). With the map in this form the Jacobian simplifies thus

$$J_h = \begin{pmatrix} 1 & 0 \\ t_u & t_v \end{pmatrix}$$

whence it is clear that $\det(J_h) = 0 \Leftrightarrow t_v = 0$. Hence $\Sigma_h = \{(u, v) : t_v = 0\}$ and by the implicit function theorem this is smooth if and only if $t_{vv} \neq 0$ or $t_{uv} \neq 0$. We now state some important propositions concerning fold and cusp maps. Proofs of these propositions and further details can be found in Lu [13] Ch.2.

[1] Which is described as an *$\mathcal{A}$–equivalent* (or *RL–equivalent*) change of coordinates.

Proposition 4.2.4 *If* $\det(J_h) = 0$ *with* Σ_h *smooth and* $h|\Sigma_h$ *an immersion at* $\mathbf{0}$ *then* h *is a fold map.*

Whitney showed that any h satisfying these criteria is $\mathcal{A}$–equivalent to the *standard fold map* $h_0 : (x, y) \mapsto (x, y^2)$ in a neighbourhood of $\mathbf{0}$. If we look at the map h_0 we can see where the term "fold" comes from since if we lift from $\mathbb{R}^2 \to \mathbb{R}^3$ using $(x, y) \mapsto (x, y, y^2)$ we form a parabolic cylinder containing the x–axis and as the left half of figure 4.3 shows this looks rather like a folded piece of paper. Now

$$J_{h_0} = \begin{pmatrix} 1 & 0 \\ 0 & 2y \end{pmatrix}$$

so that $\det(J_{h_0}) = 0$ if and only if $y = 0$ and $\Sigma_{h_0} = \{(x, y) : y = 0\}$. Hence the critical set of the map h_0 is just the x–axis. This is as we expect since Σ_{h_0} can also be thought of as the contour generator of the lifted surface viewed (in this instance) from $y = +\infty$. Also $h_0|\Sigma_{h_0} = (x, 0)$ so the apparent contour is smooth.

Proposition 4.2.5 *If* $\det(J_h) = 0$ *with* Σ_h *smooth but* $h|\Sigma_h$ *is an ordinary cusp at* $\mathbf{0}$ *then* h *is a cusp map.*

In this case Whitney showed that any such h is $\mathcal{A}$–equivalent to the map $h_1 : (x, y) \mapsto (x, xy - y^3)$ in a neighbourhood of $\mathbf{0}$. Lifting to $\mathbb{R}^3$ using $(x, y) \mapsto (x, y, xy - y^3)$ we form a surface rather like a twisted plane, as shown in the right half of figure 4.3. Now

$$J_{h_1} = \begin{pmatrix} 1 & 0 \\ y & x - 3y^2 \end{pmatrix}$$

so that $\det(J_{h_1}) = 0$ if and only if $x = 3y^2$ and $\Sigma_{h_1} = \{(x, y) : x = 3y^2\}$. Hence the critical set of the map h_1 is represented by a parabola through the origin and viewing the lifted surface from $y = +\infty$ gives an ordinary cusp at the origin as an apparent contour, hence the name. Also $h_0|\Sigma_{h_0} = (3y^2, 4y^3)$, which is clearly an ordinary cusp.

Now consider the *Gauss map* of N, i.e. the map $G_N : N \mapsto S^2$ where $p \mapsto n_p$ the oriented unit normal at p. For this map it is standard theory[2] that (i) G_N is a local diffeomorphism if and only if p is non-parabolic, (ii) G_N is a fold map if and only

[2]See Banchoff et al. [4] for a proof.

if p is parabolic but not a cusp of Gauss, and (iii) G_N is a cusp map if and only if p is an ordinary cusp of Gauss. So if G_M is the Gauss map of M then it is a local diffeomorphism (since we assume M to be non-parabolic). The map h relates points on N to points on M with parallel tangent planes and so we have the following equivalence of maps

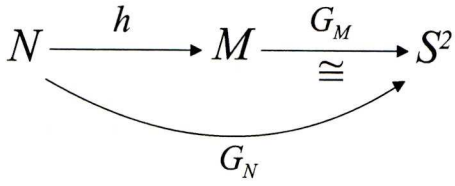

This is because the unit normal on N maps to the same unit normal on M under h. Hence $h \equiv {G_M}^{-1} \circ G_N$ and since ${G_M}^{-1}$ is also a local diffeomorphism then h and G_N have identical singularities enabling us to state:

Proposition 4.2.6 *The map $h : (u, v) \mapsto (s, t)$ is: (i) a fold map if and only if M is non-parabolic at $(0, 0, k)$ and N is parabolic but not a cusp of Gauss at $(0, 0, 0)$, (ii) a cusp map if and only if M is non-parabolic at $(0, 0, k)$ and N is an ordinary cusp of Gauss at $(0, 0, 0)$.*

The classification of map germs from the plane to the plane begins with three stable cases (local diffeomorphism, fold, cusp) and we have considered where our map h has each of these forms. We now go on to consider the codimension 1 map germs (lips, beaks). Further detail on lips and beaks maps can be found in Rieger [21].

Lips and Beaks Maps

We will restrict the level of degeneracy by insisting that the map

$$\sigma(u, v) = s_u t_v - s_v t_u \quad (= \det J_h)$$

is a *Morse function* at $\mathbf{0}$. We know from the *Morse lemma*[3] that if σ is Morse at $\mathbf{0}$ then $\Sigma_h = \sigma^{-1}(0)$ is either an isolated point ($\sigma_{uu}\,\sigma_{vv} - {\sigma_{uv}}^2 > 0$) or a transverse crossing ($\sigma_{uu}\,\sigma_{vv} - {\sigma_{uv}}^2 < 0$) and h is called a *lips map* in the first case and a *beaks*

[3]Further details on Morse functions and the Morse Lemma can be found in 'Curves and Singularities' [6] p.88–89

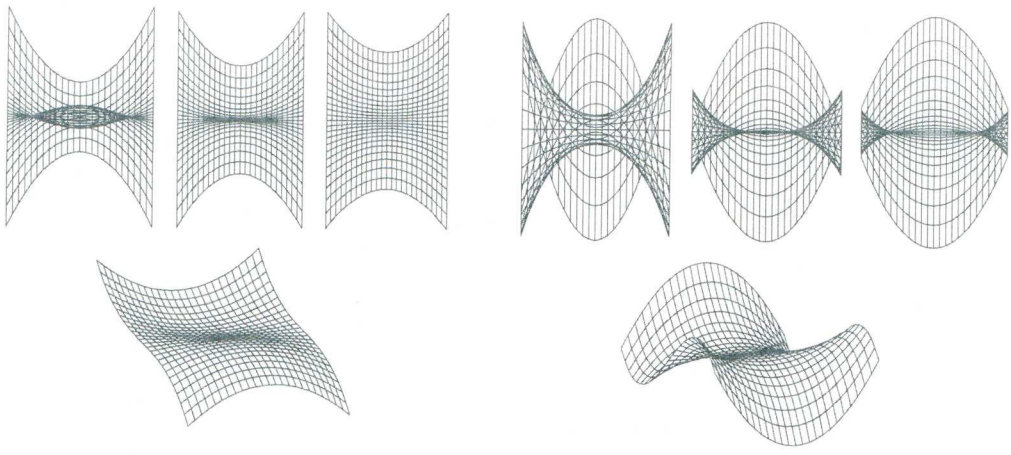

(i) Lifted Lips Map : $h_3(x, y)=(x, y, x^2y + y^3)$ (ii) Lifted Beaks Map : $h_4(x, y)=(x, y, x^2y - y^3)$

Figure 4.4: Lifted surfaces for the standard lips and beaks maps. The three upper figures in each case show the apparent contour viewed from $y = +\infty$ through a transition either side of the lips/beaks point.

map in the second. The standard form of a lips/beaks map is $h_{3,4}(x, y) = (x, x^2y \pm y^3)$ with '+' in the lips case and '–' in the beaks. Figure 4.4 shows the lifted surfaces for these two standard maps.

In order to proceed we will need some notation. We take as our starting point the initial setup described in above and assume that M is non-parabolic at $(0, 0, k)$ whilst N as parabolic at $(0, 0, 0)$. We can further simplify the calculations by rotating about the z–axis so that the principal directions to N at the origin lie along the x and y axes, with the unique asymptotic direction here being along the y–axis. This simplifies the Taylor expansion of g about $u = v = 0$ as follows

$$g(u, v) = u^2 + (g_{30}\, u^3 + g_{21}\, u^2v + g_{12}\, uv^2 + g_{03}\, v^3) + \text{h.o.t.} \tag{4.5}$$

where we have re-scaled in the z-direction to make the coefficient of u^2 equal to 1. We can write the Taylor expansion for $f(s, t)$ about $s = t = 0$ as

$$f(s, t) = (f_{20}\, s^2 + f_{11}\, st + f_{02}\, t^2) + (f_{30}\, s^3 + f_{21}\, s^2t + f_{12}\, st^2 + f_{03}\, t^3) + \text{h.o.t.} \tag{4.6}$$

and if we perform an affine transformation of the form

$$\Lambda = \begin{pmatrix} a & 0 & 0 \\ b & c & 0 \\ 0 & 0 & a^2 \end{pmatrix}, \quad a, b, c \in \mathbb{R}$$

then $\Lambda : (x,\, y,\, z) \mapsto (ax,\, bx + cy,\, a^2 z)$. This transformation preserves the y–axis, the z–axis and xy–plane, but allows us to remove the st term from the expansion of f when M is elliptic at $(0, 0, k)$ or the s^2 term when M is hyperbolic at $(0, 0, k)$. Also by choosing appropriate values for a we can ensure that the coefficients of s^2 and t^2 in the elliptic case, or st and t^2 in the hyperbolic case, are the same. Hence when M is elliptic we have

$$f(s,t) = a(s^2 + t^2) + (f_{30}\, s^3 + f_{21}\, s^2 t + f_{12}\, st^2 + f_{03}\, t^3) + \text{h.o.t.} \tag{4.7}$$

and when it is hyperbolic we have

$$f(s,t) = a(st + t^2) + (f_{30}\, s^3 + f_{21}\, s^2 t + f_{12}\, st^2 + f_{03}\, t^3) + \text{h.o.t.} \tag{4.8}$$

Using the same convention on coefficient subscripts we can write the components of h in equation (4.4) as

$$s(u,v) = (s_{10}\, u + s_{01}\, v) + (s_{20}\, u^2 + s_{11}\, uv + s_{02}\, v^2) + \text{h.o.t.}, \tag{4.9}$$

$$t(u,v) = (t_{10}\, u + t_{01}\, v) + (t_{20}\, u^2 + t_{11}\, uv + t_{02}\, v^2) + \text{h.o.t.} \tag{4.10}$$

Now $\Sigma_h = \{(u,v) : \sigma(u,v) = 0\}$ and so Σ_h is singular if and only if $\sigma_u = \sigma_v = 0$ and σ is Morse at $\mathbf{0}$ if and only if $\sigma_{uu}\sigma_{vv} \neq \sigma_{uv}^2$. Taking g in the form given by equation (4.5) and f in either of the forms of equations (4.7) or (4.8) depending as M is elliptic or hyperbolic at $(0, 0, k)$, then we can successively determine the coefficients s_{ij} and t_{ij} in equations (4.9) and (4.10) using the parallel tangency conditions $f_x = g_x$ and $f_y = g_y$. Hence we can find a series expansion for σ and the 1-jet in each case is as follows

$$j^1\sigma = \frac{g_{12}}{a^2}\, u + \frac{3\, g_{03}}{a^2}\, v \;\; (f \text{ elliptic}), \quad j^1\sigma = \frac{-4\, g_{12}}{a^2}\, u + \frac{-12\, g_{03}}{a^2}\, v \;\; (f \text{ hyperbolic}).$$

Hence in either case we have $\sigma_u = 0$ if and only if $g_{12} = 0$ and $\sigma_v = 0$ if and only if $g_{03} = 0$. For $\sigma_u = \sigma_v = 0$ (i.e. the critical set singular) we require $g_{03} = g_{12} = 0$.

We know from above that $g_{03} = 0$ means that the origin is a cusp of Gauss on N, but not an ordinary cusp of Gauss since $g_{12} = 0$. Also since $g_{12} = 0$ then the cusp of Gauss is non-degenerate provided $g_{04} \neq 0$. With $g_{03} = g_{12} = 0$ we now consider the parabolic curve on N which passes through the origin and is given by $P = g_{xx}\, g_{yy} - {g_{xy}}^2 = 0$. With g in the form of equation (4.5) the 1-jet of P is $j^1 P = 4\, g_{12}\, u + 12\, g_{03}\, v$. So $g_{12} = g_{03} = 0$ tells us that the parabolic curve is singular. If we calculate $\det(H_P) = P_{xx}P_{yy} - {P_{xy}}^2$ we find that the condition for this to be non-zero at the origin is

$$8\, g_{04}\, (g_{22} - {g_{21}}^2) - 3\, {g_{13}}^2 \neq 0. \tag{4.11}$$

By the Morse lemma, if the LHS here is positive then P is an isolated point at the origin, whilst if it is negative then P is a transverse crossing here. The condition for σ to be Morse at $\mathbf{0}$ is exactly the same as that of equation (4.11), so σ is Morse at $\mathbf{0}$ as the parabolic curve is. To decide whether h is a lips or beaks map we can use the following result by Tari [22]:

Proposition 4.2.7 *Let h be an $\mathcal{A}$-equivalent germ to $H(u,v) = (u, F(u,v))$. If we have $\partial^3 F/\partial v^3(0,0) \neq 0$, then h is a lips/beaks map if and only if its critical set is the zero set of a Morse function.*

In our case $h(u,v) = (s(u,v), t(u,v))$ and so we seek a smooth change of variables ϕ say, which will reduce h to the form of proposition 4.2.7, i.e.

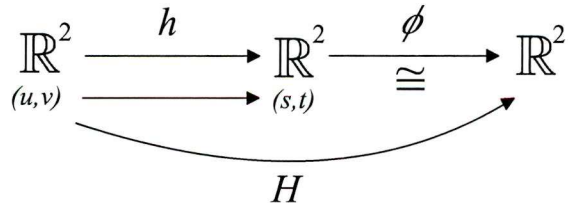

In finding the coefficients s_{ij} in the expansion for s described by equation (4.9) we find that $s_{10} = 1/a$ (f elliptic) or $s_{10} = -4/a$ (f hyperbolic). Thus $s_u \neq 0$ at the origin and by the implicit function theorem we can write $s(u,v) = U$ say, and solve for u as a function of U and v. We can then substitute this expression for u into $t(u,v)$ giving $F(U,v) = t(u(U,v),v)$ and apply the proposition. For both f elliptic and f hyperbolic the coefficient of v^3 in the expansion for F is $2\, g_{04}/a$ which is non-zero since we assume a non-degenerate cusp of Gauss on N at $\mathbf{0}$. Hence we state:

Proposition 4.2.8 *Let* $\mathbf{0}$ *on* N *be a non-degenerate cusp of Gauss at which the parabolic curve is singular but is the zero set of a Morse function. Then* $h : (u, v) \mapsto (s, t)$ *is (i) a lips map if and only if the parabolic curve has an isolated point at* $\mathbf{0}$*, and (ii) a beaks map if and only if the parabolic curve has a transverse crossing at* $\mathbf{0}$*.*

Both points Parabolic

With our notation established we can now return to the case where both points of tangency are parabolic. We can take g in the form of equation (4.5) but for f we need a parabolic form where the unique asymptotic direction is never parallel with that of g (i.e. the y–axis) to ensure that Π is locally smooth. To this end we choose f to have the form

$$f(s,t) = \varepsilon\,(as+t)^2 + (f_{30}\,s^3 + f_{21}\,s^2t + f_{12}\,st^2 + f_{03}\,t^3) + \text{h.o.t.} \tag{4.12}$$

where $\varepsilon = \pm 1$. The 1-jet of the first parallel tangency equation, $f_x - g_x = 0$, is $-2u + 2\varepsilon at + 2\varepsilon a^2 s$ so we can certainly write u as a smooth function of s, t and v. If we do this and substitute the result into the second parallel tangency equation, $f_y - g_y = 0$, then we obtain, $j^1(f_y - g_y) = 2\varepsilon t + 2\varepsilon as$, so we can write t as a smooth function of s and v. Calculation shows this to be

$$t = -as - \frac{3a^2 f_{03} - 2af_{12} + f_{21}}{2\varepsilon}\,s^2 + \frac{3g_{03}}{2\varepsilon}\,v^2 + \text{h.o.t.}$$

and substituting this into the expression for u we can write u as a smooth function of s and v thus

$$u = \frac{3\,(f_{30} + a^2 f_{12} - af_{21} - a^3 f_{03})}{2}\,s^2 + \frac{3ag_{03} - g_{12}}{2}\,v^2 + \text{h.o.t.}$$

So in this case the map relating the parameters at the two points of tangency is $h : (s, v) \mapsto (t(s, v),\ u(s, v))$. The critical set of h is $\Sigma_h = \{(s, v) : t_s\,u_v - t_v\,u_s = 0\}$ and this has 1-jet $a\,(g_{12} - 3\,a\,g_{03})\,v$. So the critical set is smooth provided $a \neq 0$ and $a \neq g_{12}/(3g_{03})$. The map h restricted to its critical set and parameterised by s is as follows

$$h|\Sigma_h = \left(-as - \frac{f_{21} - 2af_{12} + 3a^2 f_{03}}{2\varepsilon}\,s^2 + \ldots,\ \frac{3\,(f_{30} + a^2 f_{12} - af_{21} - a^3 f_{03})}{2}\,s^2 + \ldots\right)$$

which is clearly an immersion at $\mathbf{0}$ provided $a \neq 0$. Thus we state:

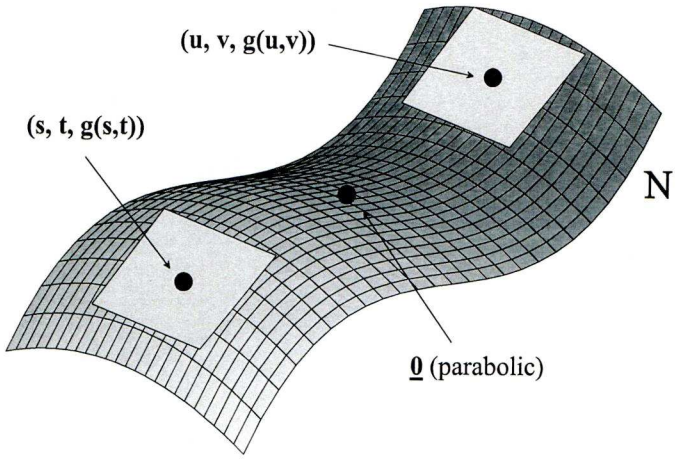

Figure 4.5: Geometry of setup for parallel tangents on a single surface piece.

Proposition 4.2.9 *With the geometry stated above, if both points of parallel tangency are parabolic then provided (i) the asymptotic directions at the two points are not parallel, and (ii) $a \neq 0$ and $a \neq g_{12}/(3g_{03})$, then t and u can be written as smooth functions of s and v and the map $h : (s, v) \mapsto (t(s, v),\ u(s, v))$ is a fold.*

4.3 The Local Case

In this section we turn our attention to neighbouring pairs of points on a single surface piece with parallel tangent planes. We are necessarily talking about pairs in a neighbourhood of a parabolic point since locally we cannot have points of parallel tangency otherwise. We will see that this case introduces complications that could not exist for disjoint surface pieces, and take particular interest in the case where the parabolic point is a cusp of Gauss where we examine the arrangement of various special curves on the surface through the cusp of Gauss. First we will describe the geometrical setting for the local case.

Let N be a smooth surface piece in $\mathbb{R}^3$ with parabolic point at the origin. We will retain the simplifications and notation of the two surface case, but now the points p and q both lie on N in a neighbourhood of the origin[4]. The equation of the surface

[4]Note: In this section we will (loosely) use p and q to designate both points in the parameter plane of the surface and same points lifted onto the surface itself.

is $N : (x, y) \mapsto (x, y, g(x, y))$ where g is of the form given in equation (4.5). The condition for parallel tangent planes on N is $g_x(s,t) = g_x(u,v)$ and $g_y(s,t) = g_y(u,v)$, and the zero set of the map

$$\pi : (p, q) \mapsto (g_x(p) - g_x(q),\ g_y(p) - g_y(q))$$

will give us those points $p = (u, v, g(u,v))$ and $q = (s, t, g(s,t))$ with parallel tangent planes on N. The geometry of this setup is shown in figure 4.5.

For this case we are faced with a problem that could not arise in the disjoint surfaces case, namely that points in the diagonal $\Delta = \{(s,t,u,v) : s = u \text{ and } t = v\}$ are always a solution of our parallel tangency equations. We encountered a similar problem in section 2.4 when we looked at the MPL to a plane curve and found that $\gamma_1 = \gamma_2$ was always an un-welcome addition to the PSS. In that case we were able to eliminate the problem by showing that the function giving pairs of points on a bi-tangent circle was a Morse function. Unfortunately this approach is not available to us here and so a different approach is required. We take g as given in equation (4.5) but use an alternative coefficient numbering scheme thus

$$g(x,y) = x^2 + b_0\,x^3 + b_1\,x^2y + b_2\,xy^2 + b_3\,y^3 + c_0\,x^4 + c_1\,x^3y + c_2\,x^2y^2 + \ldots \quad (4.13)$$

so that b_i $(i = 0\,..\,3)$ is used for the coefficients of the cubic terms, c_j $(j = 0\,..\,4)$ is used for the coefficients of the quartic terms etc. So, from our earlier definitions, if $b_3 = 0$ then $\mathbf{0}$ on N is a cusp of Gauss. The cusp of Gauss is non-degenerate if ${b_2}^2 \neq 4c_4$ and ordinary if also $b_2 \neq 0$.

If we let $F(s,t,u,v) = g_x(s,t) - g_x(u,v)$ and $G(s,t,u,v) = g_y(s,t) - g_y(u,v)$ then

$$F = (\,2s + 3b_0s^2 + 2b_1st + b_2t^2 + \ldots\,) - (\,2u - 3b_0u^2 - 2b_1uv - b_2v^2 - \ldots\,) = 0$$

whence it is clear by the implicit function theorem that we can write $s = s(t,u,v)$ or $u = u(s,t,v)$ using $F = 0$. If we choose the former and let $G_1(t,u,v) = G(s(t,u,v),t,u,v)$ then $G_1 = 0$ represents a single equation for the parallel tangent set with our troublesome points now being given by $t = v$. We can write

$$s = (s_{100}\,t + s_{010}\,u + s_{001}\,v) + (s_{200}\,t^2 + s_{020}\,u^2 + s_{002}\,v^2 + s_{110}\,tu + s_{101}\,tv + s_{011}\,uv) + \text{h.o.t.}$$

substitute into $F = 0$ and determine the coefficients s_{ijk}. Doing this we obtain

$$s = u + \frac{b_2}{2}\left(v^2 - t^2\right) + b_1\left(uv - tu\right) + \text{h.o.t.} \tag{4.14}$$

and substituting this into G_1 we expect to obtain a result of the form

$$G_1(t,u,v) = (t-v)^k H(t,u,v) = 0 \quad \text{where} \quad k \in \mathbb{N} \text{ and } (t-v) \nmid H \tag{4.15}$$

provided $t = v$ is always a solution of $G_1 = 0$. If we can find such an H then $H = 0$ will be the true parallel tangent set with the $p = q$ points removed. First we show that G_1 must have a factor $(t - v)$ using a variation of the Hadamard lemma (see 'Curves and Singularities' [6], Lemma 4.28(ii), p.86):

Proposition 4.3.1 *Given any smooth function g of three variables, say t, u and v, then $g(t,u,v) = (t-v)\,h(t,u,v)$ for some smooth h, if and only if $g(t,u,t) = 0$.*

Proof: [$\Leftarrow$] Set $x = v - t$ and let $\tilde{g}(t,u,x) = g(t,u,x+t)$. Then $\tilde{g}(t,u,0) = g(t,u,t) = 0$ which implies $\tilde{g}(t,u,x) = x\,\tilde{h}(t,u,x)$ for some smooth function $\tilde{h}$ by Hadamard's lemma, or equivalently $g(t,u,t) = 0$ implies that $g(t,u,v) = (t-v)\,h(t,u,v)$ for some smooth function h. [$\Rightarrow$] follows trivially. □

So we can be assured that G_1 has a factor $(t - v)$ and in fact calculation shows that, $G_1 = (t-v)\left(3b_3t + 2b_2u + 3b_3v + \text{h.o.t.}\right)$ so that $H = 3b_3t + 2b_2u + 3b_3v + \text{h.o.t.}$ since $H(t,u,t) = 6b_3t + 2b_2u + \text{h.o.t.} \neq 0$, i.e. $(t - v)$ is not a factor of H and $k = 1$ in equation (4.15) above. Thus t or v can be expressed uniquely as a smooth function of the other two variables when $b_3 \neq 0$ (i.e. the origin is not a cusp of Gauss). We choose to write $t = t(u,v)$ and find that

$$t = -\frac{2b_2}{3b_3}u - v + \text{h.o.t.}$$

Hence the map $h : (u,v) \mapsto (s,t)$ is of the form

$$h(u,v) = \left(u + \text{h.o.t.}, -\frac{2b_2}{3b_3}u - v + \text{h.o.t.}\right)$$

so that $\det(J_h) = -1$ at the origin and we state:

Proposition 4.3.2 *The map $h : (u,v) \mapsto (s,t)$ is a always a local diffeomorphism when the origin is a parabolic point but not a cusp of Gauss.*

Ordinary Cusp of Gauss Case

When the origin is an ordinary cusp of Gauss then $b_3 = 0$ but $b_2 \neq 0$ and since the change of variable $x \mapsto -x$ takes b_2 to $-b_2$ in equation (4.13), we can assume without loss of generality that $b_2 > 0$. Now $H = 2b_2u + \text{h.o.t.}$ and we can write u as a smooth function of t and v thus

$$u = \frac{{b_2}^2 - 4c_4}{2b_2}\,t^2 + \frac{{b_2}^2 - 4c_4}{2b_2}\,tv - \frac{2c_4}{b_2}\,v^2 + \text{h.o.t.}$$

Our expression for s obtained as equation (4.14) still holds and if we substitute this expression for u into it we obtain

$$s = -\frac{2c_4}{b_2}\,t^2 + \frac{{b_2}^2 - 4c_4}{2b_2}\,tv + \frac{{b_2}^2 - 4c_4}{2b_2}\,v^2 + \text{h.o.t.}$$

We see that the coefficients of the quadratic terms of s are the same as those of u in reverse order. This interesting pattern holds true for the coefficient sets of all orders in the expansions for s and u due to the following symmetry property:

Proposition 4.3.3 *$s(t, v) = u(v, t)$ for all t, v close to $\mathbf{0}$.*

Proof: $(\{a, b\}, \{c, d\}) \in \Pi$ if and only if $(\{c, d\}, \{a, b\}) \in \Pi$ i.e. it doesn't matter in which order we name the two points (a, b) and (c, d). Now $(\{a, b\}, \{c, d\}) \in \Pi$ gives $a = s(b, d)$ and $c = u(b, d)$, whilst $(\{c, d\}, \{a, b\}) \in \Pi$ gives $a = u(d, b)$ and $c = s(d, b)$. The result follows. □

Since s and u are parameterised by t and v the parallel tangent set here is smooth. However, it is clear that the map $h : (t, v) \mapsto (s, u)$ is highly degenerate since it has co-rank 2. Instead we will consider the pair of maps, $F_1 : (t, v) \mapsto (s(t, v), t)$ and $F_2 : (t, v) \mapsto (u(t, v), v)$. Now $F_{1,2}(t, t)$ consists of limit points of the true parallel tangent set which also lie in Δ and so:

Proposition 4.3.4 *The image of the diagonal in the tv-plane under F_1 or F_2 is the parabolic curve on N.*

Proof: We have $g_x(s(t,v),t) = g_x(u(t,v),v)$ and $g_y(s(t,v),t) = g_y(u(t,v),v)$ for all $t, v \in \Pi$. If we differentiate both of these with respect to t and v we obtain

$$\begin{aligned} g_{xx}\, s_t &+ g_{xy} &&= g_{xx}\, u_t \\ g_{xx}\, s_v & &&= g_{xx}\, u_v &+ g_{xy} \\ g_{xy}\, s_t &+ g_{yy} &&= g_{xy}\, u_t \\ g_{xy}\, s_v & &&= g_{xy}\, u_v &+ g_{yy} \end{aligned}$$

but using proposition 4.3.3 with $t = v$ we have $s_t(t,t) = u_v(t,t)$ and $s_v(t,t) = u_t(t,t)$ so the second and fourth expressions above, evaluated at (t,t), are the same as the first and third. Now if we multiply the third by g_{xx} and subtract the first multiplied by g_{xy} we obtain $g_{xx}\, g_{yy} - {g_{xy}}^2 = 0$ as required. □

Considering F_2 then

$$F_2(t,v) = \left(\frac{{b_2}^2 - 4c_4}{2b_2}\, t^2 + \frac{{b_2}^2 - 4c_4}{2b_2}\, tv - \frac{2c_4}{b_2}\, v^2 + \text{h.o.t.},\ v \right)$$

so that $det(J_{F_2}) = 0$ at the origin and $\Sigma_{F_2} = \{(t,v) : u_t = 0\}$, i.e.

$$\Sigma_{F_2} : \frac{{b_2}^2 - 4c_4}{2b_2}\,(2t + v) + \text{h.o.t.} = 0.$$

If the cusp of Gauss is ordinary then ${b_2}^2 \neq 4c_4$ and we can write $\Sigma_{F_2} : v = -2t + \text{h.o.t.}$ so that $F_2|\Sigma_{F_2}$ is an immersion at $\mathbf{0}$. A similar argument holds for the map F_1 where we have $\Sigma_{F_1} = \{(t,v) : s_v = 0\}$ and we state:

Proposition 4.3.5 *For the set of points $p = (s,t,g(s,t))$ and $q = (u,v,g(u,v))$ with parallel tangent planes in the neighbourhood of an ordinary cusp of Gauss on a smooth surface piece $z = g(x,y)$ where g is of the form of equation (4.13) with $b_3 = 0$ then (i) s and u can be written as smooth functions of t and v, and (ii) $F_1 : (t,v) \mapsto (s,t)$ and $F_2 : (t,v) \mapsto (u,v)$ are fold maps.*

For F_1 and F_2 we also have $F_1|\Sigma_{F_1} = F_2|\Sigma_{F_2}$ which is geometrically obvious since this curve represents the boundary of the region on N which contains candidate points for parallel tangent pairs. Hence we define:

Definition 4.3.6 *The Parallel Tangents Boundary Curve (PTBC) is the boundary of the region on N which contains points for which a parallel tangent partner exists.*

The projection of this curve to the parameter plane of N is

$$PTBC = \left(\frac{-{b_2}^2 - 12c_4}{8b_2} v^2 + h.o.t,\, v \right).$$

Arrangement of Special Curves through a Cusp of Gauss

Here we seek to determine the relationship between the PTBC and several other important curves which pass through the cusp of Gauss on N. The curves that we consider are: the Parabolic Curve (PC), the *Flecnodal Curve* (FC) which is the locus of points on M where some tangent line has 4-point (or higher) contact and, the *Bi-tangent Plane Curve* (BPC) which is the locus of points p on N for which there exists a distinct point q with *the same* tangent plane. Calculating parameterisations of the PC and FC projected to the parameter plane of N we obtain

$$PC = \left(\frac{{b_2}^2 - 6c_4}{b_2} v^2 + \text{h.o.t},\, v \right) \text{ and } FC = \left(\frac{2c_4({b_2}^2 - 8c_4)}{{b_2}^3} v^2 + \text{h.o.t},\, v \right).$$

For the BPC we need points $p = (s(t,v),\, t,\, g(s(t,v),t))$ and $q = (u(t,v),\, v,\, g(u(t,v),v))$ on N such that $\gamma = (p-q)\cdot N = 0$ where N is any normal vector at p or q. Calculation shows the series expansion for γ in t and v to be

$$\gamma = \frac{({b_2}^2 - 4c_4)(v-t)^3(v+t)}{4} + \text{h.o.t.}$$

The first term in the numerator here is non-zero when the cusp of Gauss is non-degenerate. The second term defines the diagonal in the tv-parameter plane which we know maps to the parabolic curve under F_1 or F_2 by proposition 4.3.4. For the last factor we seek a solution of $\gamma = 0$ of the form $t = -v + \text{h.o.t.}$ the image of which under F_1 or F_2 must be the BPC by elimination. Calculation shows this to be

$$BPC = \left(-\frac{2c_4}{b_2} v^2 + \text{h.o.t},\, v \right).$$

We can be further assured that $t = -v + \text{h.o.t.}$ is a pre-image of the BPC under F_1 or F_2 by the following proposition:

Proposition 4.3.7 *Let $\Omega = \{(t,v) : F_1(t,v)$ and $F_2(t,v)$ are contact points of a bi-tangent plane to $N\}$ then $(t,v) \in \Omega$ if and only if $(v,t) \in \Omega$.*

Proof: If $\{s = a,\ t = b\}$ is one point of bi-tangency and $\{u = c,\ v = d\}$ is the other in the (s,t) and (u,v) parameter spaces, then $F_1(b,d) = (s(b,d),b) = (u(d,b),b) = F_2(d,b)$ using proposition 4.3.3. Similarly $F_2(b,d) = (u(b,d),d) = (s(d,b),d) = F_1(d,b)$. Hence $(b,d) \in \Omega$ implies $(d,b) \in \Omega$. We now repeat the above starting with the point (d,b) and the result follows. □

We can verify that the pre-BPC has a smooth branch through the origin by:

Proposition 4.3.8 *There is a smooth branch of $\gamma = 0$ tangent to $t + v = 0$.*

Proof: Substituting $x = v - t$ in the expression for γ above we obtain $\gamma = \lambda\, x^3\,(2t + x)$ + h.o.t. where λ is a non-zero constant. We now blow up the origin by means of the substitution $x = ut$. The blowing-down map $(t,u) \mapsto (t,ut) = (t,x)$ is a local diffeomorphism away from the 'exceptional divisor' $t = 0$ (where $(0,u) \mapsto (0,0)$ for all u). The curve $\gamma = 0$ now exists in a new surface on which we can take local coordinates t, u. The exceptional divisor in this coordinate system is the line $t = 0$ and different lines through the origin are now separated (or blown up) to different points on the exceptional divisor. Doing the substitution we obtain

$$\gamma = \lambda\, u^3\, t^4\,(2 + u) + \text{terms in } t,u \text{ all divisible by } t^5.$$

If we now cancel t^4 (the highest power of t to be a factor of the whole of γ) to form the *proper transform* of γ, i.e.

$$\gamma_1 = \lambda\, u^3\,(2 + u) + \text{terms in } t,u \text{ all divisible by } t$$

then $\partial\gamma_1/\partial u$ evaluated at $\{t = 0, u = -2\}$ is $-8\lambda \neq 0$, so by the implicit function theorem there is a smooth branch of $\gamma_1 = 0$ tangent to the line $u = -2$. Under the blow-down map this goes to a smooth branch of $\gamma = 0$ tangent to $2t + x = 0$, or in the original coordinates, $\gamma = 0$ has a smooth branch tangent to $t + v = 0$. □

We now have a form for all four of our special curves on N with the y-component as v and the x-component beginning with a quadratic term in v with a coefficient involving only b_2 and c_4. Hence all of these curves are tangent to the asymptotic direction (i.e. the y–axis in our setup) at the cusp of Gauss. In deciding how these

curves relate to each other on N we need to determine the relative signs and magnitudes of these quadratic coefficients which, using our earlier convention, we will call $C_{PC}(2)$, $C_{FC}(2)$, $C_{PTBC}(2)$ and $C_{BPC}(2)$. Now, since $b_2 > 0$ the BPC lies locally in the upper or lower y half plane depending on the sign of c_4 and we can ignore the effect of the denominators in determining the signs of $C_{PC}(2)$, $C_{FC}(2)$, $C_{PTBC}(2)$ and $C_{BPC}(2)$. Some rudimentary inequality calculations lead to the following:

* $C_{PC}(2) > C_{FC}(2)$,
* $C_{PC}(2) > C_{PTBC}(2)$ when the c.o.G is hyperbolic,
* $C_{PC}(2) < C_{PTBC}(2)$ when the c.o.G is elliptic,
* $C_{FC}(2) > C_{PTBC}(2)$ when the c.o.G is hyperbolic and $c_4/{b_2}^2 < -1/32$, and
* $C_{FC}(2) < C_{PTBC}(2)$ when the c.o.G is elliptic and $c_4/{b_2}^2 > -1/32$.

From these inequalities we find that, regarding the relative signs of $C_{PC}(2)$, $C_{FC}(2)$, $C_{PTBC}(2)$ and $C_{BPC}(2)$, there are only three distinct cases depending on the value of the quotient $c_4/{b_2}^2$ as follows:

Case 1: $c_4/{b_2}^2 < -\frac{1}{12}$. Here the PC and PTBC are always on the same side of the y–axis. Within this region the BPC lies on the same side of the y–axis as the PC but the FC always lies on the opposite side of the y–axis from the PC, e.g. $g(x, y) = x^2 + xy^2 - y^4$ where the PTBC and BPC lie in the hyperbolic region.

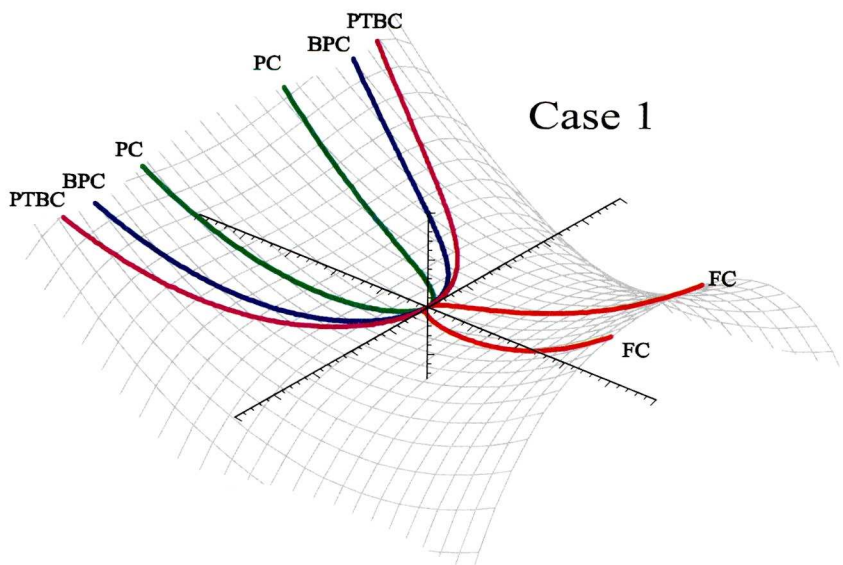

Case 2: $-\frac{1}{12} < {c_4}/{b_2}^2 < \frac{1}{6}$. Here the PC and PTBC are always on opposite sides of the y–axis. Within this region the FC and BPC could lie on either side of the y–axis, e.g. $g(x, y) = x^2 + 4xy^2 + y^4$ where the PTBC and BPC lie in the hyperbolic region.

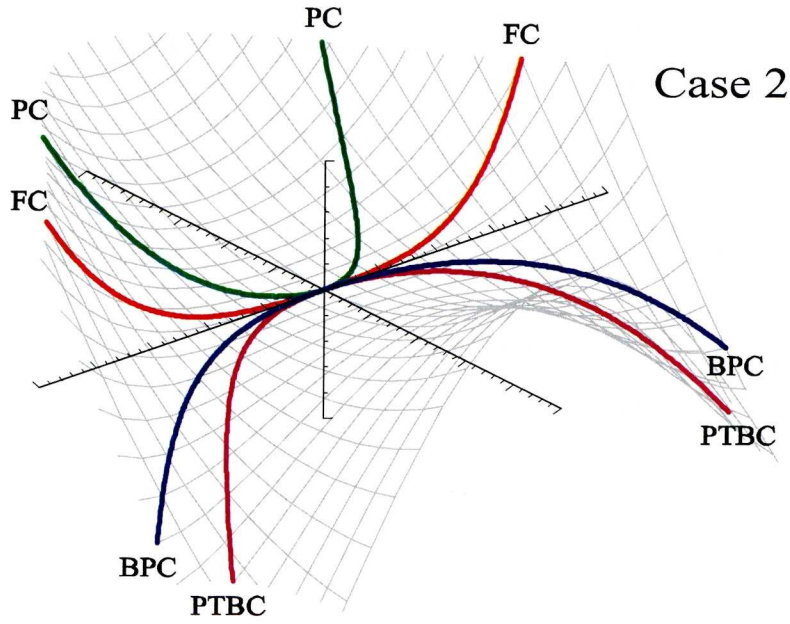

Case 3: $\frac{1}{6} < {c_4}/{b_2}^2$. Here the PC and PTBC are always on the same side of the y–axis. Within this region the FC and BPC both lie on the same side of the y–axis as the PC, e.g. $g(x, y) = x^2 + xy^2 + y^4$ where the PTBC and BPC lie in the elliptic region.

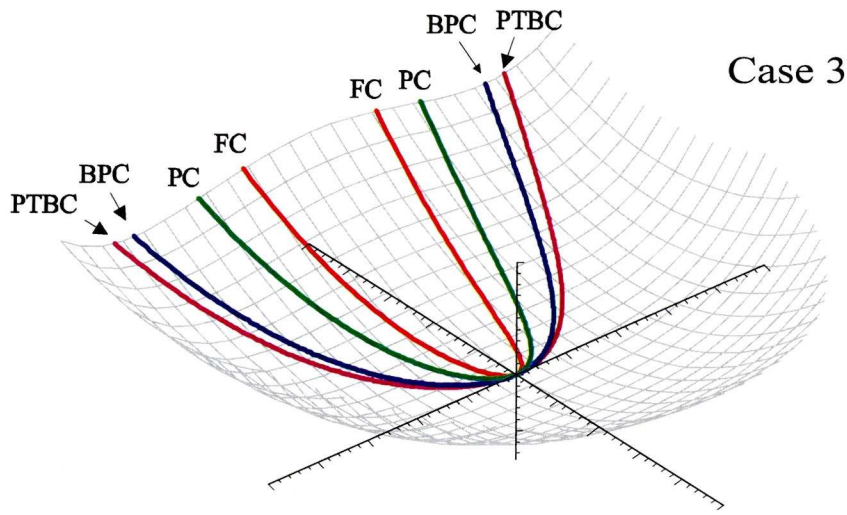

4.4 Chapter Summary

In this chapter we looked at properties of maps linking pairs of surface points with parallel tangent planes. Using local parameterisations (e.g. writing our surfaces as graphs) we denoted these parallel pairs as $p = (s, t, f(s, t))$ and $q = (u, v, g(u, v))$ and the set of all such (non-trivial) pairs as $\Pi = \{(p, q) : T_p \parallel T_q \text{ and } p \neq q\}$. The main objective was to find ways of parameterising Π and we approached this problem from two distinct standpoints: (i) p and q lie on disjoint surfaces, whence the "diagonal" pairs $(p, p) = (q, q)$ cannot exist in Π, and (ii) p and q lie local to, and either side of, the parabolic curve of a single surface piece. Here diagonal pairs do exist in Π in the limit as p and q come into coincidence on the parabolic curve.

For the disjoint case we showed in proposition 4.2.2 that Π is smooth unless both p and q are parabolic and their unique asymptotic directions are parallel. We showed in proposition 4.2.3 that the map $h : (u, v) \mapsto (s, t)$ is a local diffeomorphism when both p and q are non-parabolic, and in proposition 4.2.6 that h is (i) a fold map when one of the points is non-parabolic and the other is ordinary parabolic, and (ii) a cusp map when one of the points is non-parabolic and the other is a cusp of Gauss. In proposition 4.2.8 we found conditions for h to be a lips or beaks map. Finally in proposition 4.2.9 we showed that even when when both p and q are parabolic we can still parameterise Π using one parameter from each of the points (excluding three special cases of the relative asymptotic directions at p and q).

For the local case we showed in proposition 4.3.2 that h is a local diffeomorphism when p and q are not local to a cusp of Gauss. When p and q are local to an ordinary cusp of Gauss we showed in proposition 4.3.5 that we can parameterise Π using one parameter from each of the points and that $F_1 : (t, v) \mapsto (s, t)$ and $F_2 : (t, v) \mapsto (u, v)$ are fold maps. The fold lines of F_1 and F_2 projected onto the surface mark the boundary of the region on the surface for which points have parallel "partners". We called this boundary the Parallel Tangents Boundary Curve (PTBC). Finally we showed how the value of the ratio ${c_4}/{b_2}^2$ affects the relative arrangement of the PTBC, the parabolic curve, the flecnodal curve and the bi-tangent plane curve about a cusp of Gauss.

Chapter 5

The Affine Equidistants

5.1 Introduction

We now consider the *equidistants* of a surface (or surfaces). These are formed by points at a some fixed proportion along chords joining surface points with parallel tangent planes. Since the essential structure of the equidistants depends purely on parallelism they are affine invariants of a surface. If the points of parallel tangency are at p and q then the corresponding equidistant point is given by

$$E_\lambda(p,q) = (1-\lambda)\,p + \lambda\,q$$

where $\lambda \in [0,1]$ is the fixed proportion along the chord. Note that λ and $1-\lambda$ give rise to the same equidistant (since p and q can be interchanged) so that when $\lambda = \frac{1}{2}$ the equidistant has a special symmetry. We call this particular equidistant (which is the 3D analogue of the MPTL discussed in section 2.6) the Mid-Parallel Tangents Surface (MPTS). Its properties will feature heavily throughout this and subsequent chapters.

Note: the 3D equidistants are one of the few affinely invariant symmetry constructions to surfaces that can be computed efficiently. However for the 2D case several other options have been studied, e.g. the Affine Distance Symmetry Set (ADSS), the Affine Envelope Symmetry Set (AESS) and the Affine Area Symmetry Set (AASS). A general review of these constructions is provided in a paper by Giblin [7].

5.2 Disjoint Surfaces

If one of the points of parallel tangency is at $(s,\, t,\, k+f(s,t))$ on M and the other is at $(u\,,v,\, g(u,v))$ on N then the equidistant map $E_\lambda : \mathbb{R}^4 \to \mathbb{R}^3$ is as follows

$$E_\lambda(s,t,u,v) = \Big(\big((1-\lambda)\,s+\lambda\,u,\ (1-\lambda)\,t+\lambda\,v,\ (1-\lambda)\,(k+f(s,t))+\lambda\,g(u,v)\big)\Big)$$

with $\lambda \in \mathbb{R}$ fixed. When $\lambda = \frac{1}{2}$ we have the MPTS and we use the notation $X \equiv E_{\frac{1}{2}}$. First we prove an analogous result to proposition 2.6.3 for curves:

Proposition 5.2.1 *The tangent plane at any smooth point of E_λ is parallel to the tangent planes on M and N which gave rise to that point. Thus E_λ is formed as an envelope of planes parallel to and at a fixed proportion between pairs of parallel tangent planes on M and N.*

Proof: Recall the map π of equation (4.2) and let $\rho = (\alpha, \beta, \gamma, \delta)$ be a non-zero kernel vector of J_π, the Jacobian matrix of π given in equation (4.3). The tangent to E_λ is the image of ρ under the linear map J_X, i.e.

$$J_{E_\lambda}\,\rho = \begin{pmatrix} 1-\lambda & 0 & \lambda & 0 \\ 0 & 1-\lambda & 0 & \lambda \\ (1-\lambda)f_s & (1-\lambda)f_t & \lambda g_u & \lambda g_v \end{pmatrix} \begin{pmatrix} \alpha \\ \beta \\ \gamma \\ \delta \end{pmatrix}$$

$$= \Big((1-\lambda)\alpha+\lambda\gamma,\ (1-\lambda)\beta+\lambda\delta,\ (1-\lambda)\alpha f_s+(1-\lambda)\beta f_t+\lambda\gamma g_u+\lambda\delta g_v\Big).$$

However in the set of pairs of points with parallel tangent planes (i.e. Π) we have $f_s = g_u$ and $f_t = g_v$ so this vector can be written as

$$((1-\lambda)\alpha+\lambda\gamma)(1,0,f_s)+((1-\lambda)\beta+\lambda\delta)(0,1,f_t),\ \text{ or}$$

$$((1-\lambda)\alpha+\lambda\gamma)(1,0,g_u)+((1-\lambda)\beta+\lambda\delta)(0,1,g_v).$$

The first vector is clearly parallel to the tangent plane to M at $(s,t,f(s,t))$ whilst the second is parallel to the tangent plane to N at $(u,v,g(u,v))$. Hence the tangent to E_λ is parallel to the tangent planes at the two points which generated it, and since any smooth surface is the envelope of its tangent planes the result follows. □

Singular Points

We now go on to consider conditions under which E_λ is singular. If we assume that $\pi : \mathbb{R}^4 \to \mathbb{R}^2$ is a submersion (so that Π is smooth) then E_λ fails to be smooth when the 5×4 matrix formed as J_X stacked on top of J_π fails to have maximal rank, i.e.

$$\operatorname{rank} \begin{pmatrix} 1-\lambda & 0 & \lambda & 0 \\ 0 & 1-\lambda & 0 & \lambda \\ (1-\lambda)f_s & (1-\lambda)f_t & \lambda g_u & \lambda g_v \\ f_{ss} & f_{st} & -g_{uu} & -g_{uv} \\ f_{st} & f_{tt} & -g_{uv} & -g_{vv} \end{pmatrix} < 4.$$

Since $f_s - g_u = 0$ and $f_t - g_v = 0$ we can subtract g_u times row 1 from row 3 and g_v times row 2 from row 3 whence row 3 is rendered all zero and can be discarded. We now add column 3 to column 1 and column 4 to column 2 to obtain the following

$$\begin{pmatrix} 1 & 0 & \lambda & 0 \\ 0 & 1 & 0 & \lambda \\ f_{ss} - g_{uu} & f_{st} - g_{uv} & -g_{uu} & -g_{uv} \\ f_{st} - g_{uv} & f_{tt} - g_{vv} & -g_{uv} & -g_{vv} \end{pmatrix}$$

This 4×4 matrix is singular if and only if

$$\Big(\lambda f_{ss} + (1-\lambda)g_{uu}\Big)\Big(\lambda f_{tt} + (1-\lambda)g_{vv}\Big) - \Big(\lambda f_{st} + (1-\lambda)g_{uv}\Big)^2 = 0.$$

If H_f is the Hessian matrix of f and H_g is the Hessian matrix of g then we have:

Proposition 5.2.2 *The equidistant E_λ is smooth at a point $\wp$ when*

$$\det\left[\,\lambda\, H_f + (\,1-\lambda\,)\, H_g\,\right] \neq 0$$

where H_f and H_g are evaluated at the end points of the chord which formed $\wp$.

Example 5.2.3 We will chose simple forms for f and g, enabling us to write down exact expressions for s, t and X as functions of u and v. So we take $f(s,t) = -s^2 - t^2$, $k = 3$ and $g(u,v) = u^2 + 2v^2 + u^3$, so M and N are elliptic at $(0,0,3)$ and $(0,0,0)$ respectively. The MPTS is singular at $(0,0,3/2)$ since

$$(H_f + H_g)(\mathbf{0}) = \begin{pmatrix} 0 & 0 \\ 0 & 4 \end{pmatrix}$$

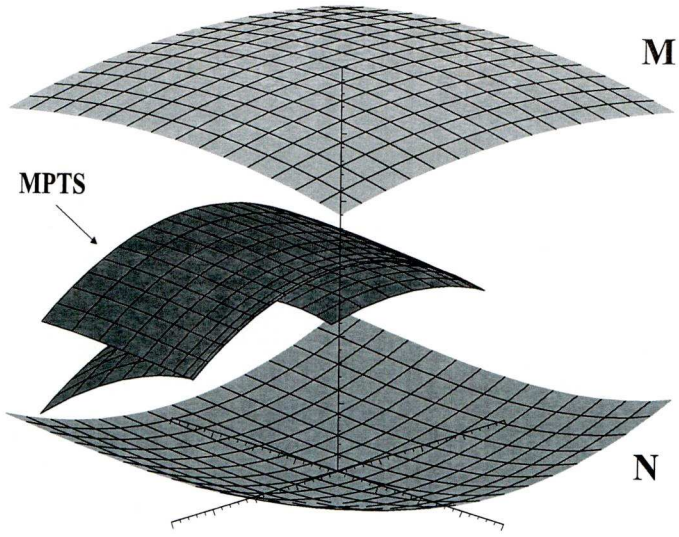

Figure 5.1: The singular MPTS of example 5.2.3.

Calculations give

$$s = -u - \frac{3u^2}{2},\ t = -2v \text{ and } X = \left(-\frac{3u^2}{4}, -\frac{v}{2}, \frac{3}{2} - v^2 - u^3 - \frac{9u^4}{8}\right)$$

whence it is clear that the MPTS is singular at $(0, 0, 3/2)$ since $X_u = (0, 0, 0)$ here. Figure 5.1 shows the two generating surface pieces with the MPTS in-between clearly singular.

Relationship between the MPTS and the CSS

We mentioned the CSS in the introduction to this chapter. Since it is formed as the envelope of chords joining points with parallel tangent planes it is clear that when the envelope point on a given chord is mid-way along the chord then the CSS and MPTS have a common point. Giblin and Zakalyukin [11] give the following method for constructing the CSS:

Let $p \in M$ and $q \in N$ be points with parallel tangent planes, then $r = \lambda p + \mu q$ is on the CSS if and only if $\mu F + \lambda G$ is a degenerate quadratic form. Here F if the matrix of the second fundamental form of M at p, G is the matrix of second fundamental of N at q, and $\lambda + \mu = 1$. An easy consequence of this is the following:

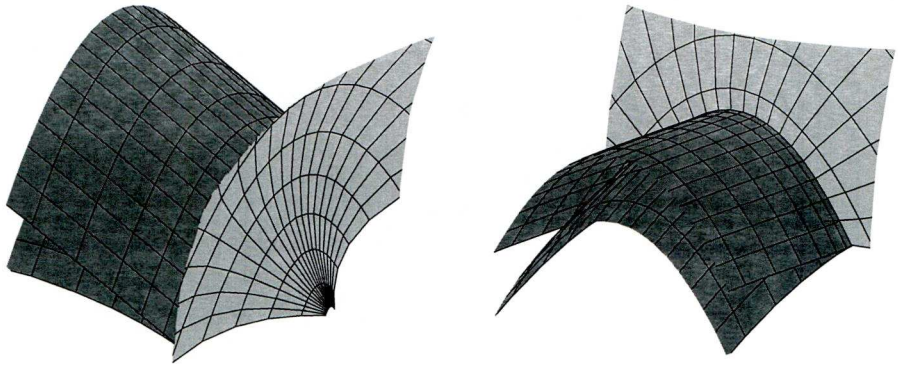

Figure 5.2: Relationship between the MPTS and the CSS from example 5.2.5.

Proposition 5.2.4 *The MPTS and CSS share a point when the MPTS is singular.*

Proof: We can assume without loss of generality that $\mu \neq 0$. Hence $|\mu F + \lambda G| = 0$ if and only if $|F + (\lambda/\mu)G| = 0$. This condition is the same as that of proposition 5.2.2 when $\lambda = \frac{1}{2}$. □

Example 5.2.5 We take the same f, g and k as example 5.2.3 so that the CSS, $B : \mathbb{R}^2 \to \mathbb{R}^3$, can be determined exactly as

$$B(u,v) = \left(\frac{3u^2}{2(2+3u)}, \frac{(3u-1)v}{2+3u}, \frac{4u^3+3u^4-8v^2+12+24v^2u}{4(2+3u)} \right).$$

We observe that $B(0,0) = (0,0,3/2)$, which is a point on the MPTS in this example. Figure 5.2 gives two views of the MPTS (the dark surface) and CSS (the light surface) in a small region around $(0,0,3/2)$. It shows how the CSS contacts the MPTS along its singular edge.

Discriminants and Unfoldings

We have shown that the MPTS can be thought of as the envelope of a certain family of planes related to the two disjoint surface pieces. With this in mind we now regard the MPTS as a discriminant and perform some unfolding calculations to ascertain the nature of its singular points. The close relationship between the MPTS and the CSS means that minor changes to the details in Giblin and Zakalyukin [11] yields the following as a generating function for the MPTS as a discriminant

$$F(s,t,u,v,p,q\,;\,x,y,z) = f(s,t) + g(u,v) + k - 2z + (s+u-2x)\,p + (t+v-2y)\,q.$$

Here $(p, q, 1)$ is an arbitrary direction vector in $\mathbb{R}^3$. Now

$$\mathcal{D}_F = \{(x, y, z) : F = F_s = F_t = F_u = F_v = F_p = F_q = 0 \text{ for some } s, t, u, v, p, q\}.$$

We have $F_s = p + f_s$ and $F_t = q + f_t$ so that $F = F_s = F_t = 0$ gives $(p, q, 1) = (-f_s, -f_t, 1)$, i.e. $(p, q, 1)$ is normal to M. Similarly $F = F_u = F_v = 0$ gives $(p, q, 1) = (-g_u, -g_v, 1)$, i.e. $(p, q, 1)$ is normal to N. Thus the tangent planes at $(s, t, f(s, t)+k)$ and $(u, v, g(u, v))$ are parallel. Finally, $F_p = s + u - 2x$ and $F_q = t + v - 2y$ so $F = F_p = F_q = 0$ gives $(x, y, z) = (\frac{1}{2}(s + u), \frac{1}{2}(t + v), \frac{1}{2}(k + f(s, t) + g(u, v)))$, i.e. the midpoint of the chord joining $(s, t, k + f(s, t))$ to $(u, v, g(u, v))$. Hence $\mathcal{D}_F$ is exactly the MPTS.

We now establish conditions for $F^{-1}(0)$ to be smooth at $(0, 0, 0, 0, 0, 0, 0, 0, k/2)$ in $\mathbb{R}^9$. This is important since if we establish smoothness here then a singularity of the MPTS at $(0, 0, k/2)$ will arise only as a result of the projection of $F^{-1}(0)$ to $\mathbb{R}^3$. Hence we ask; when does $J_* = J(F, F_s, F_t, F_u, F_v, F_p, F_q)$ evaluated at $(0, 0, 0, 0, 0, 0, 0, 0, k/2)$, have maximal rank?

$$J_* = \begin{pmatrix} 0 & 0 & 0 & 0 & 0 & 0 & 0 & 0 & -2 \\ f_{ss} & f_{st} & 0 & 0 & 1 & 0 & 0 & 0 & 0 \\ f_{st} & f_{tt} & 0 & 0 & 0 & 1 & 0 & 0 & 0 \\ 0 & 0 & g_{uu} & g_{uv} & 1 & 0 & 0 & 0 & 0 \\ 0 & 0 & g_{uv} & g_{vv} & 0 & 1 & 0 & 0 & 0 \\ 1 & 0 & 1 & 0 & 0 & 0 & -2 & 0 & 0 \\ 0 & 1 & 0 & 1 & 0 & 0 & 0 & -2 & 0 \end{pmatrix}.$$

Successive row and column operations together with deletion of any row or column with a single non-zero entry (thereby reducing the rank by one) leads to the following reduced matrix

$$\begin{pmatrix} f_{ss} & f_{st} & -g_{uu} & -g_{uv} \\ f_{st} & f_{tt} & -g_{uv} & -g_{vv} \end{pmatrix}.$$

We know by proposition 4.2.2 that this matrix has rank 2 unless both points are parabolic with the same asymptotic direction and so we have:

Proposition 5.2.6 *$F^{-1}(0)$ is smooth at $(0,0,0,0,0,0,0,0,k/2)$ in $\mathbb{R}^9$ provided (i) Either M or N is non-parabolic, or (ii) Both M and N are parabolic but with distinct asymptotic directions.*

Giblin and Zakalyukin [11] give an ingenious method for reducing the number of variables in the generating function F from 6 to 2 (which greatly simplifies the subsequent unfolding calculations). We take, $w_1 = \frac{1}{2}(s+u) - x$, $w_2 = \frac{1}{2}(t+v) - y$, $r_1 = s-u$ and $r_2 = t-v$. Now, solving for s, t, u and v we obtain, $s = w_1 + \frac{1}{2}r_1 + x$, $t = w_2 + \frac{1}{2}r_2 + y$, $u = w_1 - \frac{1}{2}r_1 + x$, and $v = w_2 - \frac{1}{2}r_2 + y$. If we now substitute these into the generating function F we obtain $F_*(\mathbf{r}, \mathbf{w}, \mathbf{x}, p, q) =$

$$f(w_1 + \frac{1}{2}r_1 + x,\ w_2 + \frac{1}{2}r_2 + y) + g(w_1 - \frac{1}{2}r_1 + x,\ w_2 - \frac{1}{2}r_2 + y) - 2z + k + 2w_1p + 2w_2q.$$

If we now take

$$H_*(\mathbf{r}, \mathbf{w}, \mathbf{x}) = f(w_1 + \frac{1}{2}r_1 + x,\ w_2 + \frac{1}{2}r_2 + y) + g(w_1 - \frac{1}{2}r_1 + x,\ w_2 - \frac{1}{2}r_2 + y) - 2z + k$$

then $F_*(\mathbf{r}, \mathbf{w}, \mathbf{x}, p, q) - H_*(\mathbf{r}, \mathbf{0}, \mathbf{x}) = 0$ when $w_1 = w_2 = 0$ so, by Hadamard's lemma,

$$F_*(\mathbf{r}, \mathbf{w}, \mathbf{x}, p, q) - H_*(\mathbf{r}, \mathbf{0}, \mathbf{x}) = w_1(2p + \Phi_1(\mathbf{r}, \mathbf{w}, \mathbf{x})) + w_2(2q + \Phi_2(\mathbf{r}, \mathbf{w}, \mathbf{x}))$$

for some smooth functions Φ_1 and Φ_2. Now if $H(\mathbf{r}, \mathbf{x}) = H_*(\mathbf{r}, \mathbf{0}, \mathbf{x})$, $p' = 2p + \Phi_1(\mathbf{r}, \mathbf{w}, \mathbf{x})$ and $q' = 2q + \Phi_2(\mathbf{r}, \mathbf{w}, \mathbf{x})$ then

$$F_*(\mathbf{r}, \mathbf{w}, \mathbf{x}, p, q) = H(\mathbf{r}, \mathbf{x}) + w_1\, p' + w_2\, q'.$$

Finally, $w_1\, p' + w_2\, q'$ is a non-degenerate quadratic form when $w_1 = w_2 = p' = q' = 0$, so the discriminants of F_* and H are diffeomorphic. Hence for the MPTS we can use H, a three parameter family of functions of two variables, to determine conditions for singular points, and to determine if these are versally unfolded by the family H.

Note: Since the direct calculations which we now describe are very involved we will restrict our investigation to A_2 and A_3 singular points of the MPTS. Later in the chapter, when we consider the local case, we will have access to *normal forms* (i.e. simplest possible versal families) for a number of singularity types, but at the time of writing such normal forms had not been determined in the disjoint surfaces case.

The A_2 Singularity

We have the family of functions, $H(\mathbf{r}, \mathbf{x}) = f(\frac{1}{2}r_1 + x, \frac{1}{2}r_2 + y) + g(-\frac{1}{2}r_1 + x, -\frac{1}{2}r_2 + y) - 2z + k$, and are interested in a singular member of this family when $(x, y, z) = (0, 0, k/2)$, i.e. $h(r_1, r_2) = f(\frac{1}{2}r_1, \frac{1}{2}r_2) + g(-\frac{1}{2}r_1, -\frac{1}{2}r_2)$. To simplify matters and also avoid the use of subscripts we will use the change of variables $r = r_1/2$ and $s = r_2/2$ in the equation for H. Thus

$$H(r, s, x, y, z) = f(r + x, s + y) + g(-r + x, -s + y) - 2z + k$$

and $h(r, s) = f(r, s) + g(-r, -s)$. If we take a general Monge form for the parallel tangency point on N then

$$g(x, y) = (g_{20}\, x^2 + g_{11}\, xy + g_{02}\, y^2) + (g_{30}\, x^3 + g_{21}\, x^2 y + g_{12}\, xy^2 + g_{03}\, y^3) + \text{h.o.t.}$$

and rotate in the z–axis so that the principal directions at the parallel tangency point on M align with the x and y axes then

$$f(x, y) = (a\, x^2 + b\, y^2) + (f_{30}\, x^3 + f_{21}\, x^2 y + f_{12}\, xy^2 + f_{03}\, y^3) + \text{h.o.t.}$$

Thus (after the change of variables $x \mapsto r$, $y \mapsto s$) we have

$$h(r, s) = (a + g_{20})\, r^2 + g_{11}\, rs + (b + g_{02})\, s^2 + (f_{30} - g_{30})\, r^3 + (f_{21} - g_{21})\, r^2 s + \ldots$$

Now h is $A_{\geq 2}$ singular if and only if its quadratic terms are a perfect square, i.e.

$$\zeta = {g_{11}}^2 - 4(a + g_{20})(b + g_{02}) = 0.$$

We may assume without loss of generality that $a + g_{20} \neq 0$ (otherwise $b + g_{02} \neq 0$ and we use the change of variables $x \mapsto y$, $y \mapsto x$) so that we can apply a change of variables $(r, s) \mapsto (r', s)$ where $r' = r + g_{11}s/(2(a + g_{20}))$ giving

$$h(r', s) = (a + g_{20}){r'}^2 + \text{h.o.t.}$$

The singularity will be exactly A_2 provided r' does not divide the cubic terms of $h(r', s)$, i.e. the coefficient of s^3 in the expansion of $h(r', s)$ is non-zero. Calculations show this coefficient to be

$$\eta = (f_{03} - g_{03}) - \left(\frac{f_{12} - g_{12}}{2\,(a + g_{20})}\right) g_{11} + \left(\frac{f_{21} - g_{21}}{4\,(a + g_{20})^2}\right) {g_{11}}^2 - \left(\frac{f_{30} - g_{30}}{8\,(a + g_{20})^3}\right) {g_{11}}^3.$$

Hence the function h has an A_2 singularity if and only if $\zeta = 0$ and $\eta \neq 0$. Note: we do not know of any geometrical significance of this expression for η.

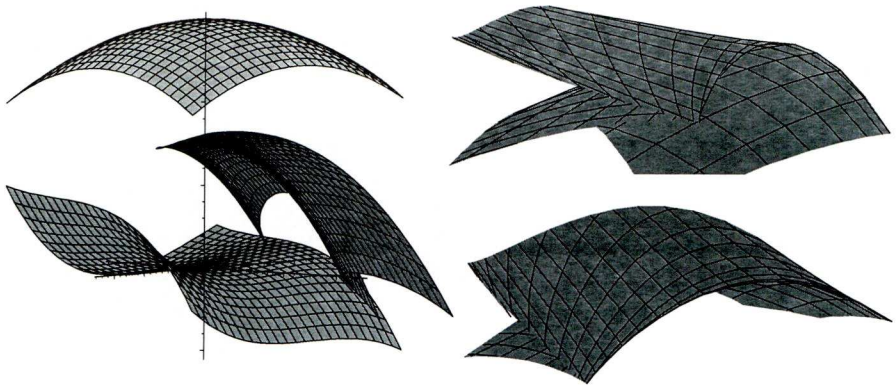

Figure 5.3: The MPTS of example 5.2.7.

Example 5.2.7 If we take $k = 3$, $f(x, y) = -x^2 - y^2$ and $g(x, y) = -x^2 + y^2 + x^3 + xy^2 + y^3$ then $\zeta = 0$ and $\eta = -1$. Hence we expect the MPTS in this example to have an A_2 singularity at $(0, 0, 3/2)$. The left half of figure 5.3 shows the two surface pieces M and N with the MPTS in-between. The right half shows two views of the MPTS in a small region around $(0, 0, 3/2)$ displaying what looks like a cuspidal edge. An unfolding calculation will be required to verify if this is the case.

We now seek to determine if the family H versally unfolds an A_2 singularity of h when $r = s = 0$. This will be the case provided the quotient, $\mathcal{E}_2/J_h$, is spanned as a real vector space by the 'initial velocities': H_x, H_y and H_z evaluated at $(0, 0, k/2)$. Here $\mathcal{E}_2$ is the ring of all smooth function germs in two variables vanishing at the origin and J_h is the Jacobian ideal of h over $\mathcal{E}_2$, i.e. $J_h = \{fh' : f \in \mathcal{E}_2\}$. We can use the general result that an A_n singularity is $(n + 1)$–determined. This means that we can work in L_2^n, the vector space of $(n + 1)$–jets of members of $\mathcal{E}_2$, rather than $\mathcal{E}_2$ itself. Hence, if $J_h = \{fh_r + gh_s : f, g \in L_2^n\}$ together with linear combinations of (the 2-jets of) H_x, H_y and H_z evaluated at $(0, 0, k/2)$ give us all monomials in r and s up to degree three, then H is versal.

Immediately we note that $H_z \mid_{(0,0,k/2)} = -2$, so we have the constant term and can now discount it from further considerations. We seek a 9×9 matrix Γ with non-zero determinant whose columns represent the monomials r, s, r^2, rs, s^2, r^3, r^2s, rs^2 and s^3 and whose rows represent linear combinations of members of J_h together with H_x and H_y evaluated at $(0, 0, k/2)$. The matrix entries represent the coefficients of the various

monomials in each linear combination. If we take h_r, $H_y \mid_{(0,0,k/2)}$, rh_r, sh_r, h_s, r^2h_r, rsh_r, s^2h_r and sh_s as the nine row entries then $\Gamma =$

$$\begin{pmatrix}
2(a+g_{20}) & g_{11} & 3(f_{30}-g_{30}) & 2(f_{21}-g_{21}) & f_{12}-g_{12} & 4(f_{40}+g_{40}) & 3(f_{31}+g_{31}) & 2(f_{22}+g_{22}) & f_{13}+g_{13} \\
-g_{11} & 2(b-g_{02}) & f_{21}+g_{21} & 2(f_{12}+g_{12}) & 3(f_{03}+g_{03}) & f_{31}-g_{31} & 2(f_{22}-g_{22}) & 3(f_{13}-g_{13}) & 4(f_{04}+g_{04}) \\
0 & 0 & 2(a+g_{20}) & g_{11} & 0 & 3(f_{30}-g_{30}) & 2(f_{21}-g_{21}) & f_{12}-g_{12} & 0 \\
0 & 0 & 0 & 2(a+g_{20}) & g_{11} & 0 & 3(f_{30}-g_{30}) & 2(f_{21}-g_{21}) & f_{12}-g_{12} \\
g_{11} & 2(b+g_{02}) & f_{21}-g_{21} & 2(f_{12}-g_{12}) & 3(f_{03}-g_{03}) & f_{31}+g_{31} & 2(f_{22}+g_{22}) & 3(f_{13}+g_{13}) & 4(f_{04}+g_{f04}) \\
0 & 0 & 0 & 0 & 0 & 2a+2g20 & g11 & 0 & 0 \\
0 & 0 & 0 & 0 & 0 & 0 & 2(a+g_{20}) & g_{11} & 0 \\
0 & 0 & 0 & 0 & 0 & 0 & 0 & 2(a+g_{20}) & g_{11} \\
0 & 0 & 0 & g_{11} & 2(b+g_{02}) & 0 & f_{21}-g_{21} & 2(f_{12}-g_{12}) & 3(f_{03}-g_{03})
\end{pmatrix}$$

Since $a + g_{20} \neq 0$ we can use $\zeta = 0$ to write $g_{02} = -b + {g_{11}}^2/(4(a + g_{20})$ whence $\det(\Gamma) = 2304\, b\, \eta^2\, (a + g_{20})^6$. We can assume, without loss of generality, that M is non-parabolic so that $a \neq 0$ and $b \neq 0$. If h is exactly A_2 then $\eta \neq 0$ so $\det(\Gamma) \neq 0$ and we state:

Proposition 5.2.8 *For generic surface pieces M and N then H versally unfolds an A_2 singularity of h when at least one of the points of parallel tangency is non-parabolic. Consequently when also $\zeta = 0$ and $\eta \neq 0$ (as given above) the MPTS is diffeomorphic to a cuspidal edge.*

Example 5.2.9 Returning to example 5.2.7 we have $g_{20} = -1$, $a = b = -1$ and $\eta = -1$ so that $\det(\Gamma) = -147456 \neq 0$ and we confirm that the MPTS of this example has a cuspidal edge through the point $(0, 0, k/2)$.

The A_3 Singularity

The function h has an $A_{\geq 3}$ singular point when $\eta = 0$ so that $(r')^2$, the repeated linear term which forms the quadratic part of h, divides the cubic part. If $a + g_{20} \neq 0$ we can carry out another change of variables, $(r', s) \mapsto (r'', s)$, to absorb the cubic terms into the quadratic. We take $r'' = r' + (\theta_0\, (r')^3 + \theta_1\, (r')^2 s + \theta_3\, r' s^3)/2$ where the θ_i's are expressions in the coefficients of the Taylor expansions of f and g, whence

$$h(r'', s) = (a + g_{20})\, (r'')^2 + \{\text{terms of degree} \geq 4\}.$$

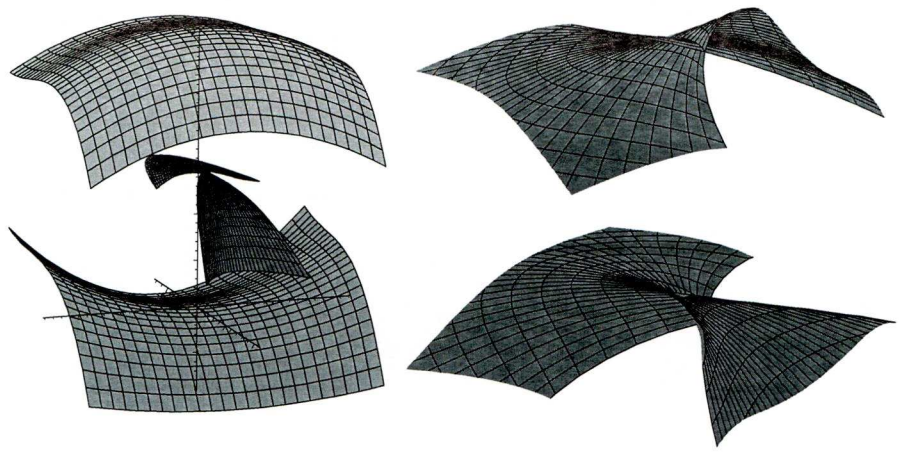

Figure 5.4: The MPTS of example 5.2.10.

The singularity will be exactly A_3 provided r'' does not divide the quartic terms of $h(r'', s)$, i.e. the coefficient of s^4 in the expansion of $h(r'', s)$ is non-zero.

Calculations show this coefficient to be $\xi =$

$$\frac{(4\,(g_{40}+f_{40})(a+g_{20})-9\,(f_{30}-g_{30})^2)\,{g_{11}}^4}{64\,(a+g_{20})^5}+\frac{(3\,(f_{21}-g_{21})(f_{30}-g_{30})-(g_{31}+f_{31})(a+g_{20}))\,{g_{11}}^3}{8\,(a+g_{20})^4}$$

$$+\frac{(-2\,(f_{21}-g_{21})^2-3\,(f_{30}-g_{30})(f_{12}-g_{12})+2\,(g_{22}+f_{22})(a+g_{20}))\,{g_{11}}^2}{8\,(a+g_{20})^3}$$

$$\frac{(-(f_{12}-g_{12})(f_{21}-g_{21})+(g_{13}+f_{13})(a+g_{20}))\,g_{11}}{2\,(a+g_{20})^2}+\frac{-(f_{12}-g_{12})^2+4\,(g_{04}+f_{04})(a+g_{20})}{4\,(a+g_{20})}$$

and when $a+g_{20} \neq 0$ the function h has an A_3 singularity if and only if $\zeta = \eta = 0$ and $\xi \neq 0$. Note: As with the expression for η above we do not know of any geometrical significance of this expression.

Example 5.2.10 If we take $k = 3$, $f(x, y) = -x^2 - y^2 + x^3$ and $g(x, y) = -x^2 + y^2 + x^3 - xy^2$ then $\zeta = \eta = 0$ and $\xi = 1/8 \neq 0$. Hence we expect the MPTS in this example to have an A_3 singularity at $(0, 0, 3/2)$. The left half of figure 5.4 shows the two surface pieces M and N with the MPTS in-between. The right half shows two views of the MPTS in a small region around $(0, 0, 3/2)$ displaying what looks like a swallowtail. Again, unfolding calculations will be required to verify if this is the case.

The unfolding calculation here is more complicated since we must consider monomials up to and including degree four. As before $H_z \,|_{(0,0,k/2)}$ gives us the constant term and we seek a 14×14 matrix Δ with non-zero determinant whose columns

represent the monomials r, s, r^2, rs, s^2, r^3, r^2s, rs^2, s^3, r^4, r^3s, r^2s^2, rs^3 and s^4 and whose rows represent linear combinations of members of J_h together with H_x and H_y evaluated at $(0,0,k/2)$. We start with a 14×18 matrix whose rows are made up by: H_x, H_y, h_r, $h_s - g_{11}h_r/(2(a+g20))$, rh_r, $rh_s - g_{11}rh_r/(2(a+g20))$, sh_r, $sh_s - g_{11}sh_r/(2(a+g20))$, r^2h_r, $r^2h_s - g_{11}r^2h_r/(2(a+g20))$, rsh_r, $rsh_s - g_{11}rsh_r/(2(a+g20))$, s^2h_r, $s^2h_s - g_{11}s^2h_r/(2(a+g20))$, r^3h_r, r^2sh_r, rs^2h_r and s^3h_r. We now impose the conditions $\zeta = \eta = 0$ and perform separate Gaussian eliminations for the cases (i) $g_{11} \neq 0$ and (ii) $g_{11} = 0$. In either case we are left with an 18×14 matrix the first fourteen rows of which are upper diagonal with the last four rows being all zero. We take Δ as these first fourteen rows and find that for case (i) $\det(\Delta) = g_{11}\,\xi^2\,\sigma_1/(2\,(a+g_{20})^8)$ where

$$\sigma_1 = \{a\,f_{21}\}\,{g_{11}}^3 + 2\,\{3\,b\,(a\,g_{30} - f_{30}\,g_{20}) - 2\,a\,f_{12}\,(a+g_{20})\}\,{g_{11}}^2 +$$

$$4\,(a+g_{20})\{3\,a\,f_{03}(a+g20) - 2\,b\,(a\,g_{21} + f_{21}\,g_{20})\}\,g_{11} + 8\,b(a+g_{20})^2\{a\,g_{12} + f_{12}\,g_{20}\}$$

whilst for case (ii) $\det(\Delta) = -8\,b\,\xi^2\,\sigma_2/(a+g_{20})^5$ where $\sigma_2 = a\,g_{12} + f_{12}\,g_{20}$. We can assume, without loss of generality, that M is non-parabolic so that $a \neq 0$ and $b \neq 0$. If h is exactly A_3 then $\xi \neq 0$ so $\det(\Delta) \neq 0$ when $\sigma_{1,2} \neq 0$ and we state:

Proposition 5.2.11 *For generic surface pieces M and N then H versally unfolds an A_3 singularity of h when at least one of the points of parallel tangency is non-parabolic and (i) $\sigma_1 \neq 0$ when $g_{11} \neq 0$ or (ii) $\sigma_2 \neq 0$ when $g_{11} = 0$. Consequently when also $\zeta = \eta = 0$ and $\xi \neq 0$ (as given above) the MPTS is diffeomorphic to an ordinary swallowtail.*

Example 5.2.12 Returning to example 5.2.10 we have $g_{11} = 0$, $b = -1$, $\xi = 1/8$ and $\sigma_2 = 1$ so that $\det(\Delta) = -\frac{1}{256} \neq 0$ and we confirm that the MPTS of this example has a swallowtail at the point $(0,0,k/2)$.

Both points Parabolic

We have seen that both the A_2 and A_3 versal unfolding criteria require at least one of the surface pieces to be non-parabolic. However, if both M and N are parabolic then we know by proposition 4.2.9 that, in general, we can write t and u as smooth

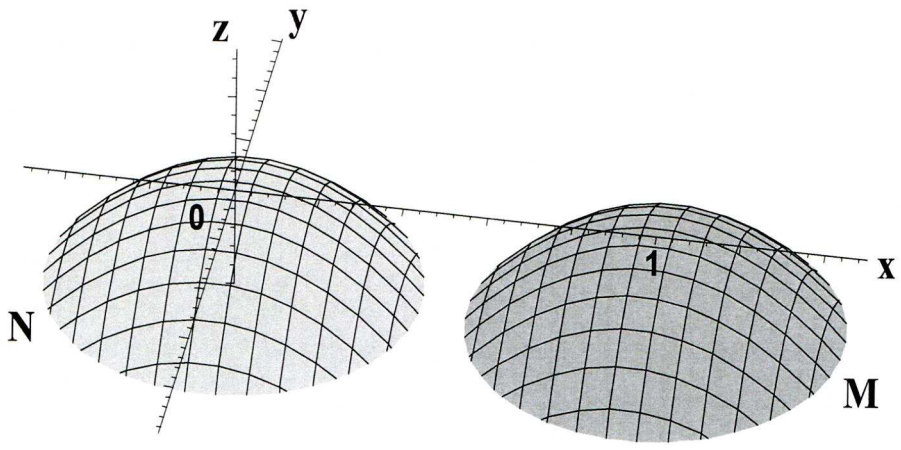

Figure 5.5: Geometrical setup for bi-tangent plane case.

functions of s and v and that the map $h : (s, v) \mapsto (t, u)$ is a fold. Calculating the components of the MPTS in this case we obtain

$$X : (s, v) \mapsto \left(\frac{s}{2} + O(2), \frac{v - as}{2} + O(2), \frac{k}{2} + O(3) \right)$$

whence it is clear that J_X has maximal rank when $s = v = 0$ and we state:

Proposition 5.2.13 *If both M and N are parabolic and certain conditions are satisfied (as stated in proposition 4.2.9) then the MPTS is always smooth.*

Bi-tangent Planes and Ruled Surfaces

We now consider the possibility that the points of parallel tangency on M and N can share the **same** tangent plane. For a standard geometry here we translate and rotate so that the point of interest on N lies at the origin with the xy–plane tangent here. We then rotate about the z–axis and re-scale in the x-direction so that the point of interest on M lies at the point $(1, 0, 0)$. Clearly the tangent plane to M at $(1, 0, 0)$ is the same as that to N at the origin and f and g will both have the general Monge form of equation (4.6). We have $M : (s, t) \mapsto (s + 1, t, f(s, t))$ and $N : (u, v) \mapsto (u, v, g(u, v))$ with $f_s = f_t = 0$ when $s = t = 0$ and $g_u = g_v = 0$ when $u = v = 0$. The geometry is shown schematically in figure 5.5. The map π relating pairs of points on M and N with parallel tangent planes is as before whilst the MPTS map is, $X : (s, t, u, v) \mapsto \left(\frac{1}{2}(s + 1 + u), \frac{1}{2}(t + v), \frac{1}{2}(f(s, t) + g(u, v))\right)$. Minor changes

to the generating function F described above gives

$$F = f(s,t) + g(u,v) - 2z + (s+1+u-2x)\,p + (t+v-2y)\,q \tag{5.1}$$

for which $\mathcal{D}_F$ is exactly the MPTS. Also, we can reduce from 6 variables to 2 by taking $w_1 = \frac{1}{2}(s+1+u) - x$, $w_2 = \frac{1}{2}(t+v) - y$, $r_1 = s - u$ and $r_2 = t - v$. This leaves us, up to diffeomorphism, with the same function $h(r_1, r_2) = f(r_1, r_2) + g(-r_1, -r_2)$ so that the A_2 and A_3 conditions are exactly the same as before. However, our main aim here is to study the relationship between a certain *ruled surface* (i.e. a surface swept out by a line moving in space) and the MPTS. The ruled surface in question, which we will call R, is formed by chords of contact of points with the same tangent plane on M and N (Note: in this section we will, rather loosely, use R and X to refer to both a map and its image in $\mathbb{R}^3$). To formulate R we need pairs of points $p = (s+1, t, f(s,t))$ on M and $q = (u, v, g(u,v))$ on N with parallel tangent planes but with the additional condition that $(p-q)\cdot N = 0$, where N is any normal vector at p or q. If we write s and t as functions of u and v in the usual manner then the condition $(p-q)\cdot N = 0$ gives us a relationship between u and v. Solving this for u as a function of v, say $u = u^*(v)$, then we can parameterise R as follows

$$R : (v,w) \mapsto \{1-w\}\,(u^*,\, v,\, g^*) + \{w\}\,(s^*+1,\, t^*,\, f^*)$$

where $g^* = g(u^*, v)$, $s^* = s(u^*, v)$, $t^* = t(u^*, v)$ and $f^* = f(s^*, t^*)$. The parameter w ranges over $\mathbb{R}$ with $w = 1$ giving the point p and $w = 0$ giving the point q. In what follows we will be interested in the structure of both X and R at the point $(\frac{1}{2}, 0, 0)$. On R this corresponds to $v = 0, w = \frac{1}{2}$ and if we evaluate the Jacobian of R here we obtain

$$J_R = \begin{pmatrix} 1 & * \\ 0 & \frac{4\,f_{20}\,g_{20}\,(f_{02}+g_{02}) - g_{20}\,{f_{11}}^2 - f_{20}\,{g_{11}}^2}{2\,g_{20}\,(4\,f_{02}\,f_{20} - {f_{11}}^2} \\ 0 & 0 \end{pmatrix}$$

where $*$ is some expression in the coefficients f_{ij}, g_{ij}. So J_R has maximal rank and R is smooth at $(\frac{1}{2}, 0, 0)$ when

$$g_{20}\,{f_{11}}^2 + f_{20}\,{g_{11}}^2 \neq 4\,f_{20}\,g_{20}\,(f_{02} + g_{02}).$$

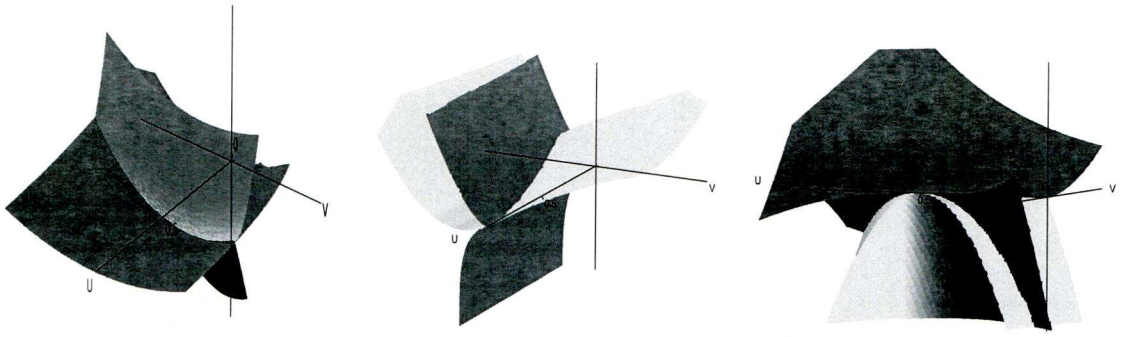

(i) X singular, R smooth (ii) X smooth, R singular (iii) X singular, R singular

Figure 5.6: In each case the lighter surface is the mid-parallel tangents surface X, whilst the darker surface is the ruled-surface R.

A similar calculation shows that J_X has maximal rank when

$$(f_{11} + g_{11})^2 \neq 4\,(f_{20} + g_{20})\,(f_{02} + g_{02}).$$

So we can clearly find examples where X is singular and R is smooth (and vice-versa) or where both are singular:

Example 5.2.14 (a) With $f = s^2 + \frac{1}{8}t^2$, $g = u^2 + u\,v + u^2\,v$ we have X singular and R smooth. See figure 5.6(i). (b) With $f = -s^2 + t^2$, $g = \frac{1}{2}u^2 + 2\,u\,v + v^2 + u^3 + u\,v^2 + v^3$ we have X is smooth and R singular. See figure 5.6(ii) (c) With $f = -s^2 - t^2$, $g = -u^2 + v^2 + u^3 + u\,v^2 + v^3$ we have X and R both singular. See figure 5.6(iii).

The above example is interesting in that the ruled surface appears (like the MPTS) to have cuspidal edges, and so we are motivated to find a generating function for it. Giblin and Zakalyukin [11] looked at bi-tangent chords in relation to the CSS and some minor modifications of their generating family yields $G(s, t, u, v, w, m, n\,;\, x, y, z) =$

$$wf + (1 - w)g - z + \{(s + 1)w + (1 - w)u - x\}m + \{wt + (1 - w)v - y\}n \quad (5.2)$$

where $(m, n, 1)$ is an arbitrary direction vector in $\mathbb{R}^3$. Simple calculations show that (i) $G = \partial G/\partial s = \partial G/\partial t = 0$ and $G = \partial G/\partial u = \partial G/\partial v = 0$ imply that the tangent planes at p and q are parallel, (ii) $G = \partial G/\partial m = \partial G/\partial n = 0$ implies that (x, y, z) is somewhere on the line through p and q (dependent on the value of w) and (iii) $G = \partial G/\partial w = 0$ implies that $(s + 1 - u,\, t - v,\, f - g) \cdot (m, n, 1) = 0$. Hence we have:

Proposition 5.2.15 *The discriminant $\mathcal{D}_G$ of the family of functions G is exactly the ruled surface described by R.*

Note: This holds only when we keep away from the end points of the chords since here $\mathcal{D}_G$ includes the surface itself. However the existence of this generating function shows that R can be regarded as a discriminant and that we can expect to see wave-front type singularities away from the end points of chords. As before a change of variables enables us to extract a non-degenerate quadratic form, simplifying G as follows

$$\tilde{G} = wf(x+w-\frac{1}{2}+\{1-w\}u, y+\{1-w\}u)+\{1-w\}g(x+w-\frac{1}{2}-wu, y-wu)-z.$$

Thus for R we could use the generating function $\tilde{G}$ of three parameters (x, y and z) and three variables (u, v and w) to determine conditions for A_2 and A_3 singularities and find versal unfolding criteria.

Common Tangent Line to X and R

In figure 5.6(iii) it looks like the respective cuspidal edges of R and X have the same limiting tangent direction at $(\frac{1}{2}, 0, 0)$. To investigate this we need some machinery which we now describe in a more general setting: Let $\mathcal{F} : \mathbb{R}^3 \times \mathbb{R}^k \mapsto \mathbb{R}^{k+1}$ be such that $\mathcal{F}(x, y, z\,;\, u_1, u_2, ..., u_k) = (F, F_{u_1}, F_{u_2}, ..., F_{u_k})$. Here x, y and z are the three unfolding parameters whilst u_1 to u_k are variables.

Let π be the projection map from $\mathbb{R}^{k+3}$ to $\mathbb{R}^3$. If we assume that $\mathcal{F}^{-1}(\mathbf{0})$ is a smooth surface $\mathcal{M} \subset \mathbb{R}^{k+3}$, with $\Sigma_{\pi|\mathcal{M}}$ smooth and $\pi|\Sigma_\pi$ an immersion (since we are looking at cuspidal edges), then the critical locus of $\pi(\mathcal{M})$ will be smooth. This critical set is found by stacking $J_\mathcal{F}$ and J_π to give a $k+4$ by $k+3$ matrix, say A, where

$$A = \begin{pmatrix} F_x & F_y & F_z & F_{u_1} & \cdots & F_{u_k} \\ F_{u_1x} & F_{u_1y} & F_{u_1z} & F_{u_1u_1} & \cdots & F_{u_1u_k} \\ \vdots & \vdots & \vdots & \vdots & \vdots & \vdots \\ \vdots & \vdots & \vdots & \vdots & \vdots & \vdots \\ F_{u_kx} & F_{u_ky} & F_{u_kz} & F_{u_ku_1} & \cdots & F_{u_ku_k} \\ 1 & 0 & 0 & 0 & \cdots & 0 \\ 0 & 1 & 0 & 0 & \cdots & 0 \\ 0 & 0 & 1 & 0 & \cdots & 0 \end{pmatrix}.$$

To find $\det(A)$ we can simplify considerably since the last k entries on the top row are all zero (as we are in $\mathcal{F}^{-1}(\mathbf{0})$) and we can use the bottom 3 rows to render everything in columns 1 to 3 to zero for rows 1 to $k+1$. Hence we can discard the top row to leave the following $k+3 \times k+3$ matrix

$$\begin{pmatrix} 0 & 0 & 0 & \mathbf{F_{u_1u_1}} & \cdots & \mathbf{F_{u_1u_k}} \\ \vdots & \vdots & \vdots & \vdots & \vdots & \vdots \\ \vdots & \vdots & \vdots & \vdots & \vdots & \vdots \\ 0 & 0 & 0 & \mathbf{F_{u_ku_1}} & \cdots & \mathbf{F_{u_ku_k}} \\ 1 & 0 & 0 & 0 & \cdots & 0 \\ 0 & 1 & 0 & 0 & \cdots & 0 \\ 0 & 0 & 1 & 0 & \cdots & 0 \end{pmatrix}.$$

The determinant of this matrix ($= \det(A)$) is just the determinant of the sub-matrix marked in bold, i.e. the hessian of F with respect to the variables u_1 to u_k. If $\Delta = \det(A)$ then we can now state:

Proposition 5.2.16 *The critical set of $\pi(\mathcal{M})$ is given by $\tilde{\mathcal{F}}^{-1}(\mathbf{0})$ where $\tilde{\mathcal{F}} : \mathbf{x}, \mathbf{u} \mapsto \mathcal{F}, \Delta$. Moreover, if $J_{\tilde{\mathcal{F}}}$ has maximal rank then a non-zero kernel vector, after projection to $\mathbb{R}^3$, will be tangent to the cuspidal edge.*

If we apply this proposition to the MPTS, so that $k = 6$ and F is given by equation (5.1), then the kernel of $J_{\tilde{\mathcal{F}}}$ after projection to $\mathbb{R}^3$ (i.e. discard all but the first three components) is the tangent to the cuspidal edge given by

$$(\, {g_{11}}^2 + f_{11}\, g_{11} - 4\, g_{02}\, (f_{20} + g_{20}),\; 2\, (f_{20}\, g_{11} - g_{20}\, f_{11}),\; 0\,)$$

as a direction vector. Applying the proposition to the ruled surface, so that $k = 7$ and $F = G$ as given by equation (5.2), then the kernel of $J_{\tilde{G}}$ after projection to $\mathbb{R}^3$ is the tangent to the cuspidal edge given by ($\mathcal{P}$, 0, 0) as a direction vector[1].

Example 5.2.17 Returning to example 5.2.14(c) where $f = -s^2 - t^2$ and $g = -u^2 + v^2 + u^3 + u\,v^2 + v^3$ then $f_{20}\,g_{11} = g_{20}\,f_{11} = 0$ and $\mathcal{P} \neq 0$ so the tangent to the cuspidal edge on both the MPTS and the ruled surface at $(\frac{1}{2}, 0, 0)$ is in the direction $(1, 0, 0)$, as anticipated.

We might wonder what an example looks like with different tangent directions to the cuspidal edges, however, if we simultaneously solve the two singularity conditions for X and R at the point $(\frac{1}{2}, 0, 0)$, i.e.

$$R \text{ singular} \;\Leftrightarrow\; g_{20}\,{f_{11}}^2 + f_{20}\,{g_{11}}^2 = 4\,f_{20}\,g_{20}\,(f_{02} + g_{02})$$

$$X \text{ singular} \;\Leftrightarrow\; (f_{11} + g_{11})^2 = 4\,(f_{20} + g_{20})\,(f_{02} + g_{02})$$

we find that both are singular $\Leftrightarrow g_{20}\,f_{11} - f_{20}\,g_{11} = 0$. This is a factor of the second component of the tangent vector to X hence we confirm:

Proposition 5.2.18 *When X and R both have a cuspidal edge at a point in $\mathbb{R}^3$ then their respective tangent directions are parallel here.*

Aside: Further Singularities of the Ruled Surface

When N has a parabolic point at $\mathbf{0}$ then R is singular at the base point on M, i.e. $(1, 0, 0)$. Since we are at an extreme of the chord we do not expect wave front type singularities and in fact what we see is a surface with self intersection terminating at a point on a cuspidal edge (see figure 5.7). In this case it is interesting to ask about the relationship of the three space curves on R which are: (i) its cuspidal edge, (ii) its curve of self-intersection and (iii) its locus of contact with the non-parabolic surface piece M.

[1]Here $\mathcal{P}$ is a polynomial in the coefficients of the 3-jets of f and g whose form is not important for our purposes.

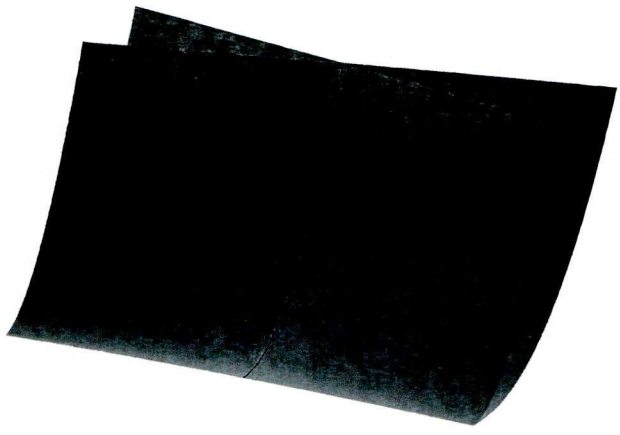

Figure 5.7: The ruled surface R when N is parabolic at $\mathbf{0}$.

To investigate this we will take $f(s,t) = s^2 + \varepsilon\, t^2$ and $g(u,v) = (au + by)^2 + g_{30}\, u^3 + g_{21}\, u^2 v + g_{12}\, uv^2 + g_{03}\, v^3$ where $\varepsilon = 1$ for an elliptic point at M and $\varepsilon = -1$ for a hyperbolic point at M. We find the three space curves as follows: (i) The cuspidal edge is the locus of points on R at which the normal vanishes. In the $\lambda\, v$ - plane this locus is

$$\lambda_{CE} = 1 - \frac{3\,(g_{30}\, b^3 - g_{21}\, a\, b^2 + g_{12}\, a^2\, b - g_{03}\, a^3)}{\varepsilon\, a^3}\, v + \text{h.o.t.}$$

(ii) For the self intersection we take two parameterisations for R, say $R(\lambda, v)$ and $R(\lambda_1, v_1)$, and find their common points. We then eliminate λ_1 and v_1. The locus of this in the $\lambda\, v$ - plane is

$$\lambda_{SI} = 1 - \frac{g_{30}\, b^3 - g_{21}\, a\, b^2 + g_{12}\, a^2\, b - g_{03}\, a^3}{a^3}\, v^3 + \text{h.o.t.}$$

(iii) The locus of contact between R and the surface M is given by $\lambda_{CP} = 1$, i.e. the end of the chord as it meets M tangentially.

Example 5.2.19 Taking $f = s^2 + t^2$ and $g = u^2 + v^3$ (so the point on M is elliptic and that on N is not a cusp of Gauss) we obtain $\lambda_{CE} = 1 + 3\, v + 9\, v^3 + \ldots$, $\lambda_{SI} = 1 + v^3 - 3\, v^6 + \ldots$ and $\lambda_{CP} = 1$. We can now plot the three curves in the $\lambda\, v$ - parameter plane to see how they interact around the point $(0, 1)$, which is mapped to the terminal point of self-intersection on R in the following manner:

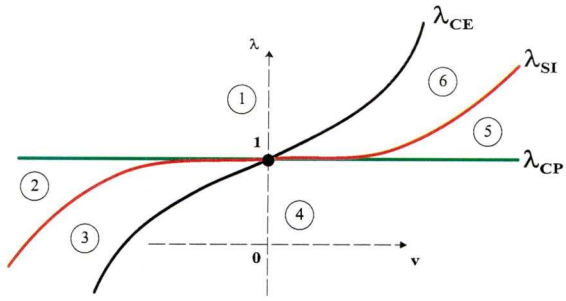

The $(\lambda\, v)$–plane is divided into six distinct regions by the three curves, as shown. If we now map these curves and regions onto the ruled surface we find that λ_{SI} maps onto R as a space curve which is smooth everywhere except the terminal point of self-intersection, where it stops and goes back along its path. λ_{CE} maps to a space curve which is smooth everywhere whilst λ_{CP} maps to a space curve with an ordinary cusp at the terminal point of self-intersection.

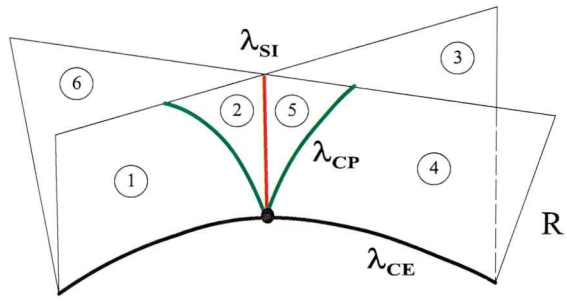

Regions 1, 2 and 3 lie on one sheet of R whilst 4, 5 and 6 lie on the other. From the graphs of the three curves in the $\lambda\, v$ - plane it is clear that λ_{CP} crosses both λ_{CE} and λ_{SI} so that the two branches of the ordinary cusp map to different sheets of R. Hence, the calculations confirm what we expect intuitively, i.e. that the surface piece M nestles into the corner created by the intersecting sheets R as follows:

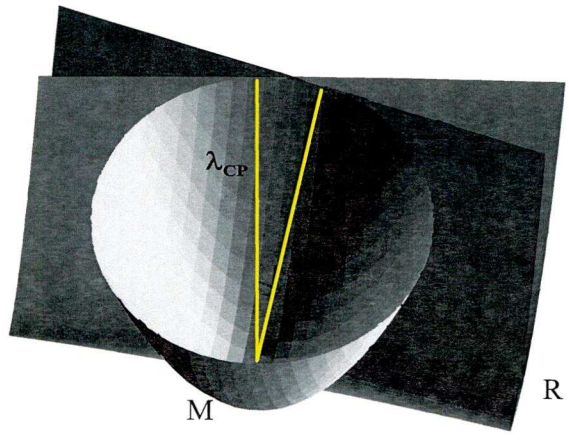

5.3 The Local Case

We now return to the local case, taking pairs of points with parallel tangent planes close to a parabolic point of a smooth surface. Our approach this time will be different in that we will introduce a table of normal forms whose discriminants give diffeomorphic versions of the equidistants in the various cases of interest. These normal forms represent the simplest possible generating family in each case. We will use them to deduce some general properties, e.g. the existence of swallowtail points on equidistants. However, since the resulting equidistants are only correct up to local diffeomorphism we also work with the full pre-normal form, which for this case is

$$G = -h + \lambda f(\mathbf{s} + \mu \mathbf{z}) + \mu f(\mathbf{s} - \lambda \mathbf{z}) \tag{5.3}$$

with $\mathbf{s} = (s_1, s_2)$ and $\mathbf{z} = (z_1, z_2)$ in the surface case, and $\lambda + \mu = 1$ (see Lemma 2.5 of Giblin et al. [10] for a proof). To further clarify some points we consider the analogous curve case and some of the examples here may even proceed directly from the surface definition.

Equidistants close to an Ordinary Parabolic Point

In section 4.3 we showed that the parallel tangency map, $\pi : (s, t, u, v) \mapsto (f_x(s,t) - f_x(u,v),\ f_y(s,t) - f_y(u,v))$ is a local diffeomorphism provided the parabolic point at the origin is not a cusp of Gauss. So we can find s and t as functions of u and v and the MPTS is parameterised in the usual manner as $X : (u, v) \mapsto \frac{1}{2}(s(u,v) + u,\ t(u,v) + v,\ f(s(u,v), t(u,v)) + f(u,v))$.

Example 5.3.1 With $f = x^2 + y^3 + y^4$ the MPTS is shown in figure 5.8. It appears as a smooth surface with a boundary along the parabolic curve of the original surface. To establish if this represents generic behaviour of the MPTS in a neighbourhood of an ordinary parabolic point we take $f = x^2 + b_0\, x^3 + b_1\, x^2\, y + b_2\, x\, y^2 + b_3\, y^3 + \text{h.o.t.}$ and look for a curve lying in the MPTS (close to the origin) at all points of which the 3×2 matrix J_X drops below maximal rank. Taking the determinant of any of the three minors of J_X we arrive at the same expression in u and v. This expression describes the singular locus of the MPTS in the (u, v)–plane.

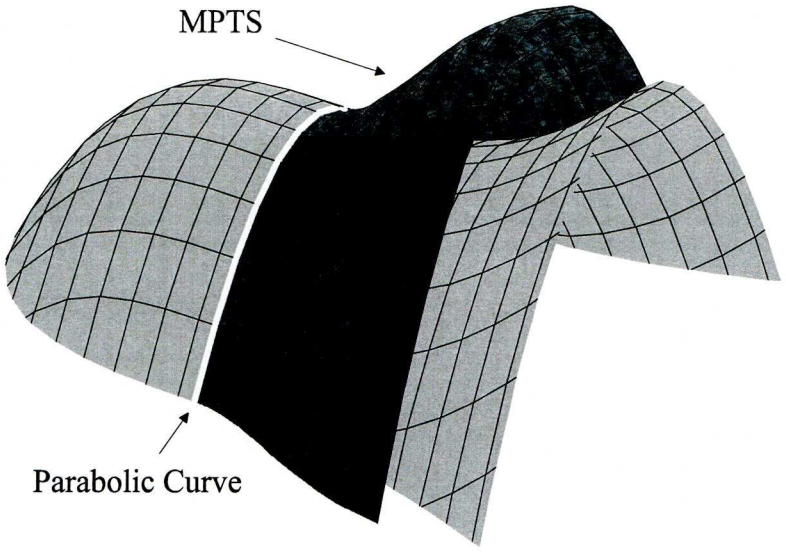

Figure 5.8: MPTS to the surface $z = x^2 + y^3 + y^4$ showing boundary along the parabolic curve.

Now, assuming $b_3 \neq 0$ (i.e. the origin is not a cusp of Gauss) then we can write v (say) as a series in u as follows

$$v = -\frac{b_2}{3\,b_3}\,u - \frac{9\,c_2\,{b_3}^2 + 6\,{b_2}^2 c_4 - 9\,{b_1}^2{b_3}^2 + 6\,{b_2}^2 b_1\,b_3 - {b_2}^4 - 9\,b_2\,c_3\,b_3}{27\,{b_3}^3}\,u^2 + \text{h.o.t.}$$

If we now calculate $P = f_{xx}\,f_{yy} - {f_{xy}}^2$ as a series in x and y and then solve for y as a series in x we obtain the same series to any given order. This strongly suggests that away from the parabolic curve of the surface the MPTS is smooth.

We can gain further insight by considering the other equidistants, i.e. those for which $\lambda \neq 0, \frac{1}{2}$ or 1. These have general equation $E_\lambda(p,q) = p + \lambda\,(q-p)$ and all represent surfaces which have *inflexional contact*[2] with the original surface along the parabolic curve then turn back, forming a cuspidal edge, before cutting the surface again away from the parabolic curve (see figure 5.9). To determine if the singular locus on these equidistants is indeed a cuspidal edge we need the following:

[2]Note: We say that two surfaces have *Inflexional Contact* at a point p if they are tangential here and moreover that their curves of intersection, in a plane through p transverse to both surfaces, have 3–point contact at p.

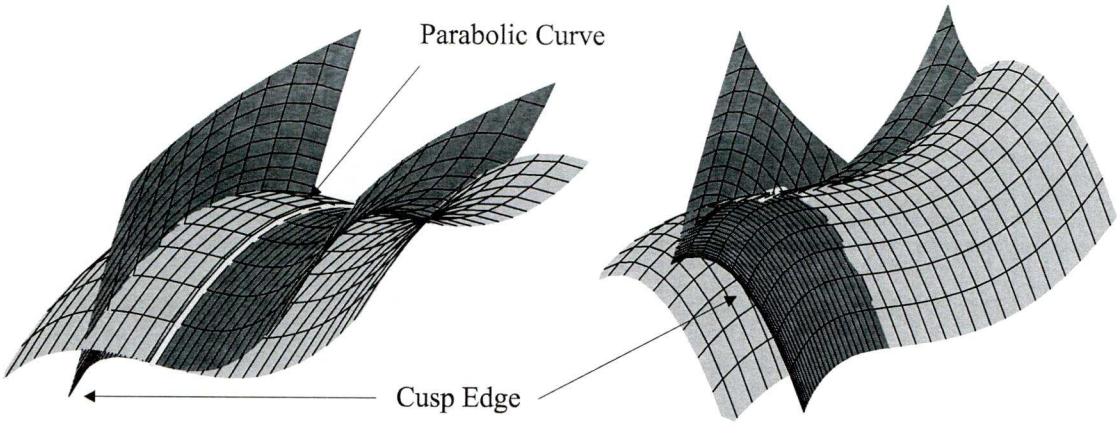

Figure 5.9: Equidistant for the surface $z = x^2+y^3+y^4$ with $\lambda = \frac{1}{4}$, showing inflexional contact and cuspidal edge.

Proposition 5.3.2 *The equidistant formed using the family G of equation (5.3) fails to be smooth if and only if*

$$\frac{\partial^2 G}{\partial z_1^2}\frac{\partial^2 G}{\partial z_2^2} - \frac{\partial^2 G}{\partial z_1 \partial z_2} = 0. \tag{5.4}$$

Proof: We simplify notation by using $\alpha = (s_1 + \mu z_1, s_2 + \mu z_2)$ and $\beta = (s_1 - \lambda z_1, s_2 - \lambda z_2)$ to denote the two points of parallel tangency in the (s_1, s_2)–parameter plane. We also use the familiar subscript notation for differentiation. Hence $G = -h + \lambda f(\alpha) + \mu f(\beta)$, $G_{z_1} = \lambda\mu(f_{z_1}(\alpha) - f_{z_1}(\beta))$ and $G_{z_2} = \lambda\mu(f_{z_2}(\alpha) - f_{z_2}(\beta))$. Consider the map $F : (s_1, s_2, z_1, z_2) \mapsto (f_{z_1}(\alpha) - f_{z_1}(\beta),\ f_{z_2}(\alpha) - f_{z_2}(\beta))$ the zero set of which we project to $\mathbb{R}^3$ using the map $E_\lambda : (s_1, s_2, z_1, z_2) \mapsto (s_1, s_2, h)$ to form the equidistant. We now stack the Jacobian matrices of these two maps and ask when the resulting 5×4 matrix has maximal rank (i.e. rank 4). This matrix is

$$\begin{pmatrix} f_{z_1z_1}(\alpha) - f_{z_1z_1}(\beta) & f_{z_1z_2}(\alpha) - f_{z_1z_2}(\beta) & \mu f_{z_1z_1}(\alpha) + \lambda f_{z_1z_1}(\beta) & \mu f_{z_1z_2}(\alpha) + \lambda f_{z_1z_2}(\beta) \\ f_{z_1z_2}(\alpha) - f_{z_1z_2}(\beta) & f_{z_2z_2}(\alpha) - f_{z_2z_2}(\beta) & \mu f_{z_1z_2}(\alpha) + \lambda f_{z_1z_2}(\beta) & \mu f_{z_2z_2}(\alpha) + \lambda f_{z_2z_2}(\beta) \\ \lambda f_{s_1}(\alpha) + \mu f_{s_1}(\beta) & \lambda f_{s_2}(\alpha) + \mu f_{s_2}(\beta) & 0\ (= G_{z_1}) & 0\ (= G_{z_2}) \\ 1 & 0 & 0 & 0 \\ 0 & 1 & 0 & 0 \end{pmatrix}.$$

Operations using rows 4 and 5 can eliminate the entries in the upper left 3×2 sub-matrix whence it is clear that the matrix has maximal rank if and only if the upper right 2×2 sub-matrix has non-zero determinant. The result follows. □

Equation (5.4) is a single condition on the parallel tangent points α and β so we expect the solution to be a space curve in $\mathbb{R}^3$. Also, when $z_1 = z_2 = 0$ we have $\alpha = \beta = (s_1, s_2)$ and using $\lambda + \mu = 1$ in equation (5.4) gives $f_{z_1 z_1} f_{z_2 z_2} - {f_{z_1 z_2}}^2 = 0$, i.e. we are on the parabolic curve (since $G_{z_1} = G_{z_2} = 0$ is automatic). Hence the parabolic curve is a space curve along which the two pieces of $\{G = G_{z_1} = G_{z_2} = 0\}$ meet (i.e. the original surface and the equidistant), which again confirms our observations with real examples. Note: any intersections of the two pieces of $\{G = G_{z_1} = G_{z_2} = 0\}$ will appear (along with the singular locus on the equidistant) as solutions to equation (5.4) but in practice we factor out the original surface in our calculations as we described above.

Example 5.3.3 In order to show that the equidistant is locally a cuspidal edge we need to work in a neighbourhood of a point where equation (5.4) is satisfied. We will do this using the surface $z = f(x, y)$ where $f(x, y) = x^2 + x\,y^2 + y^3 + y^4$ and $\lambda \neq 0$, $\frac{1}{2}$ or 1. The equidistant can be parameterised by s_2 and z_2 as follows

$$E_\lambda = \left(-3s_2 + \frac{3(\lambda - \mu)}{2} z_2 + \text{h.o.t},\ s_2,\ 9{s_2}^2 - 9(\lambda - \mu) s_2 z_2 + \frac{9(\lambda - \mu)^2}{4} {z_2}^2 + \text{h.o.t.} \right).$$

The singular locus on the equidistant is given as the solutions of equation (5.4) after substituting $s_1 = s_1(s_2, z_2)$ and $z_1 = z_1(s_2, z_2)$. Calculation shows this to be

$$z_2 \left[(6\lambda^2 - 4\lambda\mu + 6\mu^2)\, z_2 - 3(\lambda - \mu)(3s_2 + 1) \right] = 0.$$

We know that $z_2 = 0$ will correspond to intersections of the original surface and the equidistant so the term in the square brackets is the one of interest. We can solve this for s_2 as a function of z_2 when $\lambda \neq \mu$ (i.e. $\lambda \neq \frac{1}{2}$) and using $\lambda + \mu = 1$ we have

$$s_2 = \frac{(6 - 16\,\lambda + 16\,\lambda^2)\, z_2 + (3 - 6\,\lambda)}{9\,(2\,\lambda - 1)}.$$

If we substitute this s_2 into the parameterisation of E_λ and differentiate with respect to z_2 we can obtain the tangent direction to E_λ along its singular locus. Doing this we obtain $(*,\ (6 - 16\,\lambda + 16\,\lambda^2)/(18\,\lambda - 9),\ *)$ so that the middle component is always non-zero. Hence, planes $s_2 =$ constant will always be transverse to the singular locus of E_λ. We can now intersect E_λ with such a plane, $s_2 = {s_2}^*$ say, and find a parameterisation of the resulting curve γ lying in this plane. We parameterise

about the singular point on γ using say $z_2 = y + {z_2}^*$, where ${z_2}^*$ is the value of z_2 corresponding to $s_2 = {s_2}^*$ and y is the parameter on γ. Doing this we obtain

$$\gamma(y) = (a_0,\, b_0) + (a_2\, y^2,\, b_2\, y^2 + b_3\, y^3 + b_4\, y^4)$$

where the a_i's and b_i's are functions of λ and ${s_2}^*$. Now $a_2 = (-3 + 8\,\lambda - 8\,\lambda^2)/2$ which is non-zero for all λ, whilst $b_3 = 64\,\lambda\,(2\,\lambda - 1)\,(\lambda - 1)\,(2\,a_2)^3\,(1 + 3\,{s_2}^*)$ which is non-zero provided ${s_2}^* \neq -\frac{1}{3}$. Using a local diffeomorphism of the form $(X, Y) \mapsto (X,\, Y - (b_2/a_2)\,X)$ it is clear that the singular point on γ at (a_0, b_0) is an ordinary cusp. By extension the singular locus on E_λ is a cuspidal edge as expected.

So equidistants with $\lambda \neq 0, \frac{1}{2}$ or 1 cut meet the original surface with inflexional contact along the parabolic curve then turn back forming a cuspidal edge. When $\lambda = \frac{1}{2}$ we have a limiting case for which the equidistant stops along the parabolic curve before retracing its path forming a double covered smooth surface. We will now further substantiate these observations with some calculations, initially in the analogous curve case.

The Curve Case

We take the host curve as a generalised cubic with inflexion at the origin $f = x^3 + f_4\, x^4 + f_5\, x^5 + \text{h.o.t.}$ The equidistants to f for a fixed λ can be found as the discriminant of the family G of equation (5.3) with now just s in place of (s_1, s_2) and z in place of (z_1, z_2). Since we are interested in those equidistants 'close' to the MPTL we will substitute $\lambda = \frac{1}{2} + \varepsilon$ giving a family $G(h, s, \varepsilon, z) = -h + \left(\frac{1}{2} + \varepsilon\right) f\left(s + \left(\frac{1}{2} - \varepsilon\right) z\right) + \left(\frac{1}{2} - \varepsilon\right) f(s - \left(\frac{1}{2} + \varepsilon\right) z)$ whence $E_\varepsilon = \{(s, h) : \exists z \text{ with } G = \partial G/\partial z = 0\}$ with ε fixed and small. Calculation gives

$$E_\varepsilon = \left\{(s, h) : s = \varepsilon\, z - \frac{f_4}{6}\, z^2 + \text{h.o.t},\ h = \frac{\varepsilon}{4}\, z^3 - \frac{f_4}{16}\, z^4 + \text{h.o.t.}\right\}$$

whence it is clear that E_ε is inflexional at the origin for all $\varepsilon \neq 0$. Now, E_ε is clearly singular when $\frac{\partial s}{\partial z} = \frac{\partial h}{\partial z} = 0$ but we claim

Lemma 5.3.4 *For the equidistant E_ε described above we have*

$$\frac{\partial s}{\partial z} = 0 \quad \Rightarrow \quad \frac{\partial h}{\partial z} = 0.$$

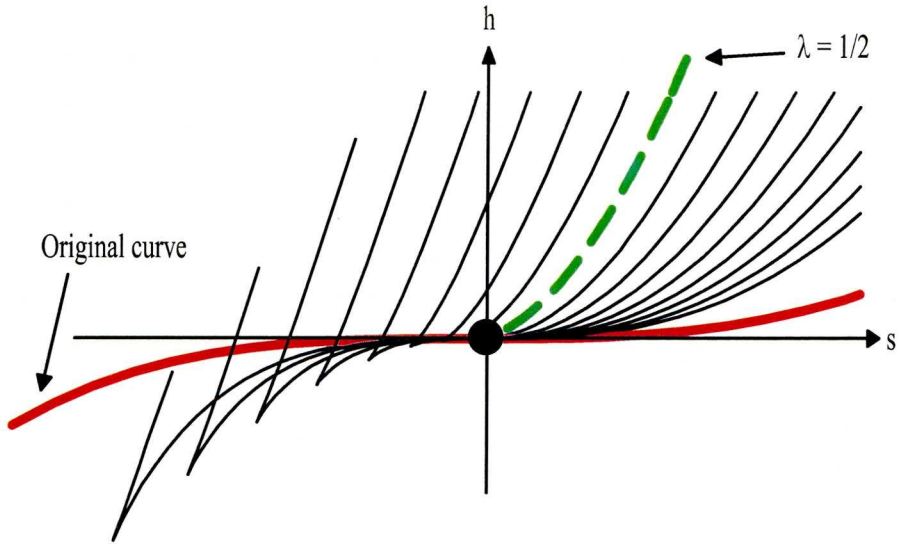

Figure 5.10: Equidistants to a curve with ordinary inflexion at the origin (bold solid). The equidistant with $\lambda = \frac{1}{2}$ terminates at the origin (bold dash). All other equidistants pass through the origin inflexionally and turn back in an ordinary cusp.

Proof: We have $\frac{\partial G}{\partial z} = \left(\frac{1}{4} - \varepsilon^2\right)\left(f'\left(s + \left(\frac{1}{2} - \varepsilon\right) z\right) - f'\left(s - \left(\frac{1}{2} + \varepsilon\right) z\right)\right)$ thus $\frac{\partial G}{\partial z} = 0$ when $z = 0$ for all s and ε. Hence by Hadamard's lemma $\frac{\partial G}{\partial z} = z\, G_1(s, \varepsilon, z)$ for some smooth function G_1. Substituting $z = 0$ into $G = 0$ just gives $h = f(s, \varepsilon)$ so that $E_\varepsilon = (s, f(s))$, i.e. the original curve. Hence the solution of interest is obtained from $G_1 = 0$ and calculation shows $G_1 = 6s + \text{h.o.t.}$ Solving $G_1 = 0$ for $s = S(\varepsilon, z)$ substituting into $h = H(\varepsilon, z)$ and differentiating with respect to z we obtain $\frac{\partial H}{\partial z} = (\frac{1}{2} + \varepsilon)\, f'(S + (\frac{1}{2} - \varepsilon)\, z)\, (\frac{\partial S}{\partial z} + \frac{1}{2} - \varepsilon) + (\frac{1}{2} - \varepsilon)\, f'(S - (\frac{1}{2} + \varepsilon)\, z)\, (\frac{\partial S}{\partial z} - \frac{1}{2} - \varepsilon)$. Thus $\frac{\partial S}{\partial z} = 0$ implies

$$\frac{\partial H}{\partial z} = \left(\frac{1}{4} + \varepsilon^2\right)\left\{f'\left(S + \left(\frac{1}{2} + \varepsilon\right) z\right) - f'\left(S - \left(\frac{1}{2} + \varepsilon\right) z\right)\right\}.$$

This is the same expression as that for $\frac{\partial G}{\partial z}$ above but with $s = S$. However $s = S(\varepsilon, z)$ solves $G_1 = 0$ and thus solves $\frac{\partial G}{\partial z} = 0$. Hence $\frac{\partial S}{\partial z} = 0$ implies $\frac{\partial H}{\partial z} = 0$ as required. □

So by the lemma we only to need solve $\frac{\partial s}{\partial z} = 0$ to find the singular points of E_ε. Doing this we obtain $z^* = 3\,\varepsilon / f_4 - 9\,(8\, {f_4}^3 - 20\, f_4\, f_5 + 9\, f_6)\, \varepsilon^4 + \text{h.o.t.}$ Substituting $z = z^* + \zeta$ into E_ε we can obtain a parameterisation for E_ε about the singular point thus

$${E_\varepsilon}^* = \left(a_0 + a_2\, \zeta^2 + a_3\, \zeta^3 + \text{h.o.t},\ b_0 + b_2\, \zeta^2 + b_3\, \zeta^3 + \text{h.o.t.}\right)$$

where the a_i's and b_i's are infinite series in ε and f_i $(i = 1...4)$. The singular point at $\zeta = 0$ is an ordinary cusp when $d^2E_\varepsilon^*/\zeta^2(0)$ and $d^3E_\varepsilon^*/d\zeta^3(0)$ are linearly independent and calculations show that

$$\det\begin{pmatrix} a_2 & b_2 \\ a_3 & b_3 \end{pmatrix} = \varepsilon\left(\frac{f_4}{12} + ...\right).$$

This is clearly non-zero for small non-zero ε when $f_4 \neq 0$. So the singular point at (a_0, b_0) is indeed an ordinary cusp. In this case the MPTL is of the form $(A\,z^2 + ..., B\,z^4 + ...)$ for non-zero constants A and B, a curve with a single smooth branch terminating at the origin. See figure 5.10.

The analysis above requires $f_4 \neq 0$ so we look at the case where $f_4 = 0$ separately by taking $f = x^3 + f_5\,x^5 + \frac{{f_6}^3}{3}\,x^6$+h.o.t (the coefficient of x^6 here is chosen to simplify the resulting expressions). In this case we have

$$E_\varepsilon = \left(\varepsilon^3\,z - \frac{{f_6}^3}{32}\,z^4 + \text{h.o.t.}\,,\ \frac{\varepsilon^3}{4}\,z^3 - \frac{{f_6}^3}{64}\,z^6 + \text{h.o.t.}\right)$$

so again E_ε is inflexional at the origin for all $\varepsilon \neq 0$. In this case z^* has three solutions of which the real one is $z^* = 2\varepsilon/f_6 + 10f_5/(3{f_6}^3)\,\varepsilon^3$+h.o.t, and substituting $z = z^* + \zeta$ into the components of E_ε we obtain

$${E_\varepsilon}^* = \left(c_0 + c_2\,\zeta^2 + c_3\,\zeta^3 + \text{h.o.t},\ d_0 + d_2\,\zeta^2 + d_3\,\zeta^3 + \text{h.o.t.}\right)$$

where

$$\det\begin{pmatrix} c_2 & d_2 \\ c_3 & d_3 \end{pmatrix} = \varepsilon^5\left(\frac{9f_6}{8} + ...\right).$$

With $f_6 \neq 0$ this is clearly non-zero when for all small non-zero ε and so the singular point is an ordinary cusp. The MPTL here is of the form $(C\,z^4 + ..., D\,z^6 + ...)$ for non-zero constants C and D. This is a curve with a higher degree of contact with the host curve at the origin, but is again a single smooth branch terminating at the origin.

Equidistants as Discriminants in $\mathbb{R}^3$

How do we describe equidistants as discriminants for the local case in $\mathbb{R}^3$, and what can we use as a valid generating function? In trying to answer these questions we are faced with the familiar problem that our two points of parallel tangency can come into coincidence. If we include such solutions of the parallel tangency equations then it is clear that any family of functions we choose will include the original surface as part of its discriminant. Hence we need to find a way of excluding them.

We start with the same reduced family that we used for the curve case but now

$$f(x,y) = x^2 + b_0\,x^3 + b_1\,x^2\,y + b_2\,x\,y^2 + b_3\,y^3 + \text{h.o.t.}$$

with $\mathbf{s} = (s_1, s_2)$ and $\mathbf{z} = (z_1, z_2)$ giving a generating family

$$G(s_1, s_2, h; z_1, z_2) = -h + \lambda\, f(s_1 + \mu\, z_1, s_2 + \mu\, z_2) + \mu\, f(s_1 - \lambda\, z_1, s_2 - \lambda\, z_2) \quad (5.5)$$

where $\lambda + \mu = 1$. This is a three parameter (s_1, s_2 and h) family of functions of two variables (z_1 and z_2) with $\mathcal{D}_G = \{(s_1, s_2, h) : G = \partial G/\partial z_1 = \partial G/\partial z_2 = 0\}$ the discriminant of G. With the host surface given by f as above we have $\partial G/\partial z_1 = 2\,\lambda\,\mu\,z_1 +$ h.o.t. So provided $\lambda\,\mu \neq 0$ (i.e. we are not at the ends of the chords) then we can certainly solve $\partial G/\partial z_1 = 0$ for z_1 as a function of s_1, s_2 and z_2, say $z_1 = w(s_1, s_2, z_2)$. We now claim the following:

Proposition 5.3.5 *The function w has a factor z_2.*

Proof: $\partial^2 G/\partial {z_1}^2 \neq 0$ when $\mathbf{s} = \mathbf{z} = \mathbf{0}$ so $\partial G/\partial z_1(s_1, s_2, z_1, 0) = 0$ has a unique solution for z_1 as a function of s_1 and s_2 by the implicit function theorem. However, $\partial G/\partial z_1(s_1, s_2, 0, 0) = f_x(s_1 + 0, s_2 + 0) - f_x(s_1 - 0, s_2 - 0) = 0$ for all s_1 and s_2 so this unique solution must be $z_1 = 0$. We know that $\partial G/\partial z_1(s_1, s_2, w(s_1, s_2, 0), 0) = 0$ for all s_1 and s_2 close to $\mathbf{0}$ so $w(s_1, s_2, 0) \equiv 0$ and hence z_2 is a factor of w by Hadamard's lemma. □

Thus $z_1 = z_2\,\bar{w}(s_1, s_2, z_2)$ and we can now substitute this into $\partial G/\partial z_2 = 0$ to get an expression in s_1, s_2 and z_2 only, say $H(s_1, s_2, z_2) = \partial G/\partial z_2(s_1, s_2, z_2\,\bar{w}, z_2)$. Now $H(s_1, s_2, z_2) = f_y(s_1 + z_2\,\bar{w}, s_2 + z_2) - f_y(s_1 - z_2\,\bar{w}, s_2 - z_2)$ so clearly $H(s_1, s_2, 0) \equiv 0$.

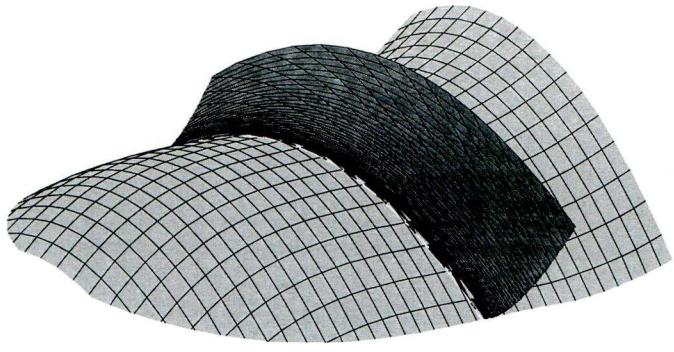

Figure 5.11: A surface diffeomorphic to the MPTS of the surface $z = x^2+x\,y^2+y^3+y^4$.

Hence z_2 is also a factor of H by Hadamard's lemma, say $H(s_1, s_2, z_2) = z_2\,K(s_1, s_2, z_2)$. Putting $z_2 = 0$ in our original family G, knowing that z_2 is a factor of $z_1 = w(s_1, s_2, z_2)$, we get $h = f(s_1, s_2)$, i.e. just the original surface. Hence the function $K(s_1, s_2, z_2) = 0$ (together with $G = 0$) gives us the part of the discriminant we are interested in and represents a surface which is diffeomorphic to an equidistant (for fixed λ) of the original surface $z = f(x, y)$. Calculation shows that

$$K(s_1, s_2, z_2) = \lambda\,\mu\,(2\,b_2\,s_1 + 6\,b_3\,s_2 + 3\,b_3\,(\mu - \lambda)\,z_2) + \text{h.o.t.} \tag{5.6}$$

So provided $b_2 \neq 0$ we can write s_1 as a unique function of s_2 and z_2. In the event that $b_2 = 0$ but $b_3 \neq 0$ then we can write s_2 as a unique function of s_1 and z_2. Finally, if $b_3 \neq 0$ and $\lambda \neq \mu$ (i.e. all proper equidistants except the MPTS) then we can write z_2 as a unique function of s_1 and s_2.

Example 5.3.6 Taking $f = x^2 + x\,y^2 + y^3 + y^4$ and $\lambda = \frac{1}{2}$ we have $G = -2\,h + 4\,z_1\,s_2\,z_2 + 2\,{z_2}^4 + 2\,{s_2}^4 + 12\,{s_2}^2{z_2}^2 + 6\,s_2\,{z_2}^2 + 2\,{s_2}^3 + 2\,s_1\,{s_2}^2 + 2\,s_1\,{z_2}^2 + 2\,{s_1}^2 + 2\,{z_1}^2$ so that $\partial G/\partial z_1 = 4\,(z_1 + s_2\,z_2)$ and $\partial G/\partial z_2 = 4\,s_1\,z_2 + 4\,z_1\,s_2 + 12\,s_2\,z_2 + 24\,{s_2}^2 z_2 + 8\,{z_2}^3$. Now $\partial G/\partial z_1 = 0$ implies that $z_1 = -s_2\,z_2$, so z_2 is a factor of $z_1 = w(s_1, s_2, z_2)$. Substituting this into $\partial G/\partial z_2 = 0$ we obtain $z_2\,(4\,s_1 + 20\,{s_2}^2 + 12\,s_2 + 8\,{z_2}^2) = 0$, so z_2 is also a factor of $H(s_1, s_2, z_2)$. We now discount the solution $z_2 = 0$ and use the second term to write s_1 as a function of s_2 and z_2. Finally we use $G = 0$ to find h as a function of s_2 and z_2 thus

$$h = {z_2}^4 + {s_2}^4 + 5\,{s_2}^2{z_2}^2 + 3\,s_2\,{z_2}^2 + {s_2}^3 + s_1\,{s_2}^2 + s_1\,{z_2}^2 + {s_1}^2.$$

A surface diffeomorphic to the MPTS of the original surface is now given by $E_{\frac{1}{2}} = (s_1(s_2, z_2), s_2, h(s_2, z_2))$. It has the familiar form of a smooth sheet terminating along the parabolic curve as shown in figure 5.11.

Normal Forms for Equidistants

In [11] Giblin and Zakalyukin determine normal forms whose discriminants give diffeomorphic versions of the CSS in the neighbourhood of various special surface points. A subsequent paper by Giblin et al. [10] employs very similar methods but using a different equivalence group, namely the group of s–equivalences, to find normal forms for equidistants. The definition of s–equivalence can be found in Chapter 6 which contains further details and some alternative arguments for the proofs of the theorems given in [10] (including those for smooth curves). Here we content ourselves with listing the relevant normal forms for the surface cases:

Table 5.1: Normal forms for Equidistants to Surfaces.

Case	$\lambda_0 =$	Normal Form ($H =$)	Comments
A_2	$1/2$	$-h + ty^2 + \varepsilon y^3 + y^4$	Half parabola $\times$ line.
A_2^*	$1/2$	$-h + ty^2 + \varepsilon y^3 + sy^4 + y^6$	Half cuspidal edge.
A_2/A_2^*	0 or 1	$-h + \varepsilon(ty^2 + y^3)$	Lies in surface when $\varepsilon = 0$.
A_2/A_2^*	Otherwise	$-h + ty^2 + y^3$	Cubic $\times$ line.
A_3	$1/2$	$-h + sy^2 + \varepsilon ty^3 + y^4$	Same as A_2 when $\varepsilon = 0$.
A_3	λ^*	$-h + sy^2 + ty^3 + (\varepsilon + t)y^4 + y^5$	Proj. of open swallowtail.
A_3	0 or 1	$-h + \varepsilon(sy^2 + ty^3 + y^4)$	Lies in surface when $\varepsilon = 0$.
A_3	Otherwise	$-h + sy^2 + ty^3 + y^4$	Folded Whitney umbrella.

Armed with these results we are now able to prove:

Proposition 5.3.7 *In the neighbourhood of an A_2 point of a smooth surface piece N all equidistants with $\lambda_0 \neq 0, \frac{1}{2}$ or 1 meet N with inflexional contact along the parabolic curve.*

Proof: From the table the correct normal form is $H = -h + t\,y^2 + y^3$ where the parameters are s and t and the variables are x and y. The equidistants are given as the

envelope of this family, $E_\lambda = \{(s,t,h) : H = \partial H/\partial y = 0\}$ (since x does not appear in the expression for H). Now, $\partial H/\partial y = y\,(2t + 3y) = 0$ so either (i) $y = 0$ with $H = 0$ giving $h = 0$ and s and t arbitrary, i.e. the (s,t)–plane in (s,t,h)–space. This represents the host surface in the diffeomorphic model, or (ii) $t = -3y/2$ with $H = 0$ giving $h = -y^3/2$ and s arbitrary. This surface (the product of a cubic curve and an interval) has inflexional contact at all points of the t–axis, which in the diffeomorphic model represents the parabolic curve. □

Remarks:

(i) For the MPTS in the neighbourhood of an A_2 point the correct normal form is $H = -h + t\,y^2 + y^4$ ($\varepsilon = 0$) whence the components of the discriminant are the (s,t)–plane (i.e. the host surface) and the surface $E_{\frac{1}{2}} = \{(s,\ -2\,y^2,\ -y^4) : y, s \in \mathbb{R}\}$. This is a parabolic cylinder with boundary along the t–axis (the parabolic curve) in line with our earlier observations with real examples.

(ii) The generating family for equidistants with $\lambda \neq 0$, $\frac{1}{2}$ or 1 results in a surface which is smooth everywhere so that the cuspidal edge that we expect to see is not represented. The reason for this is that the cuspidal edge is not part of the local structure of these equidistants. The position of the cuspidal edge depends entirely on λ with the cuspidal edge moving further away from the parabolic curve as λ moves away from the value $\frac{1}{2}$ (much as the cusp on the equidistant in the curve case moves further away from the inflexion on the original curve in fig 5.10).

Equidistants close to an $A_2{}^*$ point

So far the MPTS in the neighbourhood of a parabolic point has always been a smooth surface with boundary along the parabolic curve. However the MPTS can be singular away from the parabolic curve as we shall now demonstrate. First a definition:

Definition 5.3.8 *Consider a surface piece in Monge form given as $z = f(x,y)$ with ordinary parabolic point at the origin, i.e. $f(x,y) = x^2 + b_0x^3 + b_1x^2y + b_2xy^2 + b_3y^3 + c_0x^4 + c_1x^3y + c_2x^2y^2 + c_3xy^3 + c_4y^4 + h.o.t.$ and $b_3 \neq 0$. We call the origin an $A_2{}^*$ point of the surface if the degree 4 terms of f vanish when $x = 0$, that is $c_4 = 0$.*

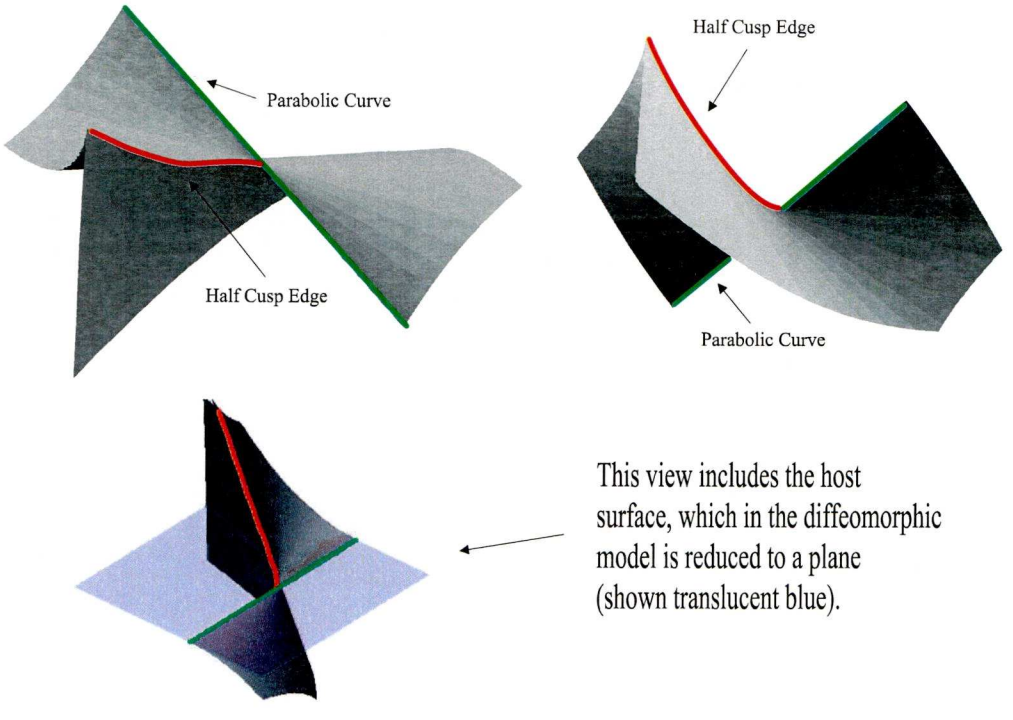

Figure 5.12: The MPTS in a neighbourhood of an $A_2{}^*$ point.

From table 5.1 the correct normal form to use with $\lambda = \frac{1}{2}$ and in the neighbourhood of an $A_2{}^*$ point is $H = -h + ty^2 + \varepsilon y^3 + sy^4 + y^6$. So $E_\varepsilon = \{(s,t,h) : H = \partial H/\partial y = 0\}$ for small fixed ε gives a diffeomorphic picture of the equidistant corresponding to $\varepsilon = \lambda - \frac{1}{2}$ and the MPTS is given by $\varepsilon = 0$. Now, solving $H = \partial H/\partial y = 0$ for h and s as functions of y and t we obtain the following parameterisation of the MPTS

$$X(s,y) = \left(s,\ -y^2(2s+3y^2),\ -y^4(s+2y^2)\right).$$

From this we can show that the Jacobian matrix of X fails to have maximal rank when $y = 0$ or $s + 3y^2 = 0$. In the model the line $y = 0$ represents the parabolic curve and so we have a second space curve lying in the MPTS, along which the MPTS is singular. If we substitute $s = -3y^2$ into the first two components of the MPTS we obtain $(-3y^2, 3y^4)$ so the singular locus is doubly covered in the (s,t)–plane, terminates at the origin and meets the parabolic line tangentially. Figure 5.12 shows three views of the MPTS with the double covered singular locus marked in red. It represents a half cuspidal edge which terminates at the origin. The parabolic curve is marked in green and shows a boundary on the MPTS in the usual manner.

Example 5.3.9 We now show the MPTS for a real $A_2{}^*$ example by taking $f(x,y) = x^2 + x^2y + y^3 + xy^3$. The origin is an ordinary parabolic point and clearly the degree 4 part of f vanishes when $x = 0$ and so the origin is an $A_2{}^*$ point. The following is a view of the MPTS close to the origin:

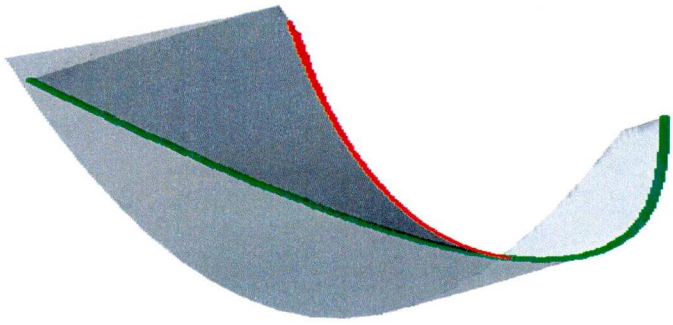

As above the red space curve indicates a half cuspidal edge, whilst the green space curve shows a boundary along the parabolic curve. The first two components of the red space curve are ($-3v^2/4$+h.o.t, $-v^4/16$+h.o.t.). Hence the projection of the red space curve onto the (s,t)–plane is a half parabola, doubly covered and terminating at the origin. We see from table 5.1 that the normal form for equidistants with $\lambda \neq 0$, $\frac{1}{2}$ or 1 is the same for $A_2{}^*$ as for the ordinary A_2 and so we would expect such equidistants to meet the original surface with inflexional contact at all points of the parabolic curve. With $\lambda = 49/100$ the resulting equidistant is as follows:

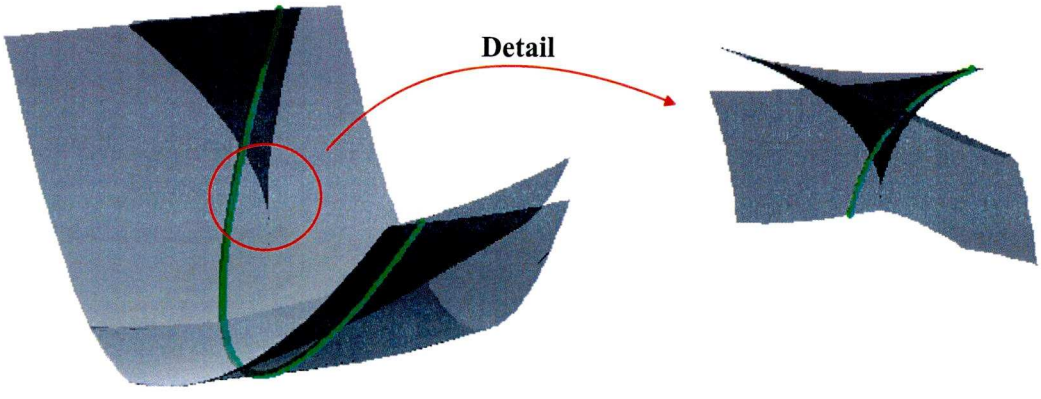

We see what looks like a cuspidal edge in the foreground and (as revealed in the blown up detail) a swallowtail away from the parabolic curve. To verify that we are

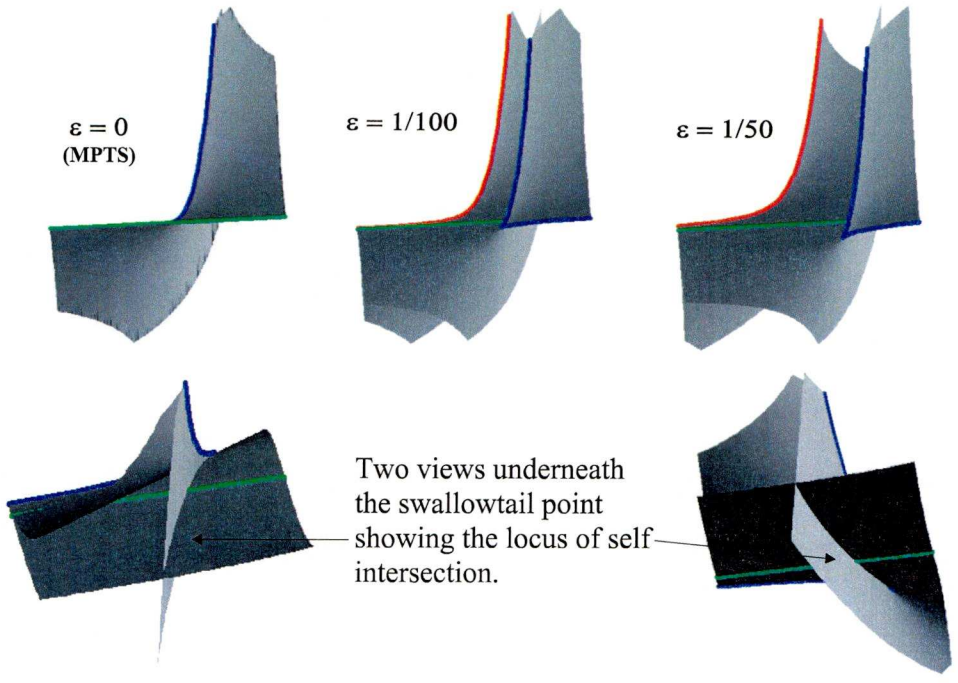

Figure 5.13: Transition from MPTS to ordinary equidistant at an $A_2{}^*$ point.

really seeing cuspidal edges and swallowtails in these examples we use the appropriate normal form from table 5.1, i.e. $H = -h + ty^2 + \varepsilon y^3 + sy^4 + y^6$. This can be regarded as a 3-parameter unfolding of a function of the single variable y. For a given y the function $H = 0$ is a plane in (s, t, h)–space and the envelope, $\mathcal{D}_H$, of these planes is the equidistant. For an A_3 of the equidistant we require $H = \partial H/\partial y = \partial^2 H/\partial y^2 = \partial^3 H/\partial y^3 = 0$ and $\partial^4 H/\partial y^4 \neq 0$ at $y = y_0$ (say) with $(h, s, t) \in \mathcal{D}_H$. Solving these equations simultaneously we obtain $y_0 = (\varepsilon/16)^{1/3}$ and $\partial^4 H/\partial y^4 \neq 0$ when $y = y_0$ so the A_3 is always non-degenerate. To determine if H is a versal unfolding of this A_3 we calculate the 2-jets with constant of $\partial H/\partial h = -1$, $\partial H/\partial s = y^4$ and $\partial H/\partial t = y^2$ at $y = y_0$, i.e. $f_i(y_0) + \eta f_i'(y_0) + \frac{1}{2!}\eta^2 f_i''(y_0)$ where f_i is the function of y that is each of these partial derivatives. The matrix of coefficients of these 2-jets is

$$\begin{pmatrix} -1 & {y_0}^4 & {y_0}^2 \\ 0 & 4y_0^3 & 2y_0 \\ 0 & 6{y_0}^2 & 1 \end{pmatrix}.$$

This has maximal rank if and only if $y_0 \neq 0$ but $y_0 = 0$ is part of the redundant component of $\mathcal{D}_H$ (i.e. the original surface) and so the unfolding is always versal.

We conclude that the equidistant at $y = y_0$ is locally diffeomorphic to a standard swallowtail. For A_2 points we require $H = \partial H/\partial y = \partial^2 H/\partial y^2 = 0$ and $\partial^3 H/\partial y^3 \neq 0$. Thus we have a locus of points on the equidistant

$$\left(\frac{3(\varepsilon + 8y^3)}{8y}, \frac{3y(-\varepsilon + 4y^3)}{4}, \frac{y^3(-\varepsilon + 8y^3)}{8} \right)$$

which are all A_2 for $y \neq (\varepsilon/16)^{1/3}$. The unfolding matrix here is just the first two rows of that above and this is also maximal if and only if $y_0 \neq 0$. So for fixed small ε the singular locus with $y \neq (\varepsilon/16)^{1/3}$ is locally diffeomorphic to a cuspidal edge.

Using the diffeomorphic model and taking small values of ε increasing from zero we can see how the MPTS transitions to an 'ordinary' equidistant in this case[3]. As figure 5.13 shows, the half cuspidal edge splits apart forming three cuspidal edges two of which (in blue) come together to form a swallowtail. Of the three cuspidal edges two (the red and one of the blue) tend towards the parabolic curve (shown in green).

Equidistants close to an Ordinary Cusp of Gauss

If our host surface has the standard Taylor expansion

$$z = x^2 + b_0\, x^3 + b_1\, x^2\, y + b_2\, x\, y^2 + b_3\, y^3 + c_0\, x^4 + c_1\, x^3\, y + c_2\, x^2\, y^2 + c_3\, x\, y^3 + c_4\, y^4 + \text{h.o.t.}$$

then we recall that the origin is a cusp of Gauss when $b_3 = 0$. If ${b_2}^2 \neq 4\, c_4$ it is non-degenerate, whilst if additionally $b_2 \neq 0$ then the cusp of Gauss is termed ordinary. First we consider how the MPTS appears in the neighbourhood of a cusp of Gauss by referring back to the notation and argument following proposition 5.3.5 above. In this case we have $\partial G/\partial z_1 = 4\, z_1 + \ldots$ so we can write z_1 uniquely as a function of s_1, s_2 and z_2 whether or not the origin is a cusp of Gauss. Equation (5.6) gives

$$K(s_1, s_2, z_2) = 4\, b_2\, s_1 - 8\, b_1\, b_2\, s_1\, s_2 + 4\, \left(6\, c_4 - {b_2}^2\right) {s_2}^2 + 4\, \left(c_2 - {b_1}^2\right) {s_1}^2 + 8\, c_4\, {z_2}^2 + \ldots$$

so we can write s_1 uniquely as a function of s_2 and z_2 when $b_2 \neq 0$. With $b_3 = 0$ and $b_2 \neq 0$ the MPTS remains a smooth surface with boundary along the parabolic curve, e.g. If we take $f = x^2 + xy^2 + y^4$ (so $b_3 = 0$ and $b_2 = 1$) then the MPTS appears as follows:

[3]Note: these are simply observations made from the pictures, we make no claim that these statements have been substantiated algebraically.

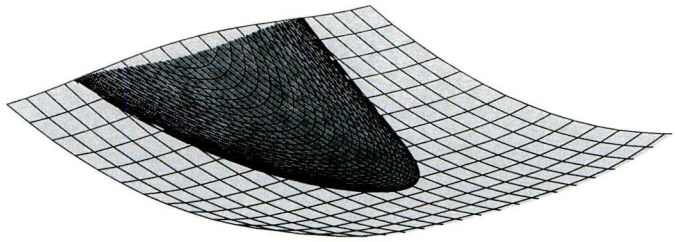

It forms a smooth 'pocket' over the surface to one side of and with boundary along the parabolic curve, which is always smooth through an ordinary cusp of Gauss. Remark: The normal form for $\lambda = 1/2$ and A_3 is the same as that for $\lambda = 1/2$ and A_2 when $\varepsilon = 0$.

For equidistants where $\lambda \neq 0$, λ^*, $\frac{1}{2}$ or 1 we see from table 5.1 that the correct normal form is $H = -h + sy^2 + ty^3 + y^4$. The discriminant of this family, shown in figure 5.14, is $\mathcal{A}$–equivalent to the standard *folded Whitney umbrella* (i.e. $(u, v) \mapsto (u, v^2, uv^3)$). In this figure the host surface is shown as the blue plane and the parabolic curve as the green line. The red and blue space curves indicate cuspidal edges while the self intersection terminates at the cusp of Gauss itself. Elsewhere on the parabolic curve the equidistant cuts meets the original surface with inflexional contact and then forms a cuspidal edge in the familiar manner.

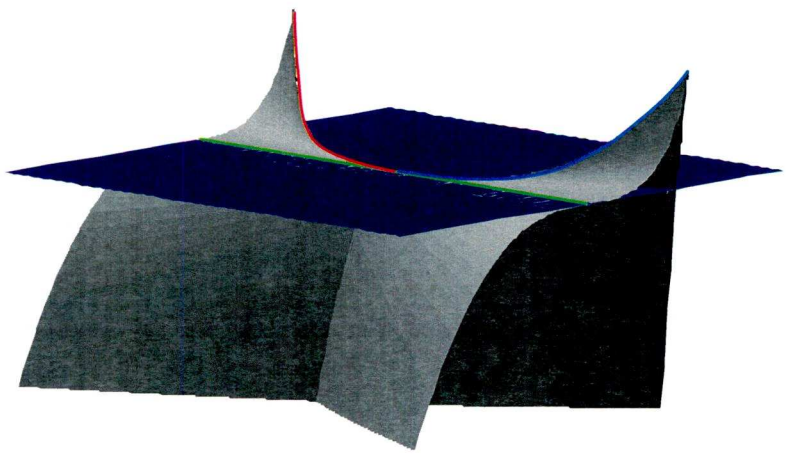

Figure 5.14: Equidistant with $\lambda \neq 0, \lambda^*$, $\frac{1}{2}$ or 1 in a neighbourhood of a cusp of Gauss.

Contact between the Equidistant and Host Surface at a Cusp of Gauss

Clearly the contact between the equidistant and the host surface is greater at the A_3 than at other parabolic points. To ascertain this we take the general form for a surface with ordinary cusp of Gauss at the origin, i.e.

$$f(x,y) = x^2 + b_0x^3 + b_1x^2y + b_2xy^2 + \text{h.o.t.}$$

So $b_2 \neq 0$, $b_3 = 0$ and we have shown previously that we can parameterise the equidistant using t and v where the pairs of parallel tangent points are given by $(s(t,v),t)$ and $(u(t,v),v)$ in the parallel tangent set Π. We now cut a plane through the cusp of Gauss which is transverse to both the equidistant and the host surface. The most obvious choice for such a plane is $y = 0$ which for the equidistant implies that $v = (\lambda - 1)\,t/\lambda$ (from equating the y–component of the parameterisation of the equidistant to zero). Note: for general f this plane will not contain the space curve of self intersection on the equidistant, although in the diffeomorphic model using $H = -h + sy^2 + ty^3 + y^4$ this is in fact the case. Now, substituting $v = (\lambda - 1)\,t/\lambda$ into the x and z components of the equidistant we obtain a parameterisation for the plane curve of intersection, say γ, lying in the plane $y = 0$. This has the form $\gamma(t) = (\alpha_2t^2 + \alpha_3t^3 + \text{h.o.t}, \beta_4t^4 + \beta_5t^5 + \text{h.o.t.})$ where

$$\alpha_2 = \frac{4({b_2}^2 - 3c_4)\lambda^2 - 4({b_2}^2 - 3c_4)\lambda + ({b_2}^2 - 4c_4)}{2b_2\lambda^2},\ \beta_4 = \frac{({b_2}^2 - 4c_4)(3\lambda^2 - 3\lambda + 1)\,\alpha_2}{2b_2\lambda^2}$$

and all coefficients α_i, β_j with $i \geq 3$, $j \geq 5$ have a factor $1 - 2\lambda$ and precede odd powered terms in t. Hence all the odd powered terms of γ vanish when $\lambda = \frac{1}{2}$, a result which follows trivially from proposition 4.3.3 after substituting $v = -t$. Now $\alpha_2 = 0$ if and only if $\lambda = \lambda^*$ where

$$\lambda^* = \frac{1}{2} \pm \frac{1}{2}\sqrt{\frac{c_4}{{b_2}^2 - 3c_4}}. \tag{5.7}$$

These two values of λ (symmetric about $\lambda = \frac{1}{2}$) have a special significance for the equidistant and require a different generating family, as indicated in table 5.1. We will return to these special cases later. Hence when $\lambda \neq \lambda^*$ then $\alpha_2 \neq 0$ but also $\beta_4 \neq 0$ since ${b_2}^2 - 4c_4 \neq 0$ at a non-degenerate cusp of Gauss and the factor which is quadratic in λ has no real roots. We now use the change of variables $(X,Y) \mapsto (X/\alpha_2,\ Y - \beta_4(X/\alpha_2)^2)$ to reduce γ to $\bar{\gamma} = (t^2 + \text{h.o.t}, \bar{\beta}_5t^5 + \bar{\beta}_6t^6 + \text{h.o.t.})$ where

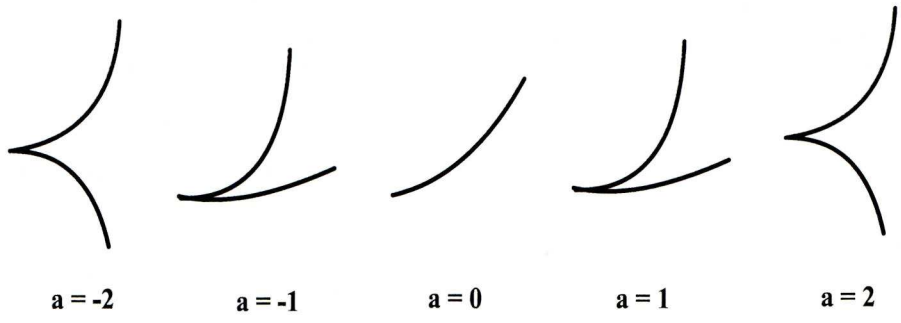

Figure 5.15: Transition about $\lambda = \frac{1}{2}$ for curve in cutting plane.

$$\bar{\beta}_5 = \frac{(1-\lambda)(1-2\lambda)}{4b_2\lambda^4}\Big[(4b_1{b_2}^3 - 2c_3{b_2}^2 - 24b_1c_4b_2 - 8d_5b_2 + 24c_3c_4)\lambda(\lambda-1) \; + \; (b_1{b_2}^3 - 8b_1c_4b_2 - 4d_5b_2 + 8c_3c_4)\Big].$$

Clearly $\bar{\beta}_5$ is generically non-zero. When $\lambda = \frac{1}{2}$ then $\bar{\beta}_5$ does vanish but

$$\bar{\beta}_6 = \frac{16{c_4}^2b_2c_2 - 8{b_2}^2d_4c_4 - 32b_0{c_4}^3 - 16b_2{b_1}^2{c_4}^2 + 8{b_2}^2c_3b_1c_4 - {b_2}^3{c_3}^2}{4{b_2}^3},$$

which again is generically non-zero. When $\lambda = \lambda^*$ then α_2 vanishes but

$$\alpha_3 = \frac{5\Phi_3\eta\sqrt{c_4\eta}}{2b_2(\eta + \sqrt{c_4\eta})^3}$$

where $\eta = {b_2}^2 - 3c_4$ and $\Phi_3 = c_3{b_2}^3 - 2b_1c_4{b_2}^2 - 4d_5{b_2}^2 + 8c_4d_5$. Clearly Φ_3 is generically non-zero and $c_4 \neq 0$ else $\lambda^* = \frac{1}{2}$ from equation (5.7). Hence $\alpha_3 \neq 0$ when $\eta \neq 0$ and by equation (5.7) this must hold for finite λ^*. Since $\alpha_2 = 0$ then $\beta_4 = 0$ but

$$\beta_5 = \frac{3b_2\eta({b_2}^2 - 4c_4)\,\alpha_3}{(\eta + \sqrt{c_3\eta})^2}$$

which is clearly non-zero when $\alpha_3 \neq 0$. Finally a change of variables of the form $(X, Y) \mapsto (X, Y/\beta_i)$ will reduce the parameterisations in these three cases to: (i) $\lambda \neq 0$, λ^*, $\frac{1}{2}$ or 1 implies $\gamma \simeq (t^2 + \text{h.o.t}, t^5 + \text{h.o.t.})$. (ii) $\lambda = \frac{1}{2}$ implies $\gamma \simeq (t^2 + \text{h.o.t}, t^6 + \text{h.o.t.})$. (iii) $\lambda = \lambda^*$ implies $\gamma \simeq (t^3 + \text{h.o.t}, t^5 + \text{h.o.t.})$. It is instructive to examine the transitions of γ about $\lambda = \frac{1}{2}$ and $\lambda = \lambda^*$. We can model the transition about $\lambda = \frac{1}{2}$ using $\gamma(t, a) = (t^2, at^5 + t^6)$. Here $\gamma(t, 0)$ gives the $\lambda = \frac{1}{2}$ moment and the transition is as shown in figure 5.15. The figure underlines the already established

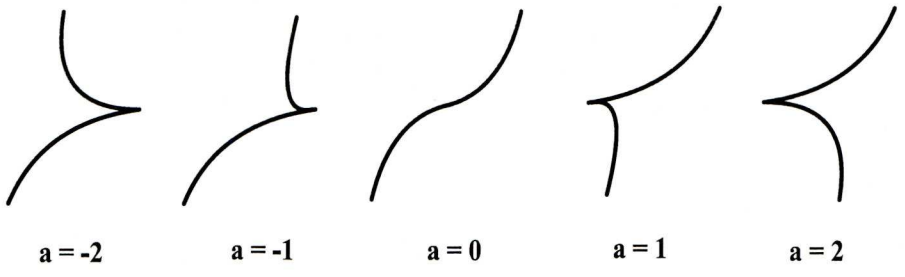

Figure 5.16: Transition about $\lambda = \lambda^*$ for curve in cutting plane.

fact that the MPTS is a limiting case of a double covered equidistant with boundary. For the transition about $\lambda = \lambda^*$ we can use $\gamma(t, a) = (at^2 + t^3,\, t^5)$. The transition is as shown in figure 5.16. When $a = 0$ the curve looks deceptively smooth at the A_3 point, but of course $\gamma'(0) = \gamma''(0) = 0$ here.

The $\lambda = \lambda^*$ Case

When $\lambda = \lambda^*$ the correct normal form from table 5.1 is

$$H = -h + sy^2 + ty^3 + (\varepsilon + t)\, y^4 + y^5$$

with $\varepsilon = 0$ giving the $\lambda = \lambda^*$ moment. The resulting equidistant, shown in figure 5.17, looks very different from the folded Whitney umbrella we obtain when $\lambda \neq 0,\ \lambda^*,\ \frac{1}{2}$ or 1. The host surface is shown as a blue plane and the parabolic curve as a green line. At ordinary parabolic points the equidistant meets the original surface with inflexional contact in the usual manner. The red and blue space curves again show a cuspidal edge but, unlike the folded Whitney umbrella, this now has a singular point at the origin. The parameterisation of the equidistant, obtained as the discriminant of H (with $\varepsilon = 0$) is

$$E_{\lambda^*} = \left(-\frac{1}{2} y\,(3t + 4yt + 5y^2),\ t,\ -\frac{1}{2} y^3\,(t + 2ty + 3y^2) \right).$$

The self-intersection is now absent which we can demonstrate algebraically as follows: Using $\Omega = E_{\lambda^*}(y_1, t) - E_{\lambda^*}(y_2, t) = \mathbf{0}$ we obtain two equations in the three unknowns t, y_1 and y_2. The x–component of Ω yields

$$(y_1 - y_2)(5{y_1}^2 + 4y_1 t + 5y_2 y_1 + 3t + 4y_2 t + 5{y_2}^2) = 0.$$

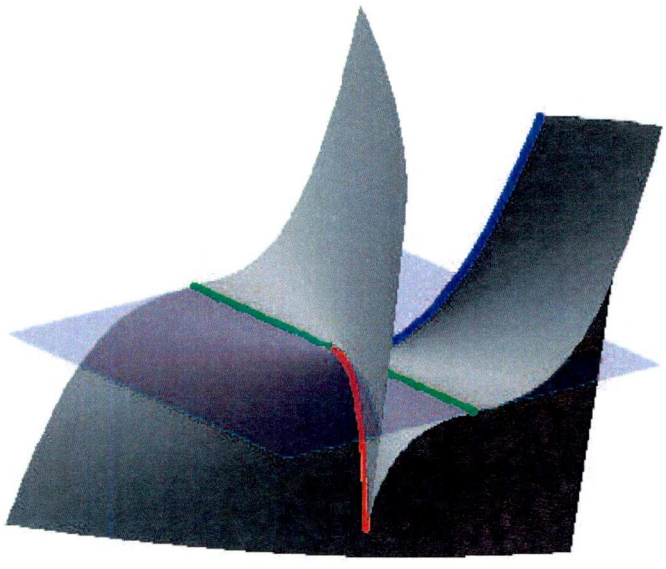

Figure 5.17: A surface diffeomorphic to the equidistant with $\lambda = \lambda^*$ in a neighbourhood of a cusp of Gauss.

Clearly we are not interested in solutions where $y_1 = y_2$ whilst the second bracket yields

$$t = \frac{-5({y_1}^2 + y_2 y_1 + {y_2}^2)}{3 + 4y_1 + 4y_2}.$$

This expression is certainly valid for small y_1, y_2 and substituting this t into the expression obtained from the z–component of Ω we obtain

$$\frac{(y_1 - y_2)^2 \left(2{y_1}^3 + 8y_2{y_1}^2 + 4{y_1}^2 + 8{y_2}^2 y_1 + 7y_2 y_1 + 2{y_2}^3 + 4{y_2}^2\right)}{3 + 4y_1 + 4y_2} = 0.$$

If we ignore the first term in the numerator and solve the second for y_1 as a series in y_2 (or vice-versa since the expression is symmetric) we obtain a series whose first term has a complex coefficient and so the only real solution is $y_1 = y_2 = 0$, i.e. the A_3 point at the origin. So the self-intersection is no longer local to the origin when $\lambda = \lambda^*$. Taking values of ε increasing from zero figure 5.18 shows the transition in this case. We see that one of the cuspidal edges (blue) persists whilst the other (red) cuts through the equidistant to create the self-intersection. A new cuspidal edge (also red) is created on the opposite side of the plane $y = 0$ as the transition progresses[4].

[4]Note: these are simply observations made from the pictures, we make no claim that these statements have been substantiated algebraically.

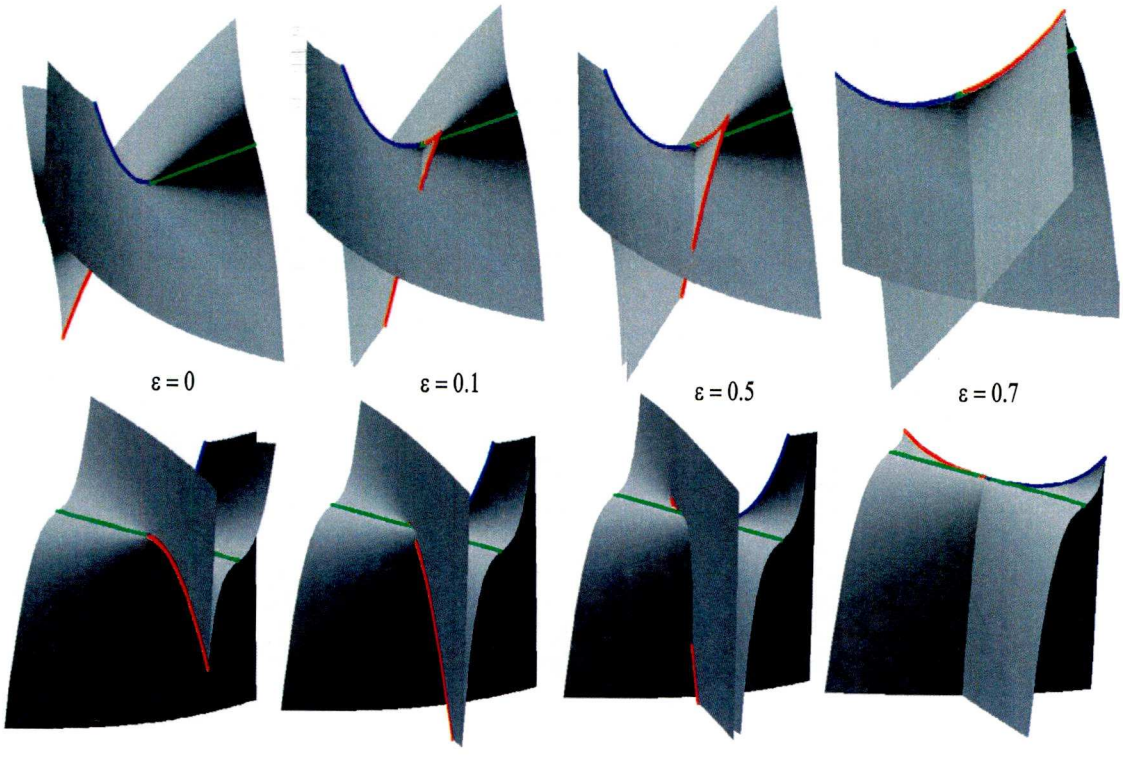

Figure 5.18: Transition from $\lambda = \lambda^*$ to ordinary equidistant at an A_3. The top and bottom rows show a sequence of 'front' and 'back' views respectively.

It is clear from equation (5.7) that for real λ^* to exist we require $c_4 \neq 0$ and ${b_2}^2 - 3c_4 \neq 0$ and moreover that these two quantities have the same sign. We know that ${b_2}^2 - 4c_4 \neq 0$ at a non-degenerate cusp of Gauss so we have four cases to consider:

1. $c_4 > 0$ and ${b_2}^2 > 4c_4$. These inequalities imply that ${b_2}^2 - 3c_4 > c_4 > 0$ so $0 < c_4/({b_2}^2 - 3c_4) < 1$. Hence, real λ^* exist and all lie in the interval $(0, 1)$.

2. $c_4 > 0$ and ${b_2}^2 < 4c_4$. Here we have two sub-cases depending as ${b_2}^2 < 3c_4$ or $3c_4 < {b_2}^2 < 4c_4$. In the former case there are no real λ^* whilst in the latter, where $1/4 < c_4/{b_2}^2 < 1/3$, real λ^* exist and all lie outside the interval $(0, 1)$.

3. $c_4 < 0$ and ${b_2}^2 > 4c_4$. Clearly $3c_4 < 0$ so ${b_2}^2 - 3c_4 > 0$. Hence c_4 and ${b_2}^2 - 3c_4$ have opposite sign and no real λ^* exist.

4. $c_4 < 0$ and ${b_2}^2 < 4c_4$. This case is impossible since ${b_2}^2 > 0$.

We can express all these results using the important ratio $c_4/{b_2}^2$. For case 1 we have $0 < c_4/{b_2}^2 < 1/4$, for case 2a we have $1/3 < c_4/{b_2}^2$, for case 2b we have $1/4 < c_4/{b_2}^2 < 1/3$ and for case 3 we have $c_4/{b_2}^2 < 0$. We can display the results on the real line as follows:

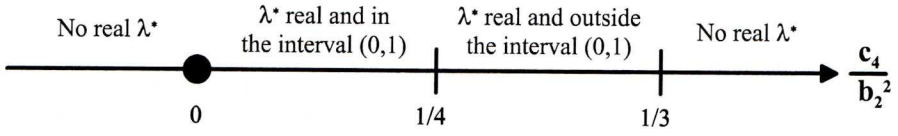

Whence it is clear that for real λ^* to exist we require c_4 to be strictly positive and the ratio $c_4/{b_2}^2$ to lie in the open interval $(0, \frac{1}{3})$.

Aside: The Open Swallowtail

In Arnold [2] the ordinary swallowtail is defined as "the surface in $\mathbb{R}^3$, consisting of all polynomials $x^4 + a\,x^2 + b\,x + c$, having multiple roots", whilst the *open swallowtail* is "the surface in $\mathbb{R}^4$, consisting of all polynomials $x^5 + A\,x^3 + B\,x^2 + C\,x + D$, having roots of multiplicity ≥ 3". In this paper he also states that "For the open swallowtail the cuspidal edge is preserved, and the self-intersection disappears". If we take the projection $(A, B, C, D) \mapsto (A, B, D)$ of the open swallowtail from $\mathbb{R}^4$ into $\mathbb{R}^3$ we obtain a surface which looks identical to that of figure 5.17, i.e. the equidistant for $\lambda = \lambda^*$ in the neighbourhood of a cusp of Gauss. The parameterisation of this projection is

$$(x,\ A) \mapsto (A,\ -10\,x^3 - 3\,A\,x,\ -6\,x^5 - A\,x^3)$$

which is essentially the same as that of E_{λ^*} given above after reordering and the removal of some lower order terms. Similar calculations to those above confirm the presence of a cuspidal edge[5] and the absence of a self intersection. We have not obtained explicit diffeomorphisms taking E_{λ^*} to the projection given above but it seems highly likely that the two surfaces are in fact diffeomorphic.

[5] As a space curve the cuspidal edge has parameterisation $(-10x^2, 20x^3, 4x^5)$ which is singular at the origin.

Equidistants when $\lambda \to 0$ (or 1)

Finally in this section we will describe the transition of the equidistant as $\lambda \to 0$ (or 1). We know that when $\lambda = 0$ (or 1) the equidistant is coincident with the host surface and figure 5.19 shows this transition using the diffeomorphic model (the host surface being represented by the translucent plane $y = 0$). During the transition the red and blue cuspidal edges move towards the green parabolic line and vanish when $\lambda = 0$. The two intersecting sheets of the equidistant come closer and closer together as the equidistant approaches the host surface. In the limit the locus of self intersection vanishes as the equidistant and surface coincide. Looking at figure 5.19 it is easy to imagine that when $\lambda = 0$ the boundary of the equidistant is coincident with the parabolic curve and that (local to the cusp of Gauss) the equidistant lies in a purely elliptic or hyperbolic region of the surface. In fact this is not the case as we will now demonstrate. We take $f(x, y) = x^2 + b_0\, x^3 + b_1\, x^2 y + b_2\, xy^2 + \text{h.o.t.}$ and assume $b_2 > 0$ (else apply the transformation $x \mapsto -x$). With the points of parallel tangency in the parameter plane of the surface denoted (s, t) and (u, v), we can parameterise Π (the parallel tangents set) using t and v whence the equidistant E_λ can be parameterised as $E_\lambda(t, v) = (\, E_1(t, v),\, E_2(t, v),\, E_3(t, v)\,)$. We now ask when the first minor of the Jacobian matrix of this mapping is zero, i.e.

$$\frac{\partial E_1}{\partial t}\,\frac{\partial E_2}{\partial v} - \frac{\partial E_1}{\partial v}\,\frac{\partial E_2}{\partial t} = 0.$$

Writing this as a series in t and v and then setting $\lambda = 0$ we find that it is linear in both t and v provided $b_2^2 \neq 4c_4$ (which holds since the cusp of Gauss is non-degenerate). Solving for t as a series in v and substituting this into the parameterisation for $E_{\lambda=0}$ gives us a space curve representing the boundary of the equidistant lying in the surface. The locus of this curve in the parameter plane of $E_{\lambda=0}$ is

$$\left(\frac{-12c_4 - b_2^2}{2b_2}\, v^2 + \text{h.o.t},\, -2v + \text{h.o.t.} \right)$$

and using a change of co-ordinates to write this in the form $(X(Y), Y)$ we obtain

$$\left(\frac{-12c_4 - b_2^2}{8b_2}\, Y^2 + \text{h.o.t},\, Y \right).$$

This is the Parallel Tangents Boundary Curve (PTBC) we encountered earlier in our discussion of special curves passing through a cusp of Gauss. The parameterisation

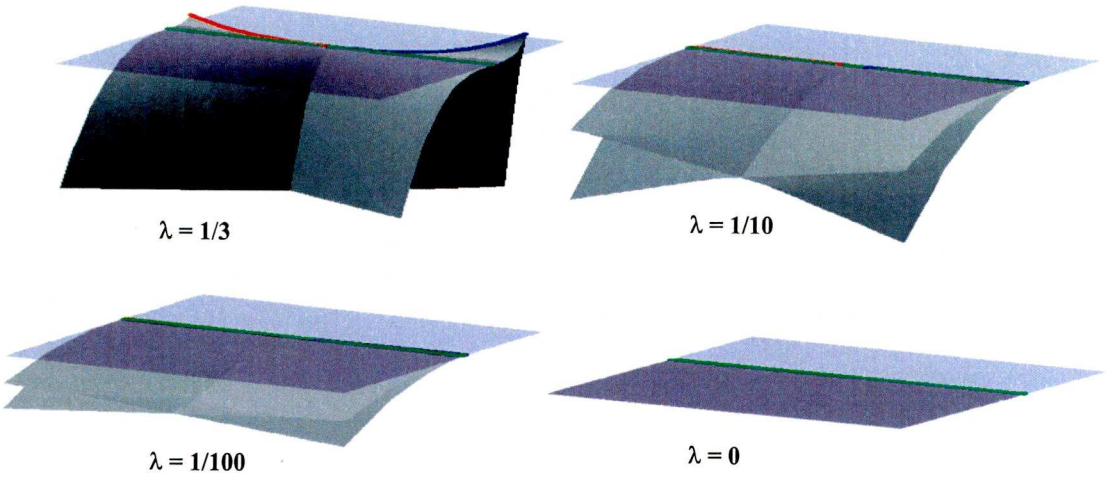

Figure 5.19: Transition of the equidistant at an A_3 as $\lambda \to 0$.

of the parabolic curve in this form is

$$\left(\frac{b_2^2 - 6c_4}{b_2} Y^2 + \text{h.o.t}, Y \right).$$

So, local to the cusp of Gauss, the PTBC lies in the elliptic region of the surface if and only if

$$\frac{-12c_4 - b_2^2}{8b_2} > \frac{b_2^2 - 6c_4}{b_2}$$

which equates to ${c_4}/{b_2}^2 > \frac{1}{4}$, i.e. the cusp of Gauss is elliptic. Conversely, local to the cusp of Gauss, the PTBC lies in the hyperbolic region of the surface if and only if the cusp of Gauss is hyperbolic. However parallel tangent partner points must lie either side and arbitrarily close to the parabolic curve so in the limit the equidistant always lies on both sides of the parabolic curve.

The orientation of the equidistant thus depends on whether the origin is an elliptic or hyperbolic cusp of Gauss as we show in the following example:

Example 5.3.10 First we take $f = x^2 + 2xy^2 + \frac{1}{2}y^4$. So ${c_4}/{b_2}^2 = \frac{1}{8} < \frac{1}{4}$ and the origin is a hyperbolic cusp of Gauss. Local to the origin the parabolic curve and PTBC lie on opposite sides of the y–axis whilst the equidistant lies in both elliptic and hyperbolic regions as follows:

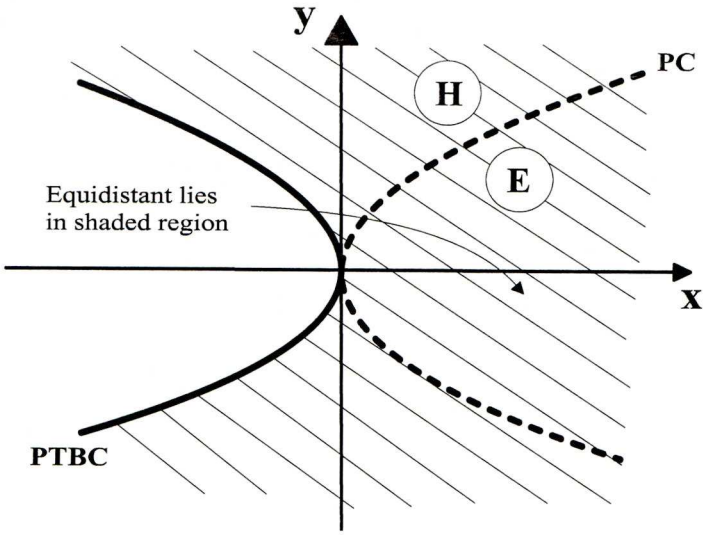

For the other possibility we take $f = x^2 + xy^2 + \frac{1}{2}y^4$. So $c_4/{b_2}^2 = \frac{1}{2} > \frac{1}{4}$ and the origin is an elliptic cusp of Gauss. Local to the origin the parabolic curve and PTBC lie on the same side of the y–axis whilst the equidistant lies in both elliptic and hyperbolic regions as follows:

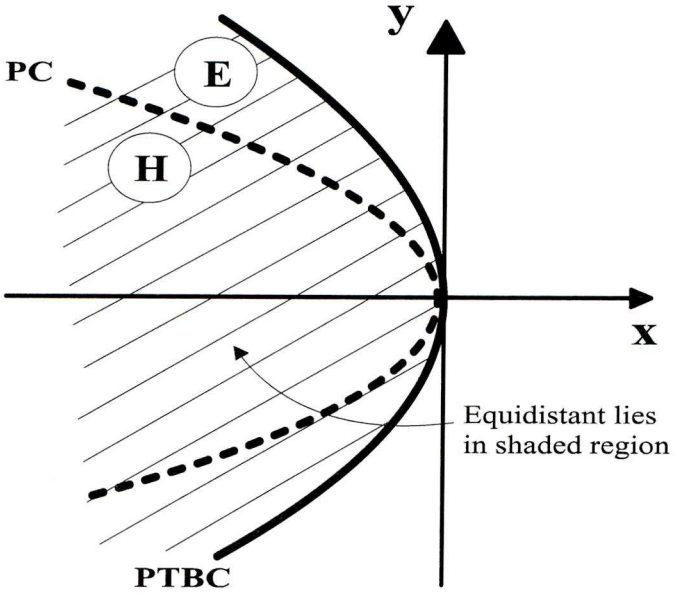

5.4 Chapter Summary

In this chapter we studied the local structure of the affine equidistants and some of their singularities. Again, due to parameterisation issues associated with the diagonal subset $\{(p,p)\}$ of Π (i.e. the set of all parallel tangent pairs), we separated the cases where the points p and q with parallel tangents lie on disjoint surfaces or on the same surface piece local to a parabolic point.

For disjoint surfaces proposition 5.2.1 states that the tangent plane to an equidistant at any point is parallel to the tangent planes at the two surface points which generated that point, whilst proposition 5.2.2 gives the condition for the equidistant to be smooth here. Proposition 5.2.4 deals with the relationship between the MPTS and the Centre Symmetry Set and shows that the singularities of the former sweep out the latter (analogous to the singularities of parallels to a plane curve sweeping out its evolute). We found a three parameter family of functions of three variables whose discriminant gave us a model of the MPTS and determined conditions for this family to versally unfold cuspidal edge (proposition 5.2.8) and swallowtail (proposition 5.2.11) points on the MPTS. We looked at the special case where the tangent plane at the two points generating a point on the MPTS is actually the same plane. The ruled surface R swept out by chords joining such points was studied in its own right and a condition for it to be smooth was determined. We showed in proposition 5.2.18 that when R shares a singular point with the MPTS then both surfaces have the same limiting tangent direction here.

For the local case we had access to *normal forms*. These represent the simplest possible versal families whose discriminants give diffeomorphic versions of the equidistants for the various cases of interest. Proofs of the validity of these normal forms are given in the next chapter but here we used them to determine general properties of the equidistants and the types of singular behaviour that they can have. In proposition 5.3.7 we showed that all proper equidistants except the MPTS meet the parabolic curve of the surface inflexionally. We showed that local to ordinary parabolic points the MPTS is a smooth surface with boundary along the parabolic curve. Local to

special parabolic points, designated A_2^*, the MPTS has a half cuspidal edge away from the parabolic curve and terminating at the A_2^* point itself. We went on to show that this cuspidal edge splits into three cuspidal edges (two of which meet to form a swallowtail point) as we move away from $\lambda = \frac{1}{2}$. Local to a cusp of Gauss we showed that the MPTS is smooth with boundary along the parabolic curve (although the contact between the MPTS and the surface is higher at the cusp of Gauss itself). For certain special values of λ, designated λ^* (which only exist when $0 < c_4/{b_2}^2 < \frac{1}{3}$), the equidistant has the structure of an "opened out" cuspidal Whitney umbrella (i.e. it has a cuspidal edge with singular point but no self intersection). All other proper equidistants are diffeomorphic to the standard cuspidal Whitney umbrella. Finally we looked at the situation of an equidistant local to a cusp of Gauss as $\lambda \to 0$ and showed that in the limit the equidistant coincides with the surface, lying entirely to one side of the PTBC but to both sides of the parabolic curve.

Chapter 6

Normal Forms for Equidistants

6.1 Introduction

In this chapter we provide further details and some alternative arguments for the proofs of the theorems given in Giblin et al. [10]. These involve the determination of normal forms for affine equidistants local to: (i) an ordinary inflexion of a smooth curve in the plane and (ii) a generic parabolic point of a smooth surface in $\mathbb{R}^3$. Such points are of particular interest as we can have pairs of points arbitrarily close to the inflexion (or parabolic point) which have parallel tangent lines (or planes). We consider all surface cases where we impose up to 2 extra conditions beyond:

$$\{\text{ordinary parabolic point, general value of } \lambda\},$$

e.g. we consider equidistants for special values of λ local to an ordinary cusp of Gauss (2 extra conditions) but not local to degenerate cusps of Gauss, A_4 or D_4 points (all 3 extra conditions) etc. The methods used are essentially the same as those used by Giblin and Zakalyukin [11] to determine generating families for the CSS but crucially a different family of equivalences is used. Here we use the so called *time-space-contact–equivalence*, or *s–equivalence* for short:

Definition 6.1.1 *The germs of families of functions $G_1(z, q, \varepsilon)$ and $G_2(z, q, \varepsilon)$, with variables $z \in \mathbb{R}^k$ and parameters $q, \varepsilon \in \mathbb{R}^n \times \mathbb{R}$, are said to be s–equivalent if there exists a non-zero function $P(z, q, \varepsilon)$ and a local diffeomorphism of the form $\theta : (z,\ q,\ \varepsilon) \mapsto (Z(z, q, \varepsilon),\ Q(q, \varepsilon),\ E(\varepsilon))$ such that $P\, G_1 = G_2 \circ \theta$.*

We showed in section 5.3 that an equidistant can be formed, for fixed ε_0, as the discriminant $\mathcal{D}_G$ of a certain generating family G. If $z = (z_1, \ldots, z_k)$ and $q = (q_1, \ldots, q_n)$ then

$$\mathcal{D}_G = \left\{ (q_1, \ldots, q_n) : G = \frac{\partial G}{\partial z_1} = \ldots = \frac{\partial G}{\partial z_k} = 0 \right\}_{\varepsilon=\varepsilon_0}.$$

The manifold formed in $\mathbb{R}^{n+1}$ as the set of all such equidistants is the big discriminant set of G, denoted $W(G)$. Since s–equivalence allows us to change ε using local diffeomorphisms of ε only, slices of $W(G)$ by hyperplanes ε = constant are diffeomorphically preserved. This is why s–equivalence is so important to this application. The generating family we need, by Lemma 2.5 of Giblin et al. [10], is

$$G(z, s, h, \lambda) = -h + \lambda f(s + \mu z) + \mu f(s - \lambda z) \tag{6.1}$$

where $\lambda + \mu = 1$. The function f describes the host curve (or surface) as a graph, with $G = z = 0$ giving $h = f(s)$ which is this host curve (or surface). The discriminant of this family $\mathcal{D}_G = \{(s, h) : G = \partial G/\partial z = 0\}$ is the equidistant for fixed λ as stated above.

With regard to the definition of s–equivalence given above the variable(s) are $z \in \mathbb{R}$ in the curve case (or $z = (x, y)$ in the surface case) whilst the parameters are $q = (s, h)$ and ε in the curve case (or $q = (s, t, h)$ and ε in the surface case). The parameter ε is usually referred to as *affine time* and its role here is played by $\varepsilon = \lambda - \lambda_0$, where λ_0 is some fixed value.

Some Technical Prerequisites

To demonstrate the s–equivalence of two families G_1 and G_2 we use the standard *Moser homotopy method* [17] by introducing a parameter τ to the family G_1 say, creating a new family G_τ. We do this in such a way that

$$G_\tau = \begin{cases} G_1 & \text{when } \tau = 1 \\ G_2 & \text{when } \tau = 0 \end{cases}$$

We now seek a family of non-zero functions $P_\tau(z, q, \varepsilon)$ and a family of diffeomorphisms of the form $\Theta_\tau : (z, q, \varepsilon) \mapsto (Z_\tau(z, q, \varepsilon), S_\tau(q, \varepsilon), H_\tau(q, \varepsilon), E_\tau(\varepsilon))$ such that

$$P_\tau \cdot G_\tau \circ \Theta_\tau = G_2$$

for any $\tau \in [0,1]$. Differentiating this expression with respect to τ we obtain[1]

$$-\frac{\partial G_\tau}{\partial \tau} = \frac{1}{P_\tau}\frac{\partial P_\tau}{\partial \tau}G_\tau + \frac{\partial G_\tau}{\partial z}\frac{\partial Z_\tau}{\partial \tau} + \frac{\partial G_\tau}{\partial s}\frac{\partial S_\tau}{\partial \tau} + \frac{\partial G_\tau}{\partial h}\frac{\partial H_\tau}{\partial \tau} + \frac{\partial G_\tau}{\partial \varepsilon}\frac{\partial E_\tau}{\partial \tau}\left(+\frac{\partial G_\tau}{\partial t}\frac{\partial T_\tau}{\partial \tau}\right)$$

with all partial derivatives of G_τ taken at the point $\Theta_\tau(z,s,h,\varepsilon)$. This is the so called *homological equation* and it tells us that for a given LHS function $\frac{\partial G_\tau}{\partial \tau}$ we need a decomposition in the form of the RHS for some smooth functions $\frac{\partial Z_\tau}{\partial \tau}$, $\frac{\partial S_\tau}{\partial \tau}$, $(\frac{\partial T_\tau}{\partial \tau})$, $\frac{\partial H_\tau}{\partial \tau}$ and $\frac{\partial E_\tau}{\partial \tau}$ in their respective variables. If we have such a decomposition then it will describe a vector field in (z,q,ε)–space which can be integrated to obtain the family of diffeomorphisms Θ_τ, with the term $\frac{1}{P_\tau}\frac{\partial P_\tau}{\partial \tau}G_\tau$ enabling us to retrieve the family P_τ. By this means we can establish the s–equivalence of G_1 and G_2. So essentially the method consists in showing that the tangent space

$$T_{G_\tau}\mathcal{Q} = \left\{-\frac{\partial G_\tau}{\partial \tau}\right\}$$

at G_τ to the space $\mathcal{Q}$ of all families of functions in z, q and ε regarded as an $\mathcal{O}_{z,q,\varepsilon}$–module[2], is contained in the tangent space

$$TO_s(G_\tau) = \left\{\tilde{P}\,G_\tau + \tilde{Z}\,\frac{\partial G_\tau}{\partial z} + \tilde{S}\,\frac{\partial G_\tau}{\partial s} + \tilde{H}\,\frac{\partial G_\tau}{\partial h} + \tilde{E}\,\frac{\partial G_\tau}{\partial \varepsilon}\left(+\tilde{T}\,\frac{\partial G_\tau}{\partial t}\right)\right\}$$

to the orbit of the group of s–equivalences through G_τ. With $\tilde{P}(z,q,\tau,\varepsilon)$, $\tilde{Z}(z,q,\tau,\varepsilon)$, $\tilde{S}(q,\tau,\varepsilon)$, $\tilde{H}(q,\tau,\varepsilon)$, $\tilde{E}(\tau,\varepsilon)$ (and $\tilde{T}(q,\tau,\varepsilon)$) being arbitrary germs in their respective variables.

The *Malgrange Preparation Theorem* is central to proving all but one of the results in this chapter and so we will state it here in full (see [14] for a proof):

Theorem 6.1.2 *Let $\mathcal{O}_{\mathbf{x}}$ be the algebra of germs at the origin of smooth functions in $\mathbf{x} \in \mathbb{R}^m$, M be a finitely generated $\mathcal{O}_{\mathbf{x}}$–module and $f : \mathbf{x}, 0 \mapsto \mathbf{y}(\mathbf{x}), 0$ be the germ of a C^∞ map from $\mathbb{R}^m$ to $\mathbb{R}^n$. If I_f is the ideal in $\mathcal{O}_{\mathbf{x}}$ generated by the components of f and the quotient algebra $M\,/\,I_f \cdot M$ is isomorphic to some finitely generated real vector space, with generators say $[g_1(\mathbf{x})], \ldots, [g_k(\mathbf{x})]$, then M regarded as an $\mathcal{O}_{\mathbf{y}(\mathbf{x})}$–module[3] is generated by $g_1, \ldots, g_k$.*

[1] The final term here, shown in round brackets, only applies in the surface case.

[2] $\mathcal{O}_{z,q,\varepsilon}$ is an R-module of monomials in z, q and ε with multiplication over the ring $\mathbb{R}$.

[3] $\mathcal{O}_{\mathbf{y}(\mathbf{x})}$ is the algebra of smooth function germs at the origin composed with the components of the map f, i.e. $\mathcal{O}_{\mathbf{y}(\mathbf{x})} = \{h(\mathbf{y_1}(\mathbf{x}), \ldots, \mathbf{y_m}(\mathbf{x}))\}$ with h an arbitrary smooth germ.

6.2 Equidistants to Curves

Here we are concerned with equidistants to a smooth plane curve $\mathcal{C}$ with ordinary inflexion at the origin. So $z, s \in \mathbb{R}$ and $\mathcal{C}$ is given as the graph of the function $f(s) = s^3 + c_4 s^4 + c_5 s^5 + \text{h.o.t}$ (following an affine transformation to make the coefficient of s^3 equal to 1). We also assume that $\mathcal{C}$ satisfies the generic condition $c_4 \neq 0$. Note: in the surface case we meet special parabolic points, denoted $A_2{}^*$, where a condition analogous to $c_4 = 0$ occurs generically. Now, the relevant theorem from [10] is

Theorem 6.2.1 *Given a smooth curve $\mathcal{C}$ with ordinary inflexion at the origin, then the germ of the family $G(z, s, \lambda_0 + \varepsilon)$ (at the origin) is s–equivalent to the germ of a family H (at the origin) where*

(i) $\lambda_0 \neq 0, \frac{1}{2}$ *or* 1 *implies* $H = -\tilde{h} + sz^2 + z^3$,

(ii) $\lambda_0 = 0$ *or* 1 *implies* $H = -\tilde{h} + \varepsilon(sz^2 + z^3)$, *and*

(iii) $\lambda_0 = \frac{1}{2}$ *implies* $H = -\tilde{h} + sz^2 + \varepsilon z^3 + z^4$.

Proof: (i) We start by substituting $f(\zeta) = \zeta^3 + c_4\zeta^4 + c_5\zeta^5 + \ldots$ into the family G of equation (6.1) with $\zeta = s \pm \lambda z$. Writing G as a series in z we obtain

$$G(z, s, \tilde{h}, \lambda, \mu) = -h + f(s) + \lambda\mu \Big\{ z^2 \,(\, 3s + 6c_4 s^2 + 10c_5 s^3 + \ldots \,) +$$

$$(\mu - \lambda)\, z^3 \,(\, 1 + 4c_4 s + 10c_5 s^2 + \ldots \,) \; + \; O(z^4) \Big\}$$

where '...' means terms of higher degree in s. Using the s–equivalent change of parameter $3s + 6c_4 s + \ldots \mapsto s$ (i.e. the coefficient of z^2 above) followed by appropriate rescalings of s and z we can write G in the form $G = -\tilde{h} + sz^2 + z^3\,(\,1 + A(z, s, \varepsilon)\,)$ for some smooth function A where $A(0) = 0$, $\tilde{h} = h - f(s)$ and $\varepsilon = \lambda - \lambda_0$. We now apply Moser's method to show that G is s–equivalent to the normal form $H = -\tilde{h} + sz^2 + z^3$ by taking a homotopy

$$G_\tau = -\tilde{h} + sz^2 + z^3\,(\,1 + \tau\, A(z, s, \varepsilon)\,), \quad \tau \in [0, 1] \tag{6.2}$$

joining $H\,(\tau = 0)$ and $G\,(\tau = 1)$. In the introduction we gave the general method of establishing s–infinitesimal stability but in this case we can simplify greatly by

showing that $T_{G_\tau}\mathcal{Q}$ is contained in a much smaller subspace of $TO_s(G_\tau)$, namely

$$T_* = \mathcal{O}_{z,s,\tilde{h},\varepsilon}\left\{z\frac{\partial G_\tau}{\partial z}\right\} + \mathcal{O}_{s,\tilde{h},\varepsilon}\left\{\frac{\partial G_\tau}{\partial s}\right\}.$$

Here $\frac{\partial G_\tau}{\partial \tau} = z^3\,A(z,s,\varepsilon)$ but we will in fact show that every element of $\mathcal{O}_{z,s,\tilde{h},\varepsilon}$ which is divisible by z^2 lies in the tangent space to the orbit of s–equivalences through G_τ. To do this we use the Malgrange preparation theorem with $M = \mathcal{O}_{z,s,\tilde{h},\varepsilon,\tau}\{z^2\}$, i.e. germs of functions in $(z,s,\tilde{h},\varepsilon,\tau)$–space at $(0,0,0,0,\tau_0)$ which are divisible by z^2, and the map f to be $f : \mathbf{x} = (z,s,\tilde{h},\varepsilon,\tau) \mapsto \mathbf{y} = (z\frac{\partial G_\tau}{\partial z}, s, \tilde{h}, \varepsilon, \tau - \tau_0)$. Note: $\frac{\partial G_\tau}{\partial \tau} \in M$ for all τ. Now

$$z\frac{\partial G_\tau}{\partial z} = s\left(2z^2\right) + z^3\left(3(1+\tau A) + z\tau\frac{\partial A}{\partial z}\right).$$

The first term on the RHS has a factor s and the second is z^3 times a function which is invertible in $\mathcal{O}_{\mathbf{x}}$. Hence $I_f = \left\langle z\frac{\partial G_\tau}{\partial z}, s, \tilde{h}, \varepsilon, \tau - \tau_0\right\rangle = \left\langle z^3, s, \tilde{h}, \varepsilon, \tau - \tau_0\right\rangle$ and

$$L = M/(I_f \cdot M) = \mathcal{O}_{\mathbf{x}}\{z^2\} \,/\, \langle z^3, s, \tilde{h}, \varepsilon, \tau - \tau_0\rangle \cdot \mathcal{O}_{\mathbf{x}}\{z^2\} \cong \mathbb{R}\{z^2, z^3, z^4\}.$$

Using $[f]$ to denote the class of a function f in the quotient space L then for any f we have $[f] = a_2[z^2] + a_3[z^3] + a_4[z^4]$ for some $a_i \in \mathbb{R}$. Hence

$$\left[z\frac{\partial G_\tau}{\partial z}\right] = 3[z^3] + a_0[z^4] \quad \text{and} \quad \left[z^2\frac{\partial G_\tau}{\partial z}\right] = 3[z^4]$$

for some $a_0 \in \mathbb{R}$. Also

$$\frac{\partial G_\tau}{\partial s} = z^2 + z^3\,\tau\frac{\partial A}{\partial s} \quad \text{so} \quad \left[\frac{\partial G_\tau}{\partial s}\right] = [z^2] + b_0[z^3] + b_1[z^4]$$

for some $b_0, b_1 \in \mathbb{R}$. Clearly $[z^2]$, $[z^3]$ and $[z^4]$ can be obtained as linear combinations of $[\frac{\partial G_\tau}{\partial s}]$, $[\frac{z\partial G_\tau}{\partial z}]$ and $[z^2\frac{\partial G_\tau}{\partial z}]$. Hence by the Malgrange preparation theorem

$$M = \mathcal{O}_{\mathbf{y}(\mathbf{x})}\left\{\frac{\partial G_\tau}{\partial s}, z\frac{\partial G_\tau}{\partial z}, z^2\frac{\partial G_\tau}{\partial z}\right\}.$$

Thus, for any $m \in M$ we can write

$$m = R_1 \cdot \frac{\partial G_\tau}{\partial s} + R_2 \cdot z\frac{\partial G_\tau}{\partial z} + R_3 \cdot z^2\frac{\partial G_\tau}{\partial z}$$

for some smooth functions $R_i \in \mathcal{O}_{\mathbf{y}(\mathbf{x})}$. Finally, we can decompose the function R_1 using Hadamard's lemma by writing $R_1 = R_1(0,s,\tilde{h},\varepsilon) + R_4 \cdot z\frac{\partial G_\tau}{\partial z}$ whence we can write any element $m \in M$ as

$$m = f_1 \cdot \frac{\partial G_\tau}{\partial s} + f_2 \cdot z\frac{\partial G_\tau}{\partial z}$$

for some functions $f_1 \in \mathcal{O}_{s,\tilde{h},\varepsilon}$ and $f_2 \in \mathcal{O}_{z,s,\tilde{h},\varepsilon}$. Thus $M \subset T_* \subset TO_s(G_\tau)$ and s–infinitesimal stability is proven. □

Proof: (ii) This case proceeds along the same lines as part (i) but with $\lambda_0 = 0$ (or 1) so that $\varepsilon = \lambda$ (or μ). Similar transformations and re-scaling to the above give the following homotopy

$$\bar{G}_\tau = -\bar{h} + \varepsilon s z^2 + \varepsilon z^3 \left(1 + \tau \bar{A}(z, s, \varepsilon)\right)$$

with $\tau \in [0, 1]$ and $\bar{A}(0) = 0$. So in this case $\frac{\partial \bar{G}_\tau}{\partial \tau} = \varepsilon z^3 \bar{A}(z, s, \varepsilon)$ and it is sufficient to show that all function germs divisible by εz^2 lie in $TO_s(\bar{G}_\tau)$. In part (i) we showed that

$$\mathcal{O}_{z,s,\tilde{h},\varepsilon}\{z^2\} = \mathcal{O}_{z,s,\tilde{h},\varepsilon}\left\{z\frac{\partial G_\tau}{\partial z}\right\} + \mathcal{O}_{s,\tilde{h},\varepsilon}\left\{\frac{\partial G_\tau}{\partial s}\right\}.$$

Multiplying both sides of this equivalence of sets by ε we obtain

$$\mathcal{O}_{z,s,\tilde{h},\varepsilon}\{\varepsilon z^2\} = \mathcal{O}_{z,s,\tilde{h},\varepsilon}\left\{z\frac{\partial \bar{G}_\tau}{\partial z}\right\} + \mathcal{O}_{s,\tilde{h},\varepsilon}\left\{\frac{\partial \bar{G}_\tau}{\partial s}\right\}.$$

Thus $\mathcal{O}_{z,s,\tilde{h},\varepsilon}\{\varepsilon z^2\} \subset TO_s(\bar{G}_\tau)$ and s-infinitesimal stability is proven. □

Proof: (iii) For the proof of this part we make use of the fact that the family G is invariant under the action of the map

$$\sigma : (z,\ \lambda,\ \mu) \mapsto (-z,\ \mu,\ \lambda)$$

since clearly $\sigma \circ G = -h + \mu f(s - \lambda z) + \lambda f(s + \mu z) = G$. Consequently we will work in $\mathcal{O}_{\mathbf{x}}^{\sigma}$, the subspace of $\mathcal{O}_{\mathbf{x}}$ containing germs which are invariant under the action of the map σ. Throughout the proof we will use the fact that every member of $\mathcal{O}_{\mathbf{x}}^{\sigma}$ is a function of the basic σ invariant functions z^2, $z\varepsilon$, ε^2 and $q = (s, \tilde{h})$ by lemma 6.2.2 (stated and proved at the end of this section).

We now proceed in a similar fashion to parts (i) and (ii) but with $\lambda_0 = \frac{1}{2}$ so that $\varepsilon = \lambda - \frac{1}{2} = \frac{1}{2} - \mu = \frac{1}{2}(\lambda - \mu)$. Again similar transformations and re-scalings to cases (i) and (ii) give the following homotopy

$$\hat{G}_\tau = -\hat{h} + s z^2 \left(1 + \tau \hat{A}^{\sigma}(s, \varepsilon^2)\right) + \varepsilon z^3 \left(1 + \tau \hat{B}^{\sigma}(s, \varepsilon^2)\right) + z^4 \left(1 + \tau \hat{C}^{\sigma}(z, s, \varepsilon)\right)$$

with $\tau \in [0,1]$ and $\hat{A}^\sigma(0) = \hat{B}^\sigma(0) = \hat{C}^\sigma(0) = 0$. For this case $\frac{\partial \hat{G}_\tau}{\partial \tau} = z^2\,\hat{D}^\sigma(z,s,\varepsilon)$ for some σ–invariant function $\hat{D}^\sigma$, and it is enough to demonstrate that all σ–invariant function germs divisible by z^2 lie in $TO_s(\hat{G}_\tau)$. We apply Poénaru's preparation theorem with $M = \mathcal{O}^\sigma_{\mathbf{x}}\{z^2\}$ and $f : \mathbf{x} = (z,\, q,\, \tau,\, \varepsilon) \mapsto \mathbf{y} = (z\,\frac{\partial \hat{G}_\tau}{\partial z},\, \hat{G}_\tau,\, q,\, \tau - \tau_0,\, \varepsilon^2)$. Now

$$z\,\frac{\partial \hat{G}_\tau}{\partial z} = s\left(2\,z^2\,(1+\tau\,\hat{A}^\sigma)\right) + \varepsilon z^3\left(3 + 3\,\tau\,\hat{B}^\sigma\right) + z^4\left(4 + 4\,\tau\hat{C}^\sigma + z\,\tau\,\frac{\partial \hat{C}^\sigma}{\partial z}\right)$$

We can write $z\frac{\partial \hat{G}_\tau}{\partial z} = 3\varepsilon z^3 + z^4\phi_1^\sigma + \alpha$ and $\hat{G}_\tau = \varepsilon z^3 + z^4\phi_2^\sigma + \beta$, where ϕ_1^σ and ϕ_2^σ are σ–invariant functions which are non-zero at the origin and $\alpha,\, \beta \in I_f$. So that

$$z\frac{\partial \hat{G}_\tau}{\partial z} - 3\hat{G}_\tau - (\alpha + 3\beta) = z^4(\phi_1 - 3\phi_2) \in I_f.$$

Now $(\phi_1 - 3\phi_2)(0) = 1 \neq 0$ so $\phi_1 - 3\phi_2$ is invertible and $z^4 \in I_f$. Similarly

$$z\frac{\partial \hat{G}_\tau}{\partial z} - \frac{\phi_1^\sigma}{\phi_2^\sigma}\,\hat{G}_\tau - \left(\alpha + \frac{\phi_1^\sigma}{\phi_2^\sigma}\beta\right) = \varepsilon z^3\left(3 - \frac{\phi_1^\sigma}{\phi_2^\sigma}\right) \in I_f.$$

since $\phi_2(0) \neq 0$. Now $(3 - \frac{\phi_1^\sigma}{\phi_2^\sigma})(0) = -1 \neq 0$ so $3 - \frac{\phi_1^\sigma}{\phi_2^\sigma}$ is invertible and $\varepsilon z^3 \in I_f$. Hence

$$M \,/\, I_f \cdot M \cong \mathbb{R}\{z^2,\, \varepsilon z^3,\, z^4\}$$

since $z^3 \notin \mathcal{O}^\sigma_{\mathbf{x}}$. So every element $m \in M$ can be written in the form $m = z^2\,f_1 + \varepsilon z^3\,f_2 + z^4\,f_3$ for some functions $f_i \in \mathcal{O}^\sigma_{\mathbf{y}(\mathbf{x})}$. Now

$$\frac{\partial \hat{G}_\tau}{\partial s} = z^2\left(1 + \tau\,\hat{A}^\sigma + s\,\tau\,\frac{\partial \hat{A}^\sigma}{\partial s}\right) + \varepsilon z^3\,\tau\,\frac{\partial \hat{B}^\sigma}{\partial s} + z^4\,\tau\,\frac{\partial \hat{C}^\sigma}{\partial s}.$$

Taking the second and third terms on the RHS over to the LHS and multiplying both sides by the inverse of the function multiplying z^2 (a σ–invariant function in ε^2 and q only) we obtain

$$z^2 = \frac{\partial \hat{G}_\tau}{\partial s}\,H^\sigma(\varepsilon^2,\, q,\, \tau) + \varepsilon z^3\,J^\sigma(z,\, q,\, \tau) + z^4\,K^\sigma(z,\, q,\, \tau)$$

for some σ–invariant functions H, J and K. We have already shown that εz^3 and z^4 can be written in terms of $z\,\frac{\partial \hat{G}_\tau}{\partial z}$ and $\hat{G}_\tau$ so

$$z^2 = \frac{\partial \hat{G}_\tau}{\partial s}\,H^\sigma(\varepsilon^2,\, q,\, \tau) + z\,\frac{\partial \hat{G}_\tau}{\partial z}\,\hat{J}^\sigma(z,\, q,\, \tau) + \hat{G}_\tau\,\hat{K}^\sigma(z,\, q,\, \tau).$$

Multiplying both sides by f_1 and decomposing the factor of $\frac{\partial \hat{G}_\tau}{\partial s}$ using Hadamard's lemma (i.e. removing those parts involving $z\,\frac{\partial \hat{G}_\tau}{\partial z}$ and $\hat{G}_\tau$ and pulling them in to the $z\,\frac{\partial \hat{G}_\tau}{\partial z}$ and $\hat{G}_\tau$ terms) we obtain

$$z^2 f_1 + \varepsilon z^3 f_2 + z^4 f_3 = \frac{\partial \hat{G}_\tau}{\partial s} P^\sigma(\varepsilon^2, q, \tau) + z \frac{\partial \hat{G}_\tau}{\partial z} Q^\sigma(z, q, \tau) + \hat{G}_\tau R^\sigma(z, q, \tau)$$

for some σ–invariant functions P^σ, Q^σ and R^σ. It follows that $\mathcal{O}^\sigma_{\mathbf{x}}\{z^2\} \subset TO_s(\hat{G}_\tau)$ and s-infinitesimal stability is proven. □

Lemma 6.2.2 *Every member of the space $\mathcal{O}^\sigma_{\mathbf{x}}$ is a function of the basic σ invariant functions z^2, $z\varepsilon$, ε^2 and $q = (s, \tilde{h})$.*

Proof: We use Poénaru's version of the preparation theorem for symmetric functions [19] with $f : (z, \varepsilon, q) \mapsto (z^2, z\varepsilon, \varepsilon^2, q)$ and $M = \mathcal{O}^\sigma_{\mathbf{x}}$. Hence the quotient space $M \,/\, I_f \cdot M$ is generated by $[1]$, $[z]$ and $[\varepsilon]$, and these elements generate M as an $\mathcal{O}_{\mathbf{y}(\mathbf{x})}$–module via f, i.e. every element $m \in M$ can be written

$$m(z, \varepsilon) = R_1(z^2, z\varepsilon, \varepsilon^2) + z\, R_2(z^2, z\varepsilon, \varepsilon^2) + \varepsilon\, R_3(z^2, z\varepsilon, \varepsilon^2)$$

for smooth germs $R_i \in \mathcal{O}_{\mathbf{y}(\mathbf{x})}$. However, $m(z, \varepsilon) = m(-z, -\varepsilon)$ since m is σ–invariant, thus $R_1 + z\, R_2 + \varepsilon\, R_3 = R_1 - z\, R_2 - \varepsilon\, R_3$ which implies that $z\, R_2 + \varepsilon\, R_3 = 0$ for all small z and ε. This can only hold if $R_2 \equiv 0$ and $R_3 \equiv 0$ so that $m(z, \varepsilon) = R_1(z^2, z\varepsilon, \varepsilon^2)$ as required. □

6.3 Equidistants to Surfaces

This time we are concerned with equidistants to a smooth surface piece $\mathcal{S}$ with parabolic curve passing through the origin. Hence we now have two variables x and y (in place of z) and an additional parameter t (so that $h = f(s,t)$ in the family G). The surface $\mathcal{S}$ is given in special Monge form as

$$f(x,y) = x^2 + a_{30}\,x^3 + a_{21}\,x^2\,y + a_{12}\,x\,y^2 + a_{03}\,y^3 + \text{h.o.t} \tag{6.3}$$

where a_{ij} is the coefficient of $x^i y^j$. Points along the parabolic curve for which the family of height functions on $\mathcal{S}$ is A_2 singular are called *ordinary parabolic points* (or just A_2 points for brevity). Generically there can also be isolated points for which the family of height functions is A_3 singular, called *cusps of Gauss* (or just A_3 points). We will deal with these two cases separately:

A_2 Cases

By using a linear change of variable $y \mapsto a_{12}\,x/(3\,a_{03}) + y/\sqrt[3]{a_{03}}$ when $a_{03} \neq 0$ (i.e. the origin is an ordinary parabolic point) we can reduce the 3–jet of f to the form

$$f(x,y) = x^2 + a_{30}\,x^3 + a_{21}\,x^2 y + y^3 + \text{h.o.t.}$$

Note: the a_{ij} here are not the same as those of equation (6.3). After this normalisation there may be isolated points for which the 4th order terms vanish when $x = 0$. We call such points A_2^* points of $\mathcal{S}$ and show below that the equidistants have a special structure local to such points. When the 4th order terms do not vanish with $x = 0$ we use the usual notation A_2. Now, using this normalised form for f and substituting into equation (6.1) with $\mathbf{z} = (x,y)$ and $\mathbf{s} = (s,t)$ we obtain

$$G(x,y,s,t,\tilde{h},\lambda) = -\tilde{h} + \lambda\mu\left(x^2 + (\mu-\lambda)(a_{30}x^3 + a_{21}x^2y + y^3) + \text{h.o.t.}\right)$$

$\tilde{h} = h - G|_{x=y=0}$. We can now state the relevant theorem from [10] regarding normal forms for equidistants local to A_2 and A_2^* points at the origin on $\mathcal{S}$:

Theorem 6.3.1 *Given a smooth surface piece $\mathcal{S}$ with an A_2 or A_2^* of the family of height functions at the origin, then the germ of the family $G(x,y,s,t,\lambda_0+\varepsilon)$ (at the origin) is s–equivalent to the germ of a family H (at the origin) where*

(i) $\mathcal{S}$ *is* A_2 *(or* A_2^**) and* $\lambda_0 \neq 0, \frac{1}{2}$ *or* 1 *implies* $H = -\tilde{h} + ty^2 + y^3$,

(ii) $\mathcal{S}$ *is* A_2 *(or* A_2^**) and* $\lambda_0 = 0$ *or* 1 *implies* $H = -\tilde{h} + \varepsilon(ty^2 + y^3)$,

(iii) $\mathcal{S}$ *is* A_2 *and* $\lambda_0 = \frac{1}{2}$ *implies* $H = -\tilde{h} + ty^2 + \varepsilon y^3 + y^4$, *and*

(iv) $\mathcal{S}$ *is* A_2^* *and* $\lambda_0 = \frac{1}{2}$ *implies* $H = -\tilde{h} + ty^2 + \varepsilon y^3 + sy^4 + y^6$, *provided* $a_{05} \neq 0$, $a_{14} \neq a_{21}a_{13}$ *and* ${a_{13}}^2 \neq 4a_{06}$.

In proving these statements we start by observing that $\partial G/\partial x = 2\lambda\mu x + \text{h.o.t.}$ So provided $\lambda \neq 0$ or 1 (i.e. the equidistant does not lie in the surface) we can solve $\partial G/\partial x = 0$ for x and substitute back into the family G giving us a family

$$\hat{G}(x, y, s, t, \tilde{h}, \lambda) = -\tilde{h} + \lambda\mu\left((\mu - \lambda)\, y^3 + (\mu^2 + \lambda^2 - \lambda\mu)\, a_{04}\, y^4 + 3t\, y^2 + \text{h.o.t.}\right).$$

This is essentially the same family as used in the curve cases above since simple rescalings will lead to equivalent homotopies. Hence the proofs of (i), (ii) and (iii) here follow in an identical fashion.

Proof: (iv) For the proof of this part we note that the family $\hat{G}$ is invariant under the action of the map $\sigma : (x, y, \lambda, \mu) \mapsto (-x, -y, \mu, \lambda)$. We set $a_{04} = 0$ (so $\mathcal{S}$ is A_2^* at the origin) and $\lambda = \frac{1}{2} + \varepsilon$ ($\mu = \frac{1}{2} - \varepsilon$) in the family $\hat{G}$ to give

$$\hat{G}(x, y, s, t, \tilde{h}, \lambda) = -\tilde{h} + \lambda\mu\Big\{y^2\left(\frac{3}{4}t + \ldots\right) + \varepsilon y^3\left(-\frac{1}{2} + \ldots\right) +$$

$$y^4\left(\frac{a_{14} - a_{21}a_{13}}{16}\, s + \frac{5a_{05}}{16}\, t + \ldots\right) + \varepsilon y^5\left(-\frac{a_{05}}{4} + \ldots\right) + y^6\left(\frac{4a_{06} - a_{13}^2}{256} + \ldots\right) + O(y^7)\Big\}.$$

We can use an s–equivalent change of t to reduce the coefficient of y^2 to just t, and provided $a_{14} - a_{21}\, a_{13} \neq 0$ we can make an s–equivalent change of s to reduce the coefficient of y^4 to just s. Provided $a_{05} \neq 0$ and $4a_{06} - a_{13}^2 \neq 0$ we can re-scale y and all parameters so that the constants in the coefficients of εy^3, εy^5 and y^6 are set to 1. After these changes we will achieve the following homotopy

$$\hat{G}_\tau = -\tilde{h} + ty^2 + \varepsilon y^3\,(1 + \tau A^\sigma(s, t, \varepsilon)) + sy^4 + \varepsilon y^5\,(1 + \tau B^\sigma(s, t, \varepsilon)) + y^6\,(1 + \tau C^\sigma(y, s, t, \varepsilon))$$

with $\tau \in [0, 1]$. Hence $\frac{\partial \hat{G}_\tau}{\partial \tau} = y^2\,(\varepsilon y A^\sigma + \varepsilon y^3 B^\sigma + y^4 C^\sigma) \in \mathcal{O}_{\mathbf{x}}^\sigma\{y^2\}$ for all τ, and

$$y\,\frac{\partial \hat{G}_\tau}{\partial y} = 2ty^2 + 4sy^4 + 3\varepsilon y^3(1 + \tau A^\sigma + 5y^2(1 + \tau B^\sigma)) + y^6(6 + 6\tau C^\sigma + \tau C_y^\sigma),$$

$$\frac{\partial \hat{G}_\tau}{\partial s} = y^4 + \varepsilon y^3(\tau A_s^\sigma + y^2 \tau B_s^\sigma) + y^6 \tau C_s^\sigma, \quad \frac{\partial \hat{G}_\tau}{\partial t} = y^2 + \varepsilon y^3(\tau A_t^\sigma + y^2 \tau B_t^\sigma) + y^6 \tau C_t^\sigma.$$

We now apply Poénaru's preparation theorem with $M = \mathcal{O}_{\mathbf{x}}^\sigma\{y^2\}$ and

$$f : (y,\, s,\, t,\, \tilde{h},\, \tau,\, \varepsilon) \mapsto \left(y\frac{\partial \hat{G}_\tau}{\partial y},\, \hat{G}_\tau,\, s,\, t,\, \tilde{h},\, \tau - \tau_0,\, \varepsilon^2 \right).$$

We can write $y\frac{\partial \hat{G}_\tau}{\partial y} = \varepsilon y^3 + y^6\phi_1^\sigma + \alpha$ and $\hat{G}_\tau = \varepsilon y^3 + y^6\phi_2^\sigma + \beta$, where ϕ_1^σ and ϕ_2^σ are σ–invariant functions which are non-zero at the origin and $\alpha,\, \beta \in I_f$. So that

$$y\frac{\partial \hat{G}_\tau}{\partial y} - \hat{G}_\tau - (\alpha + 3\beta) = y^6(\phi_1 - \phi_2) \in I_f.$$

Now $(\phi_1 - \phi_2)(0) = 3 \neq 0$ so $\phi_1 - 3\phi_2$ is invertible and $y^6 \in I_f$. Similarly

$$y\frac{\partial \hat{G}_\tau}{\partial y} - \frac{\phi_1}{\phi_2}\hat{G}_\tau - \left(\alpha + \frac{\phi_1}{\phi_2}\beta\right) = \varepsilon y^3\left(3 - \frac{\phi_1}{\phi_2}\right) \in I_f.$$

since $\phi_2(0) \neq 0$. Now $(3 - \frac{\phi_1}{\phi_2})(0) = -3 \neq 0$ so $3 - \frac{\phi_1}{\phi_2}$ is invertible and $\varepsilon y^3 \in I_f$. Hence

$$M/I_f \cdot M \cong \mathbb{R}\{y^2,\, \varepsilon y^3,\, y^4,\, y^6\}$$

since $y^3,\, \varepsilon y^2,\, \varepsilon y^4,\, y^5,\, \varepsilon y^6,\, y^7 \notin M$ and $\varepsilon y^5,\, \varepsilon y^7 \in I_f \cdot M$. We can write εy^3 and y^6 in terms of $y\frac{\partial \hat{G}_\tau}{\partial y}$ and $\hat{G}_\tau$ whilst y^2 and y^4 can be written as linear combinations of these with $\frac{\partial \hat{G}_\tau}{\partial t}$ and $\frac{\partial \hat{G}_\tau}{\partial s}$ respectively. So by Poénaru's preparation theorem

$$m = y\frac{\partial \hat{G}_\tau}{\partial y} R_1 + \hat{G}_\tau R_2 + \frac{\partial \hat{G}_\tau}{\partial s} R_3 + \frac{\partial \hat{G}_\tau}{\partial t} R_4$$

for all $m \in M$ with the R_i being smooth functions of $y\frac{\partial \hat{G}_\tau}{\partial y}$, $\hat{G}_\tau$, s, t, $\tilde{h}$, $\tau - \tau_0$ and ε^2. Decomposing R_3 and R_4 to pull the parts containing $\hat{G}_\tau$ and $y\frac{\partial \hat{G}_\tau}{\partial y}$ away from $\frac{\partial \hat{G}_\tau}{\partial s}$ and $\frac{\partial \hat{G}_\tau}{\partial t}$ we see that $\mathcal{O}_{\mathbf{x}}^\sigma\{y^2\} \subset TO_s(\hat{G}_\tau)$ and s-infinitesimal stability is proven. □

A_3 Cases

Along the parabolic curve there are special isolated points, called *cusps of Gauss*, for which the family of height functions to the surface has an A_3 singularity. With regard to equation (6.3) the condition on the coefficients of the Taylor series of f for such points is $a_{03} = 0$. If also $a_{12}^2 \neq 4a_{04}$ then the cusp of Gauss is *non-degenerate* (i.e. the singularity of the family of height functions is exactly A_3). If also $a_{12} \neq 0$ we call the

cusp of Gauss *ordinary*, and in such cases the parabolic curve is smooth through the cusp of Gauss. If we assume $a_{12} > 0$ (else perform the transformation $x \mapsto -x$) then a linear change of variable $-a_{21}\,x/(2\,a_{12}) + y/\sqrt{a_{12}} \mapsto y$ reduces the 3–jet of f to

$$f(x,y) = x^2 + a_{30}\,x^3 + xy^2 + \text{h.o.t.}$$

Substituting this normalised form for f into equation (6.1) we again find that $\partial G/\partial x = 2x + \text{h.o.t.}$ So solving $\partial G/\partial x = 0$ for x and substituting back in to G we obtain the following

$$\hat{G}(x,y,s,t,\tilde{h},\lambda) = -\tilde{h} + \lambda\mu\Big\{\, y^2\Big(\, s + \ldots\,\Big) + (\mu-\lambda)\,y^3\Big(\, a_{13}s + (4a_{04}-1)\,t + \ldots\,\Big) +$$

$$y^4\Big(\big\{4a_{04}(\mu^2-\lambda\mu+\lambda^2) - (\mu-\lambda)^2\big\} + \big\{(\mu-\lambda)^2(3a_{30}-4a_{22}) + 4a_{14}(\mu^2-\lambda\mu+\lambda^2)\big\}\,s +$$

$$\big\{5(\mu-\lambda)^2(a_{13}-2a_{05}) - 3\mu\lambda a_{13}\big\}\,t + \ldots\,\Big) +$$

$$(\mu-\lambda)\,y^5\Big(\big\{a_{13}\,(\lambda^2-\lambda\mu+\mu^2) - 2a_{05}(\mu^2+\lambda^2)\big\} + \ldots\,\Big) + O(y^6)\Big\}$$

where '...' denotes terms of order 2 and higher in s and t. We see that the constant term in the coefficient of y^4 here can vanish for certain special values of λ. There are two such values, which we denote λ^*, symmetric about $\frac{1}{2}$ and given by

$$\lambda^* = \frac{1}{2} \pm \frac{1}{2}\sqrt{\frac{a_{04}}{1-3a_{04}}}.$$

The normal form and resulting equidistants are quite different when $\lambda_0 = \lambda^*$ as we have shown in section 5.3. We now state the relevant theorem from [10] regarding normal forms for equidistants local to an ordinary cusp of Gauss at the origin on $\mathcal{S}$:

Theorem 6.3.2 *Given a smooth surface piece $\mathcal{S}$ with an A_3 of the family of height functions at the origin, then the germ of the family $G(x,y,s,t,\lambda_0+\varepsilon)$ (at the origin) is s–equivalent to the germ of a family H (at the origin) where*

(i) $\lambda_0 \neq 0, \frac{1}{2}, \lambda^*$ *or* 1 *implies* $H = -\tilde{h} + sy^2 + ty^3 + y^4$, *provided* $a_{04} \neq 0$

(ii) $\lambda_0 = 0$ *or* 1 *implies* $H = -\tilde{h} + \varepsilon(sy^2 + ty^3 + y^4)$, *provided* $a_{04} \neq 0$

(iii) $\lambda_0 = \frac{1}{2}$ *implies* $H = -\tilde{h} + sy^2 + \varepsilon ty^3 + y^4$, *provided* $a_{04} \neq 0$ *or* $\frac{1}{4}$

(iv) $\lambda_0 = \lambda^*$ *implies* $H = -\tilde{h} + sy^2 + ty^3 + (\varepsilon + t)y^4 + y^5$, *provided* $a_{04} \neq 0$, $\frac{1}{4}$ *or* $\frac{1}{3}$, $a_{13} \neq 5a_{05} - 6a_{13}a_{04}$ *and* $a_{13} \neq 4a_{05}(1 - 2a_{04})$.

Proof: (i) Here $\lambda = \lambda_0 + \varepsilon$ with $\lambda_0 \neq 0$, $\frac{1}{2}$, λ^* or 1. By inspection of $\hat{G}$ above we can make s–equivalent changes to s, t and re-scale s, t and y to give the following homotopy[4]

$$\hat{G}_\tau = -\tilde{h} + sy^2 + ty^3 + y^4\,(\,1 + \tau A(y, s, t, \varepsilon)\,)$$

with $\tau \in [0, 1]$ and $A(0) = 0$. Now $\frac{\partial \hat{G}_\tau}{\partial \tau} = y^4 A$ whilst

$$y\,\frac{\partial \hat{G}_\tau}{\partial y} = 2sy^2 + 3ty^3 + y^4\,(4 + 4\tau A + y\tau A_y).$$

We now apply the Malgrange preparation theorem with $M = \mathcal{O}_{\mathbf{x}}\{y^4\}$ and

$$f : (y, s, t, \tilde{h}, \tau, \varepsilon) \mapsto \left(y\,\frac{\partial \hat{G}_\tau}{\partial y}, s, t, \tilde{h}, \tau - \tau_0, \varepsilon \right).$$

In I_f we have $\{y\,\frac{\partial \hat{G}_\tau}{\partial y}\} = \{y^4\}$ so that

$$M/I_f \cdot M \cong \mathbb{R}\{y^4, y^5, y^6, y^7\}.$$

Now $\{y^2\,\frac{\partial \hat{G}_\tau}{\partial y}\} = \{y^5\}$, $\{y^3\,\frac{\partial \hat{G}_\tau}{\partial y}\} = \{y^6\}$ and $\{y^4\,\frac{\partial \hat{G}_\tau}{\partial y}\} = \{y^7\}$ so by the theorem

$$m = y\frac{\partial \hat{G}_\tau}{\partial y}\,\left(R_1 + y\,R_2 + y^2\,R_3 + y^3\,R_4\right)$$

for all $m \in M$ with the R_i being smooth functions of $y\frac{\partial \hat{G}_\tau}{\partial y}$, s, t, $\tilde{h}$, $\tau - \tau_0$ and ε. Clearly $\mathcal{O}_{\mathbf{x}}\{y^4\} \subset TO_s(\hat{G}_\tau)$ and s-infinitesimal stability is proven. □

Proof: (ii) We take $\lambda_0 = 0$ and after substituting $\lambda = \varepsilon$ into the expression for $\hat{G}$ above the same s–equivalent changes to s, t and y that we used in (i) give the following homotopy

$$\bar{G}_\tau = -\tilde{h} + \varepsilon sy^2 + \varepsilon ty^3 + \varepsilon y^4\,(\,1 + \tau \bar{A}(y, s, t, \varepsilon)\,)$$

with $\tau \in [0, 1]$ and $\bar{A}(0) = 0$. We showed in part (i) that

$$\mathcal{O}_{\mathbf{x}}\{y^4\} = y\frac{\partial \hat{G}_\tau}{\partial y}\,\mathcal{O}_{\mathbf{y(x)}}\{1, y, y^2, y^3\}.$$

[4]Provided $a_{04} \neq \frac{1}{4}$ and $4a_{04}(\mu^2 - \mu\lambda + \lambda^2) \neq (\mu - \lambda)^2$. Both of these conditions hold since the cusp of Gauss at the origin on $\mathcal{S}$ is ordinary and $\lambda \neq \lambda^*$.

Multiplying both sides of this expression by ε we obtain

$$\mathcal{O}_{\mathbf{x}}\{\varepsilon y^4\} = y\frac{\partial \bar{G}_\tau}{\partial y}\,\mathcal{O}_{\mathbf{y(x)}}\{1, y, y^2, y^3\}.$$

So $\mathcal{O}_{\mathbf{x}}\{\varepsilon y^4\} \subset TO_s(\bar{G}_\tau)$ and s-infinitesimal stability is proven. □

Proof: (iii) Again we restrict to the space $\mathcal{O}^\sigma_{\mathbf{x}}$ of smooth germs at the origin which are invariant under the action of the map $\sigma : (y, \varepsilon) \mapsto (-y, -\varepsilon)$. We take $\lambda = \frac{1}{2} + \varepsilon$ and substitute into the expression for $\hat{G}$ above to give

$$\hat{G} = -\tilde{h} + \lambda\mu\left\{y^2\left(\frac{1}{4}\,s + \ldots\right) + \varepsilon y^3\left(\frac{1 - 4a_{04}}{2}\,t - \frac{a_{13}}{2}\,s + \ldots\right) + y^4\left(\frac{a_{04}}{16} + \ldots\right) + O(y^5)\right\}.$$

We can now make s–equivalent changes to s, t and y in $\hat{G}$ to give the following homotopy[5]

$$\hat{G}_\tau = -\tilde{h} + sy^2 + \varepsilon t y^3 + y^4\,(\,1 + \tau A^\sigma(y, s, t, \varepsilon)\,)$$

with $\tau \in [0, 1]$ and $A^\sigma(0) = 0$. Now $\frac{\partial \hat{G}_\tau}{\partial \tau} = y^4 A^\sigma$ whilst

$$y\,\frac{\partial \hat{G}_\tau}{\partial y} = 2sy^2 + 3\varepsilon t y^3 + y^4\,(4 + 4\tau A^\sigma + y\tau A^\sigma_y).$$

We now apply Poénaru's preparation theorem with $M = \mathcal{O}^\sigma_{\mathbf{x}}\{y^4\}$ and

$$f : (y, s, t, \tilde{h}, \tau, \varepsilon) \mapsto \left(y\,\frac{\partial \hat{G}_\tau}{\partial y}, s, t, \tilde{h}, \tau - \tau_0, \varepsilon^2\right).$$

In I_f we have $\{y\,\frac{\partial \hat{G}_\tau}{\partial y}\} = \{y^4\}$ so that

$$M/I_f \cdot M \cong \mathbb{R}\{y^4, \varepsilon y^5, y^6, \varepsilon y^7\}$$

since it is clear that $\varepsilon y^4, y^5, \varepsilon y^6, y^7 \notin M$. Now $\{\varepsilon y^2\,\frac{\partial \hat{G}_\tau}{\partial y}\} = \{\varepsilon y^5\}$, $\{y^3\,\frac{\partial \hat{G}_\tau}{\partial y}\} = \{y^6\}$ and $\{\varepsilon y^4\,\frac{\partial \hat{G}_\tau}{\partial y}\} = \{\varepsilon y^7\}$ so by Poénaru's theorem we have

$$m = y\frac{\partial \hat{G}_\tau}{\partial y}\,\left(R_1 + \varepsilon y\,R_2 + y^2\,R_3 + \varepsilon y^3\,R_4\right)$$

for all $m \in M$ with the R_i being smooth functions of $y\frac{\partial \hat{G}_\tau}{\partial y}$, s, t, $\tilde{h}$, $\tau - \tau_0$ and ε^2. Clearly $\mathcal{O}^\sigma_{\mathbf{x}}\{y^4\} \subset TO_s(\hat{G}_\tau)$ and s-infinitesimal stability is proven. □

[5]Provided $a_{04} \neq 0$ or $\frac{1}{4}$ which holds since the cusp of Gauss at the origin on $\mathcal{S}$ is ordinary.

Proof: (iv) For this case there is no obvious application of the Malgrange preparation theorem and so the proof is necessarily more labourious. We take $\lambda = \lambda^* + \varepsilon$ and substitute into the expression for $\hat{G}$ above to give

$$\hat{G} = -\tilde{h} + \lambda\mu\Big\{y^2\left(\frac{4a_{04}-1}{4(3a_{04}-1)}\,s + \ldots\right) + y^3\left(\frac{-a_{13}(4a_{04}-1)\sqrt{a_{04}(1-3a_{04})}}{4(3a_{04}-1)^2}\,s - \frac{(4a_{04}-1)^2\sqrt{a_{04}(1-3a_{04})}}{4(3a_{04}-1)^2}\,t + \ldots\right) + y^4\left(\frac{(4a_{04}-1)(3a_{04}-1)\sqrt{a_{04}(1-3a_{04})}}{4(3a_{04}-1)^2}\,\varepsilon + \frac{(4a_{04}-1)(6a_{13}a_{04}-5a_{05}+a_{13})}{16(3a_{04}-1)^2}\,t + \frac{(4a_{04}-1)(4a_{22}a_{04}-3a_{30}a_{04}-a_{05})}{16(3a_{04}-1)^2}\,s + \ldots\right) + y^5\left(\frac{(4a_{04}-1)(4a_{05}-8a_{05}a_{04}-a_{13})\sqrt{a_{04}(1-3a_{04})}}{32(3a_{04}-1)^3} + \ldots\right) + O(y^6)\Big\}.$$

Now provided $a_{04} \neq 0$, $\frac{1}{3}$ or $\frac{1}{4}$ we can make s–equivalent changes to make the coefficient of y^2 the new s and the coefficient of y^3 the new t. For the coefficient of y^4 we re-scale ε to give it a unit coefficient and provided $6a_{13}a_{04} - 5a_{05} + a_{13} \neq 0$ we can do the same with t. We now re-scale y and s to re-establish unit coefficients for sy^2 and ty^3. Finally, provided $4a_{05} - 8a_{05}a_{04} - a_{13} \neq 0$ we can multiply through by the inverse of the constant term in the coefficient of y^5 and final re-scalings of all variables leads to the following homotopy

$$G_\tau = -\tilde{h} + sy^2 + ty^3 + y^4\,(\,\varepsilon + t + \tau A(s,t,\varepsilon)\,) + y^5\,(\,1 + \tau B(y,s,t,\varepsilon)\,)$$

with $\tau \in [0,1]$ and $A(0) = B(0) = 0$. However, before going on to apply Moser's method we seek a further simplification of G_τ using some standard singularity theory. Since the family G_τ is a deformation of the function germ y^5 it can be induced from the standard versal unfolding of Z^5 at 0, namely

$$H = Z^5 + \alpha_3\,Z^3 + \alpha_2\,Z^2 + \alpha_1\,Z.$$

To say that G_τ can be induced from H means that we can write

$$G_\tau(y,p) = H(Z,\alpha_1,\alpha_2,\alpha_3)$$

where now $Z = Z(y,p)$ and $\alpha_i = \alpha_i(p)$ with $p = (s,t,\tilde{h},\varepsilon)$. The family H is an unfolding of Z^5 at 0 so we must have $\alpha_i(0) = 0$ and by setting $p = 0$ we can show that $Z(y,0) = y\,(1+\tau\,B)^{\frac{1}{5}}$. However it does not necessarily follow that $Z(0,p) = 0$ and we will need this in what follows. Hence we prove the following easy lemma:

Lemma 6.3.3 *Any unfolding of the germ y^5 at $y = 0$ can be induced from the unfolding $L = T^5 + A'T^4 + B'T^3 + C'T^2 + D'T + E'$ in such a way that the origin is fixed, i.e. $y = 0$ implies $T = 0$. (This states that L is a versal unfolding of the boundary singularity y^5 at $y = 0$.)*

Proof: We start with the versal unfolding theorem which states that every unfolding of y^5 can be induced from the standard versal unfolding $K(t, P) = t^5 + At^3 + Bt^2 + Ct$ where $P = (A, B, C)$ is the parameter set. Hence given any unfolding of y^5, $F(y, p)$ say, we can write

$$F(y, p) = K(t(y, p), A(p), B(p), C(p))$$

with $A(0) = B(0) = C(0) = 0$. Now we can certainly write t in the form

$$t(y, p) = T(y, p) + Q(p)$$

where $T(0, p) = 0$ for all p, i.e. Q is that part of t which is independent of y. Substituting $t = T + Q$ into K we obtain a new family

$$L(T, P') = T^5 + A'T^4 + B'T^3 + C'T^2 + D'T + E'$$

with the required property that $y = 0$ implies $T = 0$, and furthermore

$$F(y, p) = L(T(y, p), A'(p), B'(p), C'(p), D'(p), E'(p))$$

with $A'(0) = B'(0) = C'(0) = D'(0) = E'(0) = 0$. Hence F can be induced from L in the required way. Thus we have shown that allowing only changes of coordinates which take 0 to 0, the functions T^5, T^4, ..., T and 1 form a basis for a versal unfolding of the boundary singularity y^5 at 0. (Note: Clearly the same argument can be trivially generalised to the case y^k at $y = 0$.) □

We can now induce G_τ from a family of the same form as L in the lemma, thus

$$G_\tau(y, p) = T^5 + \beta_4 T^4 + \beta_3 T^3 + \beta_2 T^2 + \beta_1 T + \beta_0$$

where $T = T(y, p)$, $\beta_i = \beta_i(p)$ and $\beta_i(0) = 0$. Setting $y = 0$ in this equation we obtain $\beta_0 = -\tilde{h}$. Differentiating once with respect to y and setting $y = 0$ we obtain $\beta_1 = 0$. Differentiating twice with respect to y and once with respect to s and setting

$y = 0$ we can show that $\beta_2 = s + \text{h.o.t.}$ Similarly, differentiating three times with respect to y and once with respect to t we can show that $\beta_3 = t + \text{h.o.t.}$ Finally, if we differentiate four times with respect to y and once with respect to ε (or t) we can show that $\beta_4 = \varepsilon + t + \text{h.o.t.}$ Thus the family G_τ has an equivalent representation of the form

$$G_\tau(y, s, t, \varepsilon) = -\tilde{h} + (s + \text{h.o.t.})\, T^2 + (t + \text{h.o.t.})\, T^3 + (\varepsilon + t + \text{h.o.t.})\, T^4 + T^5$$

where 'h.o.t.' means terms of degree two and higher in s, t and ε. Hence (after some obvious s–equivalent changes of parameter) we obtain the following homotopy

$$\hat{G}_\tau(y, s, t, \varepsilon) = -h + sy^2 + ty^3 + (\,\varepsilon + t + \tau\hat{A}(s, t, \varepsilon)\,)\, y^4 + y^5.$$

We will now apply Moser's method to the family $\hat{G}_\tau$. First we note that

$$y\frac{\partial \hat{G}_\tau}{\partial y} = 2sy^2 + 3ty^3 + 4y^4\,(\,\varepsilon + t + \tau\hat{A}(s, t, \varepsilon)\,) + 5y^5. \tag{6.4}$$

The function on the RHS here is 5-regular so by the general division theorem (e.g. Martinet [15] Ch.9) any such function, $f(y, p)$ say, can be written in the form

$$f(y, p) = Q(y, p)\left(y\frac{\partial \hat{G}_\tau}{\partial y}\right) + \gamma_2(p)\, y^2 + \gamma_3(p)\, y^3 + \gamma_4(p)\, y^4$$

for some smooth function Q and smooth functions γ_i in parameters only. We have

$$\frac{\partial \hat{G}_\tau}{\partial \tau} \subset \mathcal{O}_{y,p}\{y^2\}.$$

If N is the space $\mathcal{O}_{y,p}\{y^2\}$ quotiented by $\mathcal{O}_{y,p}\{y\frac{\partial \hat{G}_\tau}{\partial y}\}$ then the division theorem statement above is equivalent to

$$N = \mathcal{O}_{y,p}\{y^2\} \,/\, \mathcal{O}_{y,p}\left\{y\frac{\partial \hat{G}_\tau}{\partial y}\right\} \cong \mathcal{O}_p\{y^2, y^3, y^4\}.$$

If $[\,f\,]$ denotes the class of a function f in N then $[\,f\,] = \gamma_2(p)y^2 + \gamma_3(p)y^3 + \gamma_4(p)y^4$. Now $\frac{\partial \hat{G}_\tau}{\partial s} = y^2 + \tau\frac{\partial \hat{A}}{\partial s}y^4$ and $\frac{\partial \hat{G}_\tau}{\partial t} = y^3 + \left(1 + \tau\frac{\partial \hat{A}}{\partial s}\right) y^4$ so that

$$\begin{aligned}[\,f\,] &= \gamma_2\left(\frac{\partial \hat{G}_\tau}{\partial s} - \tau\frac{\partial \hat{A}}{\partial s}y^4\right) + \gamma_3\left(\frac{\partial \hat{G}_\tau}{\partial t} - \left(1 + \tau\frac{\partial \hat{A}}{\partial t}\right) y^4\right) + \gamma_4 y^4 \\ &= \gamma_2\frac{\partial \hat{G}_\tau}{\partial s} + \gamma_3\frac{\partial \hat{G}_\tau}{\partial t} + \gamma_5 y^4\end{aligned}$$

for some smooth functions γ_i in parameters. If M is the space N quotiented by $\mathcal{O}_p\{\frac{\partial \hat{G}_\tau}{\partial s}, \frac{\partial \hat{G}_\tau}{\partial t}\}$ then it follows that

$$M = N \,/\, \mathcal{O}_p \left\{ \frac{\partial \hat{G}_\tau}{\partial s}, \frac{\partial \hat{G}_\tau}{\partial t} \right\} \cong \mathcal{O}_p\{y^4\}.$$

So it is sufficient to show that any function of the form $f(y,p) = y^4\, k(p)$ lies in the factor space of the tangent space to the orbit of s–equivalences through $\hat{G}_\tau$. To this end we consider a number of germs from the tangent space $TO_S(\hat{G}_\tau)$. Clearly $\hat{G}_\tau + h \in TO_S(\hat{G}_\tau)$ and

$$\hat{G}_\tau + h = sy^2 + ty^3 + (\varepsilon + t + \tau\hat{A})y^4 = \frac{1}{5}\left(y\frac{\partial g_\tau}{\partial y} - (\varepsilon + t + \tau\hat{A})y^4 - ty^3 - sy^2 \right)$$

using equation (6.4). If $[[\, f \,]]$ is the class of a function f in M then we have

$$[[\, \hat{G}_\tau + h \,]] = \frac{1}{5}(\varepsilon + t + \Phi_1)\, [[\, y^4 \,]]$$

where $\Phi_1 \in \mathcal{M}_p^2$. Now consider the germ

$$y^2\, \hat{G}_\tau = -hy^2 + sy^4 + ty^5 + y^6\, [\, \varepsilon + t + \tau\hat{A}(s,t,\varepsilon)\,] + y^7.$$

Multiplying equation (6.4) by powers of y and using back substitution we can write the RHS here in terms of powers of y up to degree 4 only. Doing this we find

$$[[\, y^2\, \hat{G}_\tau \,]] = \frac{3}{5}(s + \Phi_2)\, [[\, y^4 \,]]$$

where $\Phi_2 \in \mathcal{M}_p^2$. Using the same method with the germ $y^4\, \hat{G}_\tau$ we obtain

$$[[\, y^4\, g_\tau \,]] = (-h + \Phi_3)\, [[\, y^4 \,]]$$

where $\Phi_3 \in \mathcal{M}_p^2$. Finally consider the germ

$$\varepsilon\frac{\partial \hat{G}_\tau}{\partial \varepsilon} = \varepsilon\left(1 + \tau\frac{\partial \hat{A}}{\partial \varepsilon}\right) y^4 \quad \text{so that} \quad \left[\left[\varepsilon\frac{\partial g_\tau}{\partial \varepsilon} \right]\right] = (\varepsilon + \Phi_4)\, [[y^4]]$$

where $\Phi_4 \in \mathcal{M}_p^2$. We now make s–equivalent changes of variable, $\frac{3}{5}(s + \Phi_2) \mapsto \tilde{s}$, $\frac{1}{5}(\varepsilon + t + \Phi_1) \mapsto \tilde{t}$ and $-h + \Phi_3 \mapsto \tilde{h}$. If we write Φ_4 in the form $\Phi_4 = \Phi_5(\varepsilon) + \Phi_6(\tilde{s}, \tilde{t}, \varepsilon)$ with $\Phi_6(0,0,\varepsilon) = 0$ for all ε, we can make a final s–equivalent change of variable, $\varepsilon + \Phi_5(\varepsilon) \mapsto \tilde{\varepsilon}$ and kill the term Φ_6 using $\tilde{s}$, $\tilde{t}$ and $\tilde{h}$. Now we can obtain $\tilde{s}\, [[\, y^4 \,]]$,

$\tilde{t}\,[[\,y^4\,]]$, $\tilde{\varepsilon}\,[[\,y^4\,]]$ and $\tilde{h}\,[[\,y^4\,]]$ using linear combinations of the germs $\hat{G}_\tau + h$, $y^2\hat{G}_\tau$, $y^4\hat{G}_\tau$ and $\varepsilon\,\frac{\partial \hat{G}_\tau}{\partial \varepsilon}$. Hence any function of the form $f(y,p) = y^4\,k(p)$ can be written as a linear combination of germs from the tangent space $TO_S(\hat{G}_\tau)$. We can now make the final statement of the proof: Any function $g \in \mathcal{O}_{\{y,p\}}\{y^2\}$ can be written in the form

$$g(y,p) = Q(y,p)\left\{y\frac{\partial \hat{G}_\tau}{\partial y}\right\} + \gamma_1(p)\left\{\frac{\partial \hat{G}_\tau}{\partial s}\right\} + \gamma_2(p)\left\{\frac{\partial \hat{G}_\tau}{\partial t}\right\} +$$

$$\gamma_3(p)\left\{\hat{G}_\tau + h\right\} + \gamma_4(p)\left\{y^2\,\hat{G}_\tau\right\} + \gamma_5(p)\left\{y^4\,\hat{G}_\tau\right\} + C_0\left\{\varepsilon\,\frac{\partial \hat{G}_\tau}{\partial \varepsilon}\right\}$$

for smooth functions Q and γ_i in their respective variables and some $C_0 \in \mathbb{R}$. This is the required s–infinitesimal stability statement and the proof is complete. □

6.4 Chapter Summary

In this chapter we proved theorems giving normal forms for equidistants, appropriate to all $\lambda \in [0,1]$, local to (i) an ordinary inflexion of a plane curve (theorem 6.2.1) and (ii) ordinary parabolic points (theorem 6.3.1) and cusps of Gauss (theorem 6.3.2) on a single smooth surface piece. These normal forms represent the simplest possible versal families whose discriminants give diffeomorphic versions of the equidistants in each case.

Chapter 7

Experimental Work for Further Study

7.1 Introduction

The bulk of this chapter concerns itself with the behaviour of equidistants in the neighbourhood of points of a smooth surface which occur in 1 and 2 parameter families. In particular we consider:

(i) Non-versal A_3 points,
(ii) A_4 points, and
(iii) D_4 (or flat umbilic) points.

All of these points are unstable in the sense that a small perturbation of the surface will remove them. They do however occur generically as transition 'moments' in families of surfaces and for the equidistants we will be interested in their structure at such special points and either side of such points in the transition. At the time of writing normal forms had not been determined for these cases as they present a number of new difficulties, and in fact unique normal forms may not even exist for these cases. Hence most of this material is of a more experimental nature. We conclude the chapter with an investigation into the birth of A_2^* points.

7.2 Non-versal A_3 Points

Referring once again to the notation and argument following proposition 5.3.5 above, then for the cusp of Gauss case when $b_2 = 0$ we have from equation 5.6

$$K = 24\, c_4\, {s_2}^2 + 4\, \left(c_2 - {b_1}^2\right) {s_1}^2 + 8\, c_4\, {z_2}^2 + \text{h.o.t.}$$

If c_4 and $c_2 - {b_1}^2$ have the same sign then $K = 0$ is locally a point in (s_1, s_2, z_2)-space, whilst if they have opposite sign it is locally a cone. We know from above that when $b_2 = b_3 = 0$ the parabolic curve is singular and (as the zero set of a Morse function) this singularity will be locally an isolated point or a node (i.e. two branches crossing transversely) at the origin. Such points are described as *non-versal* A_3 points of the surface. Our aim is to describe the structure of the equidistants about these isolated points and nodes of the parabolic curve and how they transition either side of such points. First we recall some basic theory:

In a 1-parameter family of surfaces, with b_2 passing through zero, the generic behaviour of the parabolic curve is that of the standard Morse transitions. If $z = f(x, y, t)$, using t as the transition parameter b_2, then the parabolic curve is given by the zero set of $P(x, y, t) = f_{xx}\, f_{yy} - {f_{xy}}^2$. If P has a Morse singularity (i.e. an isolated point or a node) at $x = y = t = 0$ then the condition for the family f to give a standard Morse transition is given by the *Morse Lemma with parameters* (see 'Curves and Singularities' [6] p.95 for a sketch of the proof). In this lemma we use a local diffeomorphism $\psi : (x, y) \mapsto (\psi_1(x, y, t),\ \psi_2(x, y, t))$ of the source space of P so that we can write

$$P(\psi_1(x, y, t), \psi_2(x, y, t), t) = \varepsilon_1\, x^2 + \varepsilon_2 y^2 + h(t) \tag{7.1}$$

where $\varepsilon_1 = \pm 1$ and $\varepsilon_2 = \pm 1$. The lemma states that the family f gives a standard Morse transition if and only if $h'(0) \neq 0$, i.e. h changes sign at the origin. Differentiating equation (7.1) with respect to t gives

$$\frac{\partial P}{\partial x}\,\frac{\partial \psi_1}{\partial t} + \frac{\partial P}{\partial y}\,\frac{\partial \psi_2}{\partial t} + \frac{\partial P}{\partial t} = h'(t).$$

Now when $x = y = t = 0$ then $\partial P/\partial x = \partial P/\partial y = 0$, so the first two terms on the LHS vanish leaving $\partial P/\partial t\,|_{\,(0,0,0)} = h'(0)$. This gives us an easy way to determine if the lemma is satisfied for a given family f.

Example 7.2.1 Bruce et al. [5] provide a detailed study of the evolution of parabolic curves from which we take the following family $f(x, y, t) = x^2 + t\,y^2 + \varepsilon_1\,x^2\,y^2 + \varepsilon_2\,y^4$. For this family $\partial P/\partial t\,|_{(0,0,0)} = 4$ so the Morse lemma with parameters applies. Moreover this family contains all four of the possible Morse transitions of P corresponding to the following choices of ε_1, ε_2: (i) $\varepsilon_1 = \varepsilon_2 = -1$ (ii) $\varepsilon_1 = \varepsilon_2 = 1$ (iii) $\varepsilon_1 = 1$, $\varepsilon_2 = -1$, and (iv) $\varepsilon_1 = -1$, $\varepsilon_2 = 1$. Cases (i) and (ii) represent an elliptic (or hyperbolic) region enclosed by the parabolic curve which shrinks to a point and vanishes, leaving a fully hyperbolic (or elliptic) region. In both of these cases the MPTS is a smooth surface with boundary along the parabolic curve and lying above the enclosed region. During the transition it shrinks to a point and vanishes along with the parabolic curve, e.g. with $\varepsilon_1 = \varepsilon_2 = -1$ and $t = 1$ the MPTS is as follows.

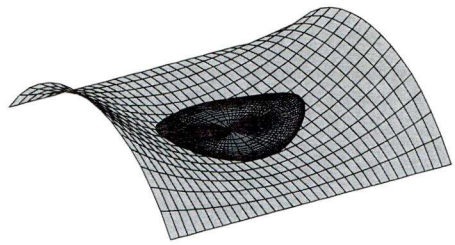

Cases (iii) and (iv) both represent transitions either side of a node on the parabolic curve. In both cases the MPTS clings to the parabolic curve throughout, lying over an elliptic region in one case and over a hyperbolic region in the other, e.g. with $\varepsilon_1 = -1$, $\varepsilon_2 = 1$ and $t = -0.1$, 0 and 0.1 the MPTS is as follows.

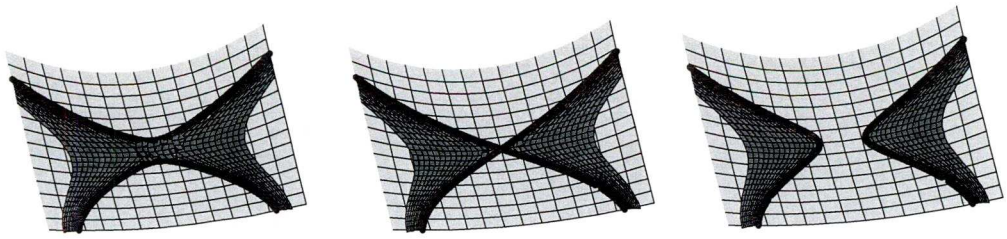

Remark: Convincing pictures for equidistants other than the MPTS are hard to produce in this case. However we know from our earlier work in diffeomorphic settings that they all have the structure of a cuspidal Whitney umbrella at the cusp(s) of Gauss and inflexional contact with the host surface elsewhere along the parabolic curve.

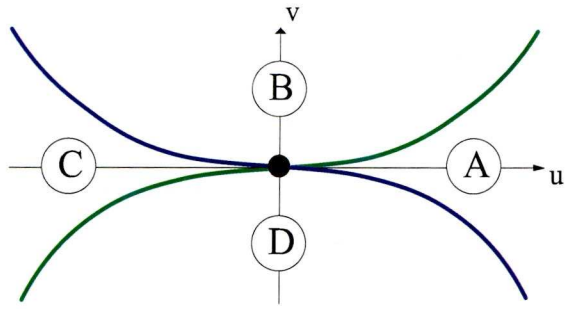

Figure 7.1: The critical locus of the map G.

Movement of Partner Points about a Node of the Parabolic Curve

For the node transition it is instructive to take points close to a node of the parabolic curve and ask where, if anywhere, other *partner points* lie (i.e. other points which have a parallel tangent plane). Any such partner points will of course generate points of an equidistant. To study the behaviour of partner points about a node we take the usual generalised form for f as follows

$$f(x,y) = x^2 + b_0x^3 + b_1x^2y + txy^2 + \text{h.o.t.}$$

with $t = 0$ giving a node on the parabolic curve at the origin. Now consider the map $G : (x,y) \mapsto (f_x, f_y)$ which is $\mathcal{A}$–equivalent to the standard Gauss map. This map determines the parallel tangent set Π for a given surface since points with parallel normals also have parallel tangent planes. By studying the number of pre-images of points in the target space of G we can say something about the existence of partner points in the parameter plane of the surface. Now, using a series of affine changes of coordinate we can reduce G to the form $(x, \pm x^2y + y^3 + \text{h.o.t.})$ and standard classification results for maps from the plane to the plane (e.g. Rieger [21]) tell us that this map is 3–$\mathcal{A}$–determined. Hence we arrive at a final form of $\mathcal{A}$–equivalent Gauss map as follows (retaining G for simplicity of notation)

$$G : (x,y) \mapsto (u,v) \text{ where } u = x \text{ and } v = \pm x^2y + y^3.$$

Now $\Sigma_G = \{(x,y) : \pm x^2 + 3y^2 = 0\}$ which implies $x = y = 0$ or $x = \pm y\sqrt{3}$. The image of this set of points under G is $\{(\pm y\sqrt{3}, -2y^3) : y \in \mathbb{R}\}$. This represents two cubic curves both of which are inflexional and intersect at the origin. Thus the target

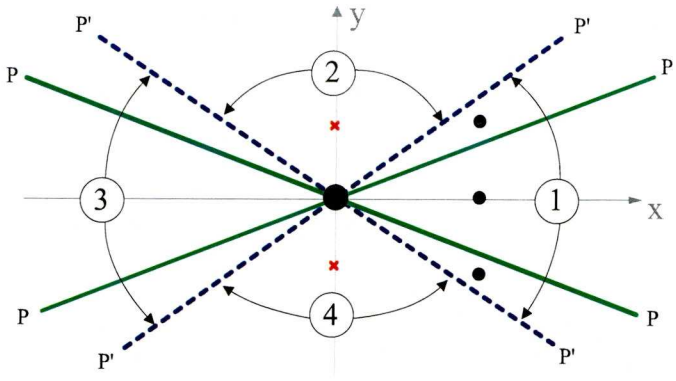

Figure 7.2: Non-versal A_3: Location of partner points.

space of G is separated into regions A, B, C and D by its critical locus, as shown in figure 7.1. We can now ask: how many pre-images do points lying in the various regions of figure 7.1 have?

1. Starting with a point on the v–axis (other than $\mathbf{0}$) this is equivalent to asking for a given v_1 ($u_1 = 0$) how many points in the parameter space of the surface map to $(0, v_1)$ under G? Since $u_1 = 0$ then $v_1 = y^3$ (from the second component of G) so for a given v_1 there is a unique point $(0, y)$ in the parameter space of the surface mapping to $(0, v_1)$. We conclude that every point in regions B and D of figure 7.1 has a single pre-image under G, and so points mapping into these regions do not generate equidistant points.

2. Repeating the exercise for the u–axis we have $x = u_1$ so $\pm {u_1}^2 y + y^3 = 0$ (from the second component of G) and choosing the '–' sign we have $y = 0$ or $y = \pm u_1$ (Note: choosing the '+' sign just yields $u_1 = y = 0$). Hence every point in regions A and C of figure 7.1 has three pre-images under G and points mapping into these regions do generate equidistant points.

3. Points on the critical locus itself are the images of points on the parabolic curve of the surface. These arise in the limit as distinct points with parallel tangent planes come into coincidence on the parabolic curve, creating a boundary on the MPTS (or inflexional contact in the case of other equidistants).

We now look at what is going on in the domain space of G, i.e. the parameter plane of the surface. The pre-image of the critical locus of G is given by those x and y

such that $(x, -x^2y + y^3) = (\pm v\sqrt{3}, -2v^3)$. So from the first components $x = \pm v\sqrt{3}$, and substituting in the second components we have $y^3 + 2v^3 - 3v^2y = 0$. Factorising we have $(y - v)^2(y + 2v) = 0$ so that $y = v$ or $y = -2v$ and the pre-images of the critical locus are $P = \{(\pm y\sqrt{3}, y)\}$ and $P' = \{(\pm y\sqrt{3}, -2y)\}$. The set P is shown as the solid lines through the origin in figure 7.2. It represents the parabolic curve of the surface (after the diffeomorphism to reduce the map G) projected onto the parameter plane. The set P' is another pre-image of the image of the parabolic curve under G and it plays an important role since it separates the parameter plane of the surface into four regions as shown in figure 7.2. Points in regions 2 and 4 have no partner points and hence cannot generate equidistant points (e.g. the marked red crosses). However, all points in regions 1 and 3 have two partner points generating equidistant points (e.g. the marked black circles). This model can provide more qualitative information about the relative movement of partner points and hence the structure of equidistants about a non-versal A_3. We use the following simple rules concerning the critical locus of G:

- Partner points always move in a continuous fashion (except for the possibility of them coming together on P).
- The only folds of the map G are on P.
- Partner points can only hit $G^{-1}(G(P))$ simultaneously (since $P \cup P'$ is the complete inverse image of the critical locus of G).

Now consider a pair of partner points previously coincident on the 'upper' branch of the parabolic curve in region 1 of figure 7.2 and now close to and either side of this line. The points are drawn red and yellow and their initial positions are indicated by a and a^* in figure 7.3. By using the three rules we can conclude the following as these points move smoothly within region 1:

1. As the red point hits the 'lower' branch of P (position b) the yellow point must hit the 'upper' branch of P' (position b^*). From here the red point moves through P but the yellow point must turn back into region 1, since otherwise it could not be a partner to the red point.

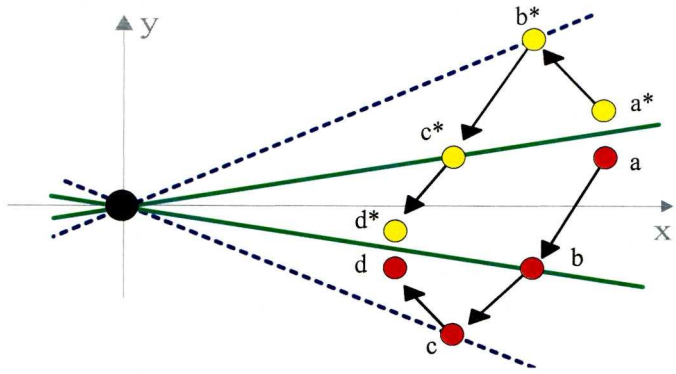

Figure 7.3: Non-versal A_3: Relative movement of partner points.

2. The red point continues on until it hits the 'lower' branch of P' (position c) whence the yellow point reaches the 'upper' branch of P (position c^*). This time the yellow point moves through P but the red point must turn back into region 1 in order to remain a partner point.

3. Both points continue on and are shown at positions d and d^* shortly before coinciding on the 'lower' branch of P.

Since the map taking Π onto the equidistants is a local diffeomorphism then the above argument tells us that points of region 1 of figure 7.2 generate an equidistant in one continuous 'sheet'. Points coming together on the parabolic curve create a boundary on the MPTS and inflexional contact with the host surface for all other equidistants. Clearly all of the above applies equally well to region 3 of figure 7.2. So equidistants in this case always consist of two distinct and continuous sheets (though joined at $\mathbf{0}$).

7.3 A_4 Points

With the surface described locally in Monge form as a graph $z = f(x, y)$ with

$$f = x^2 + b_0x^3 + b_1x^2y + b_2xy^2 + b_3y^3 + c_0x^4 + c_1x^3y + c_2x^2y^2 + c_3xy^3 + c_4y^4 + \text{h.o.t.}$$

then the origin is called an A_4 point whenever $b_3 = 0$, ${b_2}^2 = 4c_4$ and $b_1{b_2}^2 + 4d_5 \neq 2b_2c_3$. Such points occur generically in 1-parameter families of functions and are identifiable, for example, by the intersection of the surface with its tangent plane forming a rhamphoid cusp. There are two types of transition about A_4 points representing either the

birth or death of two ordinary cusps of Gauss on the parabolic curve. The parabolic curve itself remains smooth throughout these transitions (provided $b_2 \neq 0$) but its image under the Gauss map undergoes a *standard swallowtail* transition thus:

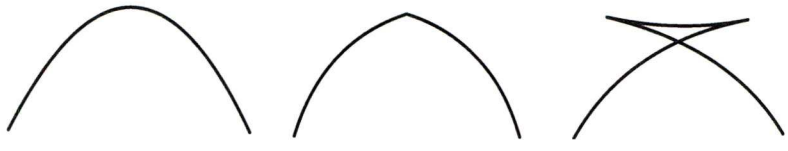

All of this is documented in detail in Bruce et al. [5]. The MPTS in this case shows the familiar behaviour of being a smooth surface with boundary along the parabolic curve. The other equidistants show the typical singularities of a surface formed as an envelope (i.e. cuspidal edges and swallowtail points).

Example 7.3.1 Taking $f(x, y) = x^2 + y^5 + 2xy^2 + y^4$ (so the origin is an A_4 point) the MPTS and equidistant with $\lambda = \frac{1}{3}$ are as follows,

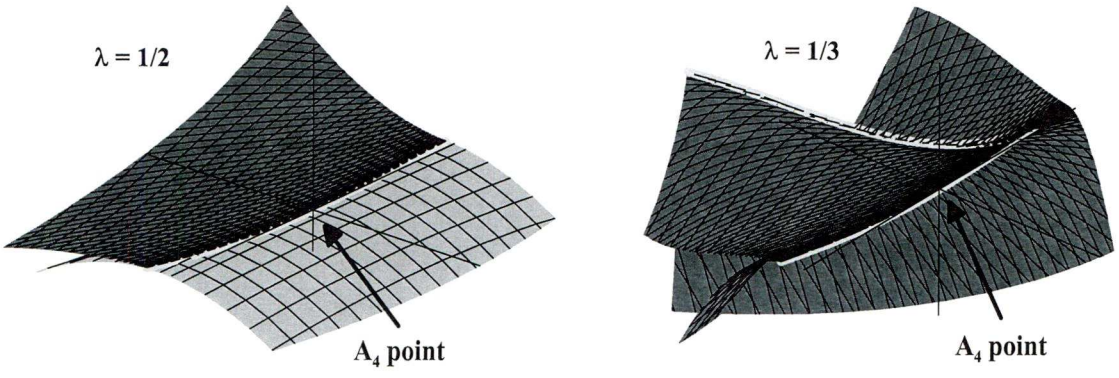

In the latter case the host surface is not shown as it obscures the equidistant which has a cuspidal edge through the A_4 point (and also a swallowtail point away from the A_4). In both figures the singular locus is marked by the lighter coloured space curve.

Singular Parabolic Curve

Here we add a special case to proposition 3.5 of Bruce et al. [5] which was not considered at the time. The proposition states that if the family of height functions, $H(x, y, t, a, b) = f(x, y, t) + ax + by$, is a versal unfolding of an A_4 then the sections $t =$ constant of the big bifurcation set of H (a swallowtail surface) are always generic. This is always true when the parabolic curve remains smooth throughout the transition but

in fact there is a further (co-dimension 2) case in which H is versal but the parabolic curve is singular leading to non-generic t = constant sections of the swallowtail surface. To show this we take f in the standard form, setting $b_2 = b_3 = 0$ (which implies $c_4 = 0$) and $d_5 \neq 0$ whence $f(x,y) = x^2 + b_0x^3 + b_1x^2y + c_0x^4 + c_1x^3y + c_2x^2y^2 + c_3xy^3 +$ h.o.t. If we write $f_1(x,y) = A_0x^2 + A_1xy + A_2y^2 + B_0x^3 + B_1x^2y + B_2xy^2 + B_3y^3 +$ h.o.t. then we can take

$$H(x,y,t,a,b) = f(x,y) + t\,f_1(x,y) + ax + by$$

and use the usual matrix method to determine conditions for H to be a versal unfolding. We need all monomials up to and including degree 3 so we construct a 9×9 matrix whose column headers relate to the monomials x, y, x^2, xy, y^2, x^3, x^2y, xy^2 and y^3. We take the matrix entries to be the coefficients of these monomials in the sequence of expressions F_a, F_b, F_t, f_x, f_y, xf_x, yf_x, xf_y and yf_y. This matrix is

$$\Upsilon = \begin{pmatrix} 1 & 0 & 0 & 0 & 0 & 0 & 0 & 0 & 0 \\ 0 & 1 & 0 & 0 & 0 & 0 & 0 & 0 & 0 \\ 0 & 0 & A_0 & A_1 & A_2 & B_0 & B_1 & B_2 & B_3 \\ 2 & 0 & 3b_0 & 2b_1 & 0 & 4c_0 & 3c_1 & 2c_2 & c_3 \\ 0 & 0 & b_1 & 0 & 0 & c_1 & 2c_2 & 3c_3 & 0 \\ 0 & 0 & 2 & 0 & 0 & 3b_0 & 2b_1 & 0 & 0 \\ 0 & 0 & 0 & 2 & 0 & 0 & 3b_0 & 2b_1 & 0 \\ 0 & 0 & 0 & 0 & 0 & b_1 & 0 & 0 & 0 \\ 0 & 0 & 0 & 0 & 0 & 0 & b_1 & 0 & 0 \end{pmatrix}$$

and $\det(\Upsilon) = -12(b_1c_3)^2A_2$. Hence the family F versally unfolds the A_4 of f at the origin if and only if $b_1 \neq 0$, $c_3 \neq 0$ and $A_2 \neq 0$.

Example 7.3.2 We take $F(x,y,t,a,b) = ax + by + x^2 + ty^2 + x^2y + xy^3 + y^5$ so $b_1 = c_3 = A_2 = 1$ and $d_5 \neq 0$. Clearly $f(x,y) = F(x,y,0,0,0)$ has an A_4 at the origin and we know from above that F is a versal unfolding of this A_4. The big bifurcation set of F is given by $\tilde{\mathcal{B}}_F = \{(t,a,b) : F_x = F_y = F_{xx}F_{yy} - {F_{xy}}^2 = 0\}$ and calculations show that we can parameterise this using x and y as follows

$$\left(\frac{-31y^4 - 12xy - 40y^3 + 4x^2}{4(y+1)},\ -2x - 2xy - y^3,\ \frac{21y^5 + 30y^4 + 6xy^2 - 6x^2y - 2x^2 - 6xy^3}{2(y+1)}\right).$$

The following figure gives a view of this surface close to the origin, showing the familiar swallowtail shape.

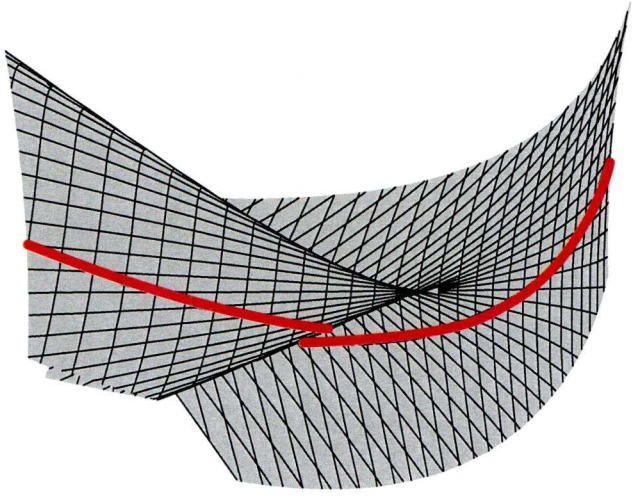

Intersection in the swallowtail surface

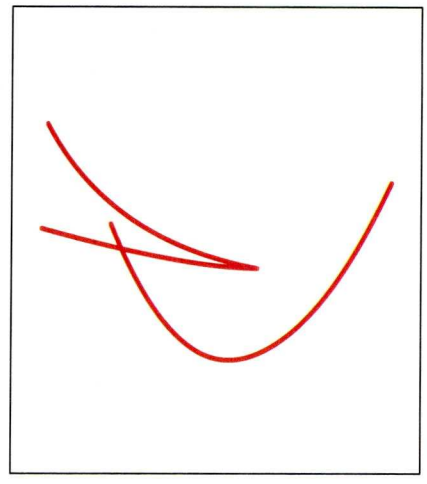

Intersection in the plane t = 0.05

The red curves indicate the intersection of the swallowtail and the plane $t = 0.05$. In examples such as these the $t =$ constant surfaces in $\mathbb{R}^3$ have a tangent plane for $t = 0$ which contains the limiting tangent line to the cuspidal edge and self-intersection of the swallowtail. Hence this family of sections is always non-generic.

7.4 D_4 Points

At D_4 points the quadratic part of f disappears completely forming what is termed a 'flat umbilic', i.e.

$$f = b_0x^3 + b_1x^2y + b_2xy^2 + b_3y^3 + \text{h.o.t.}$$

There are two types of D_4 point depending on the number of real roots of the cubic part of f: (i) elliptic D_4 (or D_4^-) when there are three real roots, and (ii) hyperbolic D_4 (or D_4^+) when there is only one real root. Affine changes of variable allow us to reduce these two types to $z = x^3 \pm xy^2 +$ h.o.t. with the '$-$' sign for D_4^- and the '$+$' sign for D_4^+. Alternatively for D_4^+ we can reduce to $z = x^3 + y^3 +$ h.o.t.

The D_4^- Case

The transition about a D_4^- is similar to the two Morse transitions about an isolated point on the parabolic curve but in this case the parabolic curve reappears after shrinking to a point. An elliptic region reappears as an elliptic region (and hyperbolic similarly) as follows:

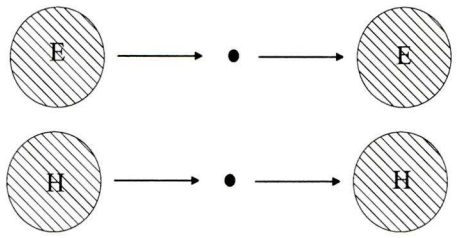

For this case we can find examples where it is possible to extract the problematic diagonal points and parameterise the parallel tangent set Π.

Example 7.4.1 We take $F(x, y, \sigma) = x^3 - xy^2 + y^4 + \sigma\, y^2$, a family which correctly realises the D_4^- transition (see Bruce et al. [5] for details). By using the substitution $a = s - u$, $b = t - v$, $c = s + u$, $d = t + v$ we can extract the diagonal points (i.e. $a = b = 0$) and so parameterise the equidistants. When $\sigma = 0$ we are at the D_4^- moment and the MPTS appears as a parabolic bowl, smooth everywhere except at its single point of contact with the host surface (the D_4^- point):

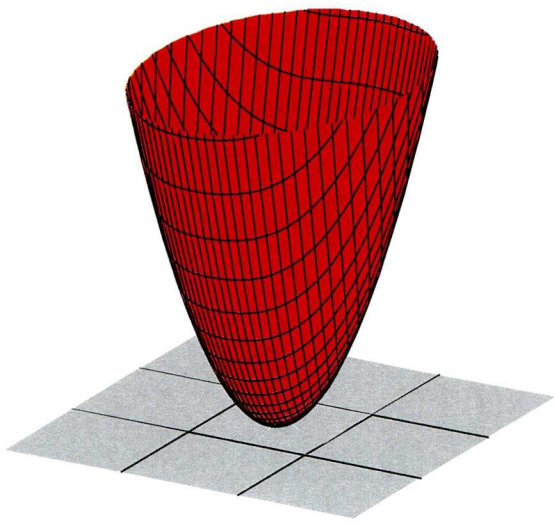

With $\sigma = 1/100$ the parabolic curve opens out into an ellipse passing through the origin and lying in the positive x–half plane. This is now a standard A_2 situation so MPTS is smooth everywhere except for a boundary along the parabolic curve (the bowl sinks into the host surface without reappearing underneath!):

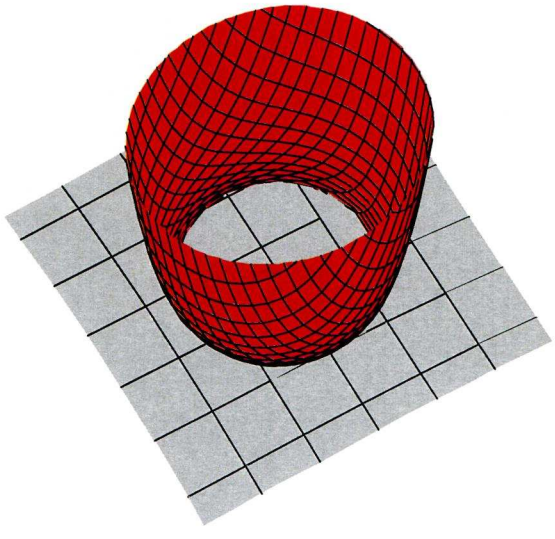

For the transition on the other side we take $\sigma = -1/100$ whence the parabolic curve is an ellipse passing through the origin, this time lying in the negative x–half plane. The MPTS is once again smooth with boundary close to the parabolic curve (left side image), but it is no longer smooth everywhere. If we zoom out slightly we start to see what appear to be cuspidal edges and swallowtails on the MPTS about the forming parabolic bowl (right side image).

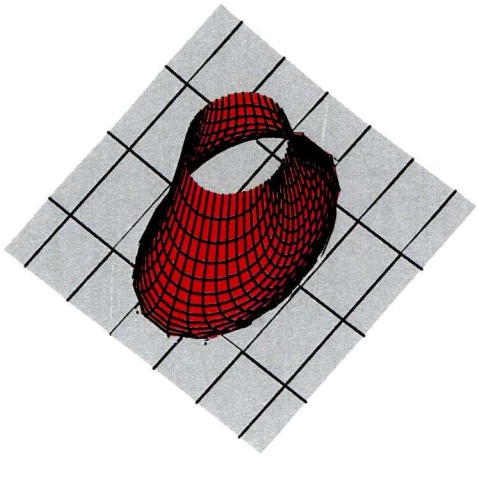

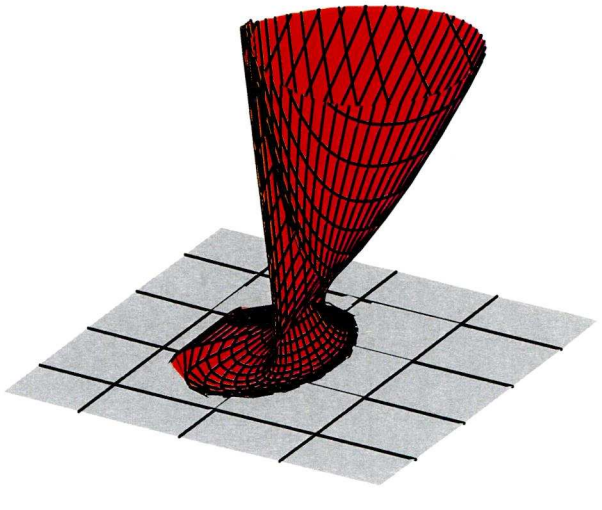

All other equidistants are very singular, e.g. With $\sigma = 0$ and $\lambda = 49/100$ the resulting equidistant looks to have three swallowtail points and several self intersections, although local to the D_4^- point the equidistant is actually smooth:

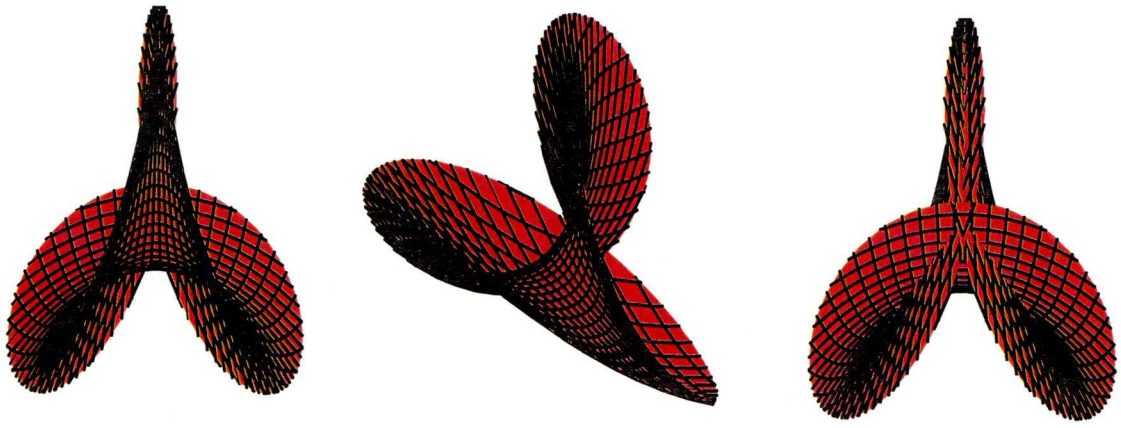

Through the transition it is difficult to produce convincing pictures of the non-halfway equidistants. However from our previous findings we expect them all to meet the original surface with inflexional contact along the parabolic curve before forming cuspidal edges, whilst at the three cusps of Gauss around the parabolic curve they will form cuspidal Whitney umbrellas.

Movement of partner points through the D_4^- transition

In an attempt to establish if this example is generic we will repeat the exercise carried out for the non-versal A_3 case by examining the existence and relative movement of parallel tangent pairs close to a cusp of Gauss after a small perturbation from the $D_4{}^-$ position. For this exercise we can use the simplest possible versal family

$$F(x, y, \sigma) = x^3 - xy^2 + \sigma y^2$$

as cusps and ordinary tangency are stable phenomena. Hence if G is the $\mathcal{A}-$equivalent Gauss map described above then we don't expect to see significant changes in the structure of $G^{-1}(G(P))$ after adding some higher order terms to give a generic example. For this case $G = (f_x, f_y) = (3x^2 - y^2, 2\sigma y - 2xy)$ and we will use u and v as coordinates in the target space of G. The parabolic curve is given by $P = -12x^2 + 12x\sigma - 4y^2 = 0$ which is an ellipse through the origin in the

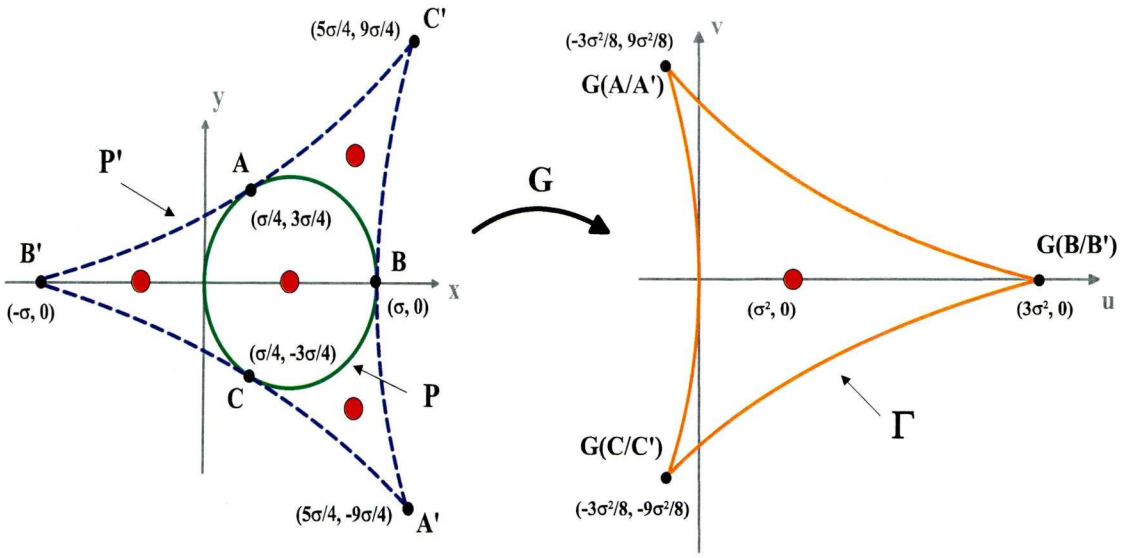

Figure 7.4: The critical locus of the $\mathcal{A}$–equivalent Gauss map and its pre-images for the surface $z = x^3 - xy^2 + \sigma y^2$, with σ fixed and small.

(x, y)–plane, shrinking to a point when $\sigma = 0$. Calculations reveal three hyperbolic cusps of Gauss around this ellipse corresponding to points with coordinates: $A = (\sigma/4, 3\sigma/4)$, $B = (\sigma, 0)$ and $C = (\sigma/4, -3\sigma/4)$. Under G the ellipse maps to a three cusped curve which has two pre-images in the (x, y)–plane; the elliptical parabolic curve P and another curve P' which also has three cusps and is tangent to P at the three cusps of Gauss. If we look at how the cusp of Gauss at B, say, is mapped under G then $G(\sigma, 0) = (3\sigma^2, 0)$. So $f_y = 2\sigma y - 2xy = 0$ which implies that $y = 0$ or $x = \sigma$. Now $y = 0 \implies x = \pm\sigma$ and $x = \sigma \implies y = 0$ so $G(\sigma, 0) = G(-\sigma, 0) = (3\sigma^2, 0)$. The point $(-\sigma, 0)$ is marked as B' in the left half of figure 7.4 and we see that B and B' map to the same cusp in the image of P (or P') under G. In a similar manner we can find points A' and C' so that A and A' map to the cusp at $(-3\sigma^2/8, 9\sigma^2/8)$ and C and C' map to the cusp at $(-3\sigma^2/8, -9\sigma^2/8)$. All of this is shown in the left half of figure 7.4 with the parabolic curve in green and the other pre-image of G shown in dotted blue.

The parabolic curve P represents the critical set of G and its image under G (called Γ in the right half of figure 7.4) gives the critical locus of G. This locus separates the (u, v)–plane into two distinct regions; the finite region within the curve and the

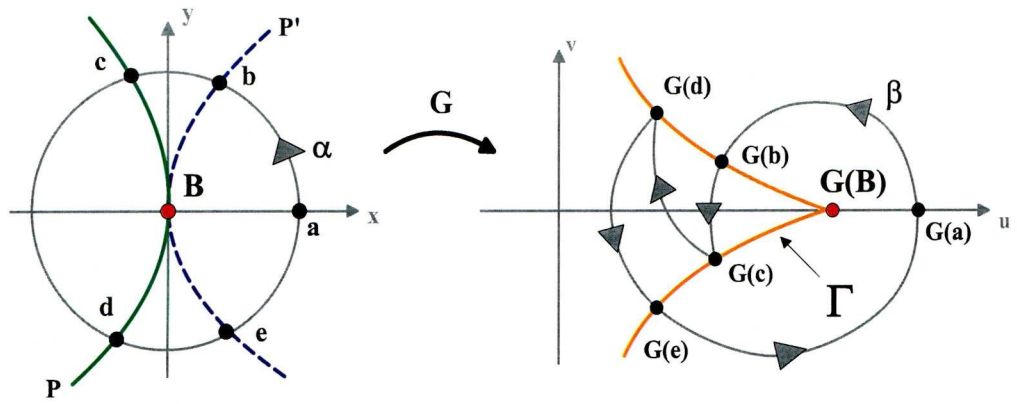

Figure 7.5: Behaviour of the Gauss map close to a Cusp of Gauss.

infinite region without. We can trivially show that G is a fold at all points of P except for the three points A, B and C where it is (by definition) a cusp map. The question arises: how many pre-images do points within these two regions have? (i) Taking the point $(\sigma^2, 0)$ inside Γ we have $(\sigma^2, 0) = (3x^2 - y^2, 2y(\sigma - x))$ for which calculation gives four points in the (x, y)–plane as follows: $(\pm\sigma/\sqrt{3}, 0)$ and $(\sigma, \pm\sigma\sqrt{2})$. The red circles in the left half of figure 7.4 show how these points are arranged, with one point in each of the regions enclosed by ABC, $A'BC$, $AB'C$ and ABC'. (ii) We now take the point $(-\sigma^2, 0)$ outside Γ and obtain two points in the $(x, y)-$plane as follows: $(\sigma, \pm 2\sigma)$. Both of these are clearly outside of P' in the (x, y)–plane. Thus we conclude that all points within Γ have four pre-images (lying in four distinct regions of the $(x, y)-$plane) whilst those outside have just two.

We now move a point α around one of the cusps of Gauss in the $(x, y)-$plane, say B, and look at the corresponding movement of its image β under the map G: (i) Starting with α outside of P' (marked as a in figure 7.5) we move around B before meeting P' at the point b. In the (u, v)–plane this corresponds to β being initially outside of Γ (marked as $G(a)$ in figure 7.5) and meeting Γ at $G(b)$. (ii) Since P' is not part of the critical set of G (except at the three cusps of Gauss) as α moves into the region enclosed by ABC' then β moves inside Γ. (iii) α now goes on to meet P at the point c. This is a fold point of G so β must 'bounce' off Γ and back into its interior as α moves into the region enclosed by the parabolic curve. (iv) α goes on to meet P again at the point d. This is also a fold point of G so β must again 'bounce' back

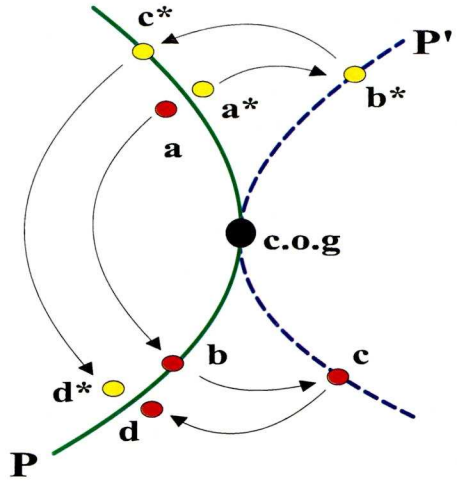

Figure 7.6: Movement of partner points either side of P.

into the interior of Γ as α moves into the region enclosed by $A'BC$. (v) α carries on to meet P' again at the point e. P' is not part of the critical set of G so as α moves into the exterior of P' its image β can finally escape from the interior of Γ. (vi) α continues on to its starting point a as β does the same in the (u, v)–plane. All of this is shown schematically in figure 7.5.

We now examine the relative movement of a pair of partner points p and q close to and either side of the parabolic curve P, having previously been coincident on P. The initial positions for p and q are a and a^* with a^* in the region enclosed by ABC' and a within P. From figure 7.6 we see that the setup is essentially the same as (one half) of the non-versal A_3 case. So again the equidistant, local to the parabolic curve, is formed as a single continuous sheet. Pairs coming together on the parabolic curve form a boundary on the MPTS and an inflexional contact on the other equidistants. As $\sigma \to 0$ the three cusps of Gauss around the parabolic curve approach each other and in the limit coincide so that the parabolic curve vanishes to a point. The example above shows that the equidistants do not similarly vanish. This is because, as shown above, a point outside of P' in the parameter plane of the surface has a unique parallel tangent partner. It is these that generate the equidistants we see about the D_4^- point in our example.

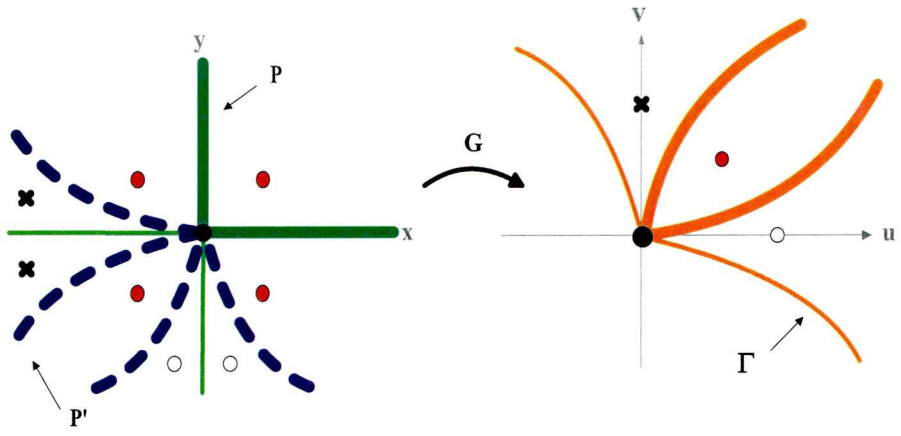

Figure 7.7: The critical locus of $G = (x^2 + y^3,\ x^3 + y^2)$ and its pre-images.

The $D_4{}^+$ Case

The transition about a $D_4{}^+$ has similarities to the two Morse transitions about a node on the parabolic curve but here the parabolic curve and arrangement of elliptic and hyperbolic regions is the same either side of the D_4^+ point as follows

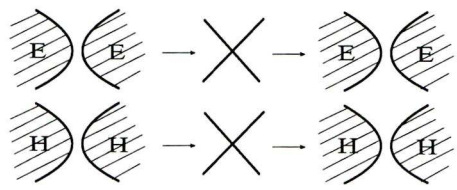

As stated above we can make smooth changes of coordinate to reduce f to the form $f = x^3 + y^3 + \phi(x, y)$ where ϕ contains all terms of degree 4 and higher. In this case the parallel tangency equations $f_x(p) = f_x(q)$, $f_y(p) = f_y(q)$ where $p = (s, t)$ and $q = (u, v)$ give $s^2 - u^2 = \phi_u - \phi_s$, $\quad t^2 - v^2 = \phi_v - \phi_t \quad$ with $\quad \phi_i \in \mathcal{M}^3$. This time we cannot always trivially eliminate two of the variables to give a parameterisation of Π, the ability to do so depends on what we choose for ϕ. The $\mathcal{A}$–equivalent Gauss map here is $G(x, y) = (x^2 + \phi_x,\ y^2 + \phi_y)$ and by an affine change of coordinates[1] followed by an application of a result of du Plessis (Ex. 3.18 of [18]) we have that G is $\mathcal{A}$–equivalent to

$$G(x, y) = (x^2 + y^3,\ x^3 + y^2)$$

[1]Note: This change of coordinates requires (i) $c_1 \neq 0$ and $c_3 \neq 0$ if the 3-jet of f is $x^3 + y^3$, or (ii) $2(c_0 - c_4) \neq \pm(c_1 - c_3)$ if the 3-jet of f is $x^3 + xy^2$.

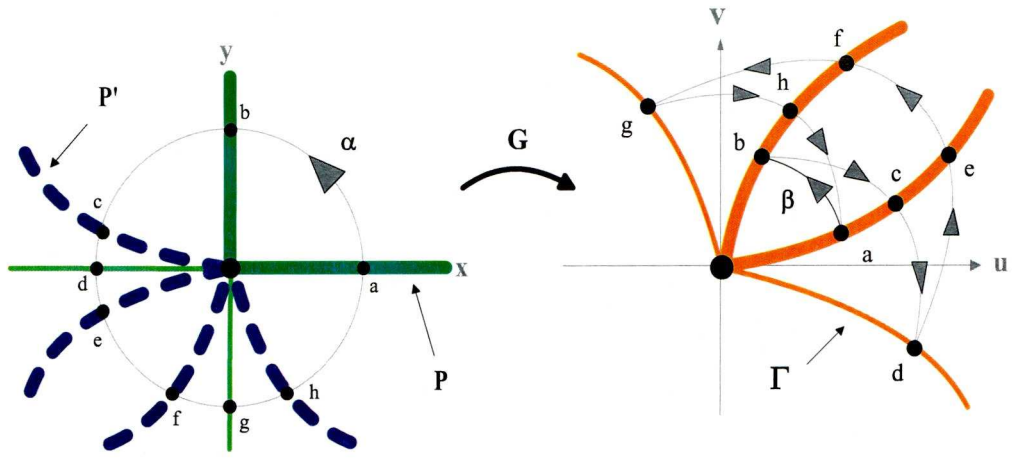

Figure 7.8: Behaviour of the Gauss map close to a D_4^+ point.

(again retaining G for simplicity of notation). The critical set of G is the parabolic curve P, which is locally just the x and y axes. The other part of $G^{-1}(G(P))$, designated P', consists of two cuspidal curves meeting at the origin. Omitting the full details this time, we find that in a neighbourhood of the origin the parameter plane of G is split into regions with either 0, 2 (the white circle or cross in figure 7.7) or 4 pre-images (the red circle in figure 7.7). Consequently the parameter plane of the surface is split into regions where a given point has either a unique partner with parallel tangent, or three partners (one in each quadrant).

Movement of partner points about a D_4^+ point

Moving a point α around the D_4^+ point in the $(x, y)-$plane we can look at the corresponding movement of its image β under G. Starting at a point a on the 'east' branch of the parabolic curve we move α anti-clockwise around the D_4^+ point. Since the green branches of $G^{-1}(G(P))$ represent fold lines then each time α crosses one in the xy–plane the point β must bounce back from the corresponding branch in the uv–plane. Whenever α crosses a blue branch in the xy–plane, β may cross the corresponding branch in the uv–plane. The resulting trajectory of β is shown in the right half of figure 7.8. Using this diagram we can look at the relative movement of a pair of partner points p and q close to and either side of a branch of the green parabolic curve P, having previously been coincident on P. This time we find that it matters

which branch of P we start either side of. First we take $p = a$ and $q = a^*$ close to and either side of the 'south' branch of P, marked red and yellow as follows:

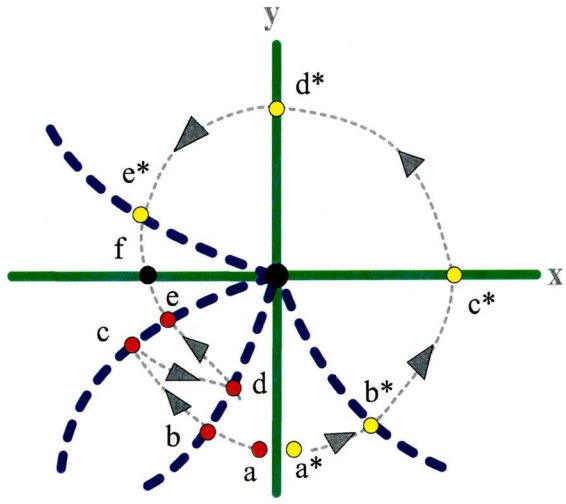

We see that when q crosses the 'east' and 'north' branches of the parabolic curve (at c^* and d^*) then p must turn around in order to remain a partner to q (at c and d). For example, p having reached c cannot continue on into the cusped region surrounding the 'west' branch of P since otherwise q must also be in this region. However, at this moment q is in the upper left quadrant outside of this cusped region. An identical situation arises if we start close to and either side of the 'west' branch of P. Hence this qualitative argument shows that we have a single continuous sheet of equidistant with a boundary (MPTS) or inflexional contact (other equidistants) along the 'west' and 'south' branches of P. If we now start $p = a$ and $q = a^*$ close to and either side of the 'north' branch of P we generate a diagram as follows:

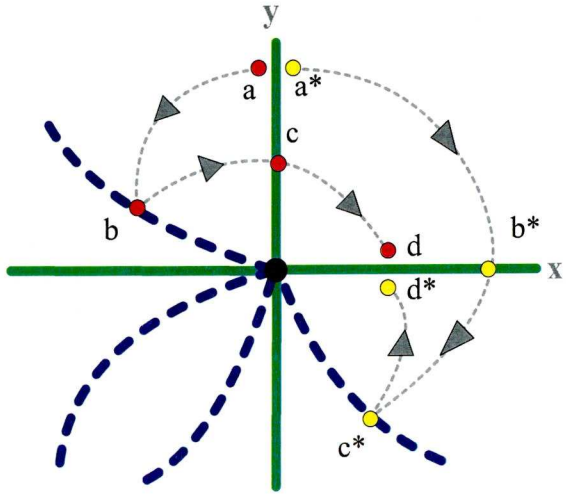

We have essentially the same diagram if we start either side of the 'east' branch of P so this time the equidistant is formed as a single continuous sheet with boundary (or inflexional contact) along the 'east' and 'north' branches of P. In its entirety then, the equidistant local to the parabolic curve is formed as two separate (though connected via the origin) and continuous sheets with boundaries (or inflexional contacts) along the 'north' and 'east' or 'south' and 'west' the branches of the parabolic curve respectively.

Example 7.4.2 We take $f = x^3 + y^3 + x^3y + xy^3$ so that $c_1 = c_3 = 1$ and the Gauss map is reducible to our 3–$\mathcal{A}$–determined form $G = (x^2 + y^3, x^3 + y^2)$. Hence the above description applies to this example. As for example 7.4.1 above we can use the substitution $a = s - u$, $b = t - v$, $c = s + u$, $d = t + v$ to extract the diagonal points and enable a parameterisation using a and b. However in order to avoid zero denominators we form the equidistants as a family of space curves through the origin using further substitutions $a = \lambda b$ and $b = \mu a$ (i.e. parameterising along lines through the origin in the (a, b)–plane). The resulting MPTS is as follows:

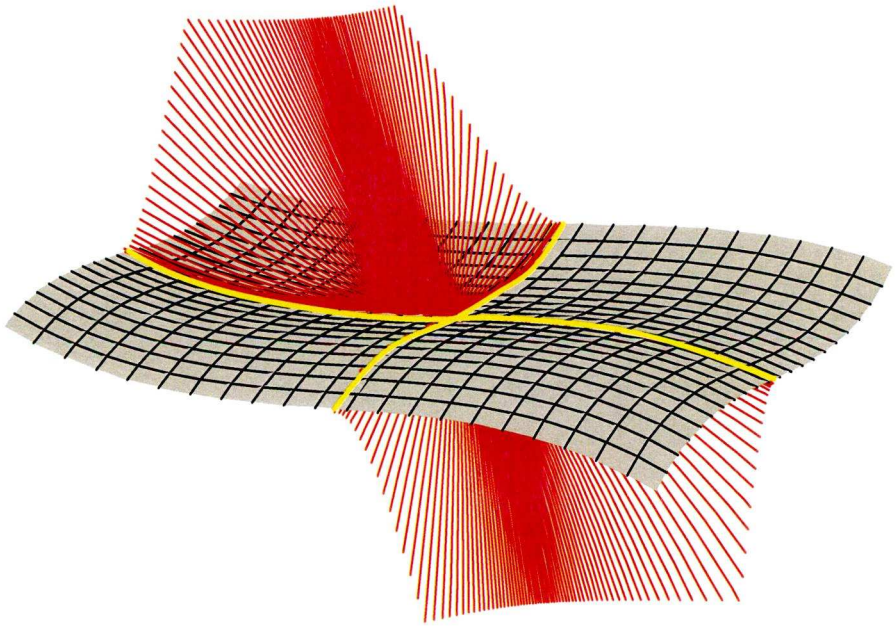

It is a smooth surface in two sheets, one on each side of the host surface. The sheet above has a boundary along the 'north' and 'east' branches of the parabolic curve (shown in yellow), whilst the sheet below has a boundary along the 'south' and 'west' branches of the parabolic curve.

So example 7.4.2 shows the exact structure we predicted in the qualitative argument above. However to illustrate how sensitive the equidistant structure is to the choice of higher order terms we provide another example:

Example 7.4.3 We take $f = x^3 + y^3 + x^4 + y^4$ so that $c_1 = c_3 = 0$. Hence this time we do not satisfy the conditions to be able to reduce the Gauss map to the 3–$\mathcal{A}$–determined form. The parallel tangency equations are: $(s-u)\,(4s^2+s+4su+u+4u^2) = 0$ and $(t-v)\,(4t^2+t+4tv+v+4v^2) = 0$ and these can be solved exactly, yielding three solution sets corresponding to (i) $s = u$ and $4t^2+t+4tv+v+4v^2 = 0$ (ii) $t = v$ and $4s^2+s+4su+u+4u^2 = 0$ and (iii) $4s^2+s+4su+u+4u^2 = 0$ and $4t^2+t+4tv+v+4v^2 = 0$. The final option, $s = u$ and $t = v$, just gives us the diagonal points. The resulting MPTS is as follows:

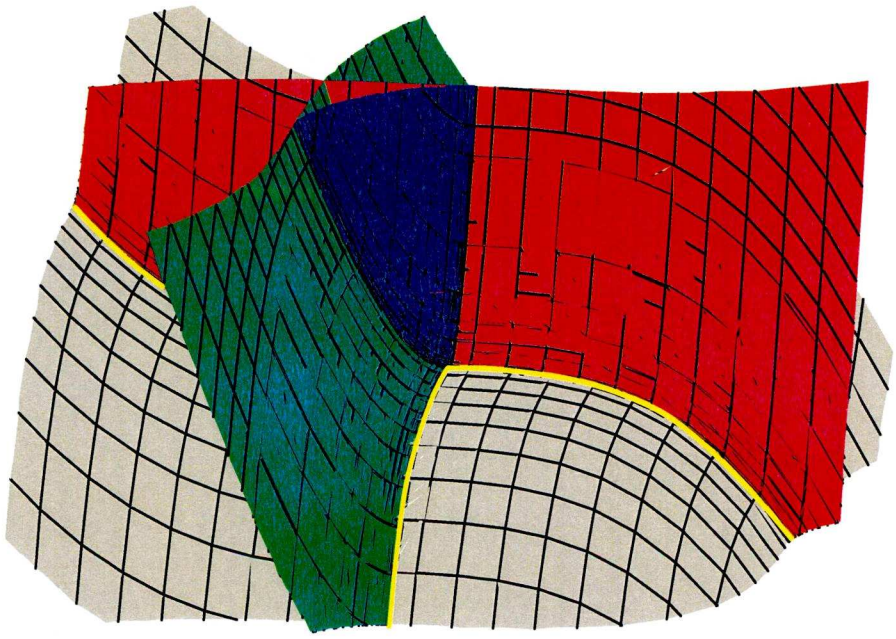

The red piece comes from the solution to (i) and is a smooth sheet with boundary along the 'north' and 'south' branches of the parabolic curve. The green piece comes from the solution to (ii) and is a smooth sheet with boundary along the 'east' and 'west' branches of the parabolic curve. The red and green pieces have a self intersection terminating at the D_4^+ point. Finally, the blue piece comes from the solution to (iii) and is a smooth sheet with boundary along parabolic curves on the red and green pieces. So it is in some sense an equidistant to the equidistant!

Remark: We can strengthen this assertion slightly by looking at a close up of the locus of contact between the blue and green pieces of the equidistant after moving away from the MPTS by taking $\lambda = \frac{5}{12}$:

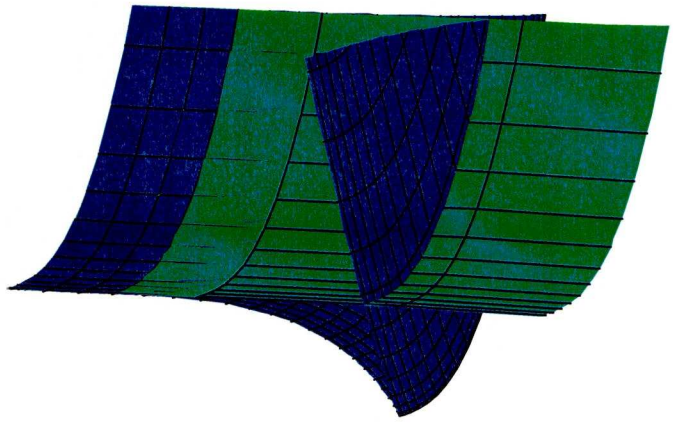

The blue piece meets the green piece with inflexional contact along the parabolic curve before turning back in a cuspidal edge. This is the classic behaviour of a non-halfway equidistant about the parabolic curve of a surface.

7.5 On the Birth of A_2^* Points

We recall that the origin on a surface placed in Monge form is A_2^* if it is ordinary parabolic and the fourth order terms of its Taylor expansion vanish along the asymptotic direction at the origin, i.e. describing the surface as a graph z = f(x,y) with $j^2 f = x^2$ we have

$$f(x,y) = x^2 + b_0x^3 + b_1x^2y + b_2xy^2 + b_3y^3 + c_0x^4 + c_1x^3y + c_2x^2y^2 + c_3xy^3 + \text{h.o.t.}$$

and $b_3 \neq 0$. We have shown above how A_2^* points give rise to special singular behaviour on the MPTS, namely a half cuspidal edge terminating at the A_2^* point itself. The obvious question arises though; how are A_2^* points born? An ellipsoid has no parabolic points but some small perturbations can lead to both A_2 and A_2^* points. In this section we eliminate a number of natural proposals for the birth of A_2^* points[2] and also provide an example which clearly demonstrates the birth event.

[2]However, at the time of writing this remains an open question.

Are A_2^* points born during the 'point' Morse transition of the parabolic curve?

This is perhaps the most obvious candidate since A_2 points are certainly born and we know that two cusps of Gauss are also born during such transitions. Consequently we might speculate that A_2^* points are born in between these cusps of Gauss, i.e.

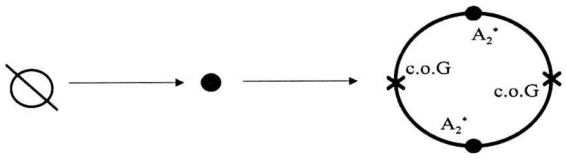

To check this we can use the family from Bruce et al. [5] which correctly models this transition, i.e. $f = x^2+\eta y^2-x^2y^2-y^4$ with η small and negative meaning no parabolic points close to the origin, and η small and positive giving a small ring of parabolic points around the origin (Note: when $\eta = 0$ the origin is not an A_2^* point). For this case we can solve the parallel tangency equations exactly and remove the diagonal points subset Δ to enable a parameterisation of the parallel tangents set Π using t and v (the points of parallel tangency being $(s,t,f(s,t))$ and $(u,v,f(u,v))$). Thus we can parameterise the MPTS exactly in the form $X(t,v) = (m_1(t,v),\ m_2(t,v),\ m_3(t,v))$. Calculating the first minor of the Jacobian matrix of the MPTS with η small and positive (say $\eta = \frac{1}{9}$) we obtain an expression of the form

$$\frac{\partial m_1}{\partial t}\frac{\partial m_2}{\partial v} - \frac{\partial m_1}{\partial v}\frac{\partial m_2}{\partial t} = \frac{(v-t)\,g(t,v)}{h(t,v)}$$

with $h(t,v) \neq 0$ for small t and v. Plotting $g(t,v) = 0$ in the (t,v)–plane gives:

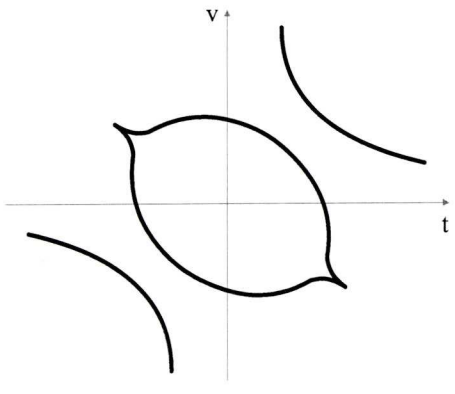

This is the locus of points in the (t,v)–plane giving rise to singular points on the MPTS other than those forming the boundary along the parabolic curve (which are

given by the term $v - t = 0$ in the above expression). Now the expression for s as a function of t, v and η is of the form

$$s(t, v) = \frac{\pm(v^2 - 1)\sqrt{\Omega(t, v, \eta)}}{k(t, v)}$$

with $k(t, v) \neq 0$ for small t and v and

$$\Omega(t, v, \eta) = (tv^3 + t^2v^2 - 2tv + t^3v - 1)(2t^2 + 2tv + 2v^2 - \eta).$$

So real s only occur when $\Omega > 0$. If we plot $\Omega = 0$ when $\eta = \frac{1}{9}$ (in red) together with the existing singular locus (in black) we obtain:

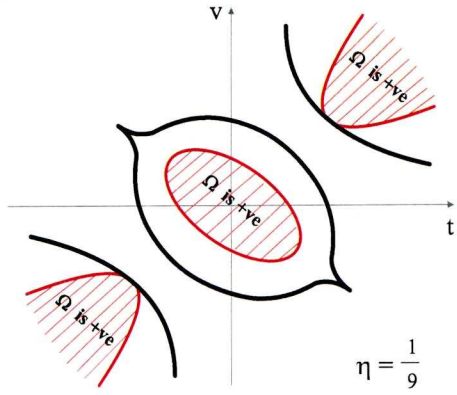

The hatched regions show where $\Omega > 0$ and it is clear that s is imaginary along the critical locus surrounding the origin. Hence the MPTS has no singular points close to the origin. If we now let $\eta \to 0$ the hatched region around the origin shrinks to a point and vanishes without ever crossing the singular locus:

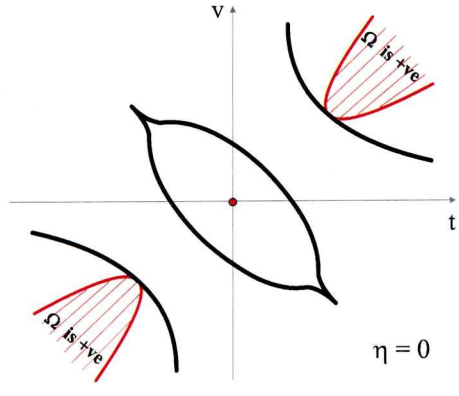

Hence we conclude that, at least generically, no A_2^* points are formed around the parabolic curve through this Morse transition.

Are A_2^* points born at special cusps of Gauss designated A_3^*?

Again we take a surface in Monge form with A_2^* point at the origin. So $z = f(x, y)$ where $f = x^2 + b_0x^3 + b_1x^2y + b_2xy^2 + b_3y^3 + c_0x^4 + c_1x^3y + c_2x^2y^2 + c_3xy^3 + \text{h.o.t.}$ The parabolic curve in the parameter plane of the surface has the parameterisation

$$\left(-\frac{b_3}{b_2}y + \text{h.o.t},\ y\right).$$

As stated above the MPTS can be parameterised using t and v as

$$X(t, v) = (m_1(t, v),\ m_2(t, v),\ m_3(t, v)).$$

Again we consider the first minor of J_X. This always has a branch $t = v$ in the (t, v)–plane. If we extract this we can parameterise another branch through the origin as follows

$$v_* = -t + \frac{3\,b_2\,c_3^2}{2\,(5\,b_2\,d_5 - b_2^2\,c_3 + 3\,b_1\,b_3\,c_3 - 3\,b_3\,d_4)}\,t^2 + \text{h.o.t.}$$

Substituting v_* into the expression for s we obtain a locus of points in the parameter plane of the surface giving rise to singular points of the MPTS other than the boundary along the parabolic curve. We shall call this the S–curve and it has the following parameterisation

$$\left(\frac{-9\,b_3\,c_3^2}{4\,(5\,b_2\,d_5 - b_2^2\,c_3 + 3\,b_1\,b_3\,c_3 - 3\,b_3\,d_4)}\,t^2 + \text{h.o.t},\ t\right).$$

So it is clear than when $b_3 \neq 0$ the parabolic curve and S–curve are never tangent at the origin whilst with $b_3 = 0$ they are always tangent here.

Definition 7.5.1 *With a smooth surface given in Monge form as $z = f(x, y)$ where $f = x^2 + b_0x^3 + b_1x^2y + b_2xy^2 + b_3y^3 + c_0x^4 + c_1x^3y + c_2x^2y^2 + c_3xy^3 + c_4y^4$ + h.o.t then if $b_3 = c_4 = 0$ the origin is a special cusp of Gauss, designated A_3^*. Note: At such points the asymptotic line has 5–point contact with the surface, so we have a bi–flecnode at a cusp of Gauss (or the case "$\rho = 0$" in the terminology of Uribe-Vargas [23]).*

A small perturbation of the surface will move such a cusp of Gauss away from the origin whence the parabolic and S–curves will have two intersections. Is this an A_2^* birth event in the following sense?

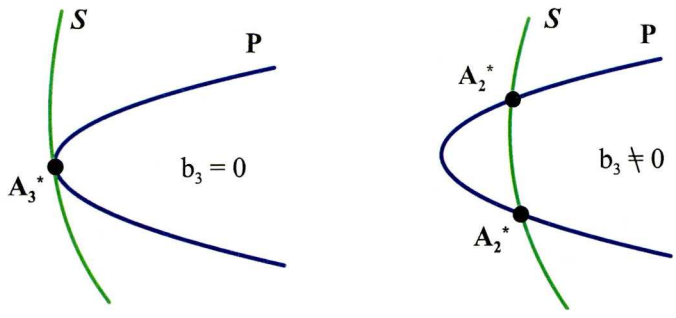

Clearly A_2^* points can only occur when the S–curve crosses the parabolic curve, but does the S–curve crossing the parabolic curve always designate an A_2^* point? We can answer this question by means of an example, taking

$$f(x, y) = x^2 + xy^2 + \varepsilon y^3 + 3xy^3 + xy^4 - y^5.$$

With $\varepsilon = 0$ the origin is an A_3^* whilst for all other values it is an A_2^*. Plotting the parabolic and S–curves for ε small negative, zero, and small positive we obtain

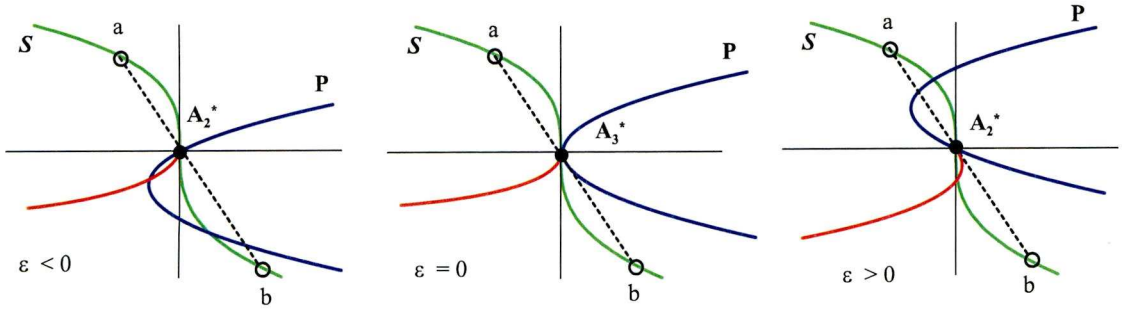

Pairs of points $a = \{s(t, v_*(t)),\, t)\}$ and $b = \{u(t, v_*(t)),\, v_*(t)\}$ on the S–curve are marked by small circles. The mid-points of lines joining them gives a locus in the parameter plane of the surface corresponding to the half cuspidal edge on the MPTS (marked in red). When $t = 0$ the points a and b come together at the A_2^* (or A_3^*) point at the origin. As t passes through zero a and b flip either side of the x–axis. So for no value of t do the points come together at the other crossing point of the parabolic and S–curves. Hence only one A_2^* exists throughout the transition. It moves along P momentarily becoming an A_3^* before carrying on along P as an A_2^*. Consequently there is no birth event, but we have shown that the MPTS also has a half cuspidal edge when the host surface has an A_3^* point at the origin.

Are A_2^* points born at singular points of the S–curve?

We start with the familiar setup of a smooth surface in Monge form with A_2^* point at the origin. If we calculate J_X in the manner described above and remove the factor $v-t$ from the expression for the determinant of its first minor we are left with a series in t and v which describes the S–curve in the (t,v)–plane. It starts as follows

$$S(t,v) = -\frac{5\,b_2\,d_5 - b_2^2\,c_3 + 3\,b_1\,b_3\,c_3 - 3\,b_3\,d_4}{2\,b_2^2}\,(t+v) + \text{h.o.t.}$$

So there is a special value of d_4 namely

$$d_4^* = \frac{5\,b_2\,d_5 - b_2^2\,c_3 + 3\,b_1\,b_3\,c_3}{3\,b_3}$$

for which the S–curve is singular at the origin. Depending on the sign of the discriminant of the quadratic part of the S–curve when $t = v = 0$ this singularity will be either a node or an isolated point. Is there an A_2^* birth event in the d_4 transition in the following manner?

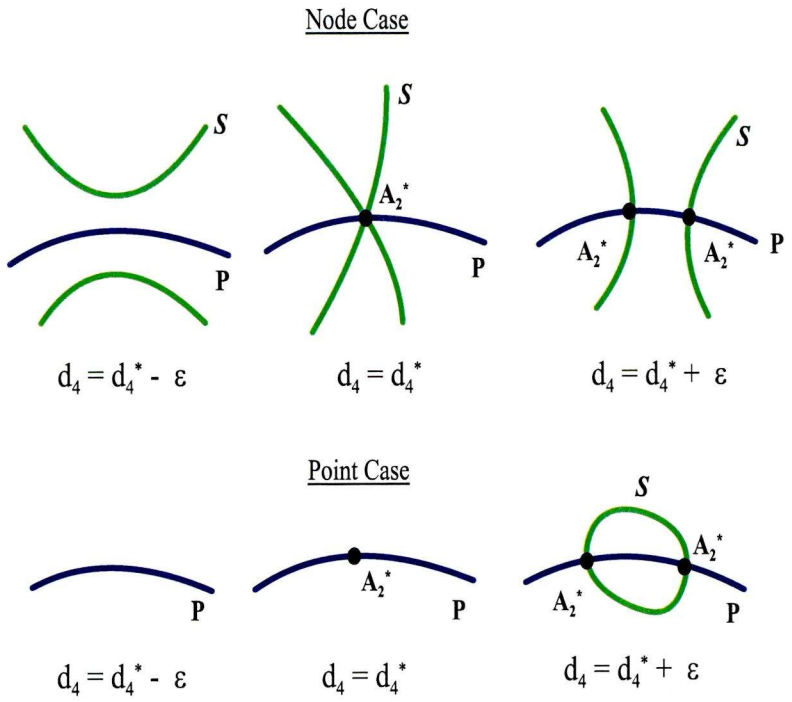

The map $(t,v) \mapsto (s,t)$ is a local diffeomorphism in a neighbourhood of the origin since $\{\frac{\partial s}{\partial v}\}_{t=v=0} = -\frac{3}{2} \neq 0$. Hence the singularities of the S–curve in the (t,v)-plane

are $\mathcal{A}$–equivalent to those of the S–curve in the (s,t)-plane. We take as a suitable example

$$f(x,y) = x^2 + x\,y^2 + y^3 + x\,y^3 + d_4\,x\,y^4 + \eta\,y^5$$

with $\eta = 1$ giving $d_4^* = \frac{4}{3}$ and the node singularity at the origin, and $\eta = -1$ giving $d_4^* = -2$ and the isolated point singularity at the origin. If we plot the S–curve in the (t,v)–plane we can still observe its interaction with the parabolic curve since this is represented by the line $t = v$. For the node case we obtain the following:

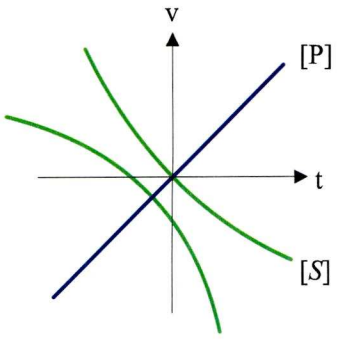

$d_4 = d_4^* - \varepsilon$

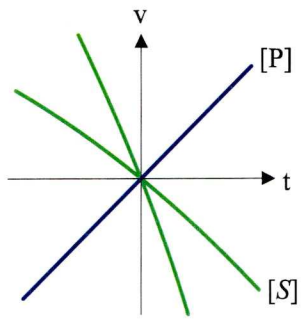

$d_4 = d_4^*$

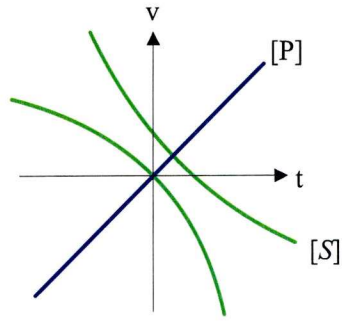

$d_4 = d_4^* + \varepsilon$

Whilst for the isolated point case we obtain:

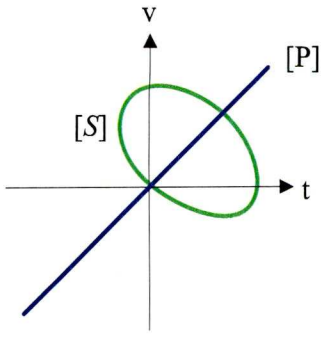

$d_4 = d_4^* - \varepsilon$

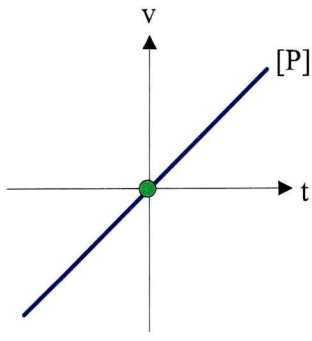

$d_4 = d_4^*$

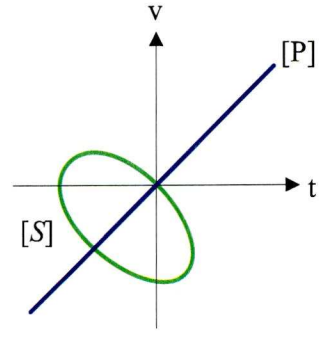

$d_4 = d_4^* + \varepsilon$

Using $[S]$ and $[P]$ to represent the S and parabolic curves in the (t,v)–plane respectively. It is clear from these pictures that there is no birth or death event in either case. The transitions of $[S]$ are similar to those of the parabolic curve in the D_4^+ and D_4^- cases in that the locus reappears either side of the transition. An examination of the movement of parallel tangent partner points (as we did for case (ii) above) shows that they only ever come together at the crossing of $[S]$ and $[P]$ at the origin. So once again there is only ever one A_2^* point throughout, remaining fixed at the origin.

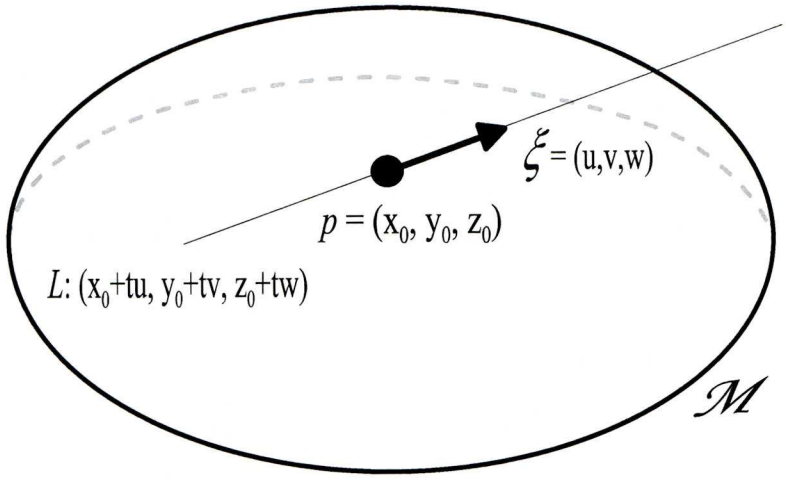

Figure 7.9: A_2^* birth: Contact between the line L and the surface $\mathcal{M}$.

An Example of A_2^* Birth

We conclude this section with an example that clearly demonstrates the birth (and death) of A_2^* points. We start with the functions

$$f(x,y) = x^2 + y^2, \quad g(x,y) = x^2 + x^2y + y^3 + xy^3.$$

Clearly $z = f(x,y)$ is a surface which is elliptic everywhere and so has no A_2^* points, whilst $z = g(x,y)$ has an A_2^* point at the origin. Now consider the surface $\mathcal{M}$ given by $z = F(x,y,\alpha)$ where

$$F(x,y,\alpha) = \alpha\, f(x,y) + (1-\alpha)\, g(x,y).$$

So when $\alpha = 1$ there are no A_2^* points on $\mathcal{M}$ and when $\alpha = 0$ there is certainly one A_2^* point on $\mathcal{M}$, at the origin. Take a point $p = (x_0, y_0, z_0)$ on $\mathcal{M}$ and an arbitrary line L passing through p with direction vector $\xi = (u,v,w)$, as shown in figure 7.9. Now consider the contact function

$$\mathcal{C}_{p,\xi}(t) = F(x0 + tu,\, y_0 + tv) - (z_0 + tw) \quad [= \mathcal{C}(t) \text{ say}]$$

between L and $\mathcal{M}$. If $\mathcal{C}(0) = \mathcal{C}'(0) = 0$ then L is tangent to $\mathcal{M}$ at p. If also $\mathcal{C}''(0) = 0$ then L is an asymptotic line to $\mathcal{M}$ at p. We place no requirement on $\mathcal{C}'''$ but if in addition we have $\mathcal{C}^{(4)}(0) = 0$ then p is an A_2^* point. Now

$$\mathcal{C}^{(4)}(0) = 24\,(\alpha - 1)\, u\, v^2$$

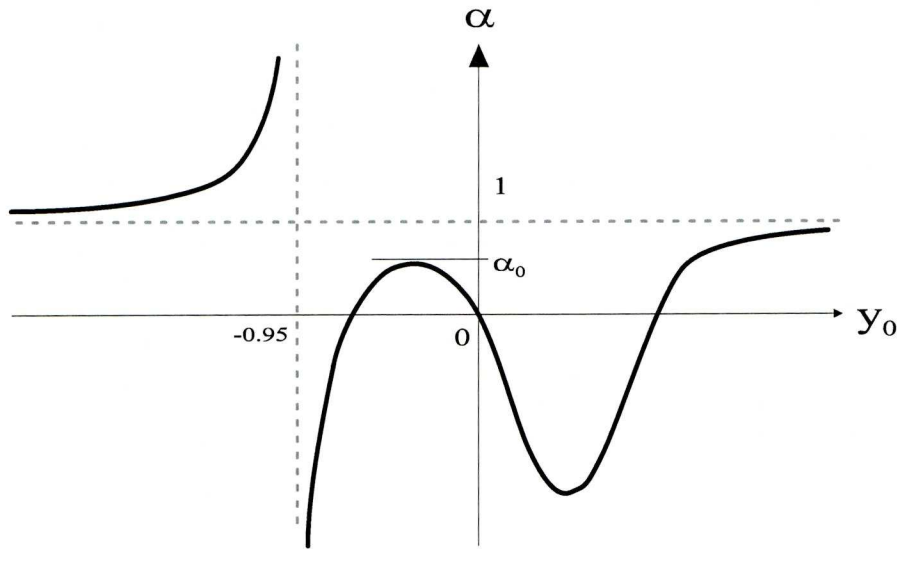

Figure 7.10: A_2^* birth: The graph of α as a function of y_0.

so we require either $u = 0$ or $v = 0$ since with $\alpha = 1$ we have no A_2^* points. If we take $v = 0$ then

$$C''(0) = -2\,u^2\,(\alpha y_0 - y_0 - 1)$$

so $u = 0$ (which implies $\xi = \mathbf{0}$, a contradiction) or $y_0 = \frac{1}{\alpha - 1}$ (which can be shown not to lead to A_2^* points on $\mathcal{M}$). Taking $u = 0$ then $C''(0) = 0$ has the form

$$\frac{\{(\alpha - 1)\,(3y_0^2 + 2\,x_0) \pm \sqrt{\theta}\}\,v}{2(\alpha y_0 - y_0 - 1)} = 0 \tag{7.2}$$

where $\theta = 0$ is the exact condition for p to be a parabolic point of $\mathcal{M}$, i.e.

$$F_{xx}\,F_{yy} - {F_{xy}}^2 = 0.$$

This equation is quadratic in x so we can solve for x_0 in terms of y_0 (provided $y_0 \neq \frac{1}{\alpha - 1}$) and substituting either solution into equation (7.2) we obtain

$$9\,(\alpha - 1)\,y_0^3 - 6\,(\alpha - 1)\,y_0 + 2\,\alpha = 0 \;\; [= \phi(y_0) \;\; \text{say}].$$

When $\alpha \neq 1$ we have a cubic in y_0 the solutions of which give the positions of A_2^* points on $\mathcal{M}$. A birth event occurs when this cubic has a double root, i.e. $\phi = \partial\phi/\partial y_0 = 0$ and these yield a solution $y_0 = -\sqrt{2}/3$ and $\alpha_0 = 6\sqrt{2} - 8$. Back substitution gives $x_0 = -1/3$ and $z_0 = 5\sqrt{2}/9 - 17/27$. So when $\alpha = 6\sqrt{2} - 8$ there is an A_2^* birth event

at the point $p_0 = (-1/3, -\sqrt{2}/3, 5\sqrt{2}/9 - 17/27)$ on $\mathcal{M}$. Solving $\phi(y_0) = 0$ for α as a function of y_0 gives

$$\alpha = \frac{3\,y_0\,(3\,y_0^2 - 2)}{3\,y_0\,(3\,y_0^2 - 2) + 2}.$$

A plot of this function is shown in figure 7.10 where the dashed lines indicate horizontal and vertical asymptotes to the graph. Taking $\alpha = \alpha_0 + \varepsilon$ with ε small and moving through zero from positive to negative we have: $\varepsilon > 0$ there are no A_2^* points close to p_0, $\varepsilon = 0$ an A_2^* point is born at p_0, and $\varepsilon < 0$ the A_2^* point splits into two distinct A_2^*'s which move away from p_0 in opposite directions along the parabolic curve.

Remarks: (i) Substituting $x = x_0$, $y = y_0$, $z = z_0$ and $u = 0$ in $\mathcal{C}$ and setting $v = 1$ (since ξ is merely a direction vector) we obtain $\mathcal{C} = 2(3 - 2\sqrt{2})\,t^3$ so in fact $\mathcal{C}'''(0) \neq 0$ at the birth point. (ii) Using our parameterisation of the parabolic curve and knowing that ξ points in the unique asymptotic direction at p_0 we can trivially show that ξ is not tangent to the parabolic curve at p_0. Both (i) and (ii) tell us that the A_2^* birth point in this example is certainly not a cusp of Gauss.

7.6 Chapter Summary

In this chapter we looked at equidistants local to special surface points that only occur in 1 and 2 parameter families and also considered the issue of how A_2^* points are born on a surface. Normal forms were not available for the cases involving 1 and 2 parameter families so our approach was of a more experimental nature, utilising carefully chosen examples and qualitative arguments to illustrate certain points. The cases considered were as follows:

(i) The non-versal A_3, which represents a cusp of Gauss at which the parabolic curve is either a node or an isolated point. By using an example which is known to versally unfold each of these types we showed that the equidistants vanish (along with the parabolic curve) to one side of the transition in the isolated point case. For the node case we used an illustrative example and also some qualitative arguments, based on properties of the Gauss map, to show that the equidistants exist in two distinct and continuous sheets, joined by a single point at the origin.

(ii) Local to A_4 points of a surface we gave an example that indicates that the MPTS is a smooth surface with boundary along the parabolic curve, whilst other equidistants have a cuspidal edge through the A_4 point. We also looked at an interesting special case where we have a family of height functions which versally unfolds an A_4, but whose big bifurcation set (a swallowtail surface) has non-generic sections.

(iii) Local to D_4^- points we again used qualitative arguments based on properties of the Gauss map to say something about the structure of the equidistants. We found that in the transition either side of the D_4^- moment the equidistants have essentially the same structure as they do to one side of the non-versal A_3 isolated point case, i.e. a smooth surface with boundary (MPTS) or inflexional contact (other equidistants) around the parabolic curve. However, unlike the non-versal A_3 case, the equidistants do not vanish at the singular moment, e.g. the MPTS is a surface which is smooth everywhere except the point where it meets the host surface at the D_4^- point.

(iv) Local to D_4^+ points the parabolic curve is nodal, much like the non-versal A_3 node case, although transitioning in an entirely different manner. We used qualitative arguments based on properties of the Gauss map to show that the equidistants exist in two continuous sheets. One having a boundary (MPTS) or inflexional contact (other equidistants) along the "north" and "east" branches of the parabolic curve, and the other similarly along the "south" and "west" branches. The branches meet at the D_4^+ point itself and we gave an example where this marked the end point of a self intersection on the equidistant. Another example with slightly different fourth order terms had no self intersection so the essential structure of the equidistants seems highly sensitive to the choice of higher order terms. This perhaps supports that notion that there is no unique model of the equidistants local to a D_4^+ point.

We concluded this chapter by looking at three obvious mechanisms by which A_2^* points could be born on a surface. None of these turned out to lead to the birth of A_2^* points and at the time of writing this remains an open question, although we have devised an example which clearly demonstrates the birth event.

Bibliography

[1] Arnold V.I, *Catastrophe Theory*, Springer (1984) (Translated from Russian)

[2] Arnold V.I, Lagrangian manifolds with singularities, asymptotic rays, and the open swallowtail, *Functional Analysis and Its Applications*, **15** (1981), 235–246.

[3] Asada H and Brady M, Smoothed Local Symmetries and their Implementation. *Massachusetts Inst. of Tech. – Tech. Reports (1984).* UMI Order No. AIM–757.

[4] Banchoff T, Gaffney T and McCrory C. Cusps of Gauss Mapping. *Pitman Advanced Publishing Program, Boston (1982).* ISBN 0-273-085360

[5] Bruce J.W, Giblin P.J. and Tari F, 'Families of Surfaces: Height Functions, Gauss Maps and Duals', *Pitman Research Notes in Maths* **333** (1995), 148–178.

[6] Bruce J.W. and Giblin P.J, Curves and Singularities. Second Edition. *Cambridge University Press* ISBN 0-521-41985-9.

[7] Giblin P.J, Affinely Invariant Symmetry Sets. *Geometry and Topology of Caustics - Caustics '06*, Banach Centre Publications, **82** (2008), 71–84.

[8] Giblin P.J and Brassett S.A, Local Symmetry of Plane Curves. *American Mathematical Monthly* **92** (1985), 689–707.

[9] Giblin P.J and Holtom P.A, 'The Centre Symmetry Set'. *Geometry and Topology of Caustics*, Banach Center Publications, **50**, (1999), 91–105.

[10] Giblin P.J, Warder J.P. and Zakalyukin V.M, Birfurcations of Affine Equidistants. To appear in Proceedings of Arnold-70 "Analysis and singularities" (2009)

[11] Giblin P.J and Zakalyukin V.M, Singularities of Centre Symmetry Sets. *Proc. London Math. Soc.* (3) **90** (2005), 132–166.

[12] Ince E.L, Ordinary Differential Equations, Second Edition (1956). *Dover Publications Inc. LoC Card No. 58-12618*

[13] Lu Y-C, Singularity theory and an introduction to catastrophe theory. *Springer, New York* ISBN 0-38790-221-X (1976)

[14] Malgrange B, Le théorème de préparation en géométrie différentiable. I. Position du problème. 1962/63 Séminaire Henri Cartan, Exp. 11 14 pp. Sec. math, Paris.

[15] Martinet J, Singularities of smooth functions and maps, *London Math. Soc. Lecture Note Series* **58**, Cambridge, 1982.

[16] Morris R.J, The Use of Computer Graphics for Solving Problems in Singularity Theory, *Visualisation and Mathematics*, Springer (1997), 53–66.

[17] Moser J, On Volume Elements on Manifold, *Trans. Amer. Math. Soc.*, **120** (1965), 280–296.

[18] du Plessis A.A, On the Determinacy of Smooth Map Germs. *Inv. Math* **58** (1980), 107–160.

[19] Poénaru V, Singularités C^{∞} en présence de symétrie: en particulier en présence de la symétrie d'un groupe de Lie compact. *Lecture Notes in Maths*, vol. **510**, Springer, 1976.

[20] Porteous I.R, Geometric Differentiation: For the Intelligence of Curves and Surfaces. 2nd Edition. *Cambridge University Press* ISBN 0-521-00264-8

[21] Reiger J.H, Families of Maps from the Plane to the Plane. Journal Lond. Math. Soc. **36** (1987), 351–369.

[22] Tari F, Some Applications of Singularity Theory to the Geometry of Curves and Surfaces. *PhD thesis, University of Liverpool* (1990).

[23] Uribe-Vargas R, A Projective Invariant for Swallowtails and Godrons and Global Theorems on the Flecnodal Curve. *Moscow Math. Journal* **6:4** (2006) 731–768.

[24] Whitney H, On Singularities of Mappings of Euclidean Space: I. Mappings from the plane to the plane. *Annals of Mathematics* **62** (1955), 374–410.